Universitat Autònoma de Barcelona

Vaccination strategies to prevent MERS CoV spillover to humans

Jordi Rodon Aldrufeu

Vaccination strategies to prevent MERS-CoV spillover to humans

Jordi Rodon Aldrufeu

Ph.D. thesis

Bellaterra, 2022

Insights into MERS-CoV disease resistance in the camelid reservoir and strategies to prevent zoonotic spillover

Jordi Rodon Aldrufeu

Ph.D. Thesis

Bellaterra, 2022

Universitat Autònoma de Barcelona

Insights into MERS-CoV disease resistance in the camelid reservoir and strategies to prevent zoonotic spillover

Doctoral thesis presented by **Jordi Rodon Aldrufeu** to obtain the Doctoral degree under the program of Animal Medicine and Health at the Faculty of Veterinary medicine from Universitat Autònoma de Barcelona, under the supervision of **Joaquim Segalés Coma**, **Albert Bensaid** and **Júlia Vergara Alert.**

Bellaterra, 2022

IRTA

CReSA

El Prof. **Joaquim Segalés i Coma**, catedràtic del Departament de Sanitat i d'Anatomia Animals de la Facultat de Veterinària de la Universitat Autònoma de Barcelona i investigador adscrit a l'Institut de Recerca i Tecnologia Agroalimentàries – Centre de Recerca en Sanitat Animal (IRTA-CReSA), el Dr. **Albert Bensaid**, investigador de l'IRTA-CReSA i la Dra. **Júlia Vergara i Alert**, investigadora de l'IRTA-CReSA,

Certifiquen:

Que la memòria titulada "**Insights into MERS-CoV disease resistance in the camelid reservoir and strategies to prevent zoonotic spillover**" presentada per **Jordi Rodon Aldrufeu** per a l'obtenció del grau de Doctor en Medicina i Sanitat Animals, s'ha realitzat sota la nostra direcció i tutoria, i n'autoritzem la seva presentació per tal de que sigui valorada per la comissió establerta.

I perquè així consti als efectes oportuns, signem la present declaració a Bellaterra (Barcelona), a 27 de juny de 2022.

Prof. Joaquim Segalés i Coma	**Dr. Albert Bensaid**	**Dra. Júlia Vergara i Alert**
Tutor i Director	Director	Director

Jordi Rodon i Aldrufeu
Doctorand

This Ph.D. thesis was performed as part of the Zoonotic Anticipation and Preparedness Initiative (ZAPI) [Innovative Medicines initiative (IMI) grant 115760] and the Veterinary Biocontained research facility Network (VetBioNet) (EU Grant Agreement INFRA-2016-1 Nº731014) projects.

Jordi Rodon Aldrufeu was partially supported by VetBioNet and the crowdfunding initiative #Yomecorono.

“Fer de la interrupció un camí nou.

Fer de la caiguda un pas de dansa,

de la por una escala,

del somni un pont,

de la recerca, una trobada.”

Fernando Sabino

Table of contents

List of abbreviations

BAL	Bronchoalveolar fluid lavage
BSL-3	Biosafety level 3
CEEA	Ethical and Animal Welfare Committee
CoV	Coronavirus
COVID-19	Coronavirus infectious disease 2019
CPE	Cytopathic effect
Cq	Quantification cycle
CReSA	Animal Health Research Center
CCHFV	Crimean-Congo haemorrhagic fever virus
DAD	Diffuse alveolar damage
DMV	Double-membrane vesicle
dpi	days post MERS-CoV inoculation
DMEM	Dulbecco's modified Eagle medium
DPP4	Dipeptidyl-peptidase 4 (or CD26)
E	Envelope protein
ERGIC	Endoplasmic reticulum-Golgi intermediate compartment
ES	Environmental samples
Fc	Fold-change value
FCS	Fetal calf serum
gDNA	Genomic DNA
HCAbs	Heavy-chain only antibodies
hDPP4	human DPP4
HEV	Hepatitis E virus
HI	Hemagglutination inhibition

hpe	h post MERS-CoV exposure
HR	Heptad repeat
IFN	Interferon
Ig	Immunoglobulin
ISG	Interferon-stimulated genes
IL	Interleukin
IRTA	Institute of Agrifood Research and Technology
KSA	Kingdom of Saudi Arabia
LAM	Llama alveolar macrophage
LIPS	Luciferase immunoprecipitation
LN	Lymph nodes
LRT	Lower respiratory tract
LS	Lumazine synthase
LU	Luminescence units
M	Membrane protein
mDPP4	mouse DPP4
MERS-CoV	Middle East respiratory syndrome coronavirus
MERSr-CoV	MERS-related CoVs
MDDCs	Monocyte-derived dendritic cells
MDMs	Monocyte-derived macrophages
MHC-I	Major histocompatibility complex class I
MHC-II	Major histocompatibility complex class II
MPSP	Multimeric protein scaffold particles
N	Nucleocapsid protein
nAbs	Neutralizing antibodies
NHP	Non-human primate

NK	Natural killer cells
NS	Nasal swabs
nsps	non-structural proteins
NTC	no-RNA template controls
ORF	Open-reading frames
PAMPs	Pathogen-associated molecular patterns
PBMCs	Peripheral blood mononuclear cells
PBS	Phosphate-buffered saline
pDCs	Plasmacytoid dendritic cells
PHA	Phytohemagglutinin P
PMA	Pphorbol 12-myristate 13-acetate
PRNT	Plaque reduction neutralization
PRR	Pattern-recognition receptor
R_0	Reproduction number
RBD	Receptor-binding domain
RBI	Receptor binding inhibition
RBM	Receptor-binding motif
RER	Rough endoplasmic reticulum
RIN	RNA Integrity Numbers
RPMI	Roswell Park Memorial Institute 1640 medium
RT-qPCR	Reverse transcription-quantitative polymerase chain reaction
Ruc	*Renilla* luciferase
RVFV	Rift Valley fever virus
S	Spike protein
$S1^A$	N-terminal domain of S1 subunit
$S1^B$	C-terminal domain of S1 subunit (or RBD)

SARS-CoV	Severe acute respiratory syndrome coronavirus
sgRNA	subgenomic RNAs
TCID	Tissue culture infectious dose
TEM	Transmission electron microscopy
TF	Transcription factor
TLR	Toll-like receptor
Tm	Melting temperature
TRS	Transcription-regulating sequence
TRS-L	Leader transcription-regulating sequence
UAE	United Arab Emirates
URT	Upper respiratory tract
VLP	Virus-like particle
WHO	World Health Organization

Abstract

Outbreaks caused by the Middle East respiratory syndrome coronavirus (MERS-CoV) are ongoing in the Arabian Peninsula. Patients with severe MERS can experience fatal pulmonary disease due to a massive infiltration of immune cells into the lungs, exacerbating lung injury. Bats and camelid species are the natural reservoirs of MERS-CoV, being dromedary camels the primary source of human infection. Camelids trigger robust and timely innate immune responses thought to resolve MERS-CoV infection and prevent disease development. A high induction of type I and III IFNs by MERS-CoV-infected nasal epithelium during the peak of infection would likely activate downstream antiviral responses along the respiratory tract. Here, we evidenced that alveolar macrophages from camelids could be important mediators of MERS-CoV clearance without eliciting pro-inflammatory responses. Outside the respiratory tract, MERS-CoV is carried to secondary lymphoid organs, but viral replication does not occur in these compartments as we determined *in vitro*. Cervical lymph nodes induced innate and adaptive cellular immune responses (i.e., IFNs, ISGs, Th1-like responses) to a secondary MERS-CoV exposure, but not inflammatory responses. Like bats, dampened inflammation in key anatomical compartments of camelids allows transient replication, shedding and transmission of MERS-CoV while remaining asymptomatic. Moreover, field data revealed waning adaptive immunity in dromedaries, allowing for rapid MERS-CoV reinfection. Thus, endemicity of MERS-CoV in dromedary camels drives viral evolution, whereas humans are merely terminal hosts suffering from zoonotic disease.

Currently, clade B strains are prevalent in the Arabian Peninsula and are being repeatedly introduced into the human population, whereas clade C

strains are restricted to African dromedaries. Although MERS-CoV is widespread in the latter ones, human disease of zoonotic origin has only been reported in the Arabian Peninsula. Serological and molecular evidence of MERS-CoV infection have been found in camel handlers, but no zoonotic MERS has been reported across Africa. Despite a continuous dromedary trade from Africa to the Arabian Peninsula, African clade C viruses are not found in this region. This Ph.D. thesis provides experimental evidence for extended Arabian clade B shedding in a camelid model compared to African clade C counterparts. Increased replicative fitness and differential transmission patterns between MERS-CoV clades support the dominance of clade B strains in the Middle east. These results might explain why MERS-CoV clade C strains fail to establish in the Arabian Peninsula. Importantly, our work recommends that the introduction of clade B strains to Africa must be avoided, as they might outcompete African clade C strains and pose a greater zoonotic threat in Africa.

Vaccination of livestock reservoir species is a recommended strategy to prevent spread of MERS-CoV among animals and potential spillover to humans. To date, there is a lack of commercial vaccines against MERS-CoV, although some prototypes for human use are being examined in regulatory pathways. We explored the capacity of two different vaccine candidates to curtail MERS-CoV transmission among camelids, using a llama direct-contact transmission set up to mimic MERS-CoV natural infection. Prototypes were based in the S1 subunit or the receptor-binding domain (RBD) of the Spike protein formulated using a registered adjuvant for animal use. Both vaccine candidates induced high levels of MERS-CoV-neutralizing antibodies. RBD vaccination only provided protection in one out of three vaccinated llamas. In contrast, immunization with the

S1 candidate elicited both mucosal and systemic protective immunity, conferring protection against MERS-CoV infection. This vaccine candidate completely prevented infectious viral shedding. Our data provide further evidence that vaccination of the reservoir host may be an economical solution to impede MERS-CoV zoonotic transmission to humans.

The present Ph.D. thesis contributes to the understanding of disease resistance mechanisms in camelid reservoir species and propose strategies to prevent MERS-CoV spillover.

Resum

El coronavirus de la síndrome respiratòria de l'Orient Mitjà (MERS-CoV) continua causant brots a la península aràbiga. Els pacients greus pateixen una pneumònia que pot ser fatal, caracteritzada per una infiltració massiva de cèl·lules immunitàries als pulmons que agreugen la malaltia. Els ratpenats i els camèlids són els reservoris naturals del MERS-CoV, mentre que els dromedaris són la principal font d'infecció d'humans. Es creu que els camèlids generen una resposta immunitària oportuna per contrarestar la infecció eficaçment i prevenir el desenvolupament de malaltia respiratòria. L'epiteli nasal infectat per MERS-CoV indueix IFNs tipus I i III durant el pic de la infecció, els quals activen respostes immunitàries antivirals al llarg del tracte respiratori. Aquest treball evidencia que els macròfags alveolars dels camèlids poden ser importants per l'eliminació del MERS-CoV sense desencadenar respostes pro-inflamatòries. Fora el tracte respiratori, el MERS-CoV és transportat cap a òrgans limfoides secundaris, on no hi ha replicació viral *in vitro*. Els nodes limfàtics cervicals produeixen respostes immunitàries cel·lulars innates i adaptatives (p. ex., IFNs, ISGs o respostes tipus Th1) en l'exposició secundaria al MERS-CoV, però no respostes inflamatòries. Com els ratpenats, els camèlids inhibeixen la inflamació en diferents compartiments anatòmics que permeten la replicació transitòria, excreció i transmissió del MERS-CoV. A més, els dromedaris desenvolupen una immunitat adaptativa minvant que ràpidament permet la re-infecció viral. Per tant, la endemicitat del MERS-CoV en dromedaris guia l'evolució viral, mentre que els humans només són hostes terminals que pateixen la malaltia zoonòtica.

Actualment, les soques del clade B circulen per Aràbia i són introduïdes a la població humana contínuament, mentre que les del clade C són àmpliament detectades en dromedaris africans. Tot i evidències serològiques i moleculars de la infecció d'humans exposats a dromedaris africans, mai s'han descrit casos de MERS zoonòtica a l'Àfrica. Hi ha un flux comercial de dromedaris des d'Àfrica cap a l'Orient Mitjà, però els virus del clade C no es troben en la darrera regió. Aquesta tesi doctoral aporta evidències experimentals de l'excreció perllongada de virus aràbics (clade B) en camèlids, en comparació amb soques africanes (clade C). La replicació i transmissió diferencial entre soques del MERS-CoV podrien explicar la dominància del clade B a l'Orient Mitjà. Remarcablement, aquest treball recomana evitar la introducció de soques del clade B a l'Àfrica, ja que podrien desplaçar les soques del clade C i incrementar l'amenaça zoonòtica en aquest continent.

La vacunació del bestiar és l'estratègia recomanada per impedir la propagació del MERS-CoV entre animals reservori i la potencial transmissió a humans. Avui en dia no existeixen vacunes contra el MERS-CoV, encara que alguns prototips per ús humà s'estan avaluant en afers regulatoris. En aquest treball hem explorat la capacitat de dos prototips de vaccí per reduir la transmissió viral entre camèlids, utilitzant un escenari de contacte directe entre llames per simular la infecció natural per MERS-CoV. Els candidats vacunals s'han basat en la subunitat S1 o el domini d'unió a receptor (RBD) de la proteïna S, combinats amb un adjuvant registrat per ús animal. Ambdós prototips indueixen nivells alts d'anticossos neutralitzants contra MERS-CoV. L'RBD només va protegir una llama de tres vacunades. Contràriament, la vacunació S1 va proporcionar immunitat sistèmica i a la mucosa respiratòria, va protegir els animals contra la infecció per MERS-CoV i va impedir l'excreció de

virus infecciós. Els nostres estudis evidencien que la vacunació de l'espècie reservori pot ser una solució econòmica per prevenir la transmissió zoonòtica del MERS-CoV a humans.

La present tesi doctoral proporciona coneixement sobre la resistència a la malaltia causada pel MERS-CoV en camèlids reservori i proposa estratègies per prevenir la infecció zoonotica.

Resumen

El coronavirus del síndrome respiratorio del Oriente Medio (MERS-CoV) continúa causando brotes en la península arábiga. Los pacientes graves sufren una neumonía que puede resultar fatal, caracterizada por una infiltración masiva de células inmunes en los pulmones que agravan la enfermedad. Los murciélagos y los camélidos son los reservorios naturales del MERS-CoV, mientras que los dromedarios son la principal fuente de infección en humanos. Se cree que los camélidos generan una respuesta inmune oportuna para contrarrestar la infección eficazmente y prevenir el desarrollo de enfermedad respiratoria. El epitelio nasal infectado por MERS-CoV induce IFNs tipo I y III durante el pico de la infección, los cuales activan respuestas inmunes antivirales a lo largo del tracto respiratorio. Este trabajo evidencia que los macrófagos alveolares de los camélidos pueden ser importantes para la eliminación del MERS-CoV sin desencadenar respuestas proinflamatorias. Fuera del tracto respiratorio, el MERS-CoV es transportado hacia órganos linfoides secundarios, dónde no hay replicación viral *in vitro*. Los linfonódos cervicales producen respuestas inmunes celulares innatas y adaptativas (p.ej., IFNs, ISGs o respuestas tipo Th1) ante la exposición secundaria al MERS-CoV, pero no respuestas inflamatorias. Como los murciélagos, los camélidos inhiben la inflamación en diferentes compartimentos anatómicos que permiten la replicación viral transitoria, excreción y transmisión del MERS-CoV. Además, los dromedarios desarrollan una inmunidad adaptativa menguante que permite la reinfección viral rápidamente. Por lo tanto, la endemicidad del MERS-CoV en dromedarios guía la evolución viral, mientras que los humanos solamente son huéspedes terminales que sufren enfermedad zoonótica.

Actualmente, las cepas del clado B circulan por Arabia y son introducidas continuamente en la población humana, mientras que las del clado C se detectan ampliamente en dromedarios africanos. A pesar de evidencias serológicas y moleculares de la infección de humanos expuestos a dromedarios infectados, nunca se han descrito casos de MERS zoonótico en África. Existe un flujo comercial de dromedarios desde África hacía el Oriente Medio, pero los viruses del clado C no se encuentran en esta última región. La presente tesis aporta evidencias experimentales de la excreción prolongada de viruses arábigos (clado B) en comparación con cepas africanas (clado C). La replicación y transmisión diferencial entre cepas de MERS-CoV podrían explicar la dominancia del clado B en el Oriente Medio. Remarcablemente, este trabajo recomienda evitar la introducción de cepas del clado B en África, ya que podrían desplazar las cepas del e incrementar la amenaza zoonótica en el continente.

La vacunación del ganado es la estrategia recomendada para impedir la propagación del MERS-CoV entre animales reservorio y la potencial transmisión a humanos. Hoy en día no existen vacunas contra el MERS-CoV, aunque algunos prototipos para uso humanos se están evaluando en vías regulatorias. En este trabajo hemos explorado la capacidad de dos prototipos vacunales para reducir la transmisión viral entre camélidos, utilizando un escenario de contacto directo entre llamas para simular la infección natural por MERS-CoV. Los candidatos vacunales se han basado en la subunidad S1 o el dominio de unión a receptor (RBD) de la proteína S, combinados con un adyuvante registrado para uso animal. Ambos prototipos inducen niveles altos de anticuerpos neutralizantes contra MERS-CoV. El RBD sólo protegió una llama de tres vacunadas. Contrariamente, la vacunación S1 proporcionó inmunidad sistémica y mucosal, protegió los animales contra la infección por MERS-CoV e

impidió la excreción de virus infeccioso. Nuestros estudios evidencian que la vacunación del reservorio animal puede ser una solución económica para prevenir la transmisión zoonótica del MERS-CoV a humanos.

La presente tesis doctoral proporciona conocimiento sobre la resistencia a la enfermedad causada por el MERS-CoV en camélidos reservorio y propone estrategias para prevenir la infección zoonótica.

Chapter 1

General introduction

1.1 Emerging infectious diseases and zoonotic coronaviruses

The frequency of emerging and re-emerging diseases with pandemic potential has been increasing over the last decades globally, driven by different socio-economic, environmental, and ecological factors [1]. More than 60% of them are of zoonotic origin [2], firstly appearing in a naïve population or have previously existed but increasing in incidence or geographical range. Zoonotic emerging diseases are caused by pathogenic agents that are naturally transmitted from vertebrate animals to humans, or vice versa, including viruses, bacteria, parasites, fungi, and prions. They emerge unpredictably, particularly viruses, and can spread efficiently across countries. In the current globalized world, pathogens with high epidemic potential pose a health risk to humans and animals of any geographical location. Furthermore, they are of huge economic impact and their rise is expected to continue in the coming years, favoured by the current climate change crisis [3]. In absence of specific vaccines and treatments to fight against most of known zoonotic diseases, the recent pandemic H1N1 influenza and coronavirus infectious disease 2019 (COVID-19) pandemics evidenced the need to investigate, anticipate, prevent, and control emerging zoonotic diseases.

Many of the recent epidemics with high fatality rates in humans are caused by zoonotic viruses, such as filoviruses (e.g., Ebola and Marburg viruses), henipaviruses (e.g., Nipah and Hendra viruses) or coronaviruses (e.g., severe acute respiratory syndrome coronavirus [SARS-CoV] and Middle East respiratory syndrome coronavirus [MERS-CoV]). In the last two decades, three emerging coronaviruses (CoVs) crossed the species barrier to cause severe respiratory diseases and human fatalities. The capability of CoVs to jump between species is mediated by complex host-pathogen

interactions [4,5]. Bats are thought to be the origin of these CoVs, although intermediate host species have been discovered before eventual human spillover [6]. SARS, MERS and now COVID-19, it is very likely that the next CoV epidemic outbreak is only a matter of time; the challenge remains in determining when and where it will occur. Therefore, it is critical to identify and investigate reservoir hosts of CoVs, such as bats and other wildlife species or livestock, to prevent future viral introductions to the human population. Organizational issues arise once they are identified, such as monitoring their populations and understanding their overlapping niche with humans, as well as controlling and interrupting zoonotic spillover of CoVs. Moreover, reservoir species possess specific mechanisms to control CoVs infection, since they have evolved to be virus-tolerant animals [7,8]. By studying natural host-pathogen interactions occurring in reservoir hosts, we can understand unique processes leading to viral infection in the absence of clinical disease. Thereafter, the ultimate and complex obstacle would be to translate their 'tolerance' mechanisms into human medicines. Thus, exploring the source of emerging viruses and exploiting their inherent biology, according to the 'One Health 'concept, would aid in finding immunological pathways critical for the control of CoVs infections in humans.

1.2. MERS-CoV: an overview

1.2.1. Discovery and history of MERS-CoV

In 2012, a 60-year-old man hospitalized in Jeddah, Saudi Arabia, developed acute pneumonia and renal failure before dying due to multi-organ failure. The disease was caused by a previously unknown coronavirus identified in his sputum [9], which was later named Middle East

respiratory syndrome coronavirus (MERS-CoV) [10]. Phylogenetic analyses evidenced that MERS-CoV could have originated in bats [11–15]. However, dromedary camels are the main reservoir hosts of MERS-CoV [16] and the primary source of transmission to humans [17–22]. MERS-CoV actively circulates among dromedaries from the Middle East and Africa [23], where it is endemic, but primary human cases seem restricted to the Arabian Peninsula [24]. In the Middle East, zoonotic spillovers continue to cause intermittent outbreaks with potential to spread globally through sustained human-to-human transmission. As of March 2022, 2,589 infections and 893 deaths (~34.5% case-fatality rate) were reported in 27 countries [25]. MERS-CoV caused sporadic, nosocomial, and community-wide outbreaks, including travel-associated clusters of transmission. In 2015, a single infected traveller from the Middle East to the Republic of Korea caused a major outbreak of 186 cases and 38 fatalities [26], evidencing that MERS-CoV is of worldwide public health concern. Nonetheless, the Kingdom of Saudi Arabia (KSA) had the highest incidence recorded so far, with 2,184 cases and 813 deaths (~37.2% case-fatality rate) [25], and outbreaks continue to appear in Middle Eastern endemic countries. Preparedness and efforts to prevent zoonotic spillover from dromedary reservoirs and controlling human outbreaks were implemented to impede MERS-CoV spread [27,28] in the current absence of prophylactic treatments and vaccines.

1.2.2. Taxonomy and phylogeny

According to the International Committee on Taxonomy of Viruses, MERS-CoV belongs the order of Nidovirales, family Coronaviridae, subfamily Orthocoronavirinae, *Betacoronavirus* genus and *Merbecovirus* subgenus [29]. Phylogenetic studies identified three different MERS-CoV

clades identified as A, B and C [16,30,31]. Clade A strains were circulating in the Arabian Peninsula during early epidemic outbreaks but became extinct and were eventually replaced by clade B strains, which currently dominate the Middle East [16,32]. Five different lineages of clade B strains (B1 to B5) have been found in Arabian dromedaries and humans [16]. On the other hand, clade C strains were only found in African dromedary camels, and lineages from West and North Africa (C1) are distinct from those of Eastern Africa (C2) [30,33,34]. Evolutionary studies support that African and Arabian strains diverged before MERS-CoV was identified [30,33]. Furthermore, a retrospective serological study indicated that MERS-CoV has been circulating in African dromedary camels for decades at least [17,22].

1.2.3. Genome organization, replication, and viral gene expression

MERS-CoV possess a large single-stranded positive-sense RNA genome composed of ~30.1 kilobases, which contains a 5' cap structure followed by a leader sequence, ten polycistronic open-reading frames (ORFs) and a 3' poly(A) tail (**Figure 1.1a**). Two-thirds of the genome is occupied by the replicase ORF1a and ORF1b, which encode for two large polyproteins (one requires a ribosomal frame shift) that are eventually cleaved into 16 non-structural proteins (nsps) [35]. These genes code for the viral replication and transcription complex interacting with the host cellular machinery [36]. Downstream, in the remaining third of the genome, nine ORFs are found encoding for structural and accessory proteins, along with multiple stem loop structures required for RNA replication and transcription [37]. Functional transcription-regulating sequence (TRS) motifs, AU-rich motif of ~10 nucleotides, are found adjacent to the 5' leader sequence (TRS-L) and upstream to most ORF [38].

A full-length negative-sense RNA genome copy is generated during viral genomic replication, which work as a template for the synthesis of new positive-sense RNA genomic copies. Concomitantly, a discontinuous viral transcription occurs during the synthesis of the negative-sense RNA strand. The replication and transcription can be interrupted upon encounter of TRS and is resumed at the TRS-L, generating nested subgenomic RNAs (sgRNAs) containing the genomic 3' and 5' co-terminal ends [38,39]. Eight different MERS-CoV sgRNAs are produced from negative-strand RNA templates [40], as shown in **Figure 1.1b**. Structural and accessory genes are translated from sgRNA. Accessory proteins are not essential for MERS-CoV replication or transcription, although some have crucial roles in viral pathogenesis by inhibiting innate immune responses [41–45].

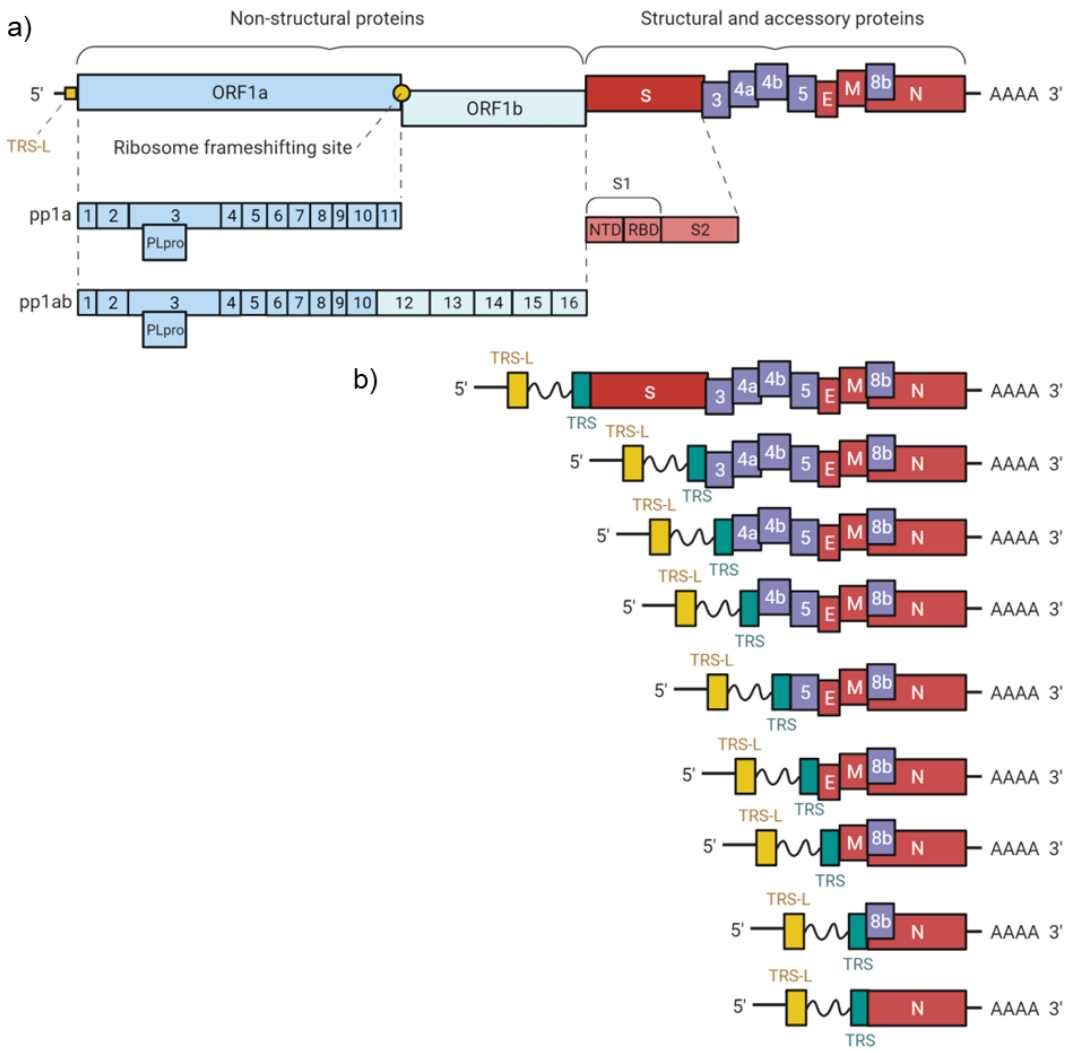

Figure 1.1. Genomic organization of MERS-CoV and subgenomes generated during viral replication. (a) A structural scheme of the single-stranded, positive sense MERS-CoV RNA genome is shown. A leader transcription-regulatory sequence (TRS) and a ribosomal frame shift are shown in yellow (square and circle, respectively). The genomic arrangement of the 16 non-structural proteins encoded by ORF1a and ORF1b are displayed in blue colors. The genomic layout of the S protein is shown in light red, including the S1 (and its subdomains) and S2 subunits. (b) The MERS-CoV subgenomic RNAs formed during viral replication are schematically represented. During viral replication, subgenomic RNAs are generated by TRS-L (yellow) joining with TRS sequences (green) found upstream each open reading frame. Created with BioRender.com. E, envelope gene; M, membrane gene; N, nucleoprotein gene; NTD, N-terminal

domain; ORF, open reading frame; PLpro, Papain-like protease; pp, polyprotein; RBD, receptor-binding domain; S, spike gene; TRS-L, leader transcription-regulatory sequence.

1.2.4. Virion structure

MERS-CoV virions are spherical particles of ~80 nm in diameter surrounded by a 'corona' or spike peplomers emanating from the viral surface [46]. Virions are composed of four structural proteins encoded by the viral genome: spike (S), envelope (E), membrane (M) and nucleocapsid (N) proteins. Each protein plays a key role in assembling the viral particle, as represented in **Figure 1.2a**. The S is a transmembrane trimeric glycoprotein expressed on the surface of the viral envelope, which has critical roles in binding, fusion, and entry into host cells. The E and M proteins form the viral core and shape the virion, besides being involved in essential functions, such as intracellular trafficking, viral assembly, or virus budding. The N protein constitutes a helical protein that binds genomic RNA molecules and allow their packaging inside the assembled virus progeny [37,42].

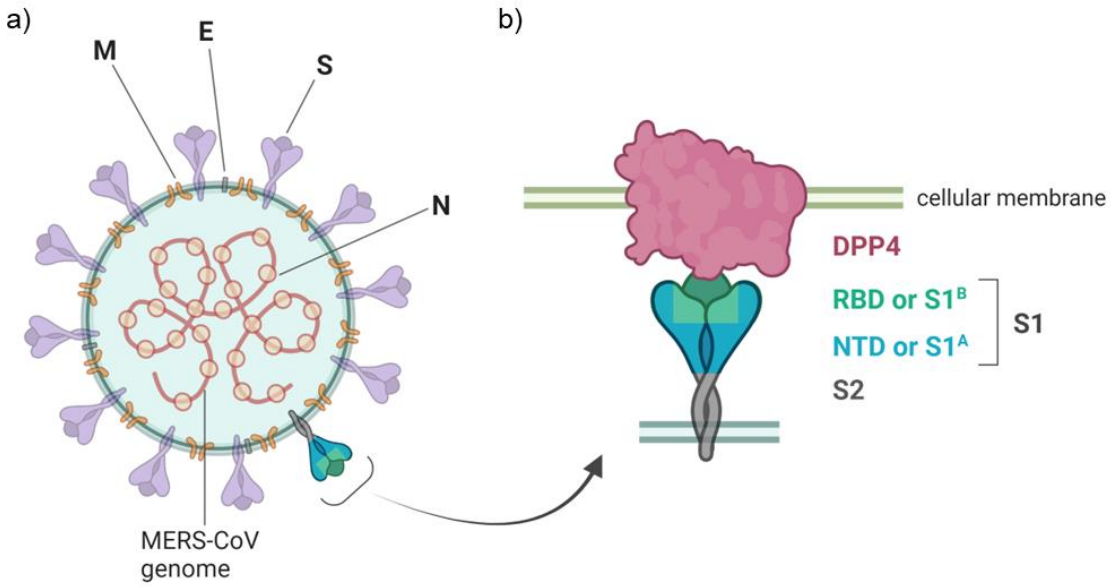

Figure 1.2. MERS-CoV virion structure and spike (S) protein interaction with dipeptidyl peptidase 4 (DPP4) receptor. (a) MERS-CoV is a spherical enveloped virus that contains a single-stranded, positive-sense RNA genome. Viral particles consist of four structural proteins: the S, envelope (E) and membrane (M) proteins confer its characteristic crown shape, while the nucleocapsid (N) proteins packs the RNA genome inside the virion. (b) The infectivity of MERS-CoV is mediated by the S protein interaction with the cellular receptor DPP4 expressed in target cells. The S protein located on the virion surface consists of the S1 and S2 subunits. The $S1^A$ subdomain (green) facilitates viral attachment to sialoglycans found on the host cell surface, and the $S1^B$ subdomain (blue) mediates the binding to the DPP4 (red). Subsequently, the S2 subunit (grey) allows viral and cellular membrane fusion and viral genome release into the cytoplasm. Created with BioRender.com. NTD, N-terminal domain; RBD, receptor-binding domain.

1.2.5. Replication cycle

The attachment of MERS-CoV to the host cell is mediated by interactions of the S protein and the dipeptidyl-peptidase 4 (DPP4, also called CD26), its cellular receptor [47]. DPP4 is a cellular membrane-bound exoprotease found in a variety of tissues and cell types that cleaves a wide range of substrates including growth factors, chemokines, neuropeptides, vasoactive peptides, and glucose metabolism hormones [48–50]. The S protein

located on the virion surface consists of two subunits, the S1 and S2 (**Figure 1.2b**). The N-terminal domain of S1 (or $S1^A$) binds to sialic acids (α2,3- and, to a lesser extent, α2,6-linked sialoglycans) found on mucins of the host cell surface and enhances infection by facilitating viral attachment [51–53]. The C-terminal part of S1 (or $S1^B$) contains the receptor-binding domain (RBD; aa residues 358–588) that binds the DPP4 receptor expressed by target cells [47,54]. Indeed, molecular studies revealed that the RBD of MERS-CoV is composed of a core subdomain and a receptor-binding motif (RBM) that mediate DPP4 receptor recognition [55]. The S2 subunit contains an internal fusion peptide and two heptad repeat (HR1 and HR2) regions that allow viral fusion to the cellular membrane [56–59]. After attachment of the RBD to DPP4, an essential step for MERS-CoV entry requires the activation of the S protein by TMPRSS2 or endosomal cathepsins [60,61]. Their proteolytical cleavage activates the S protein and separates the RBD and S2 domains. Then, the S2 subunit undergoes structural changes that enable viral and cellular membrane fusion [59,62], eventually releasing the viral RNA into the cytoplasm.

Thus, MERS-CoV S protein interaction with DPP4 at the cellular surface is the primary determinant of viral infection. Therefore, receptor binding competence determines host species range and tissue tropism. MERS-CoV RBD can bind DPP4 from several animal species beside humans, such as non-human primates (NHP), camelids, bats, and less efficiently, pigs and rabbits [63–70]. Key aa residues of DPP4 restrict species susceptibility [71–73]; for instance, wild-type mice, golden Syrian hamsters and ferrets are resistant to MERS-CoV infection [71,74,75]. Different DPP4 distribution in tissues govern MERS-CoV pathogenicity and transmission capacity in susceptible species [76].

The genome released into the cytosol directly acts as a template for mRNA translation of the replicase and other accessory genes (ORF1a and ORF1b), due to the 5' cap structure along with a 3' poly(A) tail. Among others, nsps remodel cell membranes derived from the rough endoplasmic reticulum (RER) to form double-membrane vesicle (DMV) structures, which shelter and support viral RNA replication and translation [36,77–80]. Viral genomic and subgenomic mRNAs are exported to the cytoplasm through transmembrane pores found in DMVs [78,81]. S, M and E structural viral proteins are mainly expressed at the RER and progress to the endoplasmic reticulum-Golgi intermediate compartment (ERGIC) [37,82,83]. RNA genomes are encapsidated by the N protein, which bud into the ERGIC membranes containing MERS-CoV structural proteins, assembling new virions [37,77,82]. Finally, progeny viruses are transported to the host cell surface via exocytosis and released to the extracellular space [37,77].

1.3. Epidemiology and geographical distribution

Bats are known reservoirs of many viruses, including betacoronaviruses [84]. Some hypotheses point to bats as the potential origin of MERS-CoV. Phylogenetic studies showed that MERS-CoV is genetically close to Bat CoVs HKU4 and HKU5 detected in insectivorous bats [85]. MERS-related CoVs (MERSr-CoVs) have been identified in African, Asian, Eurasian, and American bats [12,13,86–90]. Moreover, a study in the KSA found a fragment of RNA (190 nucleotides) in Taphozous bats with 100% identity to a MERS-CoV strain infecting humans [13]. Nonetheless, to date, the primary origin of MERS-CoV is not well understood and no data supports bats as the primary source of viral spillover.

Intermediate species are often involved in the spillover of emerging viruses from bats to humans [91,92]. Thus, after the emergence of MERS-CoV, scientists focused on seroepidemiological studies of livestock commonly found in the Middle East and East Africa, such as sheep, cows, goats, and dromedary camels [21,93–96]. High levels of neutralizing antibodies (nAbs) to MERS-CoV were found in dromedaries as opposed to other species [21]. Subsequent analyses revealed high seroprevalences in dromedary camels from many countries of the Middle East and Africa [17,18,101–110,21,111–114,94–100]. Antibodies to MERS-CoV were detected in sera from dromedary camels dating back to 1983 [22], suggesting that MERS-CoV has been circulating in dromedaries for at least 40 years. Seroprevalence was higher in aged dromedaries of, in big-sized herds, and in those populations mixed with individuals from other geographical origins compared to locally bred herds [23]. Also, the sub-national camel seroprevalence appears larger in the Arabian Peninsula in comparison to that of African countries [23]. Serological evidence of infection, but not active MERS-CoV circulation, has been found in other camelid species (llamas and alpacas) in the Middle East [115,116]. Serological surveys in camelids of other geographical regions (Australia, Canada, Germany, Japan, Kazakhstan, Mongolia, the Netherlands, or the USA) resulted in the absence of antibodies to MERS-CoV [21,104,108,117,118].

Active MERS-CoV infection has also been studied extensively in dromedary camels from Africa and the Middle East through the detection of viral RNA in oro-nasal samples [16,94,106,111–113,119–124,97,125,126,98–103,105]. MERS-CoV is commonly detected infecting dromedaries from these regions, and some seasonality studies showed higher RNA prevalence during the first semester of the year [16,23,119,120,124,125,127]. Higher incidence and viral loads were found in juvenile animals compared to adults

[23,98,106,112,128,129]. Importantly, most dromedary camels clear the MERS-CoV RNA shedding within two weeks after the detection onset (ranging from 7 to 45 days); however, evidence of reinfection has been observed in the field [23,120–122,130–133]. Indeed, epidemiological and phylogenetic studies revealed that African and Arabian dromedaries sustain the circulation of the different MERS-CoV lineages (see *section 1.2.2*). MERS-CoV clade B and C viruses are endemic among Arabian and African dromedaries, respectively. Movement of Arabian camels is limited to the Peninsula [134], but there is an important unilateral trade from the Horn of Africa to the Arabian Peninsula [33,135]. Intriguingly, African MERS-CoV strains have not been established in the Middle East so far, as they are rapidly outcompeted by Arabian clade B lineages [16,33,135].

Dromedary camels are not only the main reservoir for MERS-CoV, but they have also transmitted the infection to humans [19,105,130,136]. The simultaneous isolation of identical MERS-CoV strains infecting dromedaries and human contacts evidenced that MERS-CoV did not require specific mutations to jump between hosts [19]. Furthermore, previous studies found that occupational exposure to dromedary camels significantly increased the prevalence of MERS-CoV antibodies in these people compared with the general population [137,138]. Nonetheless, the routes of animal-to-human transmission are not yet clearly identified [134,139–141].

All human MERS-CoV infections reported during the last two years (July 2020 – present) were primary cases, with more than 60% of them being previously exposed to camels [126]. Therefore, people who have been in close contact with dromedary camels are considered a major source of secondary transmission events [130]. As of March 2022, the World Health

Organization (WHO) reported ~25% of primary and ~39% of secondary human cases, while the type of the remaining infections is unknown or no data is available [25]. All primary infections occurred in the Middle East, being the KSA the most affected country. Secondary cases have also been described occasionally among humans in close contact, including travel-associated outbreaks that have spread the virus in 27 countries [25]. Males account for most diagnosed cases. Furthermore, people aged 50–59 have been at the highest risk of contracting MERS-CoV infection as primary cases, while those aged 30–39 were mostly linked to secondary cases [25]. Human-to-human transmission mainly occurred in household [142–146] and nosocomial scenarios [147–154]. Large outbreaks took place in health-care facilities from, the United Arab Emirates (UAE) [153,155], Saudi Arabia [148,151,156,157] and South Korea [158–160], linked to overcrowded emergency departments, poor infection control practices, aerosol-generating procedures/nebulized medications, continuous positive pressure ventilation, cardiopulmonary resuscitation and/or superspreading events [161]. Up to five generations of MERS-CoV transmission have been reported among health-care workers [152,154]. Those who used a protective face mask (N95) were less prone to be infected with MERS-CoV compared to employees who sporadically or never wore it [162]. Asymptomatic health-care workers can spread the virus to their contacts [154,163], and their role in MERS-CoV transmission warrants further investigation. In addition, MERS-CoV environmental stability is also favoured under hospital settings, which prolong the risk for MERS-CoV acquisition in humans through fomite transmission [164]. The precise mode of human-to-human transmission is not defined yet, but MERS-CoV does not seem to be transmitted efficiently unless the contact is close [144,161,165,166]. Overall, the reproduction number of MERS-CoV during nosocomial outbreaks (R_0 of

2–5) seems higher than in other transmission scenarios ($R_0 < 1$) [144,167]. Gratefully, improvement of infection control measures has limited sustained transmission in hospitals and the recent outbreaks have been contained [161,168].

Importantly, phylodynamic modelling analyses revealed that long-term evolution of MERS-CoV is driven by dromedary camels, while infected humans are only transient dead-end hosts [127]. Indeed, recent studies indicate that MERS-CoV lineages with increased replicative fitness and higher pandemic potential are currently circulating in the Middle East [32,169]. Thus, stronger investments in vigilance programs to prevent zoonotic MERS-CoV introductions from dromedary camels are required. Spillover events might be abated by stronger surveillance of dromedary populations, restriction of camel movement in affected areas or the development of animal vaccines that curtail MERS-CoV transmission [170].

1.4. MERS-CoV infection and disease

1.4.1. MERS-CoV infection in humans

The clinical presentation of MERS is very variable. The median incubation period of MERS-CoV and the interval between onset of symptoms in successive transmission events are ~5 and ~7 days, respectively [148]. Symptoms range from absent to flu-like (cough, fever, chills, sore throat, headache, tiredness, and myalgia), shortness of breath, pneumonia, or acute respiratory distress syndrome [147,148,151,171–175]. MERS-CoV infections can also cause acute renal failure and gastrointestinal symptoms, such as abdominal pain, vomiting, and diarrhoea [9,151,173,176]. Normally, patients with dyspnoea develop severe pneumonia and require admission to intensive care unit [177]. Chest radiography and computed tomography

studies showed that mild to severe pulmonary consolidation are common features of MERS patients [173,178]. Mild to severe haematological abnormalities have also been described, as lymphopenia or thrombocytopenia [147,173]. From the age of 50 onwards, the risk of developing severe MERS and dying increases significantly [25]. Patients over 80 years-old have extremely high likelihood of succumbing because of the disease [179]. Pre-existence of comorbidities such as asthma, diabetes, renal or cardiac diseases, obesity, and hypertension, have been described as significant risk factors for severe MERS development [173,179–184]. Two studies support that acute MERS survivors experience a higher degree of pulmonary dysfunction up to 2 years after recovery, compared to those with absent or mild pneumonia [185,186]. Another common sequel is the emotional damage caused by psychological trauma after being critically ill [185].

MERS-CoV pathogenesis studies have been impaired by the limited number of patient autopsies, which have not been performed generally due to religious and cultural Islamic traditions or to prevent health-care worker contamination. Only two autopsies of MERS patients have been reported to date [187,188]. The first histopathological examination reported diffuse alveolar damage (DAD) and acute kidney injury, together with the co-localization of DPP4 and MERS-CoV antigens in pneumocytes and syncytial cells [188]. Also, lesser number of lymphoid follicles and a polymorphic population of reactive lymphocytes have been described in different lymph nodes (LN) [188]. The second study also showed focal haemorrhagic necrotising pneumonia with exudative DAD and acute kidney injury, as well as evidence of extrapulmonary viral particles detected by electron microscopy [187]. MERS-CoV-like structures were localised in pneumocytes, lung macrophages, renal epithelial cells and

macrophages infiltrating the skeletal muscles [187]. Both studies reported remarkable infiltration of leukocytes, including neutrophils, macrophages, $CD4^+$ and $CD8^+$ T lymphocytes [187,188]. This massive infiltration of immune cells into the lungs is associated with the production of a cytokine storm that exacerbates disease during late stages of infection [189,190].

Other studies focused on the distribution of the molecules that facilitate viral infection along the respiratory tract to better understand the pathogenesis of MERS-CoV. In that respect, α2,3-sialic acids and DPP4 are expressed in lower respiratory tract (LRT) airways and alveoli of humans, while DPP4 is less abundant in the upper respiratory tract (URT) [66,191,192]. These findings could explain why MERS-CoV is detected in the URT only at early stages of infection [176,193,194]. Relative low abundance of DPP4 in the URT may limit viral shedding and human-to-human transmission. At the cellular level, DPP4 expression has been identified in non-ciliated bronchial epithelial cells, type I and II pneumocytes, alveolar macrophages, endothelial cells, and some immune cell subsets, such as T, B, and natural killer (NK) cells [50,195]. Indeed, MERS-CoV was shown to infe¡ct some these target cells *in vitro* and *ex vivo* [196–202], implying that their functions may be impaired during a natural infection. Besides, DPP4 is also expressed on epithelial cells from other organs, such as kidney, intestine, liver, thymus, and bone marrow [48,49].

1.4.2. MERS-CoV infection in dromedary camels

MERS-CoV infection in dromedary camels is generally subclinical. These reservoir hosts are asymptomatic or merely display mild nasal discharge before viral clearance [141]. Although most infections are asymptomatic, muco-purulent nasal discharges, lacrimation, sneezing, coughing, fever, and loss of appetite have been described in the field in few animals

[100,124,130,131,133,136,203,204]. According to some reports [124,133], calves exhibit clinical signs more frequently than adults, but it is not clear if these symptoms could be associated to other concomitant pathologies (i.e., bacterial infections). There are only two limited histopathological studies on naturally infected dromedaries [204,205]. In Saudi Arabia, dromedary camels were screened for the presence of MERS-CoV in nasal swabs, resulting in a 41% positivity rate. Three individuals under two years of age carried high viral loads, so they were selected for histopathological analyses after regular slaughtering procedures for meat production. Importantly, antemortem examinations did not show respiratory clinical signs, or only mild rhinorrhoea in few animals, which breathed normally. However, dromedaries had some discrete lesions along the respiratory tract. Exfoliation and loss of cilia were observed in URT airways, as well as mild hyperplasia and infiltration of immune cells [204,205]. Also, typical features of interstitial pneumonia were described, such as mild thickening of alveolar septa, type II pneumocyte hyperplasia or the infiltration of alveolar macrophages [204,205]. Other mild changes were found in kidney and spleen [204]. S and N antigens of MERS-CoV were detected in epithelial cells from nasal turbinates, trachea, bronchi, alveoli, and kidney [204]. Moreover, viral labelling and lesions localized in tissues with abundant expression of DPP4 [66,206], which might explain the pathogenesis described in these organs under natural conditions.

On the other hand, MERS-CoV pathogenesis has been assessed in experimentally infected dromedary camels [141,207–210]. Mild-to-moderate rhinitis, tracheitis and bronchitis were observed after intranasal viral challenge but were resolved before 42 days post MERS-CoV inoculation (dpi) [207–210]. Importantly, although loss of cilia was noticed in respiratory epithelial layers of experimentally inoculated dromedaries, only limited

cell death or other histopathological alterations were observed. Lesions and mononuclear leukocyte infiltrations in the nose, trachea and bronchi airways [210] were like those observed in natural infections, but pneumonia was not developed upon viral inoculation [207]. Consistently, MERS-CoV antigen was found in respiratory epithelial cells, with particularly high levels of antigen in the nose epithelium, and rarely in macrophages at the nasal submucosa, but not in the alveoli [141,207,208,210]. In one animal, infectious virus was isolated from the upper right lung lobe at 5 dpi; however, it did not developed pneumonia [208]. Moreover, viral antigen and infectious MERS-CoV were detected in dendritic-like cells within secondary lymphoid organs, such as tonsils, cervical, retropharyngeal, or mediastinal LN [207,208,210]. These lymphoid tissues did not show other morphological changes than a follicular hyperplasia seen during standard antigenic presentation processes.

1.4.3. MERS-CoV infection in bats

MERS-CoV-like viruses have been found in different bat species (detailed in *section 1.3*), but the pathogenesis and clinical progression of infection in the wild are unknown. Although no specific bat species has been proposed as the original reservoir of MERS-CoV, Jamaican fruit bats (*Artibeus jamaicensis*) have been experimentally infected to understand their role as potential MERS-CoV reservoirs [211]. Bats were susceptible to MERS-CoV infection and shed viral RNA, but did not display clinical signs of apparent disease. Histopathological analyses revealed mild lesions in the respiratory tract, including mild rhinitis or interstitial pneumonia with minimal septa thickening by macrophages or neutrophils. Active MERS-CoV replication, antigen and infectious virus was detected mainly in respiratory tissues, although viral RNA was also detected to a lesser

extent in other organs, such as brain, liver, heart, spleen, bladder, duodenum colon or blood [211]. By 28 dpi, bats had cleared MERS-CoV infection. This study supports the hypothesis of a bat species being the ancestral reservoir host for MERS-CoV.

1.5. Animal models for human infection

The development of animal models to mimic the infection experienced by humans and dromedary camels has been crucial to investigate MERS-CoV pathogenesis and transmission, as well as to evaluate prophylactic and therapeutic treatments. The capacity of the S protein to bind key residues of DPP4 orthologs is the primary determinant of species susceptibility to MERS-CoV. Some small laboratory animals and domestic livestock, such as wild-type mouse, golden Syrian hamster, ferret, sheep, or horse, are not permissive to MERS-CoV infection [65,71,74,75]. The impossibility of MERS-CoV S protein to recognize and bind DPP4 of these species could be attributed to different factors, including differences in DPP4 tissular distribution, structure and/or posttranslational modifications [65,212].

1.5.1. Macaques

MERS-CoV infection of rhesus macaques (*Macaca mulatta*) and cynomolgus macaques (*Macaca fascicularis*) caused a rapid development of mild-to-moderate pneumonia, with transient MERS-CoV replication restricted to the LRT [213–216]. At 2 dpi, rhesus macaques increased body temperatures and displayed mild respiratory clinical signs, such as cough or changes in breathing rate. Transient increase in total leukocytes and neutrophiles, as well as decrease in lymphocyte counts in blood, were observed at 1-2 dpi but already returned to normal levels at 3 dpi [213]. Chest radiography and pathological examinations indicated lung consolidations

and the development of pneumonia from 3 dpi onwards. Microscopic examination revealed interstitial pneumonia characterized by thickened alveolar wall by inflammatory cells, oedema, fibrin deposition, hyaline membrane formation, haemorrhages, type II pneumocyte hyperplasia, and degeneration of bronchial epithelial cells and pneumocytes [213,215]. MERS-CoV RNA and antigen were largely restricted to the LRT and were specifically found in type I and II pneumocytes and alveolar macrophages, which expressed the DPP4 receptor [213,215,217,218]. Viral RNA was also detected in secondary lymphoid organs draining the respiratory tract but not in other tissues. Viral loads peaked early in lungs and subsequently decreased over time [213]. On the other hand, cynomolgus macaques did not experience overt clinical signs of disease, while virological and histopathological findings were similar to those described above for rhesus macaques [216]. Altogether, the macaque models reproduce mild-to-moderate features of human MERS-CoV infection but fail to recapitulate the acute pneumonia observed in severe or fatal disease.

1.5.2. Common marmoset

Common marmosets (*Callithrix jacchus*) inoculated with MERS-CoV developed mild-to-severe pneumonia [217–223]. Animals displayed respiratory clinical signs, as increased breathing rates, loss of appetite or decreased activity levels [217–219]. In one study, few animals were euthanized after exhibiting humanitarian endpoint clinical signs, such as failure to move after prompting, oral bleeding or severe hypothermia [219]. Animals developed bronchopneumonia with severe airway lesions, including degeneration of bronchial epithelial cells and pneumocytes, oedema, fibrin, haemorrhages and infiltration of neutrophils and other inflammatory cell types. Similar to the macaque model, the highest

MERS-CoV RNA and antigen loads were found in DPP4-expressing bronchial epithelial cells, type I and II pneumocytes and alveolar macrophages [217–220]. Viral RNA was also found at lower levels in oro-nasal swabs, blood, the URT, lymphoid tissues and other internal organs [219]. Overall, common marmosets infected with MERS-CoV developed a more severe pneumonia than macaques and could be useful models to mimic moderate-to-severe disease in humans. They also served as useful models to evaluate the efficacy of therapeutic compounds [222,223].

1.5.3. New Zealand white rabbit

New Zealand white rabbits experience an asymptomatic infection after MERS-CoV inoculation [70,224]. According to the DPP4 distribution [191,224], MERS-CoV replicated in upper and lower respiratory airways and was shed at low levels, but it was not transmitted to co-housed sentinels [70,224]. Gross lesions were not observed. At 3-4 dpi, mild rhinitis with epithelial necrosis and regeneration was observed, while lung lesions were absent or mild, characterized by mildly thickened alveolar septa by inflammatory cells, mild hypertrophy of type II pneumocytes and accumulation of alveolar macrophages [70,225]. In addition, rabbits developed non-neutralizing antibodies against MERS-CoV, which did not protect against re-infection and exacerbated lung inflammation [225]. Although rabbit infection did not recapitulate important clinical symptoms or histopathological changes observed in MERS patients, this small animal model could be useful to potentially screen the efficacy of prophylactic or therapeutic compounds [226].

1.5.4. hDPP4 transgenic/transduced mice

After the emergence of MERS-CoV, there was a need for small laboratory animals to facilitate the study of MERS-CoV pathogenesis and the evaluation of vaccine candidates and therapeutic drugs. However, wild type laboratory mice were not susceptible or did not develop features of severe MERS [75]. Therefore, different strategies were used to transform mice into a susceptible species, based on the heterologous expression of the human DPP4 (hDPP4). The first models were generated by intranasal transduction of a non-replicating adenovirus vector expressing the hDPP4 in different mice backgrounds [227]. These animals showed a broad expression of hDPP4 in epithelial cells and alveoli of the LRT. After challenge, MERS-CoV replicated in the lungs of all transduced animals, which did not display respiratory clinical signs except loss of weight in aged mice; animals exhibited interstitial pneumonia. No mortality was observed, and the virus was then cleared by 6–8 and 10–14 dpi in young and aged mice, respectively. The hDPP4-transduced mouse model could be used to study mild transient disease without clinical symptoms. Nonetheless, the model appears interesting because MERS-CoV infection can be produced in various mouse strains deficient in genes involved in pathways important for virus replication. Indeed, hDPP4 transduction was exploited in immunodeficient knockout mice to understand key components for viral clearance, pointing the role of innate and adaptive immunity in MERS-CoV pathogenesis [227]. However, expression of hDPP4 in transduced mice is only transient, limiting the use of such technology.

Furthermore, transgenic mouse models expressing the hDPP4 were generated [228–231]. Firstly, models expressing hDPP4 under the control of β-actin or cytokeratine 18 promoters were generated, which conferred

expression of the receptor in all tissues studied, such as lung, intestine, liver, kidney, spleen, heart, or brain, resulting in high susceptibility to MERS-CoV [228,230]. After challenge, hDPP4 transgenic mice displayed severe clinical signs, including ruffled fur, lethargy, hypothermia, immobility, but did not sneeze or cough. Moreover, animals progressively lost weight and 100% mortality was achieved by 6-7 dpi [228,230]. Transgenic mice developed early pneumonia with infiltration of macrophages and lymphocytes, and a fatal encephalitis [228,230]. No other histopathological changes were seen in other organs. High MERS-CoV loads were found in the lung and brain at 2 and 4-6 dpi, respectively, and to a lesser extent in other organs, indicative of a systemic infection [228,230]. These animal models of MERS-CoV, suffering from high lethality due to abnormal hDPP4 distribution, do not completely resemble infection in humans, but they provide a useful platform for testing vaccine prototypes and antiviral drugs.

On the other hand, a knock-in approach was used to replace the mouse (mDPP4) for the hDPP4 coding sequence, which maintained regulated expression of hDPP4 as it happens in the native mice [231]. After inoculation, these animals were asymptomatic but developed interstitial bronchopneumonia, while high titres of MERS-CoV replicating in lungs were determined at 4 dpi. Indeed, hDPP4 was found in club cells, type II pneumocytes and alveolar macrophages [231]. This knock-in mice only developed a mild MERS-CoV infection and, thus, they are not appropriate to simulate the disease observed in human patients. Nonetheless, this is a more physiologically relevant model that could be a useful tool for preclinical evaluation of MERS-CoV vaccine candidates and treatments.

1.6. Subclinical infections in camelid species

Understanding MERS-CoV infection in the highly susceptible natural reservoir host could lead to new insights into disease prevention or reveal key aspects of virus ecology and transmission. Experiments with dromedary camels are expensive and require complex biosafety level 3 (BSL-3) facilities for large animals. In addition to being big-size and dangerous irritable animals that difficult their handling, animal caretakers are exposed to a high biosafety risk [232]. In fact, camelid experimentation with MERS-CoV was only performed in three biocontainment units worldwide: the Australian Animal Health Laboratory (AAHL) of the Commonwealth Scientific and Industrial Research Organisation (CSIRO), the Animal Disease Laboratory at Colorado State University (CSU), and the Animal Health Research Center (CReSA) of the Institute of Agrifood Research and Technology (IRTA).

1.6.1. Bactrian camel

The susceptibility of Bactrian camels (*Camelus bactrianus*) to MERS-CoV was suspected since its DPP4 receptor is 98.3% similar to that of dromedary camels, also, RBM sequences are identical in both species [233]. After experimental inoculation, Bactrian camels only displayed mild respiratory clinical signs (nasal discharge or cough) and developed a transient URT infection. Only mild epithelial degeneration was observed in the URT, as well as lymphocytic sinusitis, rhinitis and tracheitis. Viral RNA was detected along the respiratory tract, but MERS-CoV antigen and infectious virus was only found in URT samples. Importantly, these animals shed abundant quantities of infectious MERS-CoV for a week after challenge, in similar levels to those observed in dromedary camels

[233]. Despite Bactrian and dromedary camels reproduce a comparable experimental infection, they are also similar in size and behaviour, making their use as animal models complicated. Additionally, this study also highlighted the importance of preventing MERS-CoV spread to western Asia, where geographical ranges of both *Camelus* species overlap.

1.6.2. New World camelids: llamas and alpacas

Evidence of natural MERS-CoV infection of llamas and alpacas was reported in the Middle East [115,116], and their susceptibility to the virus was confirmed experimentally [8,32,65,209,234,235]. When inoculated intranasally, nasal discharge was frequently reported in llamas [65] but rarely in alpacas [8,32,209,234,235]. Gross lesions were not observed in New World camelid species. Histopathological analyses revealed mild rhinitis with segmented hyperplasia or squamous metaplasia of the nasal epithelium and mild infiltration of mononuclear cells into the respiratory mucosa and submucosa and, very mildly, in lungs; no other lesions were observed [8,32,65,234]. Also, DPP4 is abundantly expressed in the upper and lower respiratory tracts of llamas and alpacas, following a similar distribution to that of dromedary camels [8,65,66]. MERS-CoV replicated extensively in epithelial cells from the URT [8,32,65,234] but only to a limited extent in the LRT and the infection was quickly cleared [8,32]. After MERS-CoV infection, respiratory epithelial cells from llamas and alpacas did not experience cilia loss as observed in dromedary camels [8,210,236]. Both species shed high amounts of infectious MERS-CoV for a week after inoculation, resembling the viral excretion kinetics observed after experimental infection of Old World camelids [65,141,207,208,233–235]. However, llamas and alpacas generally shed two-log-lower titres of infectious MERS-CoV compared to Old World camelids [65,141,207,208,233–235]. Alpacas

can transmit the virus to naïve contact animals [234], but MERS-CoV transmission among llamas have not been studied. Overall, llamas and alpacas inoculated with MERS-CoV had a similar URT infection outcome, viral shedding kinetics and clinicopathological features to those of experimentally inoculated dromedaries. Since New World camelid species are more commercially available, have smaller size and gentler behaviour than dromedary camels, they are considered useful surrogate models to study MERS-CoV infection and pathogenesis as occurs in the natural reservoir host. Since vaccination of dromedary camels is considered a realistic strategy to reduce MERS-CoV spillover to humans [170,237], llamas and alpacas are valuable models for vaccine efficacy studies and determination of antiviral immune mechanisms under controlled conditions [8,232]. Still, both animal models are also quite costly and require complex BSL-3 animal facilities.

1.7. Innate and Adaptive immune responses to MERS-CoV

1.7.1. Immune responses in humans infected with MERS-CoV

Human infections with MERS-CoV display a broad spectrum of immune responses that have been associated with disease severity outcome [190,238,239]. Innate immune data on asymptomatic infections is not available. Limited studies performed in patients with mild disease suggested that these individuals have lower immune cell counts with low levels of pro-inflammatory cytokines in sera or blood [190,239]. Contrarily, an increased number of leukocytes that infiltrate into the lungs has been identified as a hallmark of severe MERS. These cells produce a dysregulated pro-inflammatory cytokine storm that exacerbates lung injury during the later stage of infection [189,190,239,240]. Previous studies also indicated a positive

correlation between pro-inflammatory cytokine levels in blood or plasma (such as IL-6, IL-8, IL-17 and IL-1β) and disease severity [190,239].

During early stages of the infection, MERS-CoV primarily targets respiratory epithelial cells [196,241–243], where innate immune responses are initiated. Infections performed *ex vivo* and *in vitro* unravelled that viral replication in epithelial cells did not result in the induction antiviral cytokines, such as type I and III interferons (IFNs), but in a delayed and marked induction of pro-inflammatory cytokines, including IL-1β, IL-6 or IL-8 [196,241,242,244]. Based on these studies, there is a consensus that type I and III IFN responses are dampened on human respiratory epithelial cells upon MERS-CoV infection, but the chemotactic responses could explain the recruitment of immune cell subsets into the respiratory tract.

The role of different immune cell populations in the development of pulmonary inflammatory cytokine storms has been investigated [197]. Although MERS-CoV replication in human plasmacytoid dendritic cells (pDCs) was inefficient, *in vitro* infection resulted in high production of type I and III IFNs [199]. Productive MERS-CoV replication was reported in monocyte-derived macrophages (MDMs) and monocyte-derived dendritic cells (MDDCs) [200–202,245]. None of these myeloid cells triggered antiviral responses (type I and III IFNs) but MDMs induced high and persistent pro-inflammatory responses, including the expression of IL-6, IL-8, TNF-α, CCL2, CCL3 or CCL5 [199–202,245]. Therefore, infected macrophages play a key role in the development of a harmful cytokine storm that exacerbates pulmonary damage (**Figure 1.3a**). However, *in vitro* infection of lung alveolar or tissue resident macrophages has not been performed so far. Moreover, viral infection of antigen-presenting cells might impair antigen presentation processes and subsequent development of T-cell responses.

Expression of major histocompatibility complex class I (MHC-I) and class II (MHC-II) and lymphocyte co-stimulatory molecules were induced in both myeloid cell types, MDDCs and MDMs, upon *in vitro* MERS-CoV infection [201,245]. Moreover, T lymphocytes are susceptible to MERS-CoV infection, but the virus does not replicate productively; instead, these cells engage apoptotic pathways [198]. Altogether, these findings might explain the severe lymphopenia and a pronounced delay of Th1 and Th2 responses observed in MERS patients [147,173,189].

Convalescent patients develop adaptive immune responses to MERS-CoV. Previous studies described that recovered individuals efficiently developed $CD4^+$, $CD8^+$ T cells and nAbs to MERS-CoV [246,247]. Importantly, virus-specific $CD8^+$ T lymphocytes were also elicited by all MERS survivors, including those without nAbs responses [246]. In addition, levels of T-cell and nAbs responses positively correlated with the severity of infection [246,247]. Recent studies demonstrated the persistence of multifunctional memory $CD4^+$ and $CD8^+$ T-cells and nAbs in blood for up to 5 years after infection, regardless of the clinical severity that patients experienced [248,249]. Approximately half of the subjects had binding and neutralizing antibodies to the MERS-CoV S protein (S1 subunit) in sera, but a decrease in seropositivity affecting particularly nAbs was observed from the fourth year after infection onwards [249]. Also, memory T-cell responses were positively correlated with antibody responses during the first 3-4 years after infection [248]. Moreover, both memory $CD4^+$ and $CD8^+$ T-cell subsets maintained functionality against the different structural viral proteins (E, M, N and, to a lesser extent, S) during the period of the study [248]. Thus, recovered patients elicited strong and durable protective immune responses that would prevent the development of severe disease in a secondary MERS-CoV infection. However, cases of MERS-CoV re-

infection during the epidemic peak have not been documented and given the current low prevalence of the disease, issues on duration of immunity in humans might be difficult to assess.

1.7.2. Immune responses in animal models for human disease

Animal studies corroborated some of the immunological findings identified in humans. According to the mild and transient infection experienced by Rhesus macaques, rapid but self-limiting innate immune responses were noticed [213]. Antiviral, inflammatory, and chemotactic responses were elicited in lesions of infected lungs at 3 dpi but returned to basal levels earlier than 6 dpi. Mild pro-inflammatory responses were only observed at 1 dpi in PBMCs and sera of Rhesus macaques. Thus, this NHP model only recapitulate some immunological features of mild disease in humans. In that respect, common marmosets display a more severe disease but also failed to recapitulate aberrant and dysregulated immune responses observed in acute MERS patients. Despite the mild-to-severe pulmonary pathology, this model mounted robust innate and adaptive antiviral immunity upon MERS-CoV infection, evidenced by the induction of genes involved in pattern recognition receptors (PRRs), interferon-stimulated genes (ISGs), inflammatory cytokines, antigen presentation, lymphocyte stimulation, immunoglobulin (Ig) production or T-cell co-stimulatory molecules [219]. Hence, NHP models might be useful to study some immunological processes occurring upon MERS-CoV infection but do not reproduce aberrant and delayed immunity observed in severe MERS patients [221]. Importantly, treatment of Rhesus macaques with IFN-α2b and ribavirin reduced viral replication along the respiratory tract and improved the clinical outcome of infection [214]. In comparison to infected controls, treated animals expressed higher levels of antiviral innate immune genes,

such as type I and III IFNs, PRRs, or ISGs, and downregulated pro-inflammatory cytokines in the lungs. This study support that an early induction of type I IFNs after infection modulates the host innate immune response and improves clinical outcome [214].

Mice models expressing the hDPP4 were also used to study immune features of MERS-CoV infection. Transduction of immunodeficient mice with the hDPP4 unravelled crucial elements for viral clearance [227]. Viral persistence in lungs was reported in T-cell but not B-cell deficient mice, evidencing that T lymphocyte responses play a major role in MERS-CoV clearance. Also, viral clearance was delayed in the lungs of hDPP4-transduced mice with impaired toll-like receptor (TLR) and IFN signalling pathways, suggesting that these pathways are required to control MERS-CoV infection. Indeed, like Rhesus macaques treated with IFN-α2b [214], MERS-CoV was cleared faster in lungs of hDPP4-transduced mice administrated with polyI:C (TLR-3 agonist) or IFN-β [227]. Furthermore, a recent study used a hDPP4 knock-in mouse model to understand the protective role of alveolar macrophages to a mouse-adapted MERS-CoV [250]. The depletion of alveolar macrophages significantly increased lung injury and mortality in this model, indicating that they aid in viral clearance and lesion healing [250]. On the other hand, cytokine expression profiles were studied in two distinct transgenic hDPP4 mice models suffering from a systemic MERS-CoV infection and dying due to acute encephalitis [228,230]. Both transgenic mice rapidly responded with a marked peak of antiviral innate immune responses at the lung, including type I, II and III IFNs, PRRs, ISGs and pro-inflammatory cytokines, which waned over time. However, except for IFNs, higher magnitudes of the same cytokines found in lungs were detected in brain during later infection stages (4-6 dpi) [228,230]. Characterizing innate immune responses in these

models may be useful to better evaluate the efficacy of antiviral or anti-inflammatory treatments, but hDPP4-transgenic mice models suffering acute encephalitis poorly reproduce pathophysiological features of human disease. Moreover, whether murine and human genomic responses to inflammatory conditions may not be completely comparable is still debatable [251,252].

1.7.3. Immune responses in camelids

Camelids are highly adapted to harsh environmental conditions and do not show signs of disease after infection with a variety of pathogens. This could be attributed to unusual features of their immune systems. The diversity of host receptors specialized in the recognition of pathogen antigens have been associated with the capability to generate immune responses [253–255]. Besides conventional heterotetrameric antibodies, camelids also possess non-conventional dimeric IgG antibodies that lack light chain and constant region CH1 of the heavy chain [256], which are known as heavy-chain only antibodies (HCAbs). HCAbs also occur naturally in some cartilaginous fish species [257,258]. These smaller immunoglobulins can penetrate and bind to smaller antigens that conventional antibodies cannot recognize and have been exploited for diagnostic and therapeutic purposes [259–261]. Recent immunogenetic studies described the polymorphism of important camelid antigenic receptor genes, such as MHC-I and MHC-II, αβ and γδ T-cell receptors, and NK cell receptors [262]. Camelids have lower MHC gene polymorphism compared to other mammalian species [263–265]. Also, as members of Artiodactyla order, camelids exhibit a higher frequency and a wider distribution of γδ T cells compared to other mammalian species, including humans [266]. Nonetheless, camels display lower variability of γδ T cell

variable region genes, which results in a limited γδ T-cell repertoire [267]. Further diversification of γδ receptors is acquired by somatic hypermutation, a unique feature of cartilaginous fishes and camelids, which is thought to confer a more rapid adaptation to pathogen infections and changing environments [268–271]. Instead, diversity of αβ T-cell receptors genes is similar that described in pigs and ruminants, and αβ T-cell receptor variability occurs through classical somatic recombination [262,265]. A lower polymorphism of Ig-like receptors genes was also found on NK cells of camels compared to other mammals [272]. Overall, the reduced diversity of MHC and antigen recognition receptors suggest that other immunological mechanisms govern the high resistance of camelids to infectious diseases.

A previous work associated the polymorphism of some genes to MERS-CoV infection in dromedary camels [273]. Nonetheless, innate immune responses to natural MERS-CoV infection in dromedary camels have not been reported. The subclinical infection occurring in camelid species is characterized by transient MERS-CoV replication throughout the respiratory tract, with particularly high titres in the nasal cavity. The importance of local innate immune responses to control MERS-CoV infection has been previously hypothesized using an alpaca model [8,32]. After experimental infection, nasal epithelial cells infected with MERS-CoV induced robust type I and III IFN responses overlapping with the viral load peak in the URT [8]. IFN responses were not detected in non-infected nasal epithelia or infected trachea and lungs. Concomitantly, the expression of ISGs was moderate-to-highly upregulated in infected and non-infected nasal epithelial cells, their underlying nasal submucosa, trachea, and lungs. Thus, type I and III IFNs produced by nasal epithelial cells seem to promote the expression of a large array of ISGs along the

respiratory tract via paracrine and endocrine signalling, probably allowing for rapid viral clearance in tissues [8]. Importantly, despite abundance of DPP4 in alpaca lung, only low levels of infectious MERS-CoV were detected in this organ before rapid clearance, supporting the hypothesis that type I and III IFNs act in an endocrine manner to limit viral spread. Alternatively, epithelial cells from the LRT could be refractory to MERS-CoV productive infection.

During the peak of MERS-CoV infection, pro-inflammatory processes were dampened [8]. Significant induction of the anti-inflammatory IL-10 cytokine mRNA but downregulated expression of pro-inflammatory cytokines (i.e., IL-1β, IL-6 and IL-8), CARD9 (an activator of the nuclear factor κB or NF-κB), and some NLRP3 inflammasome components (NLRP3 and PYCARD) occurred in nasal tissues with high MERS-CoV replication and mild infiltration of lymphocytes and macrophages. Similar responses were found in nasal submucosa, where infiltration of leukocytes was more pronounced. Inflammatory responses were also downregulated in the trachea, while only a mild induction of pro-inflammatory cytokines was described in lungs of alpacas [8]. Also, the induction of CCL2 and CCL3 chemokines positively correlated with a mild and transient infiltration of mononuclear leukocytes in infected lungs [8]. The transcription factor IRF5, which is an important marker for M1 macrophage activation [274,275], remained in baseline levels during the infection. Altogether, these data provided insights on how camelids control inflammation in response to MERS-CoV, avoiding a pro-inflammatory cytokine storm and disease exacerbation.

Overall, strong induction of type I and III IFNs and moderate up-regulation of IL-10 at the nasal mucosa concomitant to the peak of MERS-CoV

replication, together with a dampened inflammation in respiratory tissues, are essential features characterizing a subclinical infection (**Figure 1.3b**). We also confirmed very similar qualitative and temporal similar innate immune responses to infections with a MERS-CoV clade A strain and another B strain defective in the accessory protein ORF4a [32]. In contrast to humans but like bats [7,211], camelids could be considered 'tolerant' species to MERS-CoV since high viral replication and shedding occur in these reservoir host without suffering clinical disease. Further studies would be needed to comprehend the precise mechanism underlying the fine-tune control of inflammation in viral infected tissues.

In terms of adaptive immunity, camelids develop protective humoral immune responses to MERS-CoV after natural and experimental infection [65,115,116,208,234,235]. The high prevalence of nAbs found in sera of dromedary camels from the Arabian Peninsula and African countries [23,110] evidenced that camelids mount efficient B lymphocyte responses. Therefore, successful viral antigen presentation and efficient development of specific T- and B-cell responses are thought to occur in camelids. Nonetheless, despite being important drivers of MERS-CoV clearance, cellular responses elicited by camelid reservoir species have not been studied. The endemicity of MERS-CoV in dromedary camels, as well as the re-infection of seropositive animals [23], suggest that adaptive immune responses could play a role in host disease resistance without interrupting viral circulation within dromedary populations.

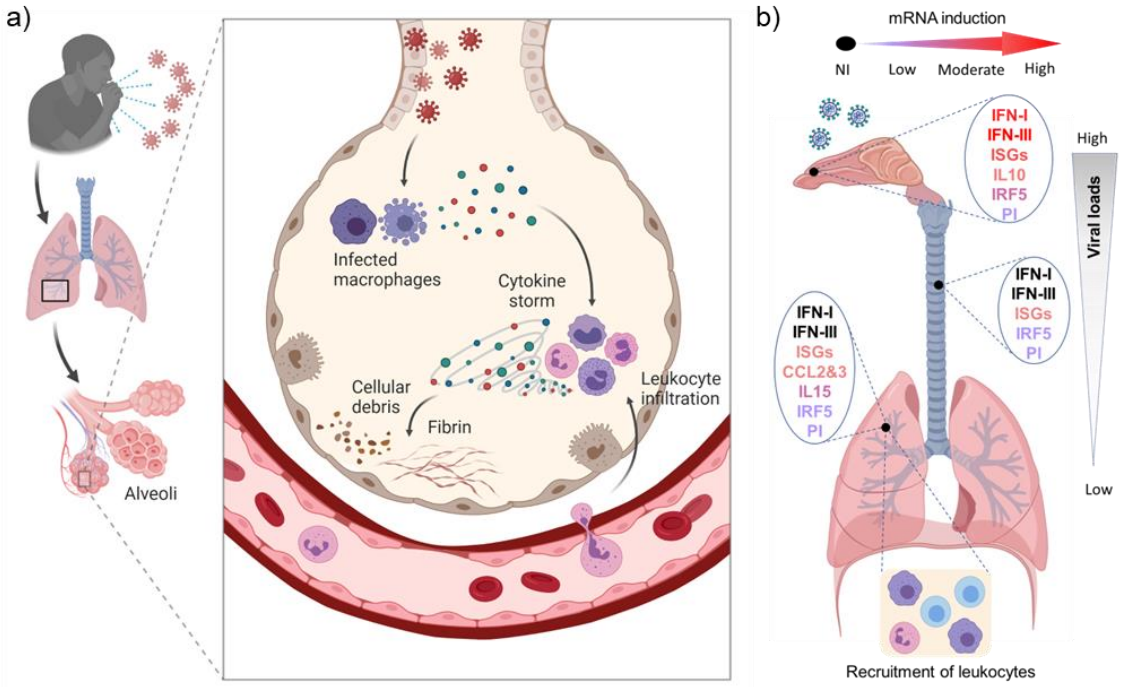

Figure 1.3. Immunopathological processes occurring after MERS-CoV infection in humans and camelids. (a) Severe MERS is characterized by disproportioned infiltration of leukocytes into the lungs of patients. These cells produce high levels of pro-inflammatory responses that exacerbate lung injury; this process is also known as inflammatory cytokine storm. MERS-CoV replicates in airway epithelial cells, which produce inflammatory cytokines and initiate the recruitment of inflammatory cells to the infection site. When viral particles reach alveoli, alveolar macrophages are infected and concomitantly induce dysregulated levels of pro-inflammatory cytokines. Chemotactic cytokine signalling leads to the recruitment of leukocytes from the bloodstream into the lungs, which contribute into the pro-inflammatory response loop and exacerbate lung lesions. Alveolar wall inflammation and lung oedema, reduce the respiratory capacity and cause severe hypoxia in human patients. Created with BioRender.com. Schematic representation shown in panel (b) was retrieved and modified from Te et al., 2021 [8]. (b) Concomitant with the peak of MERS-CoV infection in camelids, nasal epithelial cells induce robust type I and III IFN responses, ISGs, as well as anti-inflammatory IL-10 cytokine upregulation and down-regulated expression of pro-inflammatory cytokines (PI). IFN responses were not detected in infected trachea and lungs, but the expression of ISGs was significantly upregulated through a hypothetical paracrine/endocrine signalling. Inflammatory responses were lowered in the trachea. Only a mild induction of PI occurs in camelid lungs, concomitant with the induction of CCL2 and CCL3

chemokines and a mild infiltration of mononuclear immune cells. The IRF5 gene (a marker for inflammatory M1 macrophages) remained at basal levels in lungs along the infection, thus, evidencing that inflammatory processes were controlled in camelids reservoir species. NI, not induced; PI, Pro-inflammatory cytokines.

1.7.4. Immune responses in bats

Although bats have been related with the origin of MERS-CoV, studies on bat immunity upon natural infection with MERS-CoV-like viruses are lacking. A previous experimental study showed that Jamaican fruit bats (*Artibeus jamaicensis*) were infected and shed MERS-CoV without showing clinical signs of apparent disease [211]. Bats mainly replicated MERS-CoV in the respiratory tract but only suffered minimal histopathological changes in airway tissues. Analyses of gene expression revealed that bats rapidly induced a moderate peak of *MX1*, *ISG56* and *RANTES* in lungs, which gradually decreased over time. Indeed, another study showed that activation of IRF3 signalling and type I IFN inhibited MERS-CoV replication in bat Efk3 cells [276]. These results support that early induction of antiviral responses, such as IFNs and ISGs, in bats are key features to resolve MERS-CoV infection. Moreover, other studies revealed that bats possess unique first line defences, since their innate immune system can express high constitutive levels of IFNs, ISGs, TLR7 or autophagy genes [7,277,278], thus, enhancing host defence to viral infections.

Other *in vitro* works provided insights into inflammatory responses elicited by bats upon viral infection to understand why these reservoir species do not develop clinical signs of disease. Bats possess a repressor (C-Rel) for NF-κB transcription that inhibits the expression of downstream pro-inflammatory cytokines, such as TNF-α, IL-1β, IL-8 or IL-6 [279]. In addition, a dampened NLPR3 is described in bats, which impairs the

production of mature IL-1β [7,280]. This was also observed in PBMCs from bats (*Pteropus Alecto*), which did not produce of IL-1β after infection with MERS-CoV as opposed to human cells [280]. Thus, bats possess unique mechanisms to supress inflammation and prevent underlying pathology.

Limited studies on adaptive immune responses of bats have been performed due to a lack of reagents and experimental models. Some works have characterized bat immune cell subsets but there are no studies on cellular adaptive immunity in response to a specific pathogen. Nonetheless, there is a consensus that bats produce little or no humoral response to viral infections, which tends to wane quickly [281]. In accordance, only one out of six inoculated Jamaican fruit bats seroconverted and generated nAbs to MERS-CoV at 14 dpi [211]. Hence, these findings suggest that bats control MERS-CoV and other viruses with mechanisms independent from humoral immunity.

Similar to camelid species, prompt IFNs and ISGs engagement together with dampened inflammatory responses are key features contributing to viral tolerance of bats. Their innate immunological characteristics allow many viruses to persist and spread.

1.8. MERS-CoV vaccine candidates for humans and animal reservoirs

Lessons learned from previous travel-associated outbreaks [26] evidenced that the ongoing MERS-CoV outbreaks in the Middle East pose a worldwide public health threat. To date, there are no licensed vaccines or prophylactic treatments available to prevent MERS-CoV infection in humans. Nonetheless, prevention strategies have been implemented [28] and

several vaccine prototypes have been developed, some of which are under regulatory pathways.

1.8.1. MERS-CoV S protein: a key target for vaccine development

The S and N proteins are the most immunogenic MERS-CoV proteins, being the S protein the primary determinant of protective immunity [282]. Therefore, the design of vaccine candidates against MERS-CoV mainly rely on the S protein or its subdomains. The S1 subunit, which contains the N-terminal domain and the RBD that mediates viral infection, is the main target for inducing high levels of nAbs and protective responses [283–285]. The RBD is the target for most nAbs and a solid immune response against this subdomain can provide protection against MERS-CoV [285–288]. However, antibodies targeting the N-terminal domain, which mediates viral attachment to the host cell, can also provide protection against MERS-CoV in animal models [51,288]. Thus, the S protein and its subdomains are the main choice for developing effective vaccines against MERS-CoV.

1.8.2. MERS-CoV vaccine prototypes

Vaccine prototypes have been developed using different delivery platforms, such as DNA, RNA or protein-based, nanoparticle, virus-like particle (VLP), viral vector-based, live-attenuated, and inactivated vaccines [285,289–291]. Most of these vaccine candidates conferred protection to MERS-CoV-inoculated animals (hDPP4-expressing mice, New Zealand white rabbits, NHP, dromedary camels or alpacas) [285,289–291], although only some of them have been evaluated in phase I human clinical trials (GLS-5300, ChAdOx1 MERS, MVA-MERS-S and BVRS-GamVac-Combi) [292–294]. **Table 1.1** provides an updated summary of developed vaccine prototypes as well as their efficacy in animal models or

humans. All vaccination strategies have the potential to be effective for human and animal use, although each vaccine type has certain limitations that must be considered. Live-attenuated vaccines generally confer great protection but might be subjected to the reversion to a virulent phenotype or the recombination with wild-type viruses infecting the immunized individual [295–298]. The reassortment likelihood of a MERS-CoV live-attenuated vaccine with other circulating MERS-CoV-like viruses is low but could be decreased further by deleting accessory proteins that increase viral replication fitness [299]. Also, pre-existing immunity to viral vectors could reduce the efficacy of vector-based vaccines [300–303]. DNA-based vaccines frequently induce low immune responses in large animals, including humans [304,305]. Recently, mRNA-based vaccines have been designed to counteract MERS-CoV [289], but no pre-clinical efficacy studies have been conducted so far. On the other hand, the use of MERS-CoV whole-inactivated and recombinant protein-based vaccines generally require the use of adjuvants to enhance immune responses [209,306]. The adjuvant of choice can substantially influence the development of key mucosal and systemic protective immunity against CoVs [307].

Furthermore, the development of vaccine prototypes for human use is highly dependent on the availability of animal models. Previously developed animal models failed to recapitulate features of severe immunopathology observed in humans. Although the common marmoset model recapitulates a more severe infection [219], vaccine efficacy studies have not been performed in this model (**Table 1.1**). Therefore, the currently available animal models have hampered the evaluation of MERS-CoV vaccine candidates. Importantly, to date, no vaccine-associated enhancement of disease has been observed among the evaluated MERS vaccine prototypes in animal models [308].

Table1.1. Developed MERS-CoV vaccine prototypes grouped by delivery platform. Adaptive immune responses and protection efficacy in animal models or humans are shown. Humoral response indicates antibody responses generated against MERS-CoV, being nAbs in most cases. Cell-mediated responses denote viral-specific T-cell activation after immunization, such as IFN-γ production.

Vaccine Prototype	Humoral Responses	Cell-Mediated Responses	Protection	Clinical Trial	Reference
Whole inactivated					
Formaldehyde inactivated	Mouse	–	Mouse	–	[309]
UV irradiation	–	–	Mouse	–	[310]
Gamma irradiation	Mouse	Mouse	Mouse	–	[311]
Live attenuated					
rMERS-ΔE	–	–	Mouse	–	[41]
rMERS-Δ[3,4a,4b,5,E]	Mouse	–	Mouse	–	[299]
MERS-dNSP16	Mouse	–	Mouse	–	[312]
MERS-dORF3-5	Mouse	–	Mouse	–	[45]
Viral Vector or VLP					
VRP-S	Mouse	–	–	–	[282]
VRP-N	–	Mouse	Mouse	–	[313]
MVA-MERS-S	Mouse, Human, Dromedary camel	Mouse, Human	Mouse, Dromedary camel	Phase I	[207,294,314,315]
Ad5-S or Ad5-S1	Mouse	Mouse	–	–	[316,317]
Ad5-S*	Mouse	Mouse	Mouse	–	[318]
rAd5-S1 or rAd5-S1-CD40L	Mouse	–	Mouse	–	[319]
rAd/Spike rAd/NTD or rAd/RBD	Mouse	Mouse	Mouse	–	[320]
Ad41-S	Mouse	Mouse	–	–	[317]
BVRS-GamVac-Combi (Ad26/Ad5)	Mouse, Common marmoset	Mouse	Mouse	Phase I/II	[321]
PIV5/MERS-S	Mouse	Mouse	Mouse	–	[310]

ChAdOx1 MERS	Mouse, Rhesus macaque, Human, Dromedary camel	Mouse, Human	Mouse, Rhesus macaque, Dromedary camel	Phase I	[203,293,322–324]
MVvac2-S	Mouse	Mouse	Mouse	–	[325]
rLa-MERS-S	Mouse, Bactrian Camel	–	–	–	[326]
VSV-S	Mouse, Rhesus macaque	Rhesus macaque	–	–	[327]
RABV G-MERS-CoV S1	Mouse	–	Mouse	–	[328]
RV/MERS	Mouse	Mouse	–	–	[329]
RVΔP-MERS/S1	Mouse	–	–	–	[330]
cVLP MERS-S	Mouse	–	–	–	[331]
VLP (S,E,M)	Rhesus macaque	Rhesus macaque	–	–	[332]
VLP (RBD+VP2)	Mouse	Mouse	–	–	[333]
DNA					
GLS-5300	Mouse, Rhesus macaque, Human, Dromedary camel	Mouse, Rhesus macaque, Human	Rhesus macaque	Phase I/II	[292,334,335]
VRC8400-S[#]	Mouse, Rhesus macaque	–	Rhesus macaque	–	[284]
pcDNA3.1-S or pcDNA3.1-S1	Mouse	Mouse	Mouse	–	[336,337]
pSΔER or pSΔTM[+]	Mouse	Mouse	Mouse	–	[338]
AcHERV-MERS-S or AcHERV-MERS-S1	Mouse	Mouse	Mouse	–	[339]
MVA-MERS-N	–	Mouse	–	–	[340]
RNA					
RBD-mRNA	Mouse	Mouse	–	–	[289]
Recombinant protein					

S-2P	Mouse	–	–	–	[341]
NTD	Mouse	Mouse	Mouse	–	[342]
LV-MS1-Fc	Mouse	–	Mouse	–	[343]
S1	Dromedary camel, Alpaca	–	Dromedary camel, Alpaca	–	[209]
RBD	Mouse, Rabbit, Rhesus macaque	Mouse, Rhesus macaque	Mouse, Rhesus macaque	–	[54,283,306,344–347]
RBD-Fd	Mouse	–	Mouse	–	[287]
S RBD-HBD 2	Mouse	–	Mouse	–	[348]
MSPS-RBD	Rabbit	–	Rabbit	–	[226]
RBD-NP (cdGMP)	Mouse	Mouse	Mouse	–	[349]
S nanoparticles	Mouse	Mouse	Mouse	–	[318,350,351]

S, Spike protein; N, Nucleocapsid protein; RBD, receptor-binding domain; NTD, N-terminal domain; S1, Spike protein subdomain S1; E: Envelope protein; M, Membrane protein. # with S1 protein booster; * with S nanoparticles booster; + with S protein booster.

1.8.3. Target populations for vaccines

Following vaccine development, it is crucial to identify and preferentially immunize the population at higher risk of MERS-CoV infection and severe disease development. People frequently in-contact with dromedary camels and health-care workers are the most exposed to MERS-CoV, while people with pre-existing medical comorbidities or advanced age are at higher risk of developing severe MERS [161]. Particularly, immunization of camel handlers, their close contacts, and medical personnel could help preventing local or community MERS-CoV outbreaks. Moreover, as recommended by the WHO, the FAO, and the WOAH [170], vaccination of dromedary camels should be considered as the preferred option to prevent primary human cases. Developing animal vaccines could be more economical and have a faster licensing pathway than vaccines for human use [237]. Indeed,

some vaccine prototypes provided systemic and mucosal immunity in dromedary camels, as well as reduced MERS-CoV shedding upon infection [203,207,209]. Nonetheless, none of these vaccine candidates completely blocked MERS-CoV excretion in these animals and viral transmission among dromedaries could potentially occur. Thus, developing a vaccine that provides long-term mucosal immunity and curtails MERS-CoV transmission among dromedary reservoirs can be a feasible and economic solution to prevent zoonotic spillover to human population.

Chapter 2

Hypothesis and objectives

2.1. Hypothesis

Severe MERS in humans is characterized by an increased number of leukocytes that infiltrate into the lungs and produce a pro-inflammatory cytokine storm at later stages of infection [189,190,239,240]. Specifically, infected macrophages induce dysregulated pro-inflammatory responses that exacerbate lung pathology [200–202]. Contrarily, it is known that bats and camelid reservoir species induce strong antiviral responses (IFNs and ISGs) and balanced inflammatory responses to resolve MERS-CoV infection [8,211,276,280]. Although the key immunological mechanism conferring tolerance to MERS-CoV replication without suffering clinical disease remains to be elucidated in camelids, it was hypothesized that these species control inflammation and virus spread in anatomical sites important for MERS-CoV pathogenesis, such as lungs or draining lymph nodes. Indeed, the exact contribution of alveolar macrophages in virus clearance and the factors determining innate and adaptive immune responses in lymph nodes remain elusive. In that respect, the development of specific reagents for camelid species would significantly help elucidating innate and adaptive immune responses of reservoir hosts controlling MERS-CoV infection.

On the other hand, studying MERS-CoV transmission in reservoir hosts could provide new insights into viral ecology, epidemiology, and disease prevention. The challenging work with infected dromedary camels under BSL-3 conditions evidenced the need for alternative animal models [232]. In that respect, llamas and alpacas reproduce a similar MERS-CoV infection outcome than dromedary camels, therefore, they have been proposed as valuable surrogates for basic and translational research [141]. MERS-CoV can be transmitted between alpacas, but transmission among llamas has

not been determined. Moreover, an in-contact transmission model of camelids would represent a good animal model for vaccine efficacy studies because of mimicking natural transmission in the natural reservoir, the dromedary camel.

Finally, the vaccination of dromedary reservoir is advised for preventing MERS-CoV transmission to humans [170]. Despite the current vaccine candidates could reduce but not completely eliminate MERS-CoV shedding in dromedary camels [203,207,209], it was hypothesized that a vaccine providing strong immunity should be able to block MERS-CoV transmission among camelids and, thus, prevent zoonotic transmission to humans.

2.2. Objectives

1. To set up a llama direct-contact transmission model that mimics natural infection conditions, useful for assessing differential transmission of currently circulating MERS-CoV (clade B and C) strains and evaluating the efficacy of vaccine candidates under controlled conditions.

2. To design a comprehensive set of primers for quantifying camelid innate and adaptive immune responses at the transcriptomic level, as well as to optimize and validate their use in myeloid and lymphoid cells.

3. To determine whether MERS-CoV replicates in key immunological compartments of camelids, such as alveolar macrophages and lymph nodes, and to elucidate their contribution to viral clearance and disease resistance.

4. To investigate the efficacy of an RBD-based and a recombinant S1-based vaccines, using a registered adjuvant, to block MERS-CoV transmission among llamas as surrogates for dromedary camels in view of reducing zoonotic spillover.

Chapter 3

Experimental transmission of a MERS-CoV clade B strain (Qatar15/2015) among llamas

---

Chapter published as a part (I) of the article:

Rodon, J., Okba, N., Te, N., van Dieren, B., Bosch, B. J., Bensaid, A., Segalés, J., Haagmans, B. L., & Vergara-Alert, J. (2019). Blocking transmission of Middle East respiratory syndrome coronavirus (MERS-CoV) in llamas by vaccination with a recombinant spike protein. *Emerging Microbes & Infections*, *8*(1), 1593–1603. DOI: 10.1080/22221751.2019.1685912

3.1 Introduction

The dromedary camel is the main reservoir for MERS-CoV and plays a key role in the infection of primary human cases [16,352]. In New World camelid species, MERS-CoV infection in the field was evidenced by the presence of MERS-CoV nAbs [115,116]. Furthermore, MERS-CoV experimental infections in alpacas and llamas confirmed that both could serve as potential reservoirs [65,234,235]. Therefore, understanding MERS-CoV transmission in camelid reservoir hosts could provide new insights into epidemiological aspects useful for measuring virus spread within these species and disease prevention in humans.

Due to the high lethality rates in humans (~36%) and the absence of MERS-CoV-licensed vaccines or treatments, MERS-CoV has been prioritized for research and product development in the WHO R&D Blueprint for Action to Prevent Epidemics [170,237]. The WHO has suggested animal vaccination as the best strategy to control MERS-CoV infections, since reduction of virus shedding can potentially prevent both animal-to-animal and zoonotic transmissions, and might have a faster development and licensing pathway compared to human vaccination [237].

Dromedaries are large, dangerous, and irritable animals that are difficult to handle. Controlled experiments with MERS-CoV in this species are costly and require large animal BSL-3 facilities [232]. Instead, New World camelids are more commercially available and smaller in size. Llamas and alpacas experience a similar URT infection than dromedary camels [8,65,141], so they can be considered valuable animal models to understand MERS-CoV infection and pathogenesis. They might also be useful models for assessing differential MERS-CoV strain transmission and vaccine efficacy

studies under controlled conditions. It is known that alpacas can transmit the virus to in-contact sentinels [234], but MERS-CoV transmission among llamas has not been described.

In the present study, we used a MERS-CoV clade B strain to show efficient transmission among llamas in a direct-contact model.

3.2 Materials and methods

Animal welfare and ethics

Experiments with MERS-CoV were performed at the BSL-3 facilities of the Biocontainment Unit of IRTA-CReSA (Barcelona, Spain). The present study was approved by the Ethical and Animal Welfare Committee of IRTA (CEEA-IRTA) and by the Ethical Commission of Animal Experimentation of the Autonomous Government of Catalonia (file No. FUE-2017-00561265).

Cell culture and MERS-CoV

Vero E6 cells were cultured in Dulbecco's modified Eagle medium, DMEM (Lonza) supplemented with 2% fetal calf serum (FCS; EuroClone), 100 U/mL penicillin (ThermoFisher Scientific, Life Technologies), 100 µg/mL streptomycin (ThermoFisher Scientific, Life Technologies), and 2 mM glutamine (ThermoFisher Scientific, Life Technologies). A passage 2 MERS-CoV stock (Qatar15/2015 strain) was propagated in Vero cells at 37ºC in a CO_2 incubator for 3 days. The infectious virus titer was determined in Vero cells and calculated by determining the dilution that caused cytopathic effect (CPE) in 50% of the inoculated cell cultures (50% tissue culture infectious dose endpoint, $TCID_{50}$).

Experimental design

A group of llamas (n=3) were intranasally inoculated with a 10^7 $TCID_{50}$ dose of MERS-CoV Qatar15/2015 strain (GenBank Accesion No. MK280984) in 3 mL saline solution (1.5 mL in each nostril) using a nebulization device (LMA® MADgic®, Teleflex Inc.). At 2 dpi, naïve llamas (n=5) were put in contact with infected llamas (**Figure 3.1** and **Figure 3.2**). The experimental box was set up as in a previous transmission study performed in pigs [353].

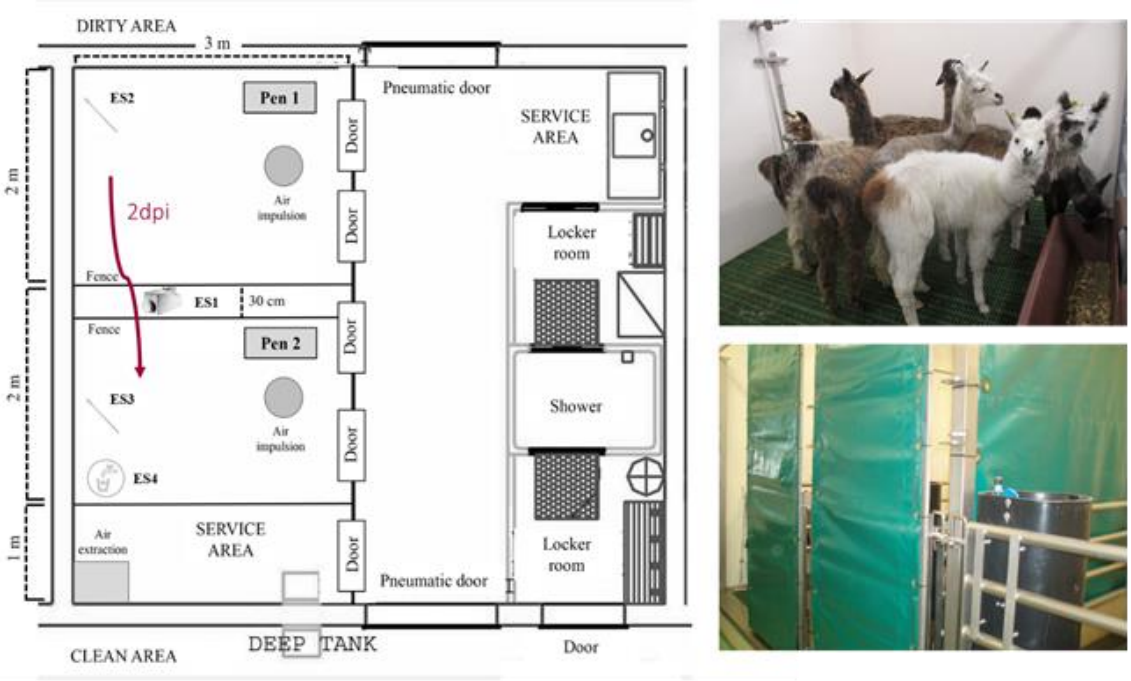

Figure 3.1. Schematic representation of an experimental animal box. Contact and inoculated groups were placed in pens 1 and 2, respectively. Tarpaulin was used to prevent contact between groups during 2 days after inoculation.

Regarding to the nomenclature used in this study, animals 1-3 corresponded to intranasally inoculated llamas. Llamas 4-8 were naïve contact animals.

Animals were monitored daily for clinical signs (sneezing, coughing, nasal discharge, or dyspnea). Rectal temperatures were recorded with a fast display digital thermometer (AccuVet®) until day 13 post-inoculation. Nasal swabs (NS) were obtained daily until day 14 pi. Serum samples were obtained prior to challenge, and weekly after the MERS-CoV challenge. Animals were euthanized 3-weeks after challenge, with an overdose of pentobarbital. An extra sampling of NS was performed prior to necropsy procedures.

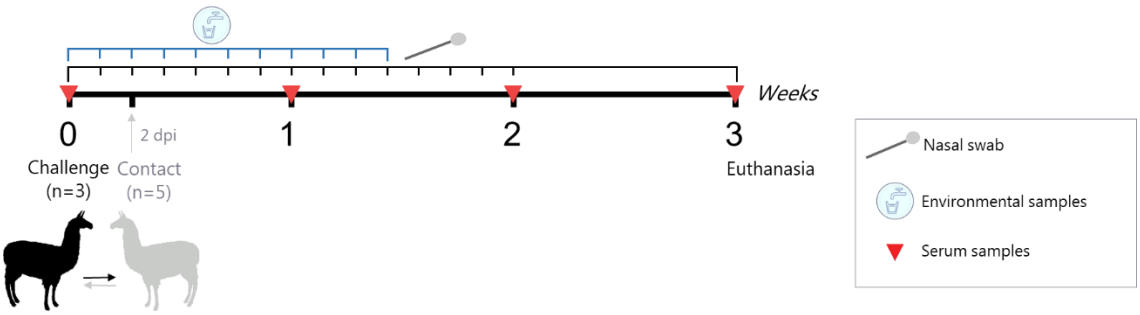

Figure 3.2. Schematic diagram of the llama transmission study. Three llamas (black, LL1-3) were intranasally inoculated with MERS-CoV (Qatar15/2015) and two days later were brought in contact with five naïve llamas (grey, LL4-8). Dpi, days post-inoculation.

Environmental samples

Three different types of environmental samples (ES) were collected to determine viral loads in the boxes throughout the study (**Figure 3.1**), as previously described [353]. An air filtering device (Sartorius MD8, Sartorius Stedim) was used for testing one thousand litres of air during 20 min (50 L/min air volume) through a gelatine membrane filter (ES1). One wall was scrubbed with two swabs (ES2 and ES3) and a water sample from the drinking point (ES4) was also obtained. ES were collected daily until 10 dpi.

Viral RNA detection by RT-qPCR

Viral RNA in collected samples was detected by RT-qPCR as previously described [65,353]. Briefly, NS and ES, except water samples, were transferred into cryotubes containing either 500 µL DMEM (Lonza) or PBS (Lonza) supplemented with 100 U/mL penicillin (ThermoFisher Scientific, Life Technologies) and 100 µg/mL streptomycin (ThermoFisher Scientific, Life Technologies), vortexed and stored at -80°C until use. Water samples were directly frozen at -80°C instead. Viral RNA from NS and ES was extracted with a NucleoSpin® RNA virus kit (Macherey-Nagel) following the manufacturer's instructions. The RNA extracts were tested by using the UpE PCR [354]. RT-qPCR was carried out using AgPath-ID™ One-Step RT-PCR Reagents (Applied Biosystems, Life Technologies), and amplification was done by using a 7500 Fast Real-Time PCR System (Applied Biosystems, Life Technologies) programmed as follows: 10 min at 50ºC, 10 sec at 95ºC, and 45 cycles of 15 s at 95ºC and 30 sec at 58ºC. Samples with a quantification cycle (Cq) value ≤40 were considered positive for MERS-CoV RNA.

Virus titration

NS and ES collected at different times pi were evaluated for the presence of infectious virus by titration in Vero cells, as previously reported [65,207]. Ten-fold dilutions were done, starting with a dilution of 1:10, and dilutions were transferred to Vero E6 cells. Plates were daily monitored under the light microscope and wells were evaluated for the presence of cytopathic effect (CPE) at 5 dpi. The infectious virus concentration in nasal swabs was calculated by determining the dilution that caused 50% CPE in cell cultures ($TCID_{50}$/mL). The limit of detection of the technique was established at 1.8 TCID50/mL.

MERS-CoV S1-ELISA

Specific S1-antibodies in serum samples from all collected time-points and from all animals were determined by a MERS-CoV S1-ELISA as previously described [65,207]. Briefly, 96-well high-binding plates (Sigma-Aldrich) were coated with 100 µL of S1 protein [355] at 1 µg/mL in PBS o/n at 4°C. After blocking with 1% bovine serum albumin/PBS/0.5% Tween20 for 1 h at 37°C, serum samples were tested at a 1:100 dilution, followed by 1 h incubation at 37°C. Plates were washed 4 times with PBS, and wells were incubated with a goat anti-llama biotin conjugate (Abcore, 1:1,000 diluted in blocking buffer), followed by incubation with streptavidin peroxidase (Sigma-Aldrich). After 1 h of incubation at 37°C, wells were washed 4 times with PBS, and a TMB substrate solution (Sigma-Aldrich) was added and allowed to develop for 8–10 min at room temperature, protected from light. Optical density was measured at 450 nm.

MERS-CoV N-LIPS

We tested llama sera for MERS-CoV nucleocapsid (N) specific antibody responses using a luciferase immunoprecipitation (LIPS) assay [356]. The N protein was expressed as an N-terminal *Renilla* luciferase (Ruc)-tagged protein (Ruc-N) using pREN2 expression vector. The cells were lysed, and the luminescence units (LU)/µL was measured in cell lysates. LIPS assay was done according to a previous protocol with minor modifications [357]. Briefly, serum samples were diluted 1:100 and mixed with 1×10^7 LU of Ruc-N in a total volume of 100 µl in buffer A (20 mM Tris, pH 7.5, 150 mM NaCl, 5 mM $MgCl_2$, 1% Triton X-100). The mixture was incubated on a rotary shaker for 1 h at room temperature. Then, the mixture was transferred into MultiScreenHTS BV Filter Plate (Merk Millipore) containing 5 µL of a 30% suspension of UltraLink protein A/G beads and

further incubated for one hour. The wells were then washed and luminescence was measured for each well after adding 100 µL of 0.1 µM coelenterazine (Nanolight Technology) in assay buffer (50 mM potassium phosphate, pH 7.4, 500 mM NaCl, 1 mM EDTA). The sera were tested in duplicates in at least two independent assays and the data was averaged to determine the LU value for each sample.

Hemagglutination inhibition (HI) assay

To test llama sera for functional antibodies against the sialic acid binding S1 N-terminal domain ($S1^A$), a nanoparticle-based HI assay was used. $S1^A$ lumazine synthase (LS) nanoparticles were produced as described previously [51,288]. Two-fold diluted sera were mixed with 4 HA units of $S1^A$-LS and incubated for 30 min at 37°C. Following incubation, 0.5% washed turkey RBCs were added and further incubated for 1 h at 4°C. HI titres were determined as the reciprocal of highest serum dilution showing inhibition of hemagglutination.

Receptor binding inhibition (RBI) assay

We tested llama sera for antibodies able to block MERS-CoV binding to its receptor (DPP4) using a competitive ELISA. ELISA plates were coated with 2 µg/mL recombinant soluble DPP4 protein [47] overnight at 4°C. The plates were washed with PBS and blocked with 1% BSA in PBS/0.1% Tween-20 at 37°C for 1 h. Serum samples were tested at a 1:20 dilution. Recombinant MERS-CoV S1-mFc was mixed with diluted sera, incubated for 1 hr at 37°C, added to the plate and further incubated for 1h. The plates were then washed, and HRP-labelled rabbit anti-mouse Igs was added to detect S1 bound to DPP4. Following 1 h of incubation, the plates were washed, and the signal was detected using TMB as described above. Optical density was measured at 450 nm.

Plaque reduction neutralization assay

Serum samples were further tested for neutralizing antibodies against MERS-CoV (Qatar15/2015 isolate) using a plaque reduction neutralization (PRNT) assay. PRNT assay was carried out using according to the previously published protocol [207] with some modification. Briefly, samples were first inactivated at 56ºC for 30 min. Then, 50 µL of 2-fold serial dilutions of heat-inactivated serum were mixed 1:1 with virus (400 PFU) prior to over-layering onto Huh7 cells. After 8 h of infection, the cells were fixed and stained using mouse anti-MERS-CoV nucleocapsid protein (SinoBiological) and HRP-conjugated goat anti-mouse IgG1 (SouthernBiotech). The number of infected cells were detected using a precipitate-forming TMB substrate (True Blue, KPL) and counted using an ImmunoSpot® Image analyser (CTL Europe GmbH). The PRNT titre was calculated based on a 50% or greater reduction in infected cells counts.

3.3 Results

Clinical signs

One naïve contact llamas showed moderate nasal mucus secretion at 13-15 dpi (see **Figure 3.3**). No animals showed a significant increase in body temperatures above 40ºC along the study.

Figure 3.3. Clinical signs after MERS-CoV infection in contact llamas. Presence of mucus excretion in llama 4 at 13 days post-challenge.

MERS-CoV RNA and infectious virus

All MERS-CoV inoculated llamas shed viral RNA in the nasal cavity during a 2-week period (**Figure 3.4A**). The amount of viral RNA was still high (Cq values < 25) in all inoculated llamas at 6-7 dpi, but a decrease in RNA load was observed from 8 dpi onwards. In-contact naïve llamas revealed evidence of infection (detectable viral RNA) 4-5 days after contact, with viral RNA loads and duration of shedding like those of the inoculated animals (**Figure 3.4A**).

RT-qPCR positive nasal swab samples were tested for the presence of infectious virus. All intranasally inoculated llamas excreted infectious MERS-CoV at some point until 6 dpi (**Figure 3.4B**). The duration of infectious virus shedding varied among individual animals ranging from 1 up to 6 consecutive days. One inoculated llama (No. 2) shed infectious virus continuously from days 1 to 6 pi (**Figure 3.4B**). Three out of the five direct contact naïve llamas shed infectious virus at 8, 9 and 10 dpi (**Figure 3.4B**). These sentinel animals (No. 4, 6 and 7) exhibited virus titres at least equal to those observed in inoculated llamas (**Figure 3.4B**). The peaks of viral RNA coincided with the highest levels of infectious virus shed.

Llama No. 4 showed low levels of MERS-CoV RNA at 1 dpi before in-contact challenge (**Figure 3.4A**). However, this animal remained negative to RT-qPCR until 5 dpi, suggesting that a contamination occurred during the collection or the processing of this sample. Additionally, no infectious virus was detected in this animal at 1 dpi (**Figure 3.4B**).

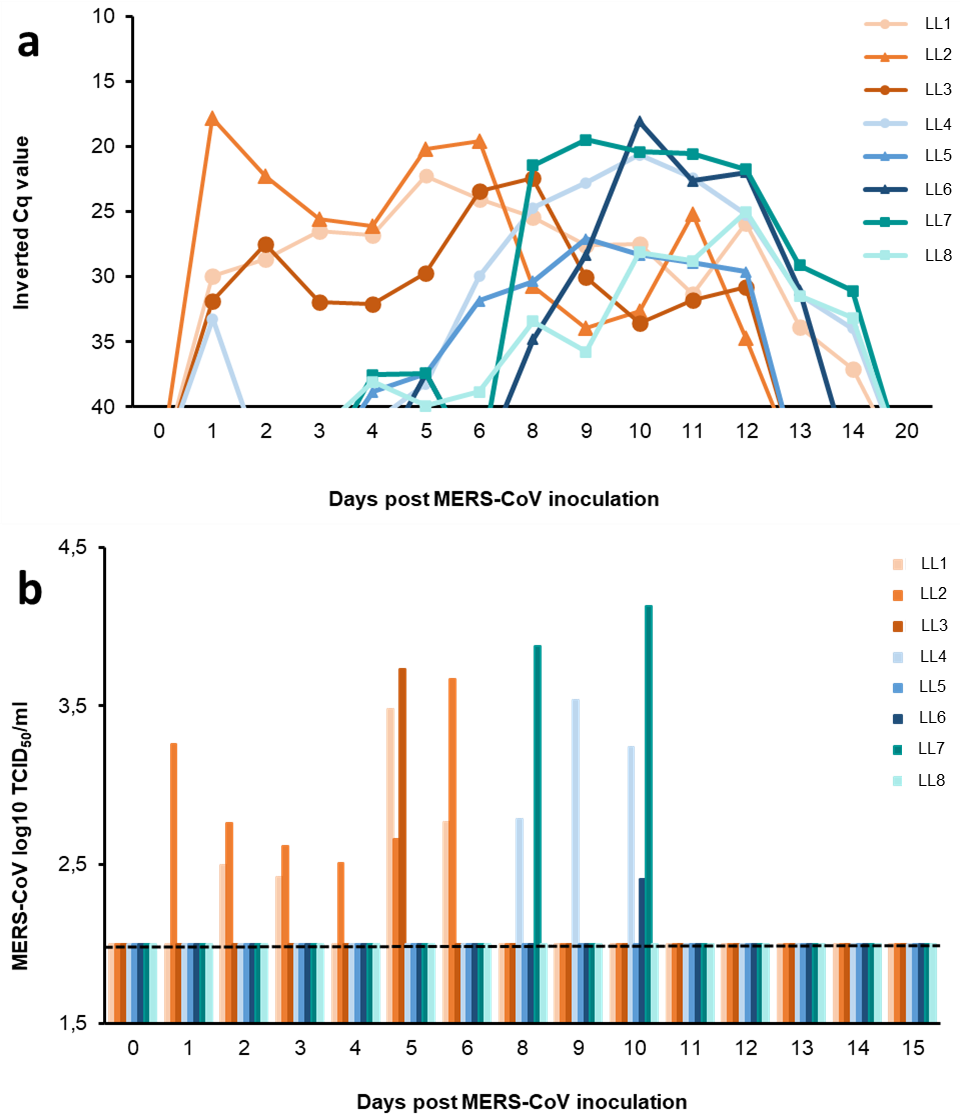

Figure 3.4. Viral shedding in llamas after experimental inoculation or contact with MERS-CoV-infected llamas. Viral RNA detected in nasal swab samples

collected from naïve **(a)** llamas at different time points after contact with directly inoculated animals. Panel **b)** displays infectious MERS-CoV in nasal swab samples collected from naïve animals at different time points after inoculation. Each line/bar represents an individual animal. Orange lines/bars indicate experimentally inoculated llamas, while blue and green lines/bars indicate in-contact naïve animals. Dashed lines depict the detection limit of the assays. Cq, quantification cycle; MERS-CoV, Middle East respiratory syndrome coronavirus; $TCID_{50}$, 50% tissue culture infective dose.

Relatively low levels of viral RNA were detected in all types of environmental samples that were taken in the boxes during the experiment (≥30 Cq) (**Table 3.1**). The highest MERS-CoV RNA levels were found in drinking water samples. However, titration of infectious virus was not successful.

Table 3.1. MERS-CoV RNA detection in environmental samples expressed in Cq values at different times after inoculation. Swabs 1 and 2 correspond to ES2 and ES3 of the **Figure 3.1**, respectively. Cq, quantification cycle; MERS-CoV, Middle East respiratory syndrome coronavirus; nc, non-collected samples.

Days post-inoculation	**0**	**1**	**2**	**3**	**4**	**5**	**6**	**7**	**8**	**9**	**10**
Sartorius	-	-	35,04	-	36,22	39,43	38,52	nc	38,21	38,72	31,91
Swab 1	-	-	-	-	36,57	-	39,53	nc	32,23	39,64	38,01
Swab 2	-	39,90	-	38,31	35,85	35,35	37,00	nc	34,30	38,12	36,58
Water	-	36,31	-	-	-	-	36,01	nc	38,70	33,42	33,24

Humoral immune response

We evaluated the MERS-CoV specific antibody responses induced in llamas following infection. All directly inoculated and in-contact naïve llamas seroconverted to MERS-CoV as detected by MERS-CoV S1 ELISA (**Figure 3.5A**) and virus neutralization (**Figure 3.5B**). In contrast, only three of those, two directly inoculated and one in-contact, also

developed anti-N antibody responses (see **Figure 3.6**). Antibodies against the $S1^A$ sialic acid binding domain were detected in one of the directly inoculated and four in-contact naïve animals using a HI assay (**Figure 3.5C**). Receptor-binding blocking (mainly RBD-directed) antibodies were detected in the sera of all directly inoculated animals and in four out of the five in-contact naïve llama sera using a competitive RBI ELISA (**Figure 3.5D**).

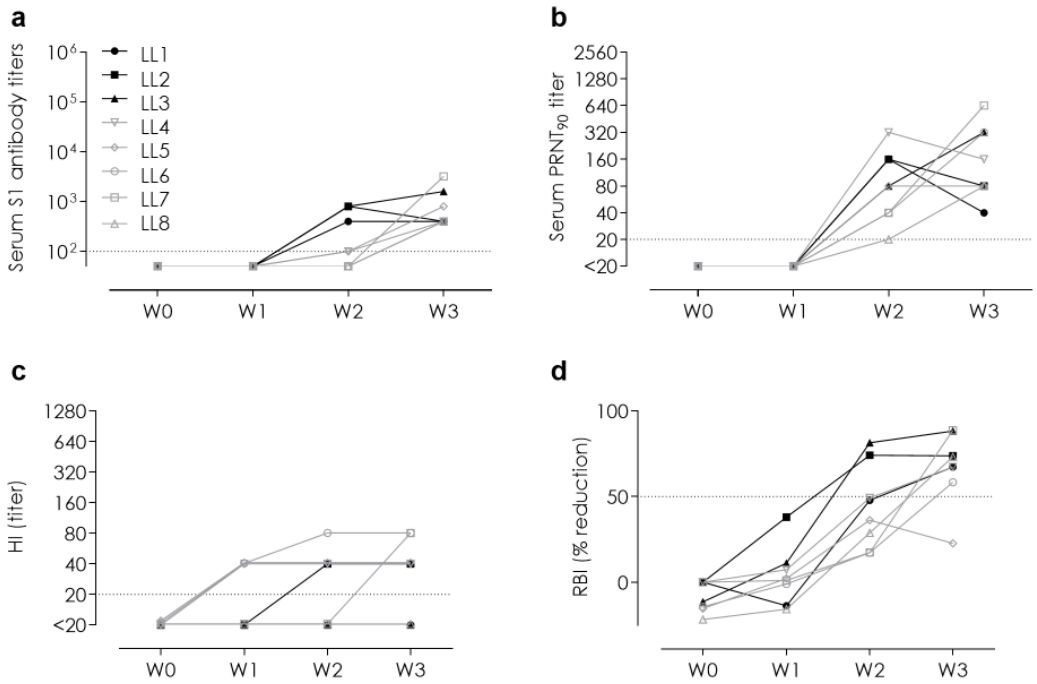

Figure 3.5. Serum antibodies elicited against MERS-CoV in inoculated and in-contact naïve llamas. **(a)** MERS-CoV spike S1, **(b)** MERS-CoV neutralizing (Qatar15/2015 strain), **(c)** hemagglutination inhibition (HI; anti-$S1^A$ N-terminal domain), and **(d)** receptor binding inhibition (RBI; anti-S1 receptor binding domain) antibodies. The horizontal dotted lines indicate the cutoff of each assay. HI, hemagglutination inhibition; LL, llama; PRNT, plaque reduction neutralization assay; RBI, receptor binding inhibition; W, week.

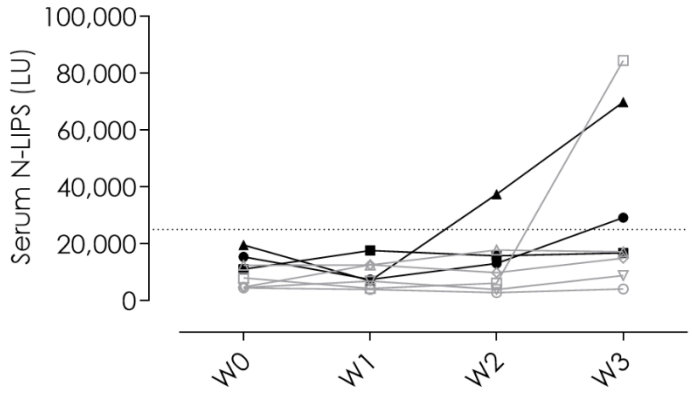

Figure 3.6. Sera MERS-CoV nucleocapsid (N)-directed antibodies elicited in inoculated (LL1-3; black) and in-contact naïve llamas (LL4-8; grey). The horizontal dotted lines indicate the cutoff of the assay. LU, luminescence units; N-LIPS, nucleocapsid luciferase immunoprecipitation assay; W, week.

3.4 Discussion

In this study, experimental MERS-CoV transmission from infected llamas to naïve in-contact llamas has been demonstrated for the first time. Consistent with previous studies [65], all MERS-CoV inoculated llamas got infected, shed infectious virus and were able to transmit the virus to all naive contact animals as assessed by MERS-CoV RNA and viral titration of the nasal swabs. We confirmed that 3 infected llamas were able to transmit MERS-CoV to at least 5 naïve animals; nonetheless, further studies are needed to determine the basic reproduction ratio of this virus transmission in camelids. Interestingly, the three contact llamas shedding infectious MERS-CoV showed the highest viral RNA loads, while the remaining two had higher Cq values and no infectious virus was isolated. Altogether, considering that (i) viral genomic replication was observed in all in-contact naïve llamas for an extended period, (ii) 3 out of 5 in-contact animals shed detectable infectious virus and (iii) one of them exhibited nasal discharges, this in-contact model of virus transmission is valuable to

test vaccine efficacy. However, before stating that llamas can be surrogates of dromedaries for vaccine testing in an in-contact model, it would be important to assess whether infectious viral pressure elicited by the experimental challenge are similar between these two animal species. In that respect, in a previous report, two dromedaries inoculated with the MERS-CoV EMC/2012 strain shed viral RNA and infectious virus for 13 and 6 days, respectively [207], like what we found in the present study in llamas infected intranasally with the MERS-CoV Qatar15/2015 strain.

Overall, this work revealed that the llama model can be a surrogate for dromedary camel in MERS-CoV transmission and vaccination studies.

Chapter 4

Experimental transmission of a MERS-CoV clade C strain (Egypt/2013) among llamas

(Manuscript submitted)

4.1 Introduction

MERS-CoV infections cause severe pneumonia, acute respiratory distress syndrome, and even lethal disease in humans. High case-fatality rates are reported in the Middle East [25], where the virus is endemic and represents a significant human health threat. Although major travel-associated outbreaks have occurred and nosocomial transmissions have been documented, MERS-CoV is known to be carried and transmitted to humans by dromedary camels, which are the natural reservoirs and main source of zoonotic events [141]. All primary human MERS-CoV cases reported during the period July – December 2021 had been previously exposed to dromedary camels [126]. Susceptible camelid species, such as dromedaries, llamas and alpacas [232], as opposed to humans, do not experience severe disease upon MERS-CoV infection, which is characterized by upper respiratory tract replication, abundant infectious viral shedding and high transmission potential [141].

Endemicity of MERS-CoV has been determined in dromedary camels from the Arabian Peninsula and Africa [110]. In fact, high incidence of MERS-CoV has been described in African dromedaries, which represent more than 80% of the worldwide camel population (https://www.fao.org/faostat). Although there is serological and molecular evidence of MERS-CoV infection in people who had been exposed to African dromedary camels [358–361], zoonotic MERS has not been reported across Africa. On the other hand, to date, zoonotic human disease has been restricted to the Arabian Peninsula. Despite a continuous dromedary camel trade into the Arabian Peninsula, African clade C MERS-CoV strains have not been established in this region. Different reasons may account for this fact. Arabian clade B strains showed increased replication competence

compared to different African clade C strains in human lung *ex vivo* cultures and in a hDPP4 knock-in mouse model [30]. An increased fitness of clade B strains could explain their dominance in the Middle East and why they rapidly outcompete clade C viruses. Nonetheless, the replication and transmission competence of African viruses in camelid reservoir species remains unknown.

In the present study, we have used a llama direct-contact transmission model (described in *Chapter 3*) to investigate the replication and transmission potential of an African MERS-CoV strain in a camelid model.

4.2 Materials and methods

Animal welfare and ethics

All animal experimentation and MERS-CoV handling were conducted at the BSL-3 facilities of the Biocontainment Unit of IRTA-CReSA. Animal handling and experimental procedures were approved by the CEEA-IRTA and by the Ethical Commission of Animal Experimentation of the Autonomous Government of Catalonia (files No. CEA-OH/10942/1).

Cell culture and viruses

Vero cells (CRL-1586, ATCC, USA) were cultured in DMEM (Lonza, Switzerland) supplemented with 5% fetal calf serum (EuroClone, Italy), 100 U/mL penicillin, 100 µg/mL streptomycin, and 2 mM glutamine (all ThermoFisher Scientific, USA). Calu-3 cells were cultured in Opti-MEM I (1X) supplemented with GlutaMAX (Gibco, USA), 100 U/mL penicillin and 100 µg/mL streptomycin. A MERS-CoV Egypt/2013 (clade C strain; GenBank accession no. KJ477103) passage-6 stock [100] was propagated for

3 days at 37◦C and 5% CO_2 in Vero cells. Infectious virus titers were determined in Vero cells and calculated by determining the dilution that caused 50% CPE in cell cultures (50% tissue culture infectious dose endpoint, $TCID_{50}$).

Study design

To study the transmission of a MERS-CoV clade C strain, five healthy llamas were purchased from a private animal facility and housed at the animal BSL-3 facilities of the IRTA-CReSA Biocontainment Unit. The experimental box was set up as described also **Figure 3.1** from *Chapter 3*. Two llamas were intranasally inoculated with $10^{6.4}$ $TCID_{50}$ of MERS-CoV Egypt/2013 strain in 3 mL saline solution, using a nebulization device (LMA® MADgic®, Teleflex Inc., USA) and administrating 1.5 mL into each nostril. At 2 dpi, inoculated llamas were placed in direct contact with the remaining three sentinel llamas (see **Figure 3.1** from *Chapter 3*). Clinical signs of all animals were monitored for 3 weeks, and rectal temperatures were recorded until 15 dpi with a fast display digital thermometer (AccuVet®, Infratec, Italy). Nasal swabs were obtained daily until 15 dpi, plus at 17 and 22 dpi. Whole blood samples of all animals were collected from the jugular vein using Vacutainer® tubes (Beckton Dickinson, USA) and serum samples were obtained before MERS-CoV challenge and at 7, 14 and 22 dpi. Animals were euthanized at 22 dpi with an overdose of pentobarbital, followed by a complete necropsy with special focus on upper and lower respiratory tract lesions.

MERS-CoV RNA detection

Viral RNA was extracted from NS samples with the IndiMag pathogen kit (Indical Biosciences, Germany) using a Biosprint 96 workstation (Qiagen,

Germany), following the manufacturer's instructions. Genomic and subgenomic RNA extracts were detected by the UpE and M mRNA RT-qPCR assays, respectively [354,362]. RT-qPCR for genomic RNA detecteion was performed as described in *Chapter 3*. To assess viral replication, subgenomic RNA form NS was tested with the M mRNA assay, according to a previously published protocol [362].

Virus titration

Infectious MERS-CoV titres in NS collected along the study were determined as previously described in *Chapter 3*.

Plaque reduction neutralization assay

Sera samples collected weekly were tested for the presence of neutralizing antibodies against MERS-CoV (EMC/2012 isolate; GenBank accession no. NC_019843.3) using a PRNT assay according to a previously published protocol [207], with minor modifications. Briefly, serum samples were inactivated at 56ºC for 30 min. Then, 50 µl of 2-fold serially diluted sera were mixed 1:1 with 400 PFU of MERS-CoV, transferred to Calu-3 cells monolayers and incubated at 37ºC and 5% CO_2. After 8 h of infection, cells were fixed, permeabilized with 70% ethanol, and stained using mouse anti-MERS-CoV nucleocapsid protein (SinoBiological, China; diluted 1:1000 in 0.1% BSA-PBS) followed by goat anti-mouse Alexa Fluor 488 antibody (Invitrogen, 1:2000 in 0.1% BSA in PBS). Plates were scanned on the Amersham Typhoon Biomolecular Imager (GE Healthcare, USA). Data was analysed using ImageQuantTL 8.2 image analysis software (GE Healthcare). The PRNT90 titre was defined as the reciprocal value of the sample dilution that showed 90% reduction of virus growth. Dose–response curves of serum samples were adjusted to a non-linear fit regression model in Graphpad Prism 9 software, with

bottom constraints of 0% and top constraints of 100%.

4.3 Results

A group of five llamas was kept inside an experimental box to study the transmission capabilities of a MERS-CoV clade C isolate (MERS-CoV/Egypt2013), obtained from an infected dromedary [100]. Rectal temperature of all animals remained at basal levels (37-40°C) and none of them displayed clinical signs throughout the study. No gross or microscopic lesions were detected in the upper and lower respiratory tracts of any studied llama, independently of their experimental group.

Animals inoculated with a high dose of MERS-CoV Egypt/2013 (clade C) had similar levels of genomic and subgenomic viral RNA in nasal swabs for 2 weeks (**Figure 4.1a** and **4.1b**). They also shed high titres of infectious virus during the first week after inoculation in a biphasic pattern (**Figure 4.1c**), evidencing that the dose used to inoculate the animals caused productive infection. The infection was characterized by a first peak of shedding at 2 dpi, a subsequent reduction in MERS-CoV loads followed by a secondary peak before viral clearance.

The African MERS-CoV isolate was transmitted to two out of three in-contact animals in this study, as determined by RT-qPCR (**Figure 4.1a** and **4.1b**), but infectious virus shedding in contact animals largely remained below threshold levels (**Figure 4.1c**). Infectious MERS-CoV Egypt/2013 could only be isolated sporadically and at titres close to the limit of detection. Of note, genomic and subgenomic MERS-CoV Egypt/2013 RNAs were detected at lower levels and cleared faster in direct-contact llamas compared to experimentally inoculated animals (**Figure 4.1a** and **b**). The remaining sentinel did not develop a productive infection but was

naturally exposed to MERS-CoV Egypt/2013, as evidenced by traces of genomic RNA in NS at 3-7, 10 and 12 dpi (Cq values > 37) and the development of serum nAbs to MERS-CoV (**Figure 4.2**). Subgenomic RNA analyses indicated no evidence for viral replication nor shedding in this llama throughout the study. Inoculated animals and in-contact sentinels developed nAbs to MERS-CoV from 2 weeks after infection onwards (**Figure 4.2**).

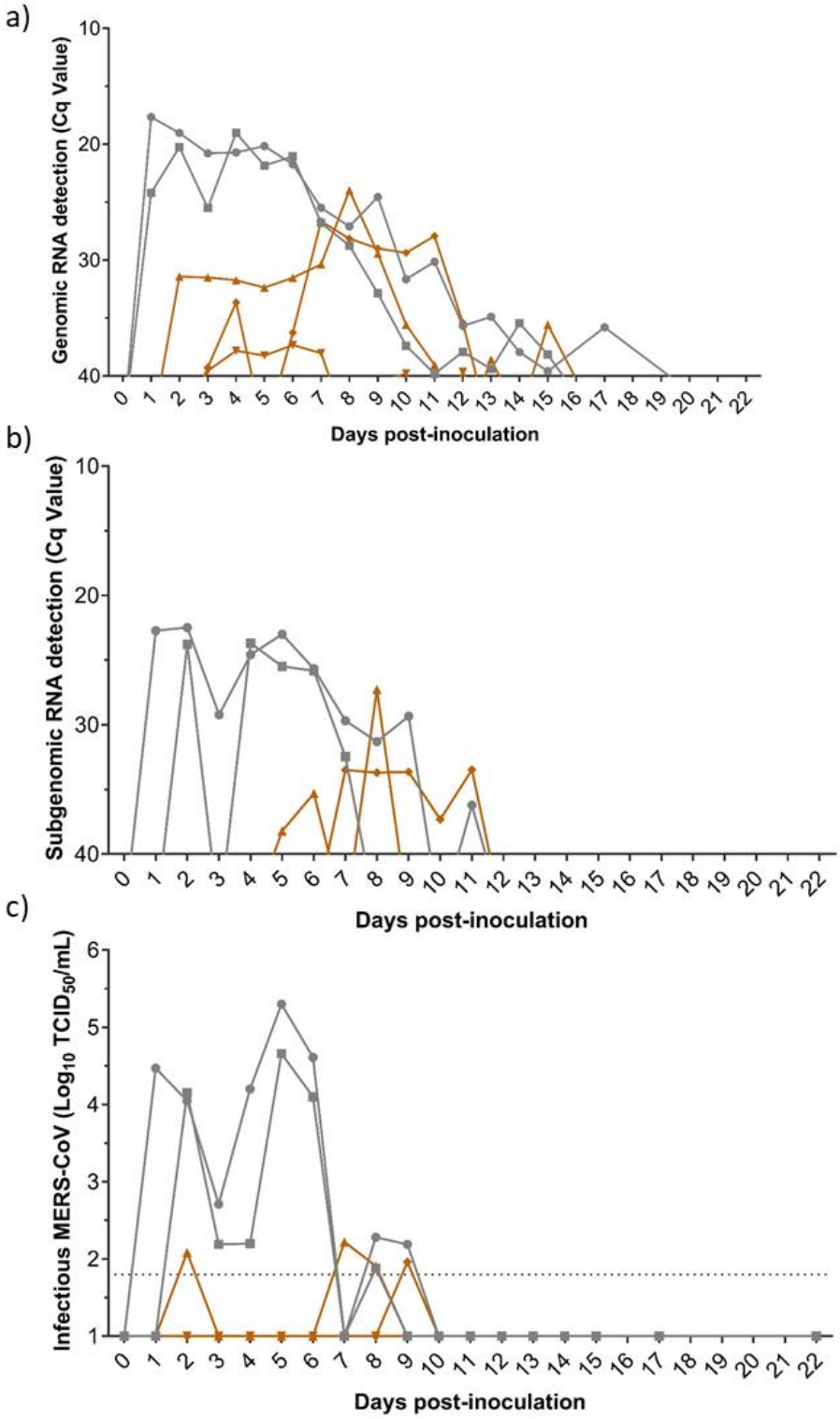
a)
Genomic RNA detection (Cq Value)
10
20
30
40
0 1 2 3 4 5 6 7 8 9 10 11 12 13 14 15 16 17 18 19 20 21 22
Days post-inoculation
b)
Subgenomic RNA detection (Cq Value)
10
20
30
40
0 1 2 3 4 5 6 7 8 9 10 11 12 13 14 15 16 17 18 19 20 21 22
Days post-inoculation
c)
Infectious MERS-CoV (Log10 TCID50/mL)
1
2
3
4
5
6
0 1 2 3 4 5 6 7 8 9 10 11 12 13 14 15 16 17 18 19 20 21 22
Days post-inoculation

Figure 4.1. MERS-CoV RNA and infectious virus shedding in llamas infected with MERS-CoV Egypt/2013. To study viral transmission, MERS-CoV Egypt/2013 experimentally-inoculated llamas (grey) were placed in contact with naïve animals (orange) two days after the inoculation procedure. Genomic (a) and subgenomic (b) viral RNA were quantified in nasal swab samples collected at different times after MERS-CoV inoculation. Plot (c) shows infectious MERS-CoV titres in nasal swabs collected on different days after MERS-CoV inoculation. Each line represents data from a different animal. Dashed lines depict the detection limits of the assays. Cq, quantification cycle; MERS-CoV, Middle East respiratory syndrome coronavirus; $TCID_{50}$, 50% tissue culture infective dose.

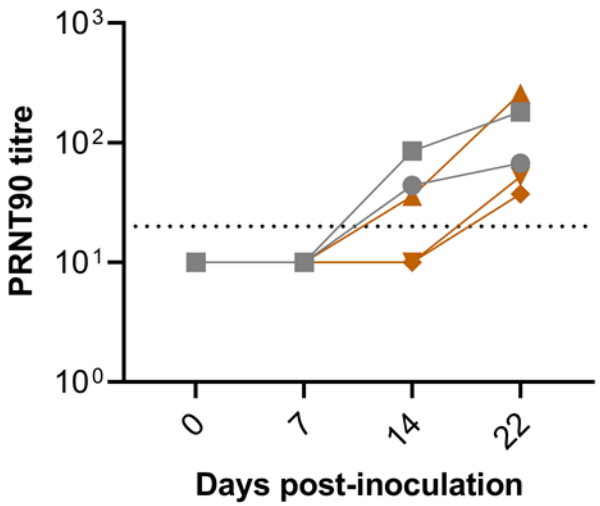

Figure 4.2. Development of neutralizing humoral responses by llamas infected with MERS-CoV Egypt/2013. The plot displays levels of serum neutralizing antibodies elicited in llamas upon MERS-CoV Egypt/2013 inoculation (grey) or direct exposition to inoculated ones (orange). Each line represents data from a different animal. Dashed lines depict the detection limits of the assays. PRNT90, 90% plaque reduction neutralization titre.

4.4 Discussion

In this study, we confirmed that a MERS-CoV clade C strain (Egypt/2013) can be transmitted among llamas in direct contact. MERS-CoV-inoculated llamas shed high levels infectious virus but were only able to transmit the virus to two out of three naive contact animals, as assessed by MERS-CoV RNA and viral titration of the nasal swabs. Furthermore, the two infected sentinels had lower viral loads and shedding than experimentally inoculated animals and cleared the infection faster. Of note, genomic and subgenomic MERS-CoV Egypt/2013 RNAs were detected at lower levels and cleared faster in direct-contact llamas, compared to sentinels infected with the MERS-CoV Qatar15/2015 strain (see *Chapter 3*). Although viral replication was not observed in one naïve-contact llama, all sentinels were exposed to MERS-CoV as evidenced by the development of serum nAbs. Sentinels infected with the Egypt/2013 strain had lower nAb levels at 14 dpi than experimentally infected animals, as well as inoculated and in-contact llamas infected with the Qatar15/2015 strain (see *Chapter 3*). However, inoculated or in-contact animals had similar levels of nAb responses at the end of the experiment, independently of the strain of infection. Altogether, the study presented in *Chapter 3* and the current one demonstrated transmission of both MERS-CoV clade B and C strains in llamas, resulting in decreased viral replication and shedding capabilities of the Egypt/2013 strain compared to the Qatar15/2015 strain in sentinel llamas infected by contact. Therefore, the Qatar15/2015 strain might have a higher potential of transmission than the Egypt/2013 strain and, consequently, is a better choice for vaccine efficacy studies using a llama contact transmission set up.

The transmission study using a MERS-CoV clade C strain also shed insights into epidemiological and ecological considerations. *Chapters 3* and *4* provide experimental data supporting a reduced replication, shedding and transmission potential of MERS-CoV clade C viruses in llamas, compared to clade B strains. These results might explain why clade B strains outcompete clade C strains in the Arabian Peninsula, which are continuously introduced to this region through the trade of infected dromedary camels. Nonetheless, additional studies using other strains are required to confirm a low-replication phenotype of African MERS-CoV lineages compared to Arabian viruses in camelid hosts. Importantly, our findings also suggest that MERS-CoV clade B strains introduced into Africa may outcompete African MERS-CoV clade C strains, allowing the virus to spread across dromedaries and pose a higher zoonotic risk in Africa.

Chapter 5

Development of a high-throughput gene expression panel to monitor immune responses in camelid PBMCs by microfluidic qPCR system

(Manuscript in preparation)

5.1 Introduction

Camelid species are livestock of great economic, sanitary, health and environmental importance in the north of Africa, central Asia, the Middle East, and South America. Number of animals is expected to grow since the camelid industry is in transition from nomadism to intensive production (FAOSTAT, 2021). In Europe, camelids are used for fine wool production but also kept as pets, guardians of other livestock, or used for recreational or leisure purposes [364]. However, these animals are susceptible to several viruses, bacteria and protozoan parasites affecting meat and milk production. As an example, Camelpox and Peste des Petits Ruminants viruses are causing recurrent epizootic outbreaks in Africa and Middle East [365]. Furthermore, there is limited information available about the role of camelids in the epidemiology of zoonotic diseases. In recent years, the most studied microbes from camelid-borne diseases included the MERS-CoV and the Rift Valley fever virus (RVFV), *Brucella* sp., and *Echinococcus granulosus* [366]. Many other less studied viruses known to be carried and transmitted by camelids, such as hepatitis E virus (HEV) or Crimean-Congo haemorrhagic fever virus (CCHFV), are of serious human health concern. Camelids are also vectors of many other fastidious bacterial diseases including tuberculosis, gastrointestinal illnesses caused by verotoxin-producing *E. coli*, campylobacteriosis, listeriosis and salmonellosis, among others, as well as protozoan parasites (*Cryptosporidium* spp., *Sarcoptes*, *Giardia duodenalis*, etc.) of veterinary and human health concern [365].

Understanding disease pathogenesis and identifying protective immune responses are prerequisites for the rational development of new anti-microbial drugs and vaccines. In addition, comparison of immune

responses between humans and domestic or wildlife species would shed insights to delineate host factors involved in disease outcome. Upon pathogen infection, the host immune system is regulated by complex mechanisms in which cytokines play a pivotal role in determining the intensity and duration of the immune response [367,368]. In some domestic species, such as pig, goat, cattle, and sheep, the quantification of cytokines, either at the protein or mRNA level, has become a widely used method to monitor immune responses upon pathogen infection [369,370]. However, cytokine detection in camelids has been hampered by the lack of specific reagents. To date, there are few reliable commercial ELISA kits available to study immune responses in camelids at the protein level. Nonetheless, camelid interferon (IFN)-α, and some Th1 cytokines, Th2 cytokines, and pro-inflammatory cytokine cDNAs have been cloned and sequenced [371–376]. Sets of primers have been derived from these sequences [377] to quantify cytokine mRNAs in peripheral blood mononuclear cells (PBMCs) of *Camelus bactrianus* upon vaccination with *Brucella abortus* strain 19 by reverse transcription quantitative polymerase chain reaction (RT-qPCR) assays [378]. Although these previous works provided tools to quantify a few camelid cytokine mRNAs, primers assays only allow for a cursory study of immune response pathways and were not optimized to function in medium to high-throughput qPCR platforms. We previously took advantage of well-annotated camelid draft genomes [379] to design a comprehensive set of primers from genes encompassing several innate immune response pathways [8,32], and demonstrated their functioning in respiratory tract samples of llamas. Here, we extended this panel of primers to characterize expression of innate and adaptive immune response genes in PHA, PMA-ionomycin and PolyI:C-stimulated PBMCs from three different camelid species (dromedaries, llama, and alpacas). We

optimized gene expression analyses in the highly sensitive and cost-effective Fluidigm Biomark microfluidic qPCR system. A full validation and standardization of these assays is provided together with an interspecies comparison characterizing camelid cytokine expression with non-specific PBMC stimuli widely used in immunological research.

5.2 Materials and methods

The present work was performed using the nomenclature and following the validation protocols proposed by the Minimum Information for publication of quantitative real-time PCR experiments (MIQE) guidelines (Bustin et al., 2009).

Animal welfare, ethics, and experimental design

Experiments with animals were performed at private animal facilities or at the BSL-3 facilities of IRTA-CReSA and were approved by the CEEA-IRTA and by the Ethical Commission of Animal Experimentation of the Autonomous Government of Catalonia (approval No. FUE-2017-00561265 and FUE-2018-00884575).

Two llamas (L1, L2) and five alpacas (A1-5) were purchased from Belgium and The Netherlands, respectively, housed at IRTA-CReSA animal facilities and used for routine blood collection. L1 and L2 were used in a previous study (*Chapter 3*), and blood was collected prior experimental infection with MERS-CoV. One healthy dromedary camel (D1) from a private zoo (Alicante, Valencian Community, Spain) was also bled once for routinely checking purposes, and extra blood samples were taken to perform this work.

Blood collection

Whole blood samples (40 to 50 mL) from each animal were collected from the jugular vein using EDTA BD Vacutainer® tubes (Beckton Dickinson, New Jersey, USA), following animal welfare protocols.

PBMC isolation

Prior PBMCs isolation, whole blood was diluted 1:1 with phosphate-buffered saline (PBS). PBMCs were harvested from blood by density-gradient centrifugation with Histopaque®-1083 (Sigma-Aldrich, St. Louis, MO, USA), according to the manufacturer's instructions. PBMCs were cultured in Roswell Park Memorial Institute 1640 (RPMI-1640) medium supplemented with antibiotics (100 U/mL penicillin, 0.1 mg/mL streptomycin) and glutamine (2 mmol/L) purchased from Life Technologies (Waltham, USA), β2-mercaptoethanol (5×10^{-5} M; Sigma-Aldrich, MO, USA), and 10% heat inactivated FCS (EuroClone, Pero, Italy). Cell viability was assessed by the Trypan blue staining exclusion method.

Cell stimulation assays

PBMCs from A1-2, D1, and L1-2 were seeded on 24-well plates at $5\cdot10^6$ cells/mL, and cultured in duplicates in medium alone (control condition), or stimulated with 10 µg/mL of phytohemagglutinin P (PHA; Sigma-Aldrich, St. Louis, MO, USA), or with a combination of 10 ng/mL phorbol 12-myristate 13-acetate (PMA; Sigma-Aldrich, St. Louis, MO, USA) and 1 µg/mL ionomycin calcium salt (Sigma-Aldrich, St. Louis, MO, USA) for 48 h at 37°C and 5% CO_2. Additionally, PBMCs from A3-5 were cultured with 250 ng/mL Poly(I:C)-LMW/LyoVec™ (PolyI:C; Invivogen, San Diego, USA) for 48 h at 37°C and 5% CO_2. Afterwards, PBMCs were carefully collected by up and down pipetting and transferred to a DNase/RNase-free tube. After centrifugation, supernatants were

removed and lysis buffer for RNA extraction was added to the cell pellet. As additional control samples, $5 \cdot 10^6$ PBMCs from the dromedary and each alpaca were freshly collected in lysis buffer before plaque seeding. All samples in lysis buffer were stored at -80°C until RNA extraction.

RNA extraction and quantification

Total RNA was extracted from PBMCs using the RNeasy® Mini Kit (Qiagen Ltd., Crawley, UK), according to the manufacturer's protocol. After RNA elution, an additional DNase I treatment was performed using the Heat&Run gDNA removal kit (ArcticZymes Technologies, Tromsø, Norway), following the manufacturer's protocol. Finally, RNase inhibitors (Invitrogen, Life Technologies, Waltham, USA) were added to the RNA samples in a final concentration of 1 U/ µL prior storage at -80°C until reverse transcription (RT) reaction was performed.

The purity, quantity and integrity of the extracted RNA were assessed using a BioDrop *µLITE* Spectrophotometer (BioDrop Ltd, Cambridge, UK) and Lab-Chip analysis (Agilent Technologies, Santa Clara, USA). The A260:A280 ratio ranged from 1.6 to 2.1, and RNA Integrity Numbers (RIN) ranged from 7 to 9.6.

cDNA synthesis

Total RNA samples were used to generate cDNA as previously described [8]. Briefly, 110 ng of RNA were retrotranscribed in a final volume of 10 µL using the PrimeScript RT reagent Kit (Takara, Kusatsu, Japan) with a combination of oligo-d(T) and random hexamers, according to the manufacturer's protocol. No-reverse transcription controls (no-RT) with all buffers and reagents supplied by the kits, but omitting the reverse transcriptase, were prepared to assess non-specific amplifications and

presence of genomic DNA (gDNA).

Additionally, control cDNA samples from stimulated PBMCs were obtained with the aim to generate standard curves and determine primer pair efficiencies. Samples were pooled by species at the same proportion per individual animal, except for the dromedary camel. For each species, pools contained cDNA samples from PMA-ionomycin and PHA-stimulated PBMCs at 1:1 proportion, while alpaca PBMCs stimulated with PolyI:C were pooled independently. Finally, samples were serially diluted by 1:4 steps (1/20, 1/80, 1/320, 1/1280, 1/5120) prior amplification reactions.

Primer design of immune associated and reference genes

Camelid genes and mRNA were found through bibliographic search or with described mRNAs in other species performing BLASTn (https://blast.ncbi.nlm.nih.gov/Blast.cgi). Primers were designed through comparative genomics of sequences deposited at the National Centre for Biotechnology Information (NCBI) GenBank database of llama (*Lama glama*), alpaca (*Vicugna pacos*), dromedary camel (*Camelus dromedarius*), bactrian camel (*Camelus bactrianus*), and wild bactrian camel (*Camelus ferus*). Comparison of mRNA and genomic sequences of each studied gene were performed with the alignment tool ClustalW to determine exon boundaries. In some instances, exons were already annotated in camelid genomes.

Primer pairs were designed with Primer3 (http://bioinfo.ut.ee/primer3-0.4.0/), Primer-Blast (https://www.ncbi.nlm.nih.gov/tools/primer-blast), or Primer Express 2.0 (ThermoFisher Scientific, Life Technologies, Waltham, USA), according to the following desirable criteria: (i) to span two or more exons, and some of them were placed at the exon-exon

boundaries, (ii) 17-23 nucleotides in length, close to the mRNA 3' end when possible, (iii) GC-content percentage between 45 and 55%, (iv) leading to an approximate 80-200 bp PCR product, (v) melting temperature (Tm) of each primer between 57-63°C with less than 2°C difference within primer pairs, and (vi) avoiding primer hairpin, self-primer dimer or cross-primer dimer formation.

The avoidance of primer secondary structure arrangement was assessed through the Beacon Designer™ program (http://www.premierbiosoft.com/ qOligo/Oligo.jsp?PID=1), selecting for primers with ΔG greater than -3.5 kcal/mol when possible. Further, primer sequence specificity was assessed using the BLASTn alignment tool against all camelid genome sequences. Potential transcription of predicted pseudogenes was assessed by carrying out promoter region analyses through the VISTA (http://genome.lbl.gov/vista/ customAlignment.shtml) and the Promoter 2.0 Prediction Server (http://www.cbs.dtu.dk/services/Promoter) softwares. Finally, the primer position within exons was checked *in silico* with their respective camelid gene sequences from the NCBI GenBank using the MapViewer tool. All the primers designed in this study are summarized in **Table 5.1**. **Appendix Table 5.1** compiles GenBank accession numbers of camelid genes and mRNA used in this study**. Appendix Table 5.2** compiles the principal characteristics of genes and derived primers used in this study. Oligonucleotides used in this study were supplied by Roche Diagnostics (Sant Cugat del Vallès, Barcelona, Spain).

Cytokine quantification by Fluidigm Biomark microfluidic RT-qPCR

cDNA obtained from PBMCs samples were used to validate the whole panel of primers designed for camelid species and to quantify gene

expression levels by a microfluidic qPCR technique. Firstly, cDNA samples were pre-amplified using the TaqMan PreAmp Master Mix (Applied Biosystems, Life Technologies, Waltham, USA), following the manufacturer's recommendations, doing an initial activation step of the AmpliTaq Gold DNA Polymerase for 10 min at 95°C, followed by 16 cycles of 15 seconds denaturation at 95°C plus 4 min annealing and extension at 60°C. Pre-amplified products were treated with Exonuclease I (New England Biolabs, Ipswich, USA) for 30 min at 37°C to eliminate the carryover of unincorporated primers. An inactivation step of the enzyme for 15 min at 80°C was included according to the manufacturer's protocol. The 96.96 Dynamic Array IFCs, the 96.96 DNA Binding Dye Sample/Loading Kit (Fluidigm Corporation, South San Francisco, USA) was prepared according to the manufacturer's instructions. Pre-amplified samples were diluted 1/20 in 1x TE Buffer, and aliquots of 2.25 µL of each sample and 0.6 µL of primer pairs at 100 µM were loaded in duplicates into their respective array inlets. Quantification of PCR reactions was performed on a Biomark HD system (Fluidigm Corporation, South San Francisco, USA). The PCR consisted in an initial activation step of 1 minute at 95°C, followed by 30 cycles of 5 seconds at 96°C plus 1 minute at 60°C. A dissociation step, increasing 1°C every 3 seconds from 60 to 95°C, was included for all reactions to confirm single specific PCR product amplification and define the Tm of each amplicon. Additionally, stimulated control samples were assayed in triplicates to create relative standard curves and calculate primer amplification efficiencies (see **Appendix Table 5.3**). No-RT controls and no-RNA template controls (NTC) were included in each assay to check for non-specific amplification or primer-dimer formation.

Relative quantification and data analysis

Expression data was collected with the Fluidigm Real-Time PCR analysis software 4.1.3 (Fluidigm Corporation, South San Francisco, USA). Cq threshold detection value was set at 0.020, quality threshold cut-off value was established at 0.65 and amplification specificity was assessed by Tm analyses for each reaction. Amplifications fulfilling the above criteria were analysed using the DAG expression software 1.0.5.6 [381] to apply the relative standard curve method (see Applied Biosystems user bulletin #2). Cq values obtained from pooled cDNA controls were used to create standard curves for each gene, species and PBMC stimulation condition, and to extrapolate the relative quantity values. R-squared values were determined for each standard curve and the specific PCR efficiencies were calculated by applying the formula (10^(-1/slope value)-1)*100 (see **Appendix Table 5.3**). Multiple reference gene normalization was performed by using *GAPDH*, *HPRT1* and *UBC* as endogenous controls. Their suitability for normalization procedures was assessed by control-gene stability analyses with the DAG expression software 1.0.5.6 [381]. The normalized quantity values of each sample and assay were used for direct comparison in relation to fresh PBMC controls (alpaca and dromedary samples) or non-stimulated PBMCs samples cultured during 48 h (llama samples). Therefore, the up- or down-regulated expression of each gene was expressed in fold changes (Fc). **Appendix Table 5.4** compiles the normalized results of all samples expressed in Fc.

Statistical analyses could only be applied in results from alpaca PBMCs cultured for 48 h with and without PolyI:C stimuli, due to the sample size. Fc values were logarithmically transformed to achieve normal distributions. Means of the transformed fold changes obtained for the different stimulation conditions were compared using unpaired t-test analyses in R and GraphPad Prism softwares. Differences were considered

significant at *p*-values < 0.05.

5.3 Results

Selection of immune-related genes and primer design

The selected genes encompass several functional categories representative of pathogen innate and adaptive immune responses, and comprised type I, II and III IFNs, PRRs, TFs, ISGs, pro- and anti-inflammatory cytokines, enzymes, adaptors, cellular receptors, and other genes involved in Th1 and Th2 responses. In addition, three reference genes, glyceraldehyde-3-phosphate dehydrogenase (*GAPDH*), hypoxanthine phosphoribosyltransferase (*HPRT1*) and ubiquitin C (*UBC*), were selected to normalize gene expression. **Table 5.1** summarizes genes and primers designed for subsequent expression analyses.

Table 5.1. Features of the selected cytokines and immune genes used for gene expression analyses, and their validated primer pair sequences for all camelid species. Genes have been grouped in functional categories: Normalizer genes, IFNs, PRRs, transcription factors, ISGs, pro- and anti-inflammatory cytokines, enzymes, adaptors, and cellular receptors.

Gene	Cytokine/Protein type and function	Primer	Sequence (5' - 3')
GAPDH	Normalizer gene	GAPDH F	GGTCGGAGTGAACGGATTTGG
		GAPDH R	TTGAGGTCAATGAAGGGGTCG
UbC	Normalizer gene	Ubc F	AGGCGAAGATCCAAGACAAGG
		Ubc R	CCAAGTGCAGAGTGGATTCCT
HPRT1	Normalizer gene	HPRT1 F	CAAAGATGGTCAAGGTCGCAA
		HPRT1 R	TCAAATCCAACAAAGTCTGGTCT
IFN-α	Type I IFN, antiviral	IFN-α F	TCTTCAGCGAGACACTTGCAA
		IFN-α R	GTTGGTCAGTGAGAATCATTTCCA
IFN-β	Type I IFN, antiviral	IFN-β F2	GCATCCTCCAAATCGCTCTCC
		IFN-β R2	ATGCCAAGTTGCTGCTCCTTT

IFN-γ	Type II IFN, antiviral activity, and mediator of cellular immunity	IFN-γ F	ACTGGAAAGAGGAGAGTGACAAAA
		IFN-γ R	CAACCGGAATTTGAATCAGCT
IFN-λ1	Type III IFN, antiviral	IFN-λ1 F	CTGCCACATGGGCTGGTT
		IFN-λ1 R	CGATTCTTCCAAGGCATCCTT
IFN-λ3	Type III IFN, antiviral	IFN-λ3 F	CCACCTGGCCCAATTCAA
		IFN-λ3 R	AGTGACTCTTCAAAGGCGTCCTT
RIG-1	PRRs and ISG, recognises dsRNA and ssRNA; induce IFN production and ISG	RIG-1 F	ACAAGTCAGAACACAGGAATGA
		RIG-1 R	CTCTTCCTCTGCCTCTGGTTT
MDA5	PRRs and ISG, recognises dsRNA and ssRNA; induce IFN production and ISG	MDA5 F	ACACCAGAGTTCAAGAGACTGTAT
		MDA5 R	CACCATCATCGTTCCCCAAGA
MAVS	PRRs, interacts with RIG-1	MAVS F	CAGCCTCCACAACTGCTACAGA
		MAVS R	CTGTGGGACTTTCTTTGAACTCTCT
TLR3	PRRs and ISG, recognises dsRNA; induce IFN production and ISG	TLR3 F	AGAAATAGACAGACAGCCAGAG
		TLR3 R	TGCTCCTTTTGATGCTATTAACGA
TLR7	PRRs and ISG, recognises ssRNA induce IFN production and ISG	TLR7 F	AGAGAGGAGTCACCAGCGTAT
		TLR7 R	GACACAAATGCAAATGGAGAC
NLRP3	PRRs, increased expression of pro-inflammatory cytokines	NLRP3 F	ATGGCCACATGGATTTTTGC
		NLRP3 R	AAACATTGGCATTGTCCCATTC
STAT1	Transcription factor activated by IFNs; increased expression of ISG	STAT1 F	TCTCTGTGTCTGAAGTTCACCCT
		STAT1 R	GGGAATCACAGGTGGGAAGGA
IRF3	Transcription factor and ISG, activated by IFNs; increased expression of ISG	IRF3 F	TCACCACGCTACACCCTCTGGT
		IRF3 R	GAGGCACATGGGCACAACCTTGA
IRF5	Transcription factor and ISG, activated by IFNs; increased expression of ISG	IRF5 F	TCAGAAGGGCCAGACCAACACC
		IRF5 R	TGCTACGGGCACCACCTGTA
IRF7	Transcription factor and ISG, activated by IFNs; increased expression of ISG	IRF7 F	CGTGATGTTGCAAGACAACTCA
		IRF7 R	TGGTTAACGCCTGGGTCTCT
NFKB1		NFKB1 F	GGGACAGTGTCTTACACTTAGCAATC

	Transcription factor activated by IFNs; increased expression of pro-inflammatory cytokines	NFKB1 R	CATCAGAAATCAAGCCAGATGTG
RELA	Transcription factor, binds to NF-κB	RELA F	AGAGTCCTTTCAATGGCCCCACCG
		RELA R	GGATGGAAGTTGAGCTGCGGGA
IKBKB	Transcription factor activated by IFNs; increased expression of pro-inflammatory cytokines	IKBKB F	TAATGAACGAAGACGAGAAGATGGT
		IKBKB R	ACCTTGCTACACGCAATCTTCAG
CXCL10	ISG, activation and migration of immune cells to the infected sites	CXCL10 F	CGTGTTGAGATTATTGCCACAATG
		CXCL10 R	GAGGTAGCTTCTCTCTGGTCCT
MX1	ISG, GTPase with antiviral activity	MX1 F	GAAGATGGTTTATTCTGACTCG
		MX1 R	TTCTCCTCGTACTGGCTGT
OAS1	ISG, antiviral enzyme; degrades viral RNA	OAS1 F	TGAAGAAGCAGCTCGGGAAAC
		OAS1 R	AGTAACTGTCTTTTCTGGGCAGC
ISG15	ISG, antiviral activity	ISG15 F	CACAGCCATGGGTGGAATC
		ISG15 R	CAGCTCCGATAACAGCATGGA
IL-10	Interleukin, inflammatory antagonist	IL-10 F	CTGCTGGAGGACTTTAAGGGT
		IL-10 R	AGGGGAGAAATCGATGACAGC
IL-1β	Interleukin, pro-inflammatory response	IL1-beta F	AGGATATGAGCCGAGAAGTGGT
		IL1-beta R	CCCTTTCATCACACAAGACAGGT
IL-6	Interleukin, pro-inflammatory response	IL-6 F	TCTGGGTTCAATCAGGAGACCT
		IL-6 R	AGGGGTGCTTACTTCTTCTGGT
IL-8	Interleukin, pro-inflammatory response	IL-8 F	TGTGTGAAGCTGCAGTTCTGT
		IL-8 R	GCAGACCTCTCTTCCATTGGC
IL-15	Interleukin, induces proliferation of antiviral natural killer cells	IL-15 F	CAGCCTACAGAAGGTCATGAAGTACTC
		IL-15 R	GGGTAACTCCTTAAGTATCGAAGAAGAG
IL-2	Interleukin, cell-mediated immunity	IL-2 F	AAACTCTCCAGGATGCTCAC
		IL-2 R	TTTCAGATCCCTTCAGTTCC
IL-4	Interleukin, humoral immunity mediator	IL-4 F	CCCTGGTCTGCTTACTGGTTT
		IL-4 R	TCTCAGTCGTGTTCTTTGGGG
IL-12p35	Interleukin, cell-mediated immunity	IL-12p35 F2	AATCACCTGGACCACCTCAGT
		IL-12p35 R2	TCTAGGGTTTGTCTGGCCTTC

TNF-α	Cytokine, pro-inflammatory response	TNF-α F	TGGCCCAGACCCTCAGATCA
		TNF-α R	TTCCAGCTTCACACCATTGGC
CCL2	Chemokine, recruite monocytes and dendritic cells at the sites of inflammation	CCL2 F	CCAGTAAGAAGATCCCCATGCA
		CCL2 R	GTGTGGTCTTGAAGATCACAGCTT
CCL3	Inflammatory chemokine, attract monocytes, macrophages and neutrophils	CCL3 F	GCTCAGCGTCATGCAGGTGCC
		CCL3 R	AGCAGGCGGTTGGGGTGTCAG
CXCL1	Chemokine, attracts neutrophils	CXCL1 F	CGTGCAGGGAATTCACTTCAA
		CXCL1 R	GAGAGTGGCTACGACTTCCGTTT
MIF	Anti-inflammatory cytokine, macrophage migration inhibitory factor	MIF F	GCGAGTTGGTCGGTTCCTGTGTT
		MIF R	ACCACGTGCACTGCGATGTACT
CASP1	Enzyme, initiates inflammatory responses	CASP1 F	ACTCCACCAAGACCTCAACCAGT
		CASP1 R	GGGTAAATCTCCGCTGACTTCTCG
CASP10	Enzyme, involved in apoptosis and inflammation	CASP10 F	CGGTAGCCACGGGAACTGAGTCAT
		CASP10 R	ATCTTGCCAGGACCCCTCCGAT
CYLD	Enzyme, involved in transcription factor NF-κB activation	CYLD F	TCGGGATGGTGGTCAGAATGGC
		CYLD R	AGTCTTCGTGCACAGCCCTGGAT
AZI2	Enzyme, NF-κB-activating kinase-associated Protein 1	AZI2 F	TGAGCGTCTCCAGCGCTAA
		AZI2 R	CTGCACTTGCGTCACCAGAT
PACT	Enzyme, protein kinase activated by double-stranded RNA	PACT F	TGCAGTTCCTGACCCCTTAATG
		PACT R	GATGAATAGCCAGTTCCTGTAGTGAA
TBK1	Enzyme, activates the transcription factor IRF3	TBK1 F	GTACAGAAAGCAGAAAATGGACCAA
		TBK1 R	AACTTGAAGGCCCCGAGAAA
TRIM25	Enzyme and ISG, ubiquitination of RIG-1	TRIM25 F	GCCCGAGCTCCTACAGTATGC
		TRIM25 R	GAAGCGACGGTGTAGGTCTTG
NFKBIA	NF-κB inhibitor	NFKBIA F	TCCCTCTTTTCCCCGCAGGTT
		NFKBIA R	TGGAGTGGAGTCTGCTGCAGGT
TRADD	Adaptor, mediates NF-κB activation and apoptosis	TRADD F	CGGCCAGGAAGCAAGATG
		TRADD R	TGAAGACTCCACAAACAGGTATGC
CARD9		CARD9 F	GGCAGTGCAAGGTCCTGAAC

	Adaptor, activates pro-inflammatory and anti-inflammatory cytokines through NF-κB	CARD9 R	CAGGAGCACACCCACTTTCC
PYCARD	Adaptor, activates caspases and inflammasome	PYCARD F	CAAGCCAGCACCGCACTT
		PYCARD R	TCTGTCAGGACCTTCCCATACA
IFNLR1	Cellular receptor of type III IFNs	IFNLR1 F	CAGGGTGTGTGATCTGGAAGAG
		IFNLR1 R	GTCTGTGTCCAGAGAAATCCAGG
IFNAR1	Cellular receptor of type I IFNs	IFNAR1 F	TGCGAGGAAACCAAACCAGGAAAT
		IFNAR1 R	ACGACGACGATACAAACACCGC

dsRNA, double-stranded RNA; IFN, interferon; ISG, interferon-stimulated gene; PRR, pattern recognition receptor; ssRNA, single-stranded RNA.

Primer sets were designed to anneal in conserved transcribed regions of genes from five camelid species (alpaca, Bactrian camel, dromedary camel, llama, and wild Bactrian camel). Some of the genes were not annotated in the genome of llama (see **Appendix Table 5.1**) but exon/intron boundaries could be found by performing a BLASTn with the mRNA of other camelid species. The main features of the designed primer pairs are listed in **Appendix Table 5.2**.

Primer amplification efficacy and specificity

Pools of cDNAs prepared from stimulated PBMCs were used to evaluate the whole panel of primers in samples from alpaca, dromedary, and llama. Number of dilutions used for the generation of each standard curve, slopes, coefficients of determination and amplification efficiencies are listed in **Appendix Table 5.3**. After 48 h of PBMC stimulation, all gene transcripts were sufficiently expressed to generate standard curves using 3 to 5 serial dilutions, except for *IFNAR1* in samples from dromedary and *IFN-λ1* in those from dromedary camel and llama (**Appendix Table 5.3**). *IFN-λ3* was not expressed in PBMCs from any species, regardless of the

stimuli type (**Appendix Table 5.3**). All calibration curves produced linear standard curves, as evidenced by high coefficients of determination (>0.95, except for 1 sample that was 0.886). Primer pairs resulted in optimal amplification efficiencies in the different camelid species, ranging from 69 to 100%. Tm analyses confirmed a single specific amplicon for all amplified gene transcripts in all three camelid species. No amplifications occurred in no-RT and NTC samples included in the microfluidic RT-qPCR assays. Thus, most of the designed primer pairs targeting camelid cytokines and immune-related genes, as well as endogenous genes, displayed optimal specificity and efficacy suitable for immune response studies in camelid PBMCs.

Gene expression analyses of llama PBMCs by microfluidic RT-qPCR

Transcriptomic gene expression profile of llama PBMCs stimulated for 48 h with PHA and PMA-ionomycin were compared to those of unstimulated cells. Relative expression of the different genes grouped by functional categories is shown in **Figure 5.1a-j**. PHA and PMA-ionomycin stimulation provoked similar gene expression profiles in llama PBMCs. Both stimuli expressed *IFN-γ* at high levels (114 and 123 Fc, respectively), but none of the other type I or III IFNs were upregulated (**Figure 5.1a**). Within the category of ISGs, only *CXCL10* expression was induced by PHA and PMA-ionomycin (Fc of 7.89 and 5.37, respectively) and *MX1* (3.12 Fc) by PHA stimulated samples (**Figure 5.1c**). PHA and PMA-ionomycin provoked the upregulation of *CCL3* (3.21 and 4.60 Fc, respectively), *TNF-α* (2.30 and 2.50 Fc, respectively), *IRF7* (2.26 and 1.39 Fc, respectively), and *NFKB1* (1.62 and 1.80 Fc, respectively) (**Figure 5.1d**, **e** and **f**). High levels of *IL-6* (Fc of 79.82 and 62.47), *IL-2* (Fc of 71.32 and 80.30) and *IL-4* (Fc of 195.78 and 145.58) expression were

found of PHA and PMA-ionomycin stimulation, respectively (**Figure 5.1e** and **j**). Transcription of other pro- or anti-inflammatory cytokines, PRRs, adaptors, enzymes and IFN receptors were not induced in llama stimulated PBMCs (**Figure 5.1b**, **e**, **g**, **h** and **i**). Globally, the results obtained in llama cells were according to the expectancy that PHA and PMA-ionomycin provoke a marked polyclonal stimulation of PBMCs.

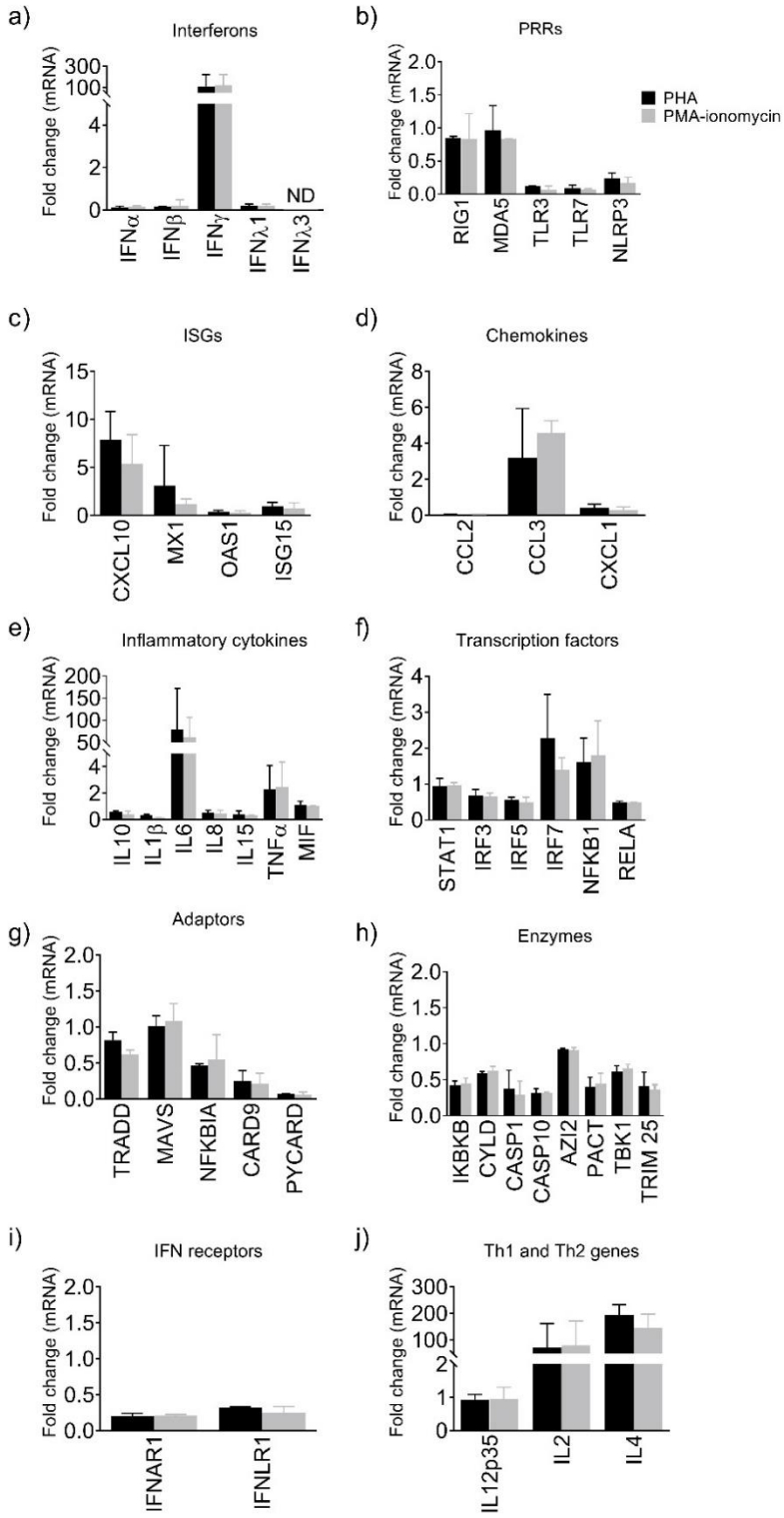
a)
Interferons
Fold change (mRNA)
300
100
4
2
0
ND
IFNα
IFNβ
IFNγ
IFNλ1
IFNλ3
b)
PRRs
Fold change (mRNA)
2.0
1.5
1.0
0.5
0.0
PHA
PMA-ionomycin
RIG1
MDA5
TLR3
TLR7
NLRP3
c)
ISGs
Fold change (mRNA)
15
10
5
0
CXCL10
MX1
OAS1
ISG15
d)
Chemokines
Fold change (mRNA)
8
6
4
2
0
CCL2
CCL3
CXCL1
e)
Inflammatory cytokines
Fold change (mRNA)
200
150
100
50
4
2
0
IL10
IL1β
IL6
IL8
IL15
TNFα
MIF
f)
Transcription factors
Fold change (mRNA)
4
3
2
1
0
STAT1
IRF3
IRF5
IRF7
NFKB1
RELA
g)
Adaptors
Fold change (mRNA)
2.0
1.5
1.0
0.5
0.0
TRADD
MAVS
NFKBIA
CARD9
PYCARD
h)
Enzymes
Fold change (mRNA)
2.0
1.5
1.0
0.5
0.0
IKBKB
CYLD
CASP1
CASP10
AZI2
PACT
TBK1
TRIM 25
i)
IFN receptors
Fold change (mRNA)
2.0
1.5
1.0
0.5
0.0
IFNAR1
IFNLR1
j)
Th1 and Th2 genes
Fold change (mRNA)
300
200
100
2
1
0
IL12p35
IL2
IL4

Figure 5.1. Relative expression of llama immune genes by microfluidic RT-qPCR. Gene expression profile of llama (L1-2) PBMCs stimulated for 48 h with PHA or PMA-ionomycin were compared to that from unstimulated cells. The relative standard curve method was applied for normalization purposes using multiple reference gene normalization (*GAPDH*, *HPRT1* and *UbC*). Immune genes were grouped by functional categories: (a) IFNs, (b) PRRs, (c) ISGs, inflammatory (d) chemokines and (e) cytokines, (f) transcription factors, downstream signalling (g) adaptors and (h) enzymes, (i) cellular receptors, and (j) cytokines involved in Th1 and Th2 response. Black and grey bars display differential expression of PHA and PMA-ionomycin stimulated PBMCs, respectively, relative to unstimulated cells. Relative expression data is displayed as mean fold-change differences ± SD. IFN, interferon; ISG, interferon-stimulated gene; PBMCs, peripheral blood mononuclear cells; PHA, phytohemagglutinin; PMA, phorbol 12-myristate 13-acetate; PRR, pattern-recognition receptor.

Gene expression analyses of alpaca PBMCs by microfluidic RT-qPCR

We utilized the same methodology to study immune gene expression in alpaca. Gene expression profile of unstimulated and stimulated PBMCs (PHA, PMA-ionomycin and PolyI:C) were compared to that of cells prior culture (**Figure 5.2**). Transcriptomic profile of unstimulated cells showed autoinduction of several genes from all categories by culturing for 48 h (**Figure 5.2a-j**). A stronger 65.74-fold upregulation was observed for *CCL2* (**Figure 5.2d**).

PHA and PMA-ionomycin stimulation triggered an upregulation of *RIG-1*, *MDA5*, *ISG15*, *CXCL1*, *IL-8*, and *TNF-α*, compared tonon-stimulated samples cultured for 48 h (**Figure 5.2b**, **c**, **d**, **e**). Moreover, expression of *IFN-γ*, *IL-10*, *IL-6*, *STAT-1*, *IRF7*, *NFKB1*, *CASP1*, *IL-2* and *IL-4* were upregulated with PHA (Figure 5.**2a**, **e**, **f**, **h** and **j**), while transcription of *CCL3*, *MX1*, *IL-15* increased in PMA-ionomycin stimulated PBMCs (**Figure 5.2d**, **c** and **e**).

On the other hand, PMBCs from three additional alpacas were cultured

with PolyI:C to ensure the functioning of primers targeting mRNA of impassive genes to PHA or PMA-ionomycin stimulation. PolyI:C exposure for 48 h resulted in the upregulation of different immune genes when compared with the previous polyclonal stimulations (*IFN-α*, *RIG-1*, *MDA5*, *TLR3*, *TLR7*, *NLRP3*, *MX1*, *OAS1*, *ISG15*, *IL-10*, *IL-6* and *IRF7*), some of them being expressed at high levels such as *IFN-β* (33.82 Fc), *CXCL10* (76.19 Fc), *CCL2* (93.33 Fc) and the transcription activator *STAT1* (18.56 Fc) (**Figure 5.2a-f**). Moreover, statistical analyses determined a significant increase in *IFN-β*, *RIG-1*, *MDA5*, *TLR7*, *NLRP3*, all ISGs, *STAT1* and *IRF7* expression levels compared to non-stimulated alpaca PBMCs cultured for 48h. Therefore, these results confirmed Poly I:C as a good *in vitro* immunostimulant of antiviral responses in alpaca PBMCs.

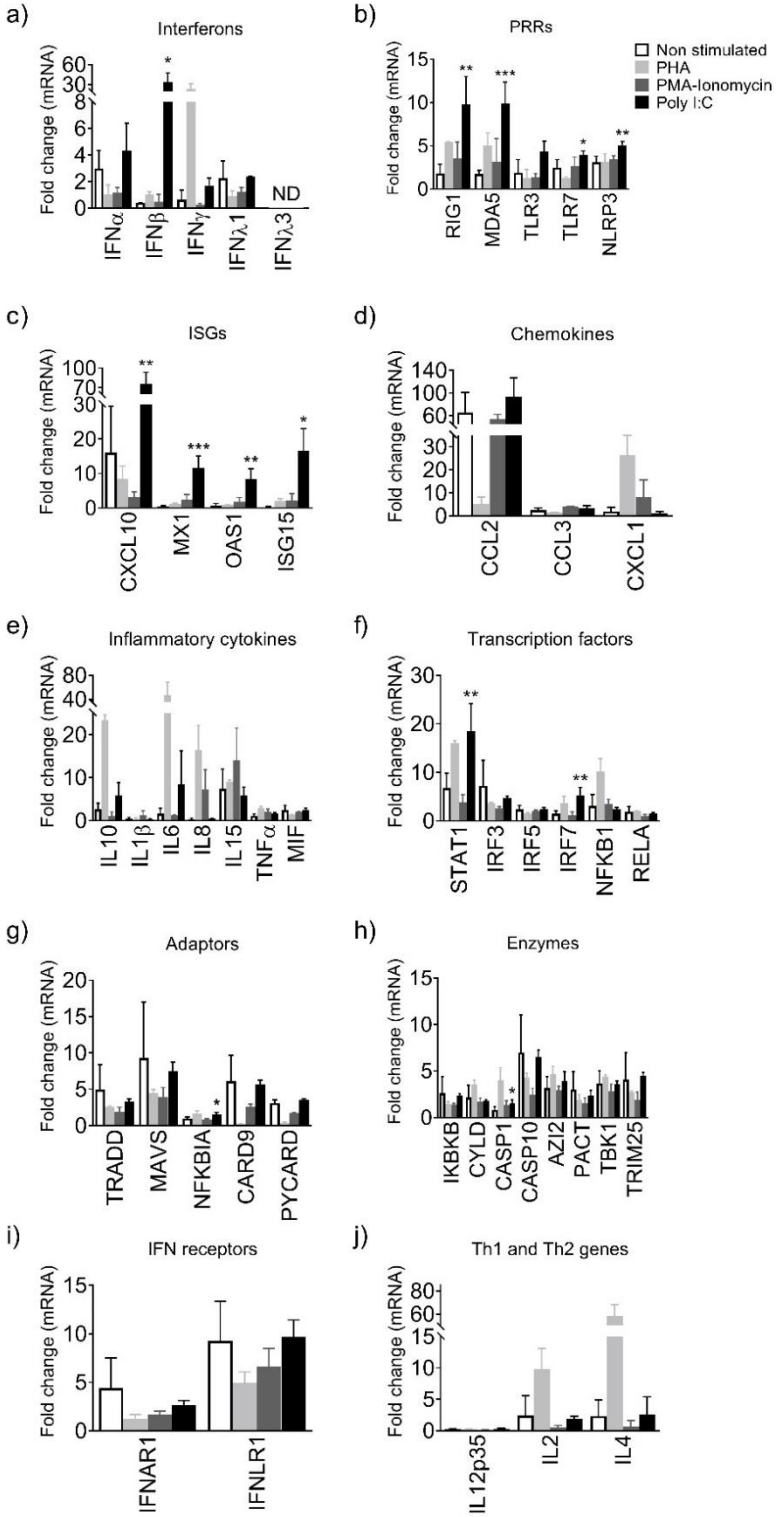
a)
Interferons
Fold change (mRNA)
IFNα
IFNβ
IFNγ
IFNλ1
IFNλ3
ND
b)
PRRs
Non stimulated
PHA
PMA-Ionomycin
Poly I:C
RIG1
MDA5
TLR3
TLR7
NLRP3
c)
ISGs
CXCL10
MX1
OAS1
ISG15
d)
Chemokines
CCL2
CCL3
CXCL1
e)
Inflammatory cytokines
IL10
IL1β
IL6
IL8
IL15
TNFα
MIF
f)
Transcription factors
STAT1
IRF3
IRF5
IRF7
NFKB1
RELA
g)
Adaptors
TRADD
MAVS
NFKBIA
CARD9
PYCARD
h)
Enzymes
IKBKB
CYLD
CASP1
CASP10
AZI2
PACT
TBK1
TRIM25
i)
IFN receptors
IFNAR1
IFNLR1
j)
Th1 and Th2 genes
IL12p35
IL2
IL4

Figure 5.2. Relative expression of alpaca immune genes by microfluidic RT-qPCR. Immune gene expression profile of alpaca PBMCs non-stimulated (empty bars) and stimulated with PHA (light grey bars), PMA-ionomycin (dark grey bars), or PolyI:C (black bars) for 48 h were compared to that from non-cultured cells. The relative standard curve method was applied for normalization purposes using multiple reference gene normalization (*GAPDH*, *HPRT1* and *UbC*). Immune genes were grouped by functional categories: (a) IFNs, (b) PRRs, (c) ISGs, inflammatory (d) chemokines and (e) cytokines, (f) transcription factors, downstream signalling (g) adaptors and (h) enzymes, (i) cellular receptors, and (j) cytokines involved in Th1 and Th2 response. Relative expression data is displayed as mean fold-change differences ± SD. Statistical significance was determined by unpaired t-test. *indicates p-value < 0.05; **indicates p-value < 0.01; ***indicates p-value < 0.001 compared with control samples obtained prior cell culture. IFN, interferon; ISG, interferon-stimulated gene; PBMCs, peripheral blood mononuclear cells; PHA, phytohemagglutinin; PMA, phorbol 12-myristate 13-acetate; PRR, pattern-recognition receptor.

Gene expression analyses of dromedary PBMCs by microfluidic RT-qPCR

Expression of dromedary immune genes in unstimulated and stimulated PBMCs were compared to that of fresh cells prior culture (**Figure 5.3a-j**). Non-stimulated PBMC samples showed that the expression of *IFN-α*, *RIG-1*, *TLR3*, *TLR7*, *IL-15*, *MIF*, *STAT1*, *IRF3*, *TRADD*, *MAVS*, *CARD9*, *PYCARD*, *IKBKB*, *CASP10*, *AZI2*, *PACT*, *TBK1*, *IL-2* and *IL-4* was upregulated after 48 h cell culture (**Figure 5.3a**, **b**, **e**, **f**, **g**, **h** and **j**). Furthermore, as depicted in **Figure 5.3d**, a higher expression of *CCL2* (20.89 Fc) was triggered by culturing PBMCs without specific stimuli, to similar levels than those induced by PHA stimulation (Fc of 21.61).

Furthermore, dromedary cells stimulated with PHA and PMA-ionomycin displayed similar transcriptomic profiles with characteristics of classical polyclonal stimulations. Relative to control samples prior culture, both PHA and PMA-ionomycin stimuli provoked the induction of *IFN-γ*, *CCL3*, *CXCL1*, *IL-6*, *IL-8*, *TNF-α*, *MIF*, *STAT1*, *NFKB1*, *TRADD*, *MAVS*, *AZI2*,

PACT, *TBK1*, *IL-2* and *IL-4* in higher relative expression levels than unstimulated PBMCs (**Figure 5.3A**, **D**, **E**, **F**, **G**, **H** and **J**). In addition, specific PHA stimulation led to an increase in the expression of *IFN-α*, *IFN-β*, *IFN-λ1*, *RIG-1*, *MDA5*, *NLPR3*, *CXCL10*, *MX1*, *OAS1*, *ISG15*, *IL-10*, *IL-15*, *IRF3*, *IRF5*, *IRF7*, *RELA*, *NFKBIA*, *IKBKB*, *CYLD*, *CASP10* and *TRIM25* in PBMCs of dromedary camels (**Figure 5.3A**, **B**, **C**, **E**, **F**, **G** and **H**). Overall, dromedary PBMCs were correctly stimulated by PHA and PMA-ionomycin, enhancing the immune-related gene expression in accordance with regular polyclonal stimulations.

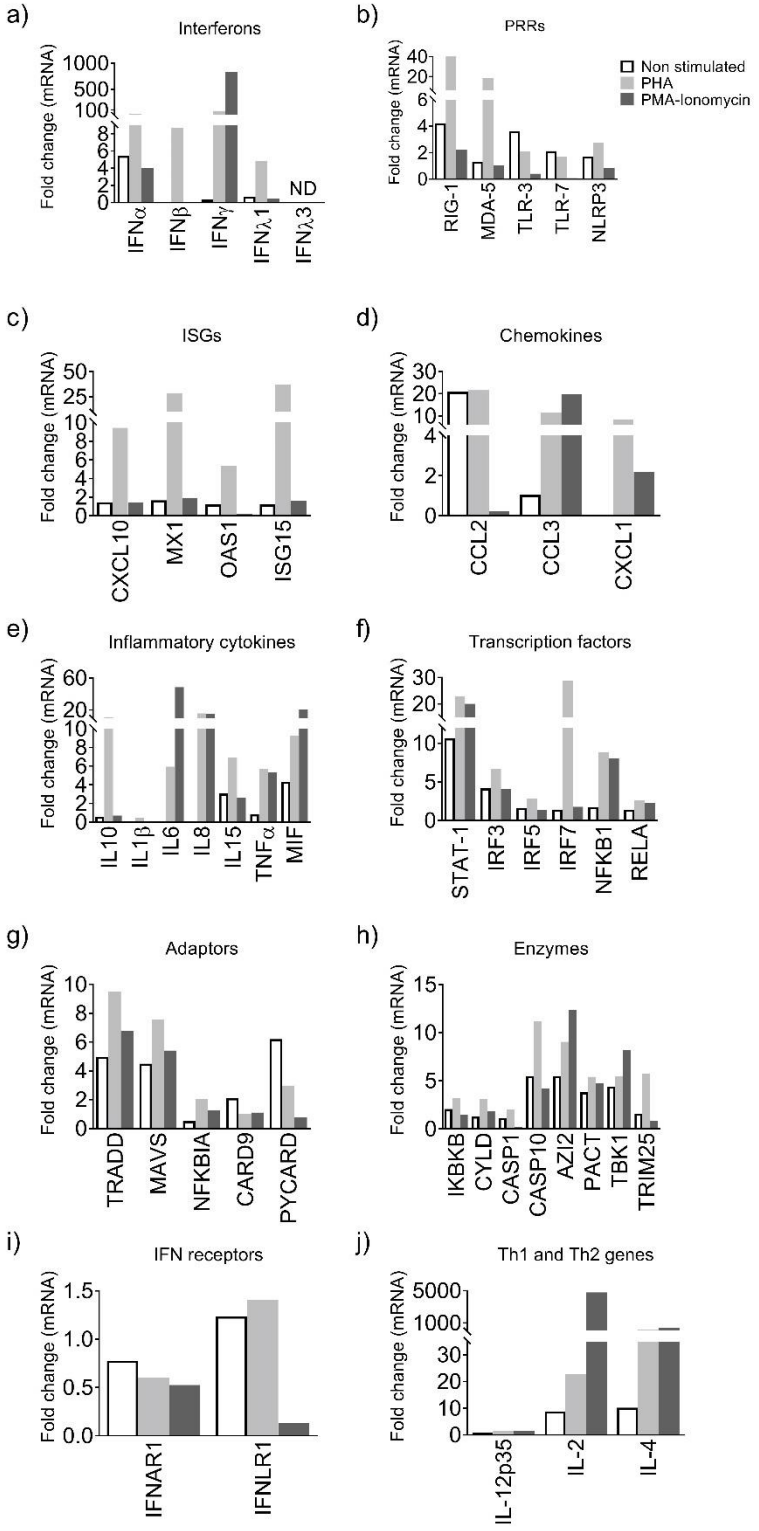
a)
Interferons
Fold change (mRNA)
1000
500
100
8
6
4
2
0
ND
IFNα
IFNβ
IFNγ
IFNλ1
IFNλ3
b)
PRRs
Fold change (mRNA)
40
20
6
4
2
0
Non stimulated
PHA
PMA-Ionomycin
RIG-1
MDA-5
TLR-3
TLR-7
NLRP3
c)
ISGs
Fold change (mRNA)
50
25
10
8
6
4
2
0
CXCL10
MX1
OAS1
ISG15
d)
Chemokines
Fold change (mRNA)
30
20
10
4
2
0
CCL2
CCL3
CXCL1
e)
Inflammatory cytokines
Fold change (mRNA)
60
20
10
8
6
4
2
0
IL10
IL1β
IL6
IL8
IL15
TNFα
MIF
f)
Transcription factors
Fold change (mRNA)
30
20
10
5
0
STAT-1
IRF3
IRF5
IRF7
NFKB1
RELA
g)
Adaptors
Fold change (mRNA)
10
8
6
4
2
0
TRADD
MAVS
NFKBIA
CARD9
PYCARD
h)
Enzymes
Fold change (mRNA)
15
10
5
0
IKBKB
CYLD
CASP1
CASP10
AZI2
PACT
TBK1
TRIM25
i)
IFN receptors
Fold change (mRNA)
1.5
1.0
0.5
0.0
IFNAR1
IFNLR1
j)
Th1 and Th2 genes
Fold change (mRNA)
5000
1000
30
20
10
0
IL-12p35
IL-2
IL-4

Figure 5.3. Relative expression of dromedary camel immune genes by microfluidic RT-qPCR. Immune gene expression profile of dromedary PBMCs non-stimulated (empty bars) and stimulated with PHA (light grey bars) or PMA-ionomycin (dark grey bars) for 48 h were compared to that from non-cultured cells. The relative standard curve method was applied for normalization purposes using multiple reference gene normalization (*GAPDH*, *HPRT1* and *UbC*). Immune genes were grouped by functional categories: (a) IFNs, (b) PRRs, (c) ISGs, inflammatory (d) chemokines and (e) cytokines, (f) transcription factors, downstream signalling (g) adaptors and (h) enzymes, (i) cellular receptors, and (j) cytokines involved in Th1 and Th2 response. Relative expression data is displayed as mean fold-change differences ± SD. Statistical significance was determined by unpaired t-test. *indicates p-value < 0.05; **indicates p-value < 0.01; ***indicates p-value < 0.001 compared with control samples obtained prior cell culture. IFN, interferon; ISG, interferon-stimulated gene; PBMCs, peripheral blood mononuclear cells; PHA, phytohemagglutinin; PMA, phorbol 12-myristate 13-acetate; PRR, pattern-recognition receptor.

5.4 Discussion

Due to the lack of reagent availability (i.e., antibodies) in several animal species, analysis of gene expression has become a common method to determine the immune transcriptomic profile after infection and/or vaccination. In this work, we developed an RT-qPCR method to monitor camelid innate and adaptive immune responses, which allow the quantification of forty-seven cytokines and immune-related genes in a single run. Importantly, the designed primer sets can be used for all camelid species using the same conditions (primer hybridization temperature) and methodology.

Several infectious diseases affect camelid species and threaten livestock productivity (Camel pox virus, trypanosomiasis and gastro-intestinal helminthiases, among others). Also, camelids are a source for several zoonotic viral and bacterial pathogens (MERS-CoV, Crimean-Congo haemorrhagic fever virus, Rickettsia spp, and others) which threaten

public health [365,382]. However, immune responses elicited upon infections of camelids remain largely unknown. Although a previous work provided tools to quantify inflammatory cytokines mRNA from llama [377], the primers were designed before annotation of camelid genomes was available [379]. Therefore, we designed new primers sets to develop more accurate assays.

First, we focused on the requirements to ensure a specific amplification of the products [383] and established a criteria for the subsequent design of primers. Although not all primer designs fulfilled all parameters of the criteria (i.e., genes with a single exon), specific amplification was determined together with the absence of amplification in no-RT and NTC controls, which ensured that gDNA amplification did not occur. In addition, three reference genes, (*GAPDH*, *HPRT1* and *UBC*) were selected to normalize gene expression [384–386]. These genes were reported to be stable for data normalization in T lymphocytes [387–389] and respiratory samples [8,390]. Choosing appropriate reference genes is crucial to achieve optimal data normalization, which is mandatory to discard sample-to-sample variations. Here, the selected normalizer genes were stable in PBMC samples from all the studied species, regardless the type of stimulation.

The designed reagents would allow to study camelid immune responses in most laboratories worldwide, including those in developing countries, which have been infrastructurally and technically upgraded to perform PCR-based assays since the recent influenza virus outbreaks and the COVID-19 pandemics. Nonetheless, to study expression analyses of a broad panel of genes in multiple samples by the gold standard RT-qPCR can result tedious and relatively expensive. Thus, we integrated the whole

set of designed primers in a unique Fluidigm Biomark microfluidic qPCR assay. Gene expression analyses showed that the transcription of some cytokines was spontaneously enhanced in camelid cells cultured without stimuli in the media. As previously reported in resting PBMCs [391,392], only mild autoinductions (2-10 Fc) were observed in camelid PBMCs, except for the higher relative expression of *CCL2* chemokine in all cultured PBMCs compared to uncultured cells. Although CCL2 regulation have been classically associated to NF-κB signalling pathway, our results support that a non-canonical upregulation of *CCL2* expression [393] occur by culturing camelid PBMCs in enriched media.

Furthermore, PHA and PMA stimulation produced strong induction of some cytokines and immune gene transcripts in camelid PBMCs, which displayed profiles commonly found in polyclonally activated lymphocytes of bovine [394] and human [395]. PBMCs from dromedary camel and llama underwent a robust increase in *IFN-γ*, *IL-2*, *IL-4*, *IL-6* expression after PHA and PMA-ionomycin exposure, and the same phenomenon occurred in alpaca PBMCs stimulated with PHA but not with PMA-ionomycin. Transcription of the pro-inflammatory *IL-8*, the anti-inflammatory *IL-10* and the transcription factor *STAT1* was also upregulated in polyclonally-stimulated alpaca and dromedary cells, but not in those from llama. Upregulation of *IL-8* and *STAT1* in camelid cells was expected since they are tightly regulated upon activation of the transcription factor NF-κB [396]. Similar to previous results [392], *IL-10* expression was only upregulated by PHA stimulation but PMA-ionomycin was ineffective. Furthermore, it is known that type I and III IFNs activate a different signalling pathway than IFN-γ does, which can lead to the expression of distinct ISGs (Sen et al., 2018; W. Wang et al., 2017). CXCL10 and CCL3 are typically classified as ISGs induced by IFN-γ [397,399]. Upregulation of these chemokines was

observed in all camelid samples expressing high levels of *IFN-γ*, apart from *CCL3* in PHA-stimulated PBMCs from alpaca, and *CXCL10* in dromedary cells stimulated with PMA-ionomycin. Generally, the stimulation of camelid cells using PHA and PMA-ionomycin did not activate the transcription of PRRs, adaptors, enzymes and IFN receptors compared to unstimulated controls. As observed in other mammalian species [394,400–403], PHA and PMA-ionomycin are potent antigen surrogate activators of Th1 and Th2 cytokine expression in alpaca, dromedary, and llama PBMCs. Our results support that PHA and PMA-ionomycin used for camelid T-cell activation, proliferation, and effective cytokine production.

Curiously, a broader gene expression profile was observed in dromedary PBMCs 48 h after PHA stimulation. Besides the activation of type II IFN signalling pathway, PHA also upregulated the expression of type I and III IFNs, as well as downstream genes regulated upon IFN signalling cascade activation. Consequently, strong induction of PRRs and ISGs occurred in dromedary samples but not in those from alpaca or llama. Expression of *IRF7* and *IL-10* were also exclusively upregulated in in PHA-stimulated dromedary PBMCs, in agreement with previous reports showing that both type I and III IFNs increase the transcription of *IRF7* factor *in vitro* [404], and that IL-10 production is enhanced as a type III IFN-stimulated gene [405]. Further analyses involving samples from more animals would help to rule out individual animal variations in cytokine levels and confirm whether dromedary camels have a broader immune response after PHA stimulation than other camelid species.

In vitro stimulation of PBMCs with PolyI:C is known to elicit the expression of other cytokines, mimicking certain aspects of viral infection

[406]. After 48 h stimulation, alpaca PolyI:C sensed PBMCs and increased the expression of type I IFNs, all studied PRRs and ISGs, along with the transcription factors *STAT1* and *IRF7*. Contrary to human PBMCs [407], alpaca lymphocytes exposed to PolyI:C induced type I but not type III IFNs. Previous investigations indicated that IFN-α was not produced by ovine and bovine PBMCs treated with PolyI:C [408], hence future studies could shed light on differential antiviral immune responses among livestock species. Globally, PolyI:C stimulation of camelid PBMCs yielded similar results than porcine and human PBMCs did [406,409,410]. Thus, we proved that Poly I:C is a good immunostimulant of antiviral responses in alpaca PBMCs. Despite it is highly probable, further research is needed to determine if other camelid species elicit similar immune responses.

Choosing an appropriate stimulus for studying immune responses is key to validate techniques in development and to use as positive control samples in subsequent established assays. In that respect, PHA and PMA-ionomycin stimulated a different signalling pathway than PolyI:C. Nonetheless, our assays revealed some differences in gene regulation between PHA and PMA-ionomycin stimulations. In line with previous works [392], PHA stimulation promoted the expression of a broader range of cytokines than PMA-ionomycin. This finding was expected because PMA-ionomycin stimulation bypasses T cell receptor-mediated activation and might reflect camelid lymphocyte stimulation with less physiological accuracy. A stronger induction of cytokines might be achieved by the stimulation of camelid cells with a combination of both PHA and PMA-ionomycin [391]. In the current work, regardless of the stimuli used to boost cytokine expression, none of the PBMC stimulation assays in any species showed detectable levels of *IFN-λ3* expression. The failure of a newly

developed reagent to detect a specific target gene raises concerns about its proper functionality. However, we previously demonstrated an appropriate quantification of *IFN-λ3* expression in the nasal epithelium of MERS-CoV infected alpacas [8,32], evidencing optimal functionality of the developed reagents. Primers targeting *IFN-λ3* were also designed to anneal mRNA of all camelid species, therefore, a correct functioning is also expected in samples from other camelids, although further studies are needed to confirm this hypothesis.

In summary, we developed a RT-qPCR method for the simultaneous quantification of cytokines and immune-related genes involved in major immune response signalling pathways of different camelid species. The novel assay was set up after the design of primers targeting immune genes and performing data normalization with three reference genes. The assays were validated using PBMCs from alpaca, dromedary camel and llama PBMCs after stimulation with PHA, PMA-ionomycin or PolyI:C. Microfluidic RT-qPCR results indicated that PBMCs from all camelid species stimulated with PHA and PMA-ionomycin mount robust Th1 and Th2 responses, besides PHA activation of type I and III IFN signalling pathways in dromedary lymphocytes. PolyI:C stimulation produced a marked antiviral response in alpaca PBMCs.

Appendix 5

Appendix Table 5.1. NCBI accession numbers of camelid gene sequences used for comparative analyses and primer design.

Gene	Species	GenBank accession number
GAPDH	Camelus dromedarius	XM_010990867.2
	Camelus bactrianus	XM_010957730.1
	Vicugna pacos	XM_006210852.2
	Camelus ferus	XM_006181646.3
HPRT1	Camelus dromedarius	XM_031446174.1
	Camelus bactrianus	XM_010968460.1
	Vicugna pacos	XM_031671409.1
	Camelus ferus	XM_032474943.1
UbC	Camelus dromedarius	XM_031442494.1
	Camelus bactrianus	XM_010969735.1
	Vicugna pacos	XM_031670203.1
	Camelus ferus	XM_032471921.1
IFN-α	Camelus dromedarius	XM_010999340.2
	Camelus bactrianus	XM_010946010.2
	Vicugna pacos	XM_015242649.2
	Camelus ferus	XM_032477607.1
IFN-β	Camelus dromedarius	XM_010988144.1
	Camelus bactrianus	XM_010958977.2
	Vicugna pacos	XM_006208258.1
	Camelus ferus	XM_006180372.1
IFN-γ	Lama glama	AB107652.1
	Camelus dromedarius	XM_031462226.1
	Camelus bactrianus	XM_010970501.1
	Vicugna pacos	XM_006205835.2
	Camelus ferus	XM_006189690.2
IFN-λ1	Camelus dromedarius	XM_010978654.2
	Camelus bactrianus	XM_010958621.1
	Vicugna pacos	XM_006206664.2
	Camelus ferus	XM_006174985.2
IFN-λ3	Camelus dromedarius	XM_010985161.1
	Camelus bactrianus	XM_010947318.1
	Vicugna pacos	XM_006219677.1

	Camelus ferus	XM_006195351.1
RIG-1 (DDX58)	Camelus dromedarius	XM_010975810.2
	Camelus bactrianus	XM_010967358.2
	Vicugna pacos	XM_031676595.1
	Camelus ferus	XM_006192497.3
MDA5 (IFIH1)	Camelus dromedarius	XM_010985569.2
	Camelus bactrianus	XM_010971381.1
	Vicugna pacos	XM_006196223.3
	Camelus ferus	XM_006190090.2
MAVS (VISA)	Camelus dromedarius	XM_010988239.2
	Camelus bactrianus	XM_010972744.1
	Vicugna pacos	XM_006207415.3
	Camelus ferus	XM_006187131.3
TLR3	Camelus dromedarius	XM_010995734.2
	Camelus bactrianus	XM_010953279.2
	Vicugna pacos	XM_015249164.2
	Camelus ferus	XM_014553913.2
TLR7	Camelus dromedarius	XM_010993639.2
	Camelus bactrianus	XM_010966214.1
	Vicugna pacos	XM_006212620.2
	Camelus ferus	XM_006193069.2
NLRP3	Camelus dromedarius	XM_010997883.2
	Camelus bactrianus	XM_010950280.2
	Vicugna pacos	XM_031673306.1
	Camelus ferus	XM_006177988.3
STAT1	Camelus dromedarius	XM_010979711.2
	Camelus bactrianus	XM_010948718.2
	Vicugna pacos	XM_031678037.1
	Camelus ferus	XM_006186813.3
IRF3	Camelus dromedarius	XM_010993178.2
	Camelus bactrianus	XM_045510710.1
	Vicugna pacos	XM_006208451.3
	Camelus ferus	XM_006173792.3
IRF5	Camelus dromedarius	XM_010975643.2
	Camelus bactrianus	XM_010947554.2
	Vicugna pacos	XM_006202276.3

	Camelus ferus	XM_032483311.1
IRF7	Camelus dromedarius	XM_031448349.1
	Camelus bactrianus	XM_010956145.2
	Vicugna pacos	XM_015251986.1
	Camelus ferus	XM_032490347.1
NFKB1	Camelus dromedarius	XM_010980636.2
	Camelus bactrianus	XM_010953589.2
	Vicugna pacos	XM_031690344.1
	Camelus ferus	XM_006188020.3
RELA	Camelus dromedarius	XM_031448012.1
	Camelus bactrianus	XM_010957140.2
	Vicugna pacos	XM_031690897.1
	Camelus ferus	XM_032489838.1
IKBKB	Camelus dromedarius	XM_031440029.1
	Camelus bactrianus	XM_010957873.2
	Vicugna pacos	XM_031691563.1
	Camelus ferus	XM_006188385.3
CXCL10	Camelus dromedarius	XM_010983050.2
	Camelus bactrianus	XM_010969313.2
	Vicugna pacos	XM_006198241.3
	Camelus ferus	XM_006176316.3
MX1	Camelus dromedarius	XM_031459860.1
	Camelus bactrianus	XM_010958347.2
	Vicugna pacos	XM_006204960
	Camelus ferus	XM_032461929.1
OAS1	Camelus dromedarius	XM_031443284.1
	Camelus bactrianus	XM_010969608.2
	Vicugna pacos	XM_031670190.1
	Camelus ferus	XM_032472237.1
ISG15	Camelus dromedarius	XM_010999398.2
	Camelus bactrianus	XM_010957998.2
	Vicugna pacos	XM_015237784.2
	Camelus ferus	XM_014551219.2
IL-10	Lama glama	AB107649.1
	Camelus dromedarius	JQ917916.1
	Camelus bactrianus	NM_001303520.1
	Vicugna pacos	XM_006215461.3
	Camelus ferus	XM_006182265.3

IL-1β	Lama glama	AB107644.1
	Camelus dromedarius	XM_010984994.2
	Camelus bactrianus	XM_010958977.2
	Vicugna pacos	XM_006203828.3
	Camelus ferus	XM_006183589.3
IL-6	Lama glama	AB107647.1
	Camelus dromedarius	XM_010987177.2
	Camelus bactrianus	AB107656.1
	Vicugna pacos	XM_006201793.2
	Camelus ferus	XM_006179204.2
IL-8 (CXCL8)	Camelus dromedarius	KF843702.1
	Camelus bactrianus	XM_010969343.2
	Vicugna pacos	XM_006212530.3
	Camelus ferus	XM_006188697.3
IL-15	Camelus dromedarius	XM_010978726.2
	Camelus bactrianus	XM_010954603.2
	Vicugna pacos	XM_015249496.2
	Camelus ferus	XM_006193545.3
IL-2	Lama glama	AB107651.1
	Camelus dromedarius	NM_001303548.1
	Camelus bactrianus	AB246671.1
	Vicugna pacos	KM205215.1
	Camelus ferus	XM_006180708.3
IL-4	Lama glama	AB107648.1
	Camelus dromedarius	HM051106.1
	Camelus bactrianus	AB246673.1
	Vicugna pacos	XM_006212826.3
	Camelus ferus	XM_006179596.2
IL-12p35	Lama glama	AB107653.1
	Camelus dromedarius	XM_010986258.2
	Camelus bactrianus	AB246672.1
	Vicugna pacos	XM_031679452.1
	Camelus ferus	XM_006190436.3
TNF-α	Lama glama	AB107646.1
	Camelus dromedarius	NM_001319880.1
	Camelus bactrianus	NM_001319779.1
	Vicugna pacos	XM_006215316.2
	Camelus ferus	XM_006178751.3

MCP-1 (CCL2)	Camelus dromedarius	XM_010979035.2
	Camelus bactrianus	XM_010970431.2
	Vicugna pacos	XM_006212021.3
	Camelus ferus	XM_006185837.3
MIP-1α (CCL3)	Camelus dromedarius	XM_010990500.2
	Camelus bactrianus	XM_010949170.2
	Vicugna pacos	XM_006213334.3
	Camelus ferus	XM_006174846.3
CXCL1	Camelus dromedarius	XM_031462577.1
	Camelus bactrianus	XM_010969410.2
	Vicugna pacos	XM_031684028.1
	Camelus ferus	XM_032458086.1
MIF	Camelus dromedarius	XM_031442393.1
	Camelus bactrianus	XM_010955454.2
	Vicugna pacos	NM_001287197.1
	Camelus ferus	XM_014552697.2
CASP1	Camelus dromedarius	XM_010993435.2
	Camelus bactrianus	XM_010953176.2
	Vicugna pacos	XM_015249739.2
	Camelus ferus	XM_014560469.2
CASP10	Camelus dromedarius	XM_010991974.2
	Camelus bactrianus	XM_010971860.2
	Vicugna pacos	XM_006205263.3
	Camelus ferus	XM_006189972.3
CYLD	Camelus dromedarius	XM_031458461.1
	Camelus bactrianus	XM_010961754.2
	Vicugna pacos	XM_015242273.2
	Camelus ferus	XM_006183539.3
AZI2	Camelus dromedarius	XM_010977820.2
	Camelus bactrianus	XM_010959645.2
	Vicugna pacos	XM_006200749.3
	Camelus ferus	XM_032459400.1
PACT (PRKRA)	Camelus dromedarius	XM_010991356.2
	Camelus bactrianus	XM_010959971.2
	Vicugna pacos	XM_006210217.3
	Camelus ferus	XM_032479782.1

TBK1	Camelus dromedarius	XM_031462774.1
	Camelus bactrianus	XM_010970514.2
	Vicugna pacos	XM_031683111.1
	Camelus ferus	XM_032493328.1
TRIM25	Camelus dromedarius	XM_010990378.2
	Camelus bactrianus	XM_010951086.2
	Vicugna pacos	XM_031685141.1
	Camelus ferus	XM_014556519.2
NFKBIA	Camelus dromedarius	XM_010983796.2
	Camelus bactrianus	XM_010967860.2
	Vicugna pacos	XM_031678782.1
	Camelus ferus	XM_032481888.1
TRADD	Camelus dromedarius	XM_031458299.1
	Camelus bactrianus	XM_010962447.2
	Vicugna pacos	XM_006203676.3
	Camelus ferus	XM_032486508.1
CARD9	Camelus dromedarius	XM_031450838.1
	Camelus bactrianus	XM_010955930.2
	Vicugna pacos	XM_006218359.3
	Camelus ferus	XM_032478794.1
PYCARD	Camelus dromedarius	XM_010980820.2
	Camelus bactrianus	XM_010972413.2
	Vicugna pacos	XM_015236916.2
	Camelus ferus	XM_006181480.3
IFNLR1	Camelus dromedarius	XM_010989801.2
	Camelus bactrianus	XM_045518428.1
	Vicugna pacos	XM_031683805.1
	Camelus ferus	XM_032495478.1
IFNAR1	Camelus dromedarius	XM_010981032.2
	Camelus bactrianus	XM_010956566.2
	Vicugna pacos	XM_006216038.3
	Camelus ferus	XM_014561608.2

Appendix Table 5.2. Features of the primer pairs designed for the quantification of camelid immune and reference genes by RT-qPCR. For primers designed at exon-exon boundaries, the percentage of nucleotides annealing each exon respect to the total number of nucleotides of the primer is indicated.

Gene name	Primer Name	Primers (5' - 3')	Exon location	Length (bp)	Tm (°C)	GC%	GC Clamp	Cross Dimer (ΔG)	Self Dimer (ΔG)	Hairpin (ΔG)	Product size (bp)
GAPDH	GAPDH F	GGTCGGAGTGAACGGATTTGG	2 (71%)/3 (29%)	21	58.53	57.14	2	-0.9	0.0	0.0	108
	GAPDH R	TTGAGGTCAATGAAGGGGTCG	3	21	57.19	52.38	2	-0.9	-2.0	-0.7	
UbC	UbC F	AGGCGAAGATCCAAGACAAGG	2	21	57.27	52.38	2	-3.8	-2.0	0.0	129
	UbC R	CCAAGTGCAGAGTGGATTCCT	2	21	57.18	52.38	2	-3.8	-3.4	-1.5	
HPRT1	HPRT1 F	CAAAGATGGTCAAGGTCGCAA	6	21	56.37	47.62	3	-1.5	0.0	0.0	82
	HPRT1 R	TCAAATCCAACAAAGTCTGGTCT	7 (43%)/8 (57%)	23	55.85	39.13	3	-1.5	0.0	-1.5	
IFN-α	IFN-α F	TCTTCAGCGAGACACTTGCAA	1	21	57.43	47.62	2	-2.5	-5.7	-0.7	87
	IFN-α R	GTTGGTCAGTGAGAATCATTTCCA	1	24	57.1	41.67	2	-2.5	-1.5	-1.5	
IFN-β	IFN-β F2	GCATCCTCCAAATCGCTCTCC	1	21	58.39	57.14	2	-2.9	0	0.0	99
	IFN-β R2	ATGCCAAGTTGCTGCTCCTTT	1	21	58.27	47.62	2	-2.9	-0.7	-0.5	
IFN-γ	IFN-γ F	ACTGGAAAGAGGAGAGTGACAAAA	3	24	57.67	41.67	1	-1.8	-0.8	-0.8	199
	IFN-γ R	CAACCGGAATTTGAATCAGCT	3 (80%) /4 (20%)	21	54.39	42.86	1	-1.8	-4.3	-0.7	
IFN-λ1	IFN-λ1 F	CTGCCACATGGGCTGGTT	1	18	56.6	61.11	2	-3.9	-2.4	-2.4	82
	IFN-λ1 R	CGATTCTTCCAAGGCATCCTT	1	21	55.57	47.62	2	-3.9	-2.4	-2.4	
IFN-λ3	IFN-λ3 F	CCACCTGGCCCAATTCAA	1	18	53.77	55.56	1	-2.4	-4.4	0.0	81
	IFN-λ3 R	AGTGACTCTTCAAAGGCGTCCTT	1 (52.2%) / 2 (47.8%)	23	59.71	47.83	1	-2.4	-2.4	-2.4	
RIG-1	RIG-1 F	ACAAGTCAGAACACAGGAATGA	15 (73%)/16 (27%)	22	55.01	40.91	1	-3.7	-0.9	-0.9	199

	RIG-1 R	CTCTTCCTCTGCCTCTGGTTT	16 (43%)/17 (57%)	21	56.55	52.38	1	-3.7	0.0	0.0	
MDA5	MDA5 F	ACACCAGAGTTCAAGAGACTGTAT	14 (60%)/15 (40%)	24	57.00	41.67	1	0.0	-1.1	-1.1	129
	MDA5 R	CACCATCATCGTTCCCCAAGA	15 (5%)/16 (95%)	21	57.26	52.38	1	0.0	0.0	0.0	
MAVS	MAVS F	CAGCCTCCACAACTGCTACAGA	4	22	59.68	54.55	1	-4.7	-1.8	-1.8	106
	MAVS R	CTGTGGGACTTTCTTTGAACTCTCT	4 (16%) / 5 (84%)	25	58.73	44	1	-4.7	-0.6	-0.6	
TLR3	TLR3 F	AGAAATAGACAGACAGCCAGAG	5	22	54.72	45.45	1	-2.2	0.0	0.0	197
	TLR3 R	TGCTCCTTTTGATGCTATTAACGA	5	24	56.69	37.5	1	-2.2	-0.8	0.0	
TLR7	TLR7 F	AGAGAGGAGTCACCAGCGTAT	3	21	57.23	52.38	2	-1.5	0.0	0.0	104
	TLR7 R	GACACAAATGCAAATGGAGAC	3	21	53.34	42.86	2	-1.5	-3.4	0.0	
NLRP3	NLRP3 F	ATGGCCACATGGATTTTTGC	1	20	54.55	45	2	-3.9	-7.2	-0.5	91
	NLRP3 R	AAACATTGGCATTGTCCCATTC	1 (31.8%) / 2 (68.2%)	22	55.51	40.91	2	-3.9	-1.5	-1.5	
STAT1	STAT1 F	TCTCTGTGTCTGAAGTTCACCCT	25 (65%)/26 (35%)	23	58.56	47.83	3	-4.3	-2.0	-1.3	191
	STAT1 R	GGGAATCACAGGTGGGAAGGA	27	21	58.59	57.14	3	-4.3	-1.3	0.0	
IRF3	IRF3 F	TCACCACGCTACACCCTCTGGT	7	22	62.69	59.09	2	-2.9	-2.9	-2.9	102
	IRF3 R	GAGGCACATGGGCACAACCTTGA	7 (17.4%) / 8 (86.6%)	23	63.25	56.52	2	-2.9	-2.3	-1.3	
IRF5	IRF5 F	TCAGAAGGGCCAGACCAACACC	7	22	61.84	59.09	2	-2.4	-4.4	0.0	121
	IRF5 R	TGCTACGGGCACCACCTGTA	7(20%) / 8 (80%)	20	60.25	60	2	-2.4	-2.0	-2.0	
IRF7	IRF7 F	CGTGATGTTGCAAGACAACTCA	3	22	57.22	45.45	1	-2.4	-5.7	-2.4	96
	IRF7 R	TGGTTAACGCCTGGGTCTCT	3 (25%) / 4 (75%)	20	57.72	55	1	-2.4	-4.3	0.0	
NFKB1	NFKB1 F	GGGACAGTGTCTTACACTTAGCAATC	13 (26.9%) /14 (73.1%)	26	59.8	46.15	1	-1.3	-4.0	-4.0	90
	NFKB1 R	CATCAGAAATCAAGCCAGATGTG	14	23	55.79	43.48	1	-1.3	-2.1	-2.1	
RELA	RELA F	AGAGTCCTTTCAATGGCCCCACCG	7 (66.7%) / 8 (33.3%)	24	64.61	58.33	3	-2.4	-4.4	0.0	81

	RELA R	GGATGGAAGTTGAGCTGCGGGA	8	22	62.27	59.09	3	-2.4	-3.0	0.0	
IKBKB	IKBKB F	TAATGAACGAAGACGAGAAGATGGT	18	25	58.16	40	2	-4.4	0.0	0.0	91
	IKBKB R	ACCTTGCTACACGCAATCTTCAG	18 (78.3%) /19 (21.7%)	23	59.11	47.83	2	-4.4	-3.1	-3.1	
CXCL10	CXCL10 F	CGTGTTGAGATTATTGCCACAATG	2 (54%)/3 (46%)	24	57.13	41.67	1	-2.3	-1.7	-1.7	184
	CXCL10 R	GAGGTAGCTTCTCTCTGGTCCT	4	22	57.76	54.55	1	-2.3	-3.0	-1.3	
MX1	MX1 F	GAAGATGGTTTATTCTGACTCG	2	22	52.21	40.91	2	-0.7	-0.7	-0.7	146
	MX1 R	TTCTCCTCGTACTGGCTGT	3	19	54.29	52.63	2	-0.7	-2.0	0.0	
OAS1	OAS1 F	TGAAGAAGCAGCTCGGGAAAC	8	21	58.11	52.38	1	-1.8	-3.0	0.0	198
	OAS1 R	AGTAACTGTCTTTTCTGGGCAGC	9 (22%)/10 (78%)	23	58.72	47.83	1	-1.8	-1.1	-1.1	
ISG15	ISG15 F M	CACAGCCATGGGTGGAATC	1 (47.4%) / 2 (52.6%)	19	55.19	57.89	1	-4.2	-6.1	-1.5	91
	ISG15 R M	CAGCTCCGATAACAGCATGGA	2	21	57.43	52.38	1	-4.2	-3	-1.8	
IL-10	IL-10 F	CTGCTGGAGGACTTTAAGGGT	2 (85%) /3 (15%)	21	56.54	52.38	3	-3.5	-0.8	0.0	187
	IL-10 R	AGGGGAGAAATCGATGACAGC	3 (24%)/4 (76%)	21	57.06	52.38	3	-3.5	-5.0	0.0	
IL-1β	IL1-β F	AGGATATGAGCCGAGAAGTGGT	5 (82%)/6 (18%)	22	58.08	50.00	2	-1.8	-0.5	0.0	125
	IL1-β R	CCCTTTCATCACACAAGACAGGT	6	23	58.39	47.83	2	-1.8	-1.3	-1.3	
IL-6	IL-6 F	TCTGGGTTCAATCAGGAGACCT	3 (68%)/4 (32%)	22	57.86	50.00	2	-1.5	-1.5	-1.5	192
	IL-6 R	AGGGGTGCTTACTTCTTCTGGT	5	22	58.4	50.00	2	-1.5	0.0	0.0	
IL-8	IL-8 F	TGTGTGAAGCTGCAGTTCTGT	1 (43%)/2 (57%)	21	57.62	47.62	1	-3.5	-6.5	-0.6	176
	IL-8 R	GCAGACCTCTCTTCCATTGGC	3	21	58.24	57.14	1	-3.5	-1.5	-0.7	
IL-15	IL-15 F	CAGCCTACAGAAGGTCATGAAGTACTC	2 (66.7%) / 3 (33.3%)	27	61.09	48.15	1	-2.4	-4.9	-1.3	93
	IL-15 R	GGGTAACTCCTTAAGTATCGAAGAAGAG	3	28	59.22	42.82	1	-2.4	-3.9	-1.0	

IL-2	IL-2 F*	AAACTCTCCAGGATGCTCAC*	2	20	54.17	50	1	-2.3	-1.3	0.0	202
	IL-2 R	TTTCAGATCCCTTCAGTTCC	3 (50%) /4 (50%)	20	51.6	45	1	-2.3	-2.0	0.0	
IL-4	IL-4 F	CCCTGGTCTGCTTACTGGTTT	1	21	57.10	52.38	2	-2.5	0.0	0.0	168
	IL-4 R	TCTCAGTCGTGTTCTTTGGGG	2 (38%)/3 (62%)	21	57.14	52.38	2	-2.5	0.0	0.0	
IL-12p35	IL-12p35 F	AATCACCTGGACCACCTCAGT	2	21	57.88	52.38	1	-1.5	-1.5	-1.1	140
	IL-12p35 R	TCTAGGGTTTGTCTGGCCTTC	2 (15%)/3 (85%)	21	56.55	52.38	1	-1.5	-4.4	-1.3	
TNF-α	TNF-α F	TGGCCCAGACCCTCAGATCA	2 (75%)/3 (25%)	20	59.30	60.00	1	-2.4	-4.4	0.0	143
	TNF-α R	TTCCAGCTTCACACCATTGGC	4	21	58.63	52.38	1	-2.4	-3.0	-1.5	
CCL2	CCL2 F	CCAGTAAGAAGATCCCCATGCA	2	22	57.23	50	2	-2	-3.4	0.0	93
	CCL2 R	GTGTGGTCTTGAAGATCACAGCTT	2 (41.6%) / 3 (58.4%)	24	59.15	45.83	2	-2	-3.0	-2.7	
CCL3	CCL3 F	GCTCAGCGTCATGCAGGTGCC	1	21	63.98	66.67	3	-2.4	-3.4	0.0	113
	CCL3 R	AGCAGGCGGTTGGGGTGTCAG	2	21	64.45	66.67	3	-2.4	0.0	0.0	
CXCL1	CXCL1 F	CGTGCAGGGAATTCACTTCAA	3	21	56.37	47.62	1	-2.5	-4.3	-1.3	91
	CXCL1 R	GAGAGTGGCTACGACTTCCGTTT	3 (56.5%) / 4 (43.5%)	23	60.15	52.17	1	-2.5	-1.9	-1.9	
MIF	MIF F	GCGAGTTGGTCGGTTCCTGTGTT	1	23	63.19	56.52	1	-2.9	-1.8	-1.8	176
	MIF R	ACCACGTGCACTGCGATGTACT	1 (9%) / 2 (91%)	22	62.18	54.55	1	-2.9	-6.8	0.0	
CASP1	CASP1 F	ACTCCACCAAGACCTCAACCAGT	2	23	60.97	52.17	1	-1.5	-0.8	-0.8	164
	CASP1 R	GGGTAAATCTCCGCTGACTTCTCG	3 (62.5%) / 4 (37.5%)	24	60.92	54.17	1	-1.5	0.0	0.0	
CASP10	CASP10 F	CGGTAGCCACGGGAACTGAGTCAT	5	24	64.12	58.33	1	-2.4	-0.9	0	107
	CASP10 R	ATCTTGCCAGGACCCCTCCGAT	5 (18.2%) / 6 (82.8%)	22	62.6	59.09	1	-2.4	-1.3	-1.3	
CYLD	CYLD F	TCGGGATGGTGGTCAGAATGGC	17 (41%) / 18 (59%)	22	62.02	59.09	3	-2.4	0.0	0.0	135
	CYLD R	AGTCTTCGTGCACAGCCCTGGAT	18	23	63.83	56.52	3	-2.4	-6.8	0.0	

AZI2	AZI2 F	TGAGCGTCTCCAGCGCTAA	6 (68.4%) / 7 (31.6%)	19	58.03	57.89	2	-2.9	-7.7	-4.1	86
	AZI2 R	CTGCACTTGCGTCACCAGAT	6	20	57.95	55	2	-2.9	-3.4	-1.1	
PACT	PACT F	TGCAGTTCCTGACCCCTTAATG	3	22	57.71	50	1	-1.1	-3.4	-1.1	92
	PACT R	GATGAATAGCCAGTTCCTGTAGTGAA	3 (38.5%) / 4 (61.5%)	26	58.84	42.31	1	-1.1	-1.1	-1.1	
TBK1	TBK1 F	GTACAGAAAGCAGAAAATGGACCAA	7	25	58.05	40	2	-0.7	-2.0	0.0	81
	TBK1 R	AACTTGAAGGCCCCGAGAAA	7 (35%) / 8 (65%)	20	56.42	50	2	-0.7	-4.4	0.0	
TRIM25	TRIM25 F	GCCCGAGCTCCTACAGTATGC	7 (81.0%) / 8 (19.0%)	21	59.86	61.9	2	-5.2	-6.2	0.0	93
	TRIM25 R	GAAGCGACGGTGTAGGTCTTG	8	21	58.29	57.14	2	-5.2	-1.1	-1.1	
NFKBIA	NFKBIA F	TCCCTCTTTTCCCCGCAGGTT	2	21	60.88	57.14	2	-3.5	-1.3	-1.3	138
	NFKBIA R	TGGAGTGGAGTCTGCTGCAGGT	2 (40.1%) / 3 (59.9%)	22	62.96	59.09	2	-3.5	-6.5	-1.1	
TRADD	TRADD F	CGGCCAGGAAGCAAGATG	1 (38.9%) / 2 (61.1%)	18	54.92	61.11	1	-2.0	-4.4	0.0	81
	TRADD R	TGAAGACTCCACAAACAGGTATGC	2	24	58.91	45.83	1	-2.0	0.0	0.0	
CARD9	CARD9 F	GGCAGTGCAAGGTCCTGAAC	1	20	58.5	60	1	-4.3	-3.4	-1.1	92
	CARD9 R	CAGGAGCACACCCACTTTCC	1 (45%) / 2 (55%)	20	57.85	60	1	-4.3	-1.3	-1.3	
PYCARD	PYCARD F	CAAGCCAGCACCGCACTT	2 (44.4%) / 3 (65.6%)	18	57.69	61.11	1	-1.1	-0.5	-0.5	105
	PYCARD R	TCTGTCAGGACCTTCCCATACA	3	22	57.69	50	1	-1.1	-1.3	-1.3	
IFNLR1	IFNLR1 F	CAGGGTGTGTGATCTGGAAGAG	6	22	57.81	54.55	1	-5.6	-2.0	-1.1	90
	IFNLR1 R	GTCTGTGTCCAGAGAAATCCAGG	6 (17.4%) / 7 (82.6%)	23	58.29	52.17	1	-5.6	-2.4	-2.4	
IFNAR1	IFNAR1 F	TGCGAGGAAACCAAACCAGGAAAT	9 (84.3%) / 10 (16.7%)	23	61.12	45.83	1	-2.9	0.0	0.0	83
	IFNAR1 R	ACGACGACGATACAAAACACCGC	11	24	61.75	52.17	1	-2.9	0.0	0.0	

The asterisk (*) indicates a primer described by Odbileg et al. (2008). Tm was calculated for each primer at 3 mM of free Mg^{2+} concentration. bp, base pairs; C, cytosine; G, guanine; GC clamp, presence of a guanine or cytosine base in the last 5 bases (3′ end) of a primer; Tm, melting temperature.

Appendix Table 5.3. Performance of the primer pairs designed for the quantification of mRNA expression of camelid immune and reference genes. Each primer pair was validated using PBMCs of alpaca, dromedary camel and llama stimulated with a mixture of PHA and PMA-ionomicyn or PolyI:C.

Gene	Species	Stimulus	N. of standard dilutions	Slope	R^2	Efficacy	Efficacy (%)
GAPDH	Alpaca	PHA/PMA-ionomycin	5	-3.76	1.00	1.84	84.38
	Alpaca	Poly I:C	5	-3.78	1.00	1.84	83.96
	Llama	PHA/PMA-ionomycin	5	-3.76	1.00	1.85	84.52
	Dromedary	PHA/PMA-ionomycin	5	-3.73	0.99	1.85	85.49
HPRT1	Alpaca	PHA/PMA-ionomycin	5	-3.77	1.00	1.84	84.32
	Alpaca	Poly I:C	5	-3.84	1.00	1.82	82.24
	Llama	PHA/PMA-ionomycin	5	-3.85	1.00	1.82	81.92
	Dromedary	PHA/PMA-ionomycin	5	-3.90	1.00	1.81	80.60
UbC	Alpaca	PHA/PMA-ionomycin	5	-3.68	1.00	1.87	86.85
	Alpaca	Poly I:C	5	-3.66	1.00	1.88	87.58
	Llama	PHA/PMA-ionomycin	5	-3.75	1.00	1.85	84.80
	Dromedary	PHA/PMA-ionomycin	5	-3.78	1.00	1.84	83.75
IFN-α	Alpaca	PHA/PMA-ionomycin	5	-3.69	1.00	1.87	86.63
	Alpaca	Poly I:C	5	-3.66	1.00	1.88	87.52
	Llama	PHA/PMA-ionomycin	4	-3.91	0.98	1.80	80.26
	Dromedary	PHA/PMA-ionomycin	5	-3.45	0.98	1.95	94.91
IFN-β	Alpaca	PHA/PMA-ionomycin	4	-3.97	1.00	1.79	78.64
	Alpaca	Poly I:C		Poorly expressed in this tissue			
	Llama	PHA/PMA-ionomycin		Poorly expressed in this tissue			
	Dromedary	PHA/PMA-ionomycin	4	-3.66	0.95	1.88	87.64
IFN-γ	Alpaca	PHA/PMA-ionomycin	4	-4.27	0.99	1.72	71.53
	Alpaca	Poly I:C	4	-4.19	0.99	1.73	73.20
	Llama	PHA/PMA-ionomycin	5	-3.96	1.00	1.79	78.86
	Dromedary	PHA/PMA-ionomycin	5	-3.87	1.00	1.81	81.43
IFN-λ1	Alpaca	PHA/PMA-ionomycin	4	-3.44	0.97	1.95	95.31
	Alpaca	Poly I:C	3	-3.45	0.99	1.95	95.01
	Llama	PHA/PMA-ionomycin		Poorly expressed in this tissue			
	Dromedary	PHA/PMA-ionomycin		Poorly expressed in this tissue			
IFN-λ3	Alpaca	PHA/PMA-ionomycin		Not expressed in this tissue			
	Alpaca	PHA/PMA-ionomycin		Not expressed in this tissue			
	Alpaca	Poly I:C		Not expressed in this tissue			
	Llama	PHA/PMA-ionomycin		Not expressed in this tissue			
	Dromedary	PHA/PMA-ionomycin		Not expressed in this tissue			
RIG-1	Alpaca	PHA/PMA-ionomycin	5	-3.76	1.00	1.85	84.52
	Alpaca	Poly I:C	5	-3.91	1.00	1.80	80.22
	Llama	PHA/PMA-ionomycin	5	-3.95	1.00	1.79	79.18

	Dromedary	PHA/PMA-ionomycin	5	-3.98	1.00	1.78	78.45
MDA5	Alpaca	PHA/PMA-ionomycin	5	-3.83	1.00	1.82	82.40
	Alpaca	Poly I:C	5	-3.87	1.00	1.81	81.37
	Llama	PHA/PMA-ionomycin	5	-3.99	0.99	1.78	78.07
	Dromedary	PHA/PMA-ionomycin	3	-3.90	0.89	1.80	80.37
MAVS	Alpaca	PHA/PMA-ionomycin	5	-3.72	1.00	1.86	85.67
	Alpaca	Poly I:C	5	-3.72	1.00	1.86	85.82
	Llama	PHA/PMA-ionomycin	5	-3.75	0.99	1.85	84.85
	Dromedary	PHA/PMA-ionomycin	5	-3.84	0.99	1.82	82.21
TLR3	Alpaca	PHA/PMA-ionomycin	4	-4.05	0.99	1.77	76.62
	Alpaca	Poly I:C	4	-4.13	0.99	1.75	74.70
	Llama	PHA/PMA-ionomycin	4	-3.79	0.99	1.84	83.67
	Dromedary	PHA/PMA-ionomycin	4	-4.15	0.98	1.74	74.19
TLR7	Alpaca	PHA/PMA-ionomycin	5	-3.88	1.00	1.81	81.08
	Alpaca	Poly I:C	5	-3.94	1.00	1.79	79.43
	Llama	PHA/PMA-ionomycin	5	-3.73	0.99	1.85	85.38
	Dromedary	PHA/PMA-ionomycin	5	-3.77	0.99	1.84	84.32
NLRP3	Alpaca	PHA/PMA-ionomycin	5	-3.79	1.00	1.84	83.69
	Alpaca	Poly I:C	5	-3.84	1.00	1.82	82.02
	Llama	PHA/PMA-ionomycin	5	-3.83	0.99	1.83	82.51
	Dromedary	PHA/PMA-ionomycin	5	-3.97	1.00	1.79	78.50
STAT1	Alpaca	PHA/PMA-ionomycin	5	-3.94	1.00	1.79	79.34
	Alpaca	Poly I:C	5	-3.99	1.00	1.78	77.99
	Alpaca	Poly I:C	4	-3.93	1.00	1.80	79.70
	Llama	PHA/PMA-ionomycin	4	-4.04	1.00	1.77	76.91
	Dromedary	PHA/PMA-ionomycin	5	-3.89	1.00	1.81	80.72
IRF3	Alpaca	PHA/PMA-ionomycin	5	-3.83	1.00	1.83	82.54
	Alpaca	Poly I:C	5	-3.91	1.00	1.80	80.30
	Llama	PHA/PMA-ionomycin	5	-3.87	1.00	1.81	81.34
	Dromedary	PHA/PMA-ionomycin	5	-3.86	0.99	1.82	81.61
IRF5	Alpaca	PHA/PMA-ionomycin	5	-3.83	1.00	1.82	82.40
	Alpaca	Poly I:C	5	-3.85	1.00	1.82	81.88
	Llama	PHA/PMA-ionomycin	5	-3.84	1.00	1.82	82.02
	Dromedary	PHA/PMA-ionomycin	5	-3.82	1.00	1.83	82.67
IRF7	Alpaca	PHA/PMA-ionomycin	5	-3.77	1.00	1.84	84.11
	Alpaca	Poly I:C	5	-3.78	1.00	1.84	83.94
	Llama	PHA/PMA-ionomycin	5	-3.77	1.00	1.84	84.24
	Dromedary	PHA/PMA-ionomycin	3	-3.84	0.96	1.82	82.14
NFKB1	Alpaca	PHA/PMA-ionomycin	5	-3.77	1.00	1.84	84.07
	Alpaca	Poly I:C	5	-3.81	1.00	1.83	82.88
	Llama	PHA/PMA-ionomycin	5	-3.77	1.00	1.84	84.07
	Dromedary	PHA/PMA-ionomycin	5	-3.79	1.00	1.84	83.73
RELA	Alpaca	PHA/PMA-ionomycin	5	-3.91	1.00	1.80	80.15
	Alpaca	Poly I:C	5	-3.91	1.00	1.80	80.24
	Llama	PHA/PMA-ionomycin	5	-3.96	1.00	1.79	78.74

	Dromedary	PHA/PMA-ionomycin	5	-3.92	1.00	1.80	79.97
IKBKB	Alpaca	PHA/PMA-ionomycin	5	-3.78	1.00	1.84	83.88
	Alpaca	Poly I:C	5	-3.80	1.00	1.83	83.29
	Llama	PHA/PMA-ionomycin	5	-3.80	1.00	1.83	83.23
	Dromedary	PHA/PMA-ionomycin	5	-3.81	1.00	1.83	83.12
CXCL10	Alpaca	PHA/PMA-ionomycin	5	-3.84	1.00	1.82	82.14
	Alpaca	Poly I:C	5	-4.01	0.99	1.78	77.53
	Llama	PHA/PMA-ionomycin	5	-3.88	1.00	1.81	80.91
	Dromedary	PHA/PMA-ionomycin	5	-3.85	0.99	1.82	81.75
MX1	Alpaca	PHA/PMA-ionomycin	5	-3.80	1.00	1.83	83.21
	Alpaca	Poly I:C	5	-3.86	1.00	1.82	81.69
	Llama	PHA/PMA-ionomycin	5	-3.79	1.00	1.84	83.54
	Dromedary	PHA/PMA-ionomycin	5	-3.86	1.00	1.82	81.56
OAS1	Alpaca	PHA/PMA-ionomycin	5	-3.73	1.00	1.85	85.35
	Alpaca	Poly I:C	5	-3.88	0.99	1.81	81.02
	Llama	PHA/PMA-ionomycin	5	-3.67	0.99	1.87	87.27
	Dromedary	PHA/PMA-ionomycin	5	-3.87	1.00	1.81	81.19
ISG15	Alpaca	PHA/PMA-ionomycin	5	-3.76	1.00	1.84	84.39
	Alpaca	Poly I:C	5	-3.86	0.99	1.82	81.52
	Llama	PHA/PMA-ionomycin	5	-3.81	1.00	1.83	82.88
	Dromedary	PHA/PMA-ionomycin	5	-3.81	1.00	1.83	82.92
IL-10	Alpaca	PHA/PMA-ionomycin	5	-3.85	0.99	1.82	81.86
	Alpaca	Poly I:C	5	-3.96	1.00	1.79	78.83
	Llama	PHA/PMA-ionomycin	5	-3.75	0.99	1.85	84.66
	Dromedary	PHA/PMA-ionomycin	5	-3.74	0.99	1.85	85.17
IL-1β	Alpaca	PHA/PMA-ionomycin	5	-3.79	1.00	1.84	83.66
	Alpaca	Poly I:C	5	-3.82	1.00	1.83	82.79
	Llama	PHA/PMA-ionomycin	5	-3.81	1.00	1.83	83.00
	Dromedary	PHA/PMA-ionomycin	5	-3.81	0.99	1.83	83.00
IL-6	Alpaca	PHA/PMA-ionomycin	5	-3.75	0.98	1.85	84.78
	Alpaca	Poly I:C	5	-3.80	0.99	1.83	83.25
	Llama	PHA/PMA-ionomycin	5	-3.91	1.00	1.80	80.25
	Dromedary	PHA/PMA-ionomycin	5	-3.88	1.00	1.81	81.12
IL-8	Alpaca	PHA/PMA-ionomycin	5	-3.81	1.00	1.83	82.90
	Alpaca	Poly I:C	5	-3.61	1.00	1.89	89.21
	Llama	PHA/PMA-ionomycin	5	-3.59	1.00	1.90	89.75
	Dromedary	PHA/PMA-ionomycin	5	-3.70	1.00	1.86	86.48
IL-15	Alpaca	PHA/PMA-ionomycin	5	-3.80	1.00	1.83	83.38
	Alpaca	Poly I:C	5	-3.79	1.00	1.83	83.48
	Llama	PHA/PMA-ionomycin	5	-4.02	1.00	1.77	77.27
	Dromedary	PHA/PMA-ionomycin	5	-3.81	1.00	1.83	83.13
IL-2	Alpaca	PHA/PMA-ionomycin	5	-3.54	0.96	1.92	91.61
	Alpaca	Poly I:C	4	-3.96	0.98	1.79	78.74
	Llama	PHA/PMA-ionomycin	5	-4.03	1.00	1.77	77.13
	Dromedary	PHA/PMA-ionomycin	5	-3.91	1.00	1.80	80.21

IL-4	Alpaca	PHA/PMA-ionomycin	3	-3.44	0.99	1.95	95.18
	Alpaca	Poly I:C	5	-3.32	0.97	2.00	99.94
	Llama	PHA/PMA-ionomycin	5	-3.99	1.00	1.78	78.06
	Dromedary	PHA/PMA-ionomycin	5	-4.00	0.99	1.78	77.89
IL-12p35	Alpaca	PHA/PMA-ionomycin	4	-3.92	0.98	1.80	79.85
	Alpaca	Poly I:C	3	-3.30	0.98	2.01	100.96
	Llama	PHA/PMA-ionomycin	4	-3.80	0.97	1.83	83.42
	Dromedary	PHA/PMA-ionomycin	5	-3.40	0.97	1.97	96.97
TNF-α	Alpaca	PHA/PMA-ionomycin	5	-3.67	0.99	1.87	87.35
	Alpaca	Poly I:C	5	-3.87	0.99	1.81	81.35
	Llama	PHA/PMA-ionomycin	5	-3.84	1.00	1.82	82.04
	Dromedary	PHA/PMA-ionomycin	5	-3.95	0.99	1.79	79.07
CCL2	Alpaca	PHA/PMA-ionomycin	5	-3.72	1.00	1.86	85.78
	Alpaca	Poly I:C	5	-3.63	1.00	1.89	88.58
	Llama	PHA/PMA-ionomycin	5	-3.87	1.00	1.81	81.31
	Dromedary	PHA/PMA-ionomycin	5	-3.77	1.00	1.84	84.27
CCL3	Alpaca	PHA/PMA-ionomycin	5	-3.77	1.00	1.84	84.16
	Alpaca	Poly I:C	5	-3.83	1.00	1.82	82.46
	Llama	PHA/PMA-ionomycin	5	-3.77	1.00	1.84	84.20
	Dromedary	PHA/PMA-ionomycin	5	-3.81	1.00	1.83	83.01
CXCL1	Alpaca	PHA/PMA-ionomycin	5	-3.79	1.00	1.83	83.46
	Alpaca	Poly I:C	5	-3.73	1.00	1.85	85.37
	Llama	PHA/PMA-ionomycin	5	-3.76	1.00	1.84	84.39
	Dromedary	PHA/PMA-ionomycin	5	-3.79	1.00	1.84	83.57
MIF	Alpaca	PHA/PMA-ionomycin	5	-3.90	1.00	1.80	80.37
	Alpaca	Poly I:C	5	-3.80	1.00	1.83	83.25
	Llama	PHA/PMA-ionomycin	5	-3.93	1.00	1.80	79.70
	Dromedary	PHA/PMA-ionomycin	5	-3.76	0.99	1.84	84.42
CASP1	Alpaca	PHA/PMA-ionomycin	5	-3.82	0.99	1.83	82.74
	Alpaca	Poly I:C	5	-3.79	1.00	1.83	83.49
	Llama	PHA/PMA-ionomycin	5	-3.88	0.99	1.81	80.97
	Dromedary	PHA/PMA-ionomycin	4	-3.72	1.00	1.86	85.64
CASP10	Alpaca	PHA/PMA-ionomycin	5	-3.79	1.00	1.84	83.62
	Alpaca	Poly I:C	5	-3.77	1.00	1.84	84.27
	Llama	PHA/PMA-ionomycin	5	-3.80	1.00	1.83	83.21
	Dromedary	PHA/PMA-ionomycin	5	-3.84	1.00	1.82	82.22
CYLD	Alpaca	PHA/PMA-ionomycin	5	-3.83	1.00	1.82	82.50
	Alpaca	Poly I:C	5	-3.85	1.00	1.82	81.82
	Llama	PHA/PMA-ionomycin	5	-3.85	1.00	1.82	81.74
	Dromedary	PHA/PMA-ionomycin	5	-3.81	0.99	1.83	82.91
AZI2	Alpaca	PHA/PMA-ionomycin	5	-3.73	1.00	1.85	85.31
	Alpaca	Poly I:C	5	-3.66	0.99	1.87	87.44
	Llama	PHA/PMA-ionomycin	5	-3.78	0.99	1.84	83.92
	Dromedary	PHA/PMA-ionomycin	5	-3.86	0.99	1.82	81.69
PACT	Alpaca	PHA/PMA-ionomycin	5	-3.87	1.00	1.81	81.18

	Alpaca	Poly I:C	5	-3.74	0.99	1.85	85.22
	Llama	PHA/PMA-ionomycin	5	-3.82	1.00	1.83	82.78
	Dromedary	PHA/PMA-ionomycin	5	-3.95	0.99	1.79	79.22
TBK1	Alpaca	PHA/PMA-ionomycin	5	-3.81	1.00	1.83	82.95
	Alpaca	Poly I:C	5	-3.91	1.00	1.80	80.09
	Llama	PHA/PMA-ionomycin	5	-3.77	1.00	1.84	84.08
	Dromedary	PHA/PMA-ionomycin	5	-3.88	1.00	1.81	80.89
TRIM25	Alpaca	PHA/PMA-ionomycin	5	-3.76	1.00	1.85	84.53
	Alpaca	Poly I:C	5	-3.79	1.00	1.84	83.72
	Llama	PHA/PMA-ionomycin	5	-3.73	1.00	1.85	85.42
	Dromedary	PHA/PMA-ionomycin	5	-3.88	1.00	1.81	80.96
NFKBIA	Alpaca	PHA/PMA-ionomycin	5	-3.86	1.00	1.82	81.56
	Alpaca	Poly I:C	5	-3.83	1.00	1.82	82.45
	Llama	PHA/PMA-ionomycin	5	-3.77	1.00	1.84	84.09
	Dromedary	PHA/PMA-ionomycin	5	-3.83	0.99	1.82	82.34
TRADD	Alpaca	PHA/PMA-ionomycin	5	-3.80	1.00	1.83	83.34
	Alpaca	Poly I:C	5	-3.89	1.00	1.81	80.80
	Llama	PHA/PMA-ionomycin	5	-3.90	0.99	1.81	80.50
	Dromedary	PHA/PMA-ionomycin	5	-3.84	1.00	1.82	82.02
CARD9	Alpaca	PHA/PMA-ionomycin	5	-3.65	1.00	1.88	87.82
	Alpaca	Poly I:C	5	-3.69	0.99	1.87	86.56
	Llama	PHA/PMA-ionomycin	5	-3.86	0.98	1.82	81.55
	Dromedary	PHA/PMA-ionomycin	4	-3.81	0.99	1.83	83.08
PYCARD	Alpaca	PHA/PMA-ionomycin	5	-3.71	1.00	1.86	86.13
	Alpaca	Poly I:C	5	-3.81	1.00	1.83	82.99
	Llama	PHA/PMA-ionomycin	5	-3.71	0.97	1.86	86.09
	Dromedary	PHA/PMA-ionomycin	5	-3.93	1.00	1.80	79.63
IFNLR1	Alpaca	PHA/PMA-ionomycin	5	-3.73	1.00	1.85	85.25
	Alpaca	Poly I:C	5	-3.89	0.99	1.81	80.67
	Llama	PHA/PMA-ionomycin	5	-3.70	1.00	1.86	86.17
	Dromedary	PHA/PMA-ionomycin	3	-3.92	0.93	1.80	79.97
IFNAR1	Alpaca	PHA/PMA-ionomycin	5	-4.25	1.00	1.72	72.02
	Alpaca	Poly I:C	5	-4.38	1.00	1.69	69.08
	Llama	PHA/PMA-ionomycin	5	-4.31	0.99	1.71	70.60
	Dromedary	PHA/PMA-ionomycin		Poorly expressed in these cells			

PBMCs, peripheral blood mononuclear cells; PHA, phytohemagglutinin; PMA, phorbol 12-myristate 13-acetate.

Appendix Table 5.4 is available online at:

https://drive.google.com/drive/folders/1Ltz1bGtYWrmTBvfYz2YBalGhXT1azwIC

Chapter 6

MERS-CoV internalized by llama alveolar macrophages does not result in virus replication or induction of pro-inflammatory cytokines

6.1 Introduction

Severe MERS is microscopically characterized by diffuse alveolar damage, which mainly occurs due to massive infiltration of immune cells into the lungs. These cells produce an excessive and aberrant host-cytokine storm that exacerbates disease during late MERS-CoV infection stages [189]. High and prolonged secretion of pro-inflammatory cytokines (such as IL-6, IL-8, IL-17 and IL-1β), as well as discrepancy in levels of antiviral cytokines (IFNs or TNF-α), have been observed in sera and bronchoalveolar fluid lavages (BAL) of acutely affected patients [190,238–240,244,411,412]. Indeed, cytokine production positively correlated with the number of leukocytes in blood and disease severity [190,239,240].

Abortive infection and induction of apoptosis were described in T cells [198], suggesting that these cells do not play a major role in proinflammatory cytokine storm production. Moreover, while inefficient replication was described in pDCs [199], productive MERS-CoV replication was only reported in MDMs [200–202] and MDDCs [200,202,245]. Upon viral infection, pDCs could elicit higher levels of antiviral responses than MDDCs, such as type I and III IFNs, but none of these cells triggered the secretion of inflammatory cytokines [199,200,202,245]. Instead, MERS-CoV replication in MDMs resulted in impaired antiviral responses (type I and III IFNs) but dysregulated and persistent production of inflammatory cytokines, such as IL-6 and TNF-α [199–202,413]. Thus, macrophages are thought to be the main drivers of the inflammatory cytokine storm leading to exacerbated lung tissue damage in human MERS-CoV infections.

Dromedary camels are the natural reservoir of MERS-CoV and primary hosts involved in virus transmission to humans [16,141,352]. Other camelid species are also susceptible to MERS-CoV under natural and experimental conditions (Adney et al., 2016; Crameri et al., 2016; David et al., 2018; Reusken et al., 2016; Vergara-Alert, van den Brand, et al., 2017). Contrary to humans, camelids experience a subclinical infection characterized by abundant viral replication in the upper respiratory tract [141,207,208]. The action of robust and timely innate immune responses at the nasal mucosa of camelids is thought to play a key role in MERS-CoV infection clearance, preventing disease development (Te et al., 2021; Te, Rodon, et al., 2022). Furthermore, a transient MERS-CoV replication has been observed in the lower respiratory tract of experimentally-infected camelids (Haagmans et al., 2016; Te et al., 2021; Te, Rodon, et al., 2022). Importantly, infiltration of mononuclear leukocytes at the lower respiratory tract was also observed in both naturally and experimentally infected camelids, although to a limited extent [8,32,204]. Nonetheless, besides being the key determinants of cytokine storms in human infections, the role of macrophages during MERS-CoV infection in camelids remains unknown.

The present work aimed to elucidate if llama alveolar macrophages (LAMs) are susceptible to MERS-CoV infection *in vitro* and could elicit a pro-inflammatory response potentially contributing to disease severity.

6.2 Materials and methods

Animal welfare and ethics

All animal and laboratory experimentation involving MERS-CoV were performed at the BSL-3 facilities of the Biocontainment Unit of IRTA-

CReSA. Animal experimentation procedures were evaluated and approved by the CEEA-IRTA and by the Ethical Commission of Animal Experimentation of the Autonomous Government of Catalonia (file No. CEA-OH/10942/1).

Cell culture and MERS-CoV

LAMs were cultured in RPMI (Lonza, Switzerland) supplemented with 10% fetal calf serum (FCS; EuroClone, Italy), 100 U/mL penicillin, 100 µg/mL streptomycin, and 2 mM glutamine (all ThermoFisher Scientific, USA). Vero E6 cells (CRL-1586, ATCC, USA) were cultured in DMEM (Lonza, Switzerland) supplemented with 5% FCS, 100 U/mL penicillin, 100 µg/mL streptomycin, and 2 mM glutamine.

A passage-3 MERS-CoV Qatar15/2015 strain stock was propagated and titrated on Vero E6 cells as indicated in *Chapter 3*.

Isolation of llama alveolar macrophages

Two llamas were euthanized and BAL were performed to collect alveolar macrophages. One lung lobe was washed with sterile saline solution (1x PBS). Alveolar macrophages were concentrated by centrifugation and fluid was discarded. Red blood cells were removed using ACK lysing buffer (ThermoFisher Scientific, USA) according to the manufacturer's instructions, and alveolar macrophages were resuspended in culture media. These cells were initially tested to ensure negativity to MERS-CoV.

MERS-CoV exposure assays

LAMs were isolated and cultured in triplicates. One million cells/well were seeded onto 24-well plates in 1 mL RPMI medium containing

MERS-CoV (MOI of 0.1), or only cultured in media for 48 h at 37ºC and 5% CO_2. Culture supernatants and cells were collected at 0, 24 and 48 h post viral exposure (hpe), as schematically represented in **Figure 6.1a**. Additional fresh control samples were also collected before seeding in culture plates.

Virus titration in cell culture

The presence of infectious MERS-CoV in culture supernatants was evaluated on Vero E6 cells, as previously described in *Chapter 3*.

Cellular RNA extraction

LAMs were detached from culture wells by mechanically pipetting and total RNA was extracted using the Direct-zol RNA Miniprep (Zymo research, USA), following the manufacturer's protocol. After RNA extraction, an additional HL-dsDNase treatment using the Heat&Run gDNA removal kit (ArcticZymes Technologies, Norway) was performed according to the manufacturer's protocol. Finally, 1 U/µL RNase inhibitors (Invitrogen, Life Technologies, Waltham, USA) were added to the RNA samples, which were stored at -75°C until subsequent analyses. The purity and quantity of RNA were assessed using a BioDrop *µLITE* Spectrophotometer (BioDrop Ltd, UK). A260:A280 ratio ranged from 1.6 to 1.9, which are optimal values for RNA purity.

cDNA synthesis

cDNA was generated from as previously described in *Chapter 5*.

Transcriptomic analyses by microfluidic RT-qPCR

Expression of cytokines and immune-related genes, as well as normalizer genes, were quantified using a previously validated

technique to monitor camelid immune responses (see *chapter 5*). A Fluidigm Biomark microfluidic RT-qPCR assay was used to quantify gene expression of LAMs. Additionally, specific primers for the detection of subgenomic viral RNA were added to the assay [362]. Each reaction was coupled with Tm analysis to ensure that specific amplifications occurred. Non-template controls with nuclease-free water were also included in the assays.

Relative immune response gene quantification and data analysis

Gene expression analyses were calculated as previously described in *chapter 5*, with minor modifications. Briefly, data were collected with the Fluidigm Real-Time PCR Analysis 4.1.3 (Fluidigm Corporation, USA) and analyzed with the DAG expression software 1.0.5.6 [381]. The relative standard curve method (see Applied Biosystems user bulletin #2) was applied to compare gene expression levels of alveolar macrophages cultured in different conditions against those of freshly collected LAMs (prior culture), using multiple reference gene normalization (GAPDH, HPRT1 and UbC). Relative expression of IFN-λ1 and IFN-λ3 was calculated according to the $2^{-\Delta\Delta CT}$ method [415] using the same normalizer genes, since expression levels of these genes in control samples were too low to generate standard curves. The relative expression of each studied gene was expressed in mean Fc values and is shown in **Appendix Table 6.1**.

Unpaired t-test analyses were performed using GraphPad Prism 9.3.1 (GraphPad Software, USA) to compare gene expression levels of alveolar macrophages exposed to MERS-CoV against those of cells cultured in media only. Differences were considered significant at *p*-values < 0.05.

Transmission electron microscopy

LAMs were chemically fixed at 24 h or 48 h post infection. Cells were mechanically detached from plates and transferred into 1.5 mL Eppendorf tubes. After centrifugation at 500g for 10 min, supernatants were discarded, and pellets were fixed with 4% paraformaldehyde for 2 hours at 4°C. In a second step, cells were fixed with 1% glutaraldehyde in PBS for 1 hour at 4°C. Post-fixation of cell pellets was done on ice with 1% osmium tetroxide + 0.8% potassium ferrocyanide in water. Afterwards the pellets were dehydrated on ice with increasing concentrations of acetone and processed for embedding in the epoxy resin EML-812 (TAAB Laboratories, UK), as previously described [416,417]. After infiltration with epoxy resin at RT, samples were polymerized at 60°C for 48h. Ultrathin sections (50-70 nm) were obtained with a Leica UC6 microtome and collected on uncoated 300 mesh copper grids. Sections were contrasted with 4% uranyl acetate and Reynold's lead citrate. Images were taken with a Tecnai G2 TEM operated at 120kV with a Ceta camera. At least 50 cells per condition were studied by TEM.

6.3 Results

LAMs were isolated and cultured in the presence of MERS-CoV for 0, 24 and 48 h, as summarized in **Figure 6.1a**. The amount of infectious virus in supernatants assessed on Vero E6 cells constantly decreased throughout the study (**Figure 6.1b**), evidencing that progeny viruses were not generated and released to the media. Consistently, cell-associated MERS-CoV RNA waned over time as determined by microfluidic RT-qPCR (**Figure 6.1c**). Therefore, MERS-CoV was

unable to productively replicate *in vitro* in LAMs. Furthermore, we performed transmission electron microscopy (TEM) analyses to confirm if MERS-CoV was able to interact with LAMs. As shown in **Figure 6.1d**, **e** and **f**, non-exposed llama cells exhibited a size and round morphology with pseudopodia characteristic of macrophages, with good preservation of organelles, cytosol and nuclei. Large vacuoles that contained electron-dense material and membranes were also observed in these cells. At 24 h post-MERS-CoV exposure hpe, LAMs looked similar to non-exposed cell controls and no viral structures were seen (**Figure 6.1g**, **h** and **i**). However, at 48 hpe (**Figure 6.1j**, **k** and **l**), virus-like particles were detected inside vesicles, vacuoles, and dense globular compartments of LAMs (**Figure 6.1k** and **l**). We found MERS-CoV virions attached to the plasma membrane or invaginations of it (**Figure 6.1k**), as well as in larger membranous compartments eventually leading to viral degradation (**Figure 6.1l**), as already described for other coronaviruses [417]. In addition, clusters of DMVs, which are virus-induced replication organelles of coronaviruses [78,79], were not formed in cells internalizing MERS-CoV throughout the study. Around 10% of the cells contained viral structures in cellular compartments in the plane of the section. Hence, MERS-CoV was successfully captured and internalized by camelid alveolar macrophages, being subsequently processed and degraded.

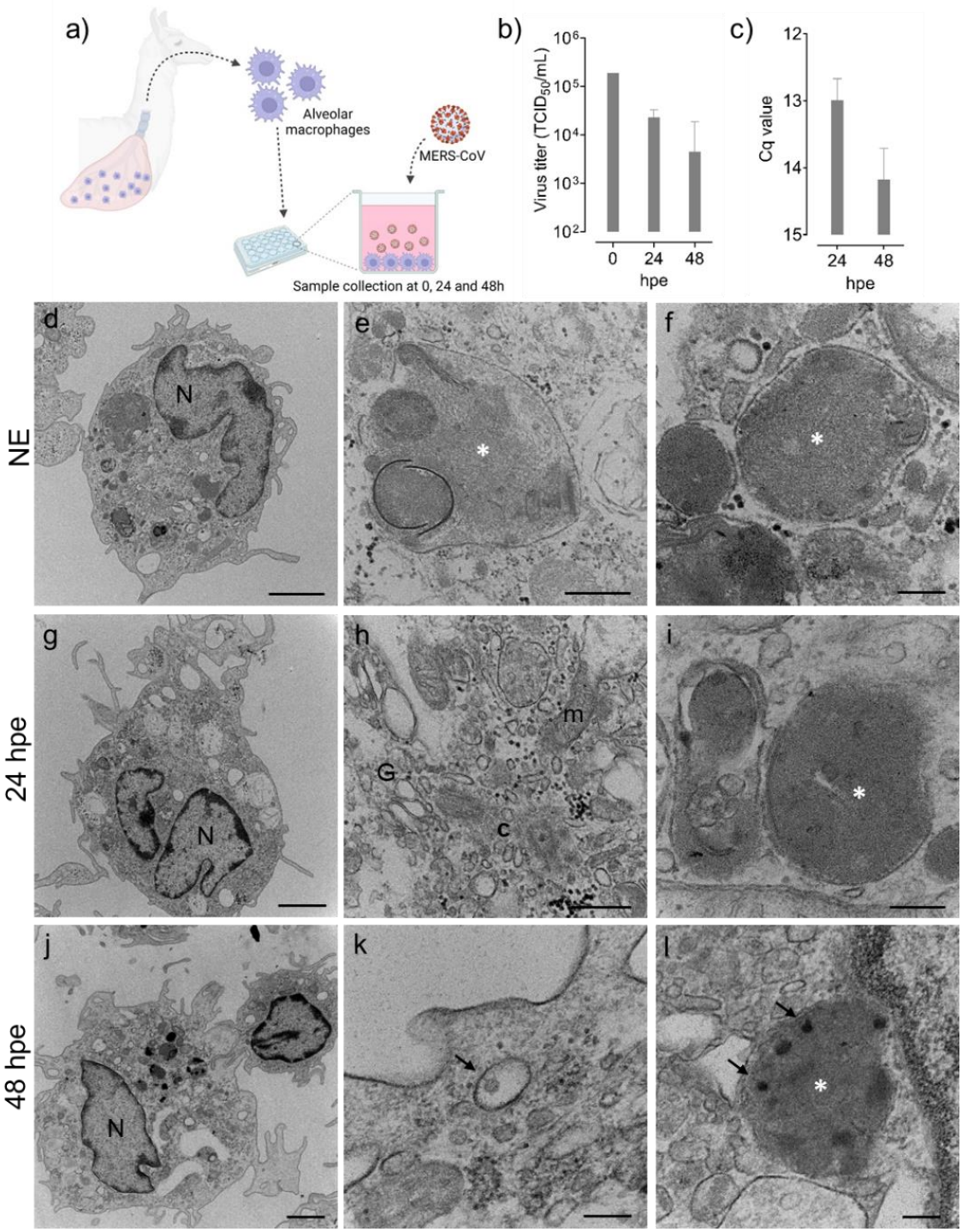

Figure 6.1. Susceptibility of llama alveolar macrophages (LAMs) to MERS-CoV. LAMs were isolated and exposed to MERS-CoV as represented in panel (a). Mean values (± SEM) of infectious virus in culture supernatants (b) and

cell-associated viral RNA (c) were monitored throughout the study. Transmission electron microscopy analyses of mock- and MERS-CoV-exposed macrophages were performed over time. Panels (d) to (f) show ultrathin sections of non-exposed (NE) cells. Low (d) and high (e, f) magnification images of NE macrophages with characteristic nucleus (N) and vacuoles with dense material and membranes (asterisks) are shown. Panels (g) to (i) display cells exposed for 24 h to MERS-CoV. Low (g) and high (h, i) magnification images of normal nucleus (N), mitochondria (m), Golgi complex (G), a centrosome (c) and vacuoles with dense material (asterisk) are shown. Panels (j) to (l) show cells exposed for 48 h to MERS-CoV. Low (j) and high (k, l) magnification images of cells with normal nuclei are displayed. Arrow in (k) points to a viral particle attached to an invagination of the plasma membrane. Arrows in (l) point to virus-like particles inside a dense vacuole (asterisk). Scale bars, 2 µm in D, G and J; 500 nm in E and H; 200 nm in f, i, k and l.

We also studied whether LAMs could induce cytokine mRNA expression upon MERS-CoV sensing, using a previously described microfluidic RT-qPCR array in *Chapter 5*. Expression levels of 43 immune-related genes from LAMs exposed to MERS-CoV and non-exposed controls were compared to those of freshly collected cells prior culture. The transcriptomic profiles included the analyses of type I, II and III IFNs, PRRs, TFs, ISGs, and cytokines involved in inflammatory responses, among other immune-related genes (**Figure 6.2a**). Remarkably, most of the cytokines studied in LAMs inoculated with MERS-CoV were expressed at similar levels than in mock-treated cells. Moreover, when compared to freshly collected LAMs, expression of pro-inflammatory cytokines and chemokines associated with the cytokine storm occurring in humans, such as IL-6, IL-1β or TNF-α, decreased in MERS-CoV and mock-treated cells. Only the chemokine IL-8 was upregulated similarly in MERS-CoV and mock-treated cells upon culture (**Figure 6.2a**). In agreement, transcription of genes involved in inflammasome complex formation (NLRP3, CASP1 and PYCARD) was not induced upon viral sensing (**Figure 6.2a**). Moreover, the expression

of anti-inflammatory IL-10 slightly increased over time compared to mock-treated cells (**Figure 6.2b**). Thus, these data evidenced that LAMs internalizing MERS-CoV did not elicit antiviral nor pro-inflammatory responses.

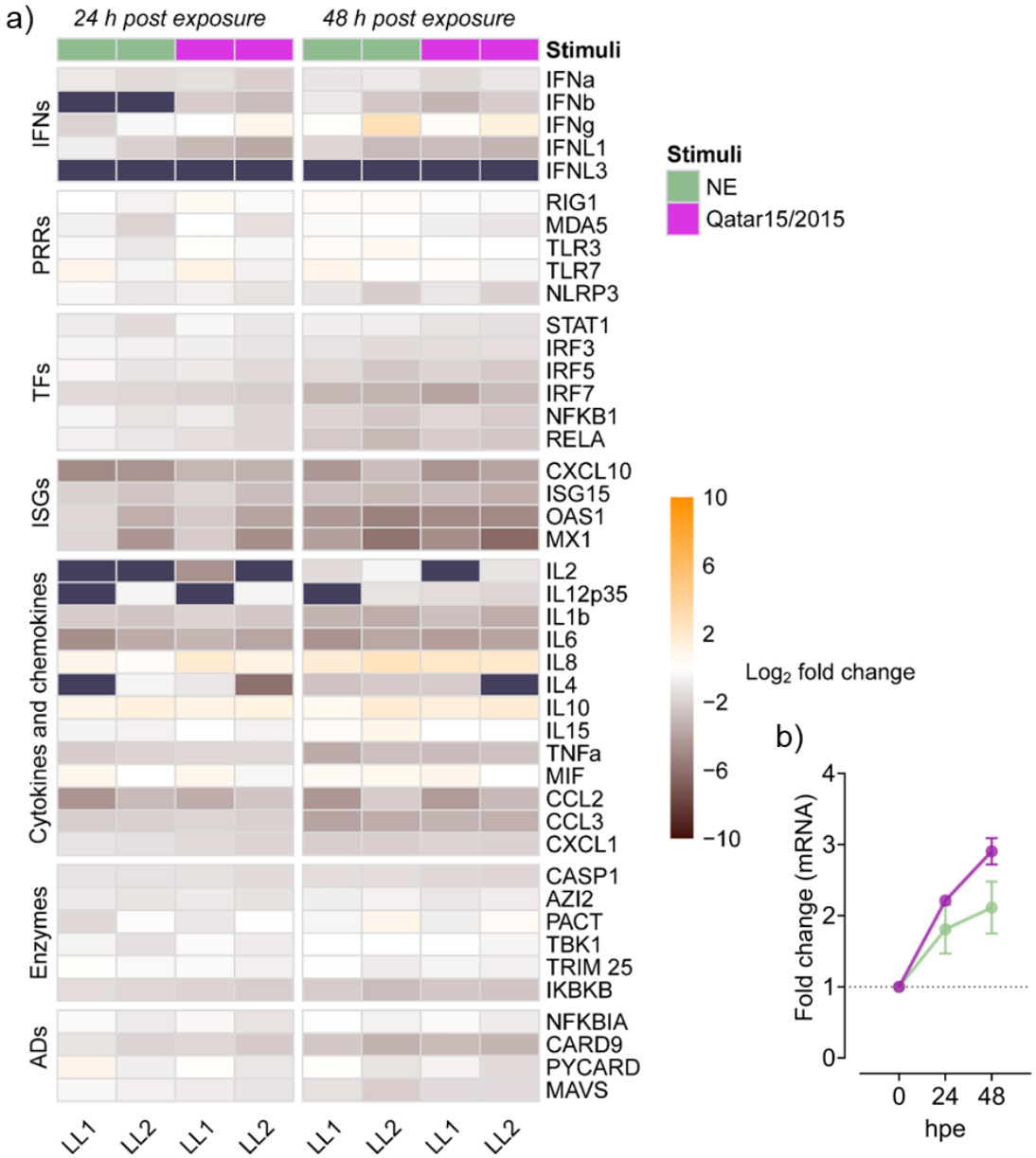

Figure 6.2. Kinetics of immune response genes expressed by llama alveolar macrophages (LAMs) sensing MERS-CoV. The Fluidigm Biomark

microfluidic RT-qPCR assay was used to quantify transcripts of immune-related genes at different h post-MERS-CoV exposure (hpe). After relative normalization, fold-change values of LAMs exposed for 24 and 48 h to MERS-CoV (Qatar15/2015, pink rectangles), or cultured in media only (NE, green rectangles) were calculated respective to freshly collected control LAMs. Panel (a) shows a heat-map plot with color variations corresponding to log2 fold-change values of expression for each studied gene; orange for upregulated and black for downregulated gene expression, respectively. Dark blue rectangles indicate absence of expression of the corresponding gene. IFNs, interferons; PRRs, pattern-recognition receptors; TFs, transcription factors; ISGs, IFN stimulated genes; ADs, adaptors; LL, llama. Panel (b) display the anti-inflammatory IL-10 expression over time in LAMs exposed to MERS-CoV (pink line) or cultured in media only (green line).

6.4 Discussion

Here we identified the ultrastructural and transcriptomic features of LAMs exposed to MERS-CoV *in vitro*. This virus causes a subclinical infection in camelid reservoirs that is rapidly cleared, especially in the lower respiratory tract [141]. We confirmed that LAMs do not support MERS-CoV infection but can capture MERS-CoV particles, which are eventually degraded. Our findings support that mild infiltration of macrophages into the lungs of infected camelids (Alnaeem et al., 2020; Te et al., 2021; Te, Rodon, et al., 2022) contributes to the efficient viral clearance observed in reservoir hosts. Indeed, depletion of alveolar macrophages in a human dipeptidyl-peptidase 4 *knock-in* mouse model resulted in increased morbidity and mortality to a mouse-adapted MERS-CoV [250].

We previously described that the mild infiltration of mononuclear cells in lungs of infected alpacas was concomitant to a moderate up-regulation of TNF-α, IL-1β and NLPR3. Moreover, chemotactic cytokines (CCL2, CCL3) were strongly correlated with the abundance of mononuclear

cells in lungs [8,32]. Here, we determined that LAMs internalizing MERS-CoV did not induce effective antiviral or pro-inflammatory immune responses throughout the experiment, but slightly increased anti-inflammatory IL-10 transcription levels. These results suggest a minor contribution of macrophages in the transcriptional induction of pro-inflammatory cytokines in lungs of infected camelids. Indeed, contrary to human macrophages contributing to acute lung inflammation and cytokine storm [189,201,202,413], our findings support that camelid macrophages degrade MERS-CoV without activating a disproportionate pro-inflammatory response. Accordingly, IRF5, an important TF involved in M1 macrophage polarization [274,275], was downregulated in cultured LAMs. Consequently, together with robust antiviral innate immune responses occurring at the mucosal level [8,32], camelid reservoir species own unique effective mechanisms to impede disease development and experience asymptomatic MERS-CoV infection.

Overall, we show that LAMs are resistant to MERS-CoV infection, although these cells effectively capture, internalize, and degrade viral particles. Also, contrary to human MDMs, these cells do not induce pro-inflammatory cytokine responses upon viral sensing.

Appendix 6

Appendix Table 6.1 is available online at:

https://drive.google.com/drive/folders/1Ltz1bGtYWrmTBvfYz2YBalGhXT1azwIC

Chapter 7

Enhanced antiviral immunity and dampened inflammation in llama lymph nodes upon MERS-CoV sensing

7.1 Introduction

Currently, MERS-CoV clade B strains have a high incidence in the Arabian Peninsula, while clade C strains, restricted to Africa, are not causing outbreaks despite that reactive virus-specific T-cells were found African camel handlers [361]. MERS-CoV was reported to abortively infect human T cells *in vitro* and concomitantly induce apoptosis pathways [198], which might explain the severe lymphopenia commonly reported in MERS patients [147,173]. Altogether, these findings could lead to aberrant or delayed induction of antiviral T cell responses, as observed in acute phase patients [189,238,247,412], and contribute to the high pathogenicity of MERS-CoV. Regarding to the relevance of T-cell responses in protection, recovered patients mount effective T cell responses that play a major role in the outcome of MERS. Remarkably, virus-specific $CD8^+$ T cell responses were also developed by all survivors studied, including those with undetectable antibody responses [246], suggesting that convalescent patients would trigger early cellular protective immune responses upon a subsequent MERS-CoV infection. Moreover, the crucial role of T cell responses to counteract MERS-CoV infection was quickly unravelled in animal model studies. Contrary to B-cell deficient and control animals, viral persistence was reported in the lungs of T-cell deficient mice [227]. Thus, development of robust and functional T cell responses is required to fully achieve MERS-CoV clearance.

MERS-CoV is transmitted to humans by dromedary camels, the main reservoir host [16,141,352], although other camelid species are also susceptible to viral infection [65,115,116,234,235]. These species only develop a subclinical infection, which typically show upper respiratory tract replication and abundant MERS-CoV shedding before eventual infection

clearance [141,207,208]. Camelids elicit strong innate immune responses with dampened inflammation at the mucosal level [8,32], which is similar to those described in bat cells [246,279,280]. Indeed, bats are tolerant to many viruses including MERS-CoV-like viruses [7] and can be experimentally infected with MERS-CoV without suffering from disease [211]. These two reservoir species can be reinfected [7,203], allowing viral maintenance and eventual spread. Therefore, innate and adaptive immune responses elicited by camelids must be important determinants of infection clearance and host disease resistance, but do not interrupt viral circulation and maintenance within these animal populations.

Protective humoral immune responses against MERS-CoV are known to occur in camelids after natural and experimental infection [65,115,116,208,234,235]. Efficient antigen presentation in draining LNs is essential to ensure successful induction of specific T and B cell adaptive immune responses. Previous experimental studies have shown the presence of infectious MERS-CoV in LN of dromedary camels [207,208]. Moreover, in llamas, abundant nucleoprotein antigen was observed within dendritic-like cells in cervical LNs at 4 dpi and MERS-CoV RNA persisted until 24 dpi [236]. Although no tissue damage was observed, it is unclear whether the virus could replicate in these lymphoid organs. In this study, we mimicked a secondary exposure to MERS-CoV clade B and C strains *in vitro* cervical LN cells from previously inoculated llamas to investigate viral replication and cellular immune responses at the transcriptional level.

7.2 Materials and methods

Animal welfare and ethics

Animal samples used in this work were obtained during necropsy procedures of previous studies (*Chapter 3* and *4*), approved by the CEEA-IRTA and the Ethical Commission of Animal Experimentation of the Autonomous Government of Catalonia, as detailed in *Chapters 3* and *4*.

Cell culture and MERS-CoV

Vero E6 cells were cultured as described in *Chapter 3*. MERS-CoV Qatar15/2015 and Egypt/2013 stocks were prepared as indicated in *Chapters 3* and *4*.

Animal infection and sampling

Two llamas were experimentally infected with the Qatar15/2015 strain (*Chapter 3*) and two other llamas with the Egypt/2013 strain (*Chapter 4*). Infection was monitored for 3 weeks. Nasal swabs samples were obtained daily until 15 dpi, plus at 17 and 22 dpi. Sera samples were obtained before MERS-CoV challenge and at 7, 14 and 22 dpi, when animals were euthanized and necropsied.

Cervical lymph node cell isolation

Cervical LNs were collected in RPMI supplemented with 100 U/mL penicillin, 100 µg/mL streptomycin, 2 mM glutamine and 10% FCS and kept at 4°C until transferred to the lab. LNs were mechanically disaggregated. Cells were filtered through 70 µm strainers (Corning, USA) and concentrated by centrifugation. Red blood cells were removed using ACK lysing buffer (ThermoFisher Scientific, USA), according to the manufacturer's instructions. LN cells were resuspended and cultured in RPMI (Lonza, Switzerland) supplemented with 10% fetal calf serum (FCS; EuroClone, Italy), 100 U/mL penicillin, 100 µg/mL streptomycin,

2 mM glutamine (all ThermoFisher Scientific, USA) and 5×10^{-5} M β-mercaptoethanol (Sigma-Aldrich, USA).

MERS-CoV exposure to lymph node cells

After isolation, LN cells were cultured in triplicates. One million cells were seeded onto 24-well plates in 1 mL final volume of cell culture medium alone (mock) or containing MERS-CoV Qatar15/2015 or Egypt/2013 strain (MOI of 0.1) and cultured for 48 h at 37ºC and 5% CO_2. Culture supernatants and cells were collected at 0, 24 and 48 hpe. Additional fresh control LN cells were also collected prior culture.

Viral and cellular RNA extraction

Viral RNA was extracted from supernatant samples using the IndiMag pathogen kit (Indical Biosciences, Germany) and a Biosprint 96 workstation (Qiagen, Germany), according to the manufacturer's instructions. Total RNA was extracted from llama LN cells using the Direct-zol RNA Miniprep (Zymo research, USA), following the manufacturer's protocol. After RNA extraction, an additional HL-dsDNase treatment using the Heat&Run gDNA removal kit (ArcticZymes Technologies, Norway) was performed according to the manufacturer's protocol to completely remove the reminiscent genomic DNA. Finally, 1 U/µL RNase inhibitors (Invitrogen, Life Technologies, Waltham, USA) were added. Samples were stored at -75°C until further analyses. The purity and quantity of the extracted RNA were assessed using a BioDrop *µLITE* Spectrophotometer (BioDrop Ltd, UK). A260:A280 ratio ranged from 1.6 to 1.8.

MERS-CoV RNA detection by RT-qPCR

Viral genomic RNA was detected in culture supernatant by performing

the UpE RT-qPCR assay [354], with minor modifications as previously described in *Chapter 3*. Samples with a Cq value ≤40 were considered positive.

cDNA synthesis

cDNA was generated from as previously described in *Chapter 5*.

Fluidigm Biomark microfluidic RT-qPCR

Transcription of cytokines and immune-related genes were quantified using a previously validated protocol to study camelid immune responses (*chapter 5*). A Fluidigm Biomark microfluidic RT-qPCR assay was used to quantify immune-gene expression of LN cell samples. As described in *Chapter 6*, specific primers for the quantification of MERS-CoV subgenomic RNA were added to the assay [362]. Amplification reactions were coupled with Tm analyses to ensure that specific amplifications occurred. Non-template controls were also included in the assays.

Relative quantification and data analysis

Gene expression analyses and data analyses were performed as previously described in *Chapter 6*. The relative expression of each gene in a particular sample was expressed in mean Fc values and are shown in **Appendix Table 7.1**.

7.3 Results

Four llamas were primed by experimental inoculation with MERS-CoV Qatar15/2015 (*n = 2)* or Egypt/2013 (*n = 2)* strains, causing productive infection resolved at 8 to 9 dpi. None of the inoculated llamas displayed

clinical signs throughout the study. Genomic and subgenomic viral RNA were detected for both strains at similar levels in nasal swabs (**Fig. 7.1a** and **b**). Thus, llamas shed high titers of infectious virus independently of the strain causing infection (**Fig. 7.1c**). Animals from both groups seroconverted to MERS-CoV with similar levels of nAbs that were detected from 2 weeks after infection onwards (**Fig. 7.1d**). Overall, llamas followed similar trends in viral shedding and development of humoral responses regardless of the MERS-CoV strain inoculated.

Three weeks after infection, llama cervical LN were collected and their cells were cultured in the presence of MERS-CoV for 0, 24 and 48 h, as schematically represented in **Figure 7.1e**. Cells were exposed to the same MERS-CoV strain used for priming. We monitored viral titres in culture supernatants and seeded cells. Importantly, MERS-CoV was not found in cervical LN cells at 22 dpi, as evidenced by the absence of viral RNA in mock-treated cells (**Figure 7.1f** and **g**). Independently of the strain used to pulse cells, viral loads in supernatant samples decreased over time, as determined by RT-qPCR for genomic RNA detection (**Figure 7.1f**). Also, microfluidic RT-qPCR results indicated that cell-associated MERS-CoV RNA declined (**Figure 7.1g**). Therefore, cervical LN cells of llama did not support MERS-CoV replication upon *in vitro* exposure.

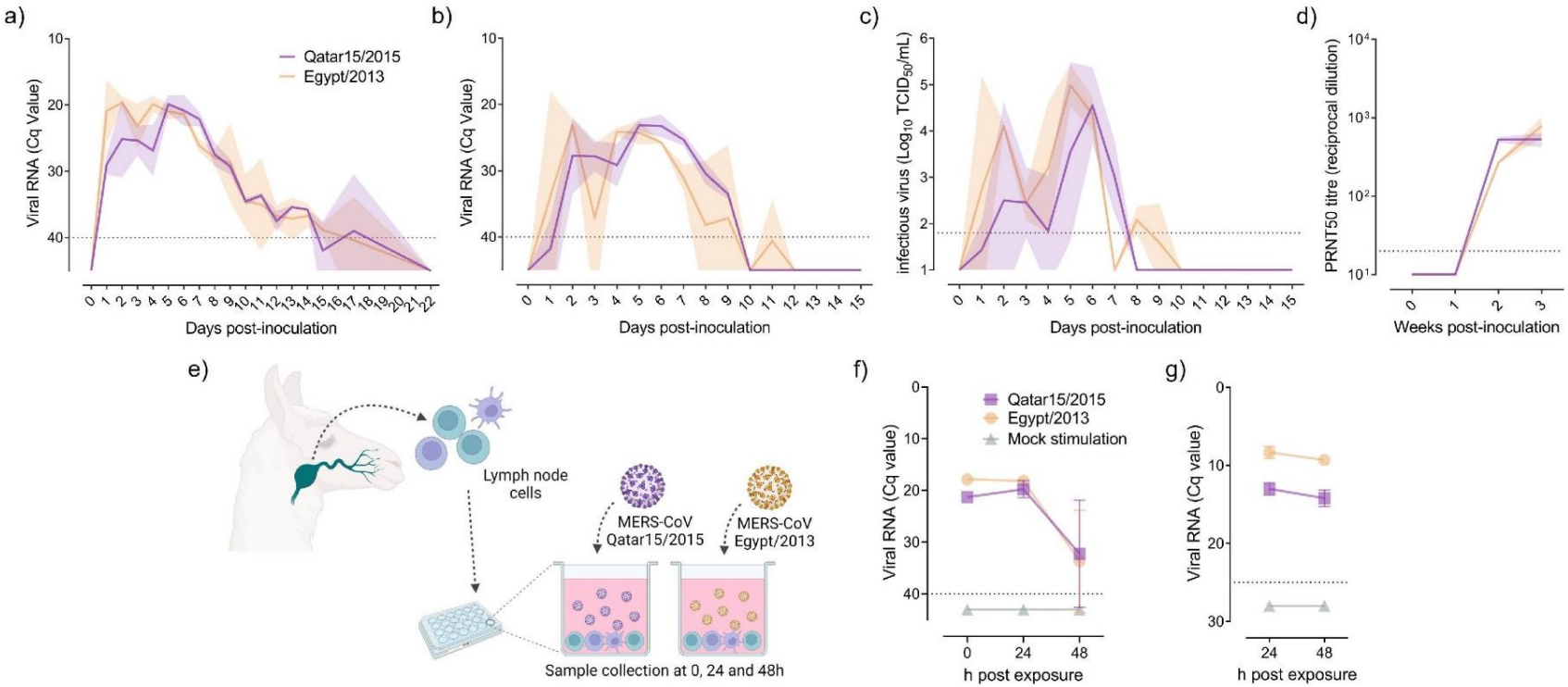
a)
Viral RNA (Cq Value)
Qatar15/2015
Egypt/2013
Days post-inoculation
b)
Viral RNA (Cq Value)
Days post-inoculation
c)
infectious virus (Log10 TCID50/mL)
Days post-inoculation
d)
PRNT50 titre (reciprocal dilution)
Weeks post-inoculation
e)
Lymph node cells
MERS-CoV Qatar15/2015
MERS-CoV Egypt/2013
Sample collection at 0, 24 and 48h
f)
Viral RNA (Cq value)
Qatar15/2015
Egypt/2013
Mock stimulation
h post exposure
g)
Viral RNA (Cq value)
h post exposure

Figure 7.1. Experimental inoculation of llamas with MERS-CoV and susceptibility of llama lymph node (LN) cells to infection. Llamas were intranasally inoculated (primed) with MERS-CoV Egypt/2013 (orange) or Qatar15/2015 (purple). Genomic (a) and subgenomic (b) viral RNA, and (c) infectious MERS-CoV titres were quantified in nasal swab samples collected at different days post-MERS-CoV inoculation (dpi). Plot (d) shows serum-neutralizing antibodies elicited against MERS-CoV in experimentally inoculated llamas. Solid lines indicate mean values and light represent standard deviation intervals. At 22 dpi, llama LN cells were isolated and pulsed with the same MERS-CoV strain used for inoculation, as represented in panel (e). Panels (f) and (g) display data from llama LN cells seeded in triplicates and exposed for 24 and 48 h to MERS-CoV Qatar15/2015 (purple rectangles), Egypt/2013 (orange circles) or cultured in media only (green triangles). Mean values (± SD) of genomic viral RNA detection in culture supernatants (f) and cell-associated viral RNA (g) were monitored throughout the study. Grey dashed lines depict the detection limits of the assays. Cq, quantification cycle; MERS-CoV, Middle East respiratory syndrome coronavirus; PRNT50, 50% plaque reduction neutralization titre; $TCID_{50}$, 50% tissue culture infective dose.

We also studied whether LN cells could mount immune responses to a secondary viral exposure *in vitro*. Transcriptomic profiles from 43 immune response genes were obtained using a previously described microfluidic RT-qPCR assay (*Chapter 5*), which included the quantification of type I, II and III IFNs, PRRs, TFs, ISGs, cytokines and chemokines involved in inflammatory responses, among other immune-related genes (**Figure 7.2a**). Afterwards, gene expression levels of LN cells exposed to MERS-CoV and mock-treated samples were compared to those from freshly isolated cells. Mock-exposed cells experimented a mild increase of immune response genes transcription and this was more evident at 48 h post *in vitro* culture (**Figure 7.2a** and **b**). *IFN-γ* expression was significantly up-regulated in MERS-CoV-treated cells and progressively increased over time (**Figure 7.2a** and **b**). Although not statistically significant, a stronger induction of *IFN-γ* occurred in cells

exposed to the Qatar15/2015 strain than the ones exposed to the Egypt/2013 (**Figure 7.2b**). Expression levels of *IL-2* and *IL-12* similarly increased at 24 hpe and subsequently returned to basal levels (**Figure 7.2b**). On the other hand, contrary to cells exposed to the MERS-CoV Egypt/2013 strain, an increase of *IL-4* expression was only reported in cells treated with the Qatar15/2015 strain (**Figure 7.2a** and **b**). Remarkably, the induction of *IL-10* mRNA was not detected in any llama cells. Overall, results are reminiscent of a Th1 response elicited in LN cells after re-exposure to MERS-CoV, regardless of the strain used for stimulation.

Innate immune gene responses were also monitored. Transcription of *IFN-λ3* mRNA was markedly upregulated in cells treated with both MERS-CoV strains, being significantly higher in those stimulated with the Qatar15/2015 strain (**Figure 7.2b**). However, type I IFNs (*IFN-α* and *IFN-β*) were only upregulated in LN cells exposed to the Qatar15/2015 strain at 24 hpe (**Figure 7.2b**). Expression of TFs (*STAT1* and *IRF7*), ISGs (*CXCL10, MX1, OAS1* and *ISG15*), and PRRs (*RIG-1*, *MDA-5* and *TLR-7*) was enhanced in cells according to levels of IFNs (**Figure 7.2a** and **b**). Thus, the Egypt/2013 strain moderately induced the above-mentioned genes at 24 hpe, while higher upregulations occurred in cells exposed to the Qatar15/2015 strain that waned over time for both strains (**Figure 7.2b**). In addition, a mild but significant upregulation of *TRIM25*, *CCL3*, and *IL-15* was mostly observed at 24 hpe by cells exposed to the Qatar15/2015 strain (**Figure 7.2a**). Importantly, pro-inflammatory responses were not induced throughout the study. These results evidenced that early and transient antiviral cellular immune responses were effectively triggered in LNs of llamas re-exposed to MERS-CoV. Responses induced by the MERS-CoV Qatar/2015 strain

were significantly more pronounced than those provoked by the Egypt/2013 strain.

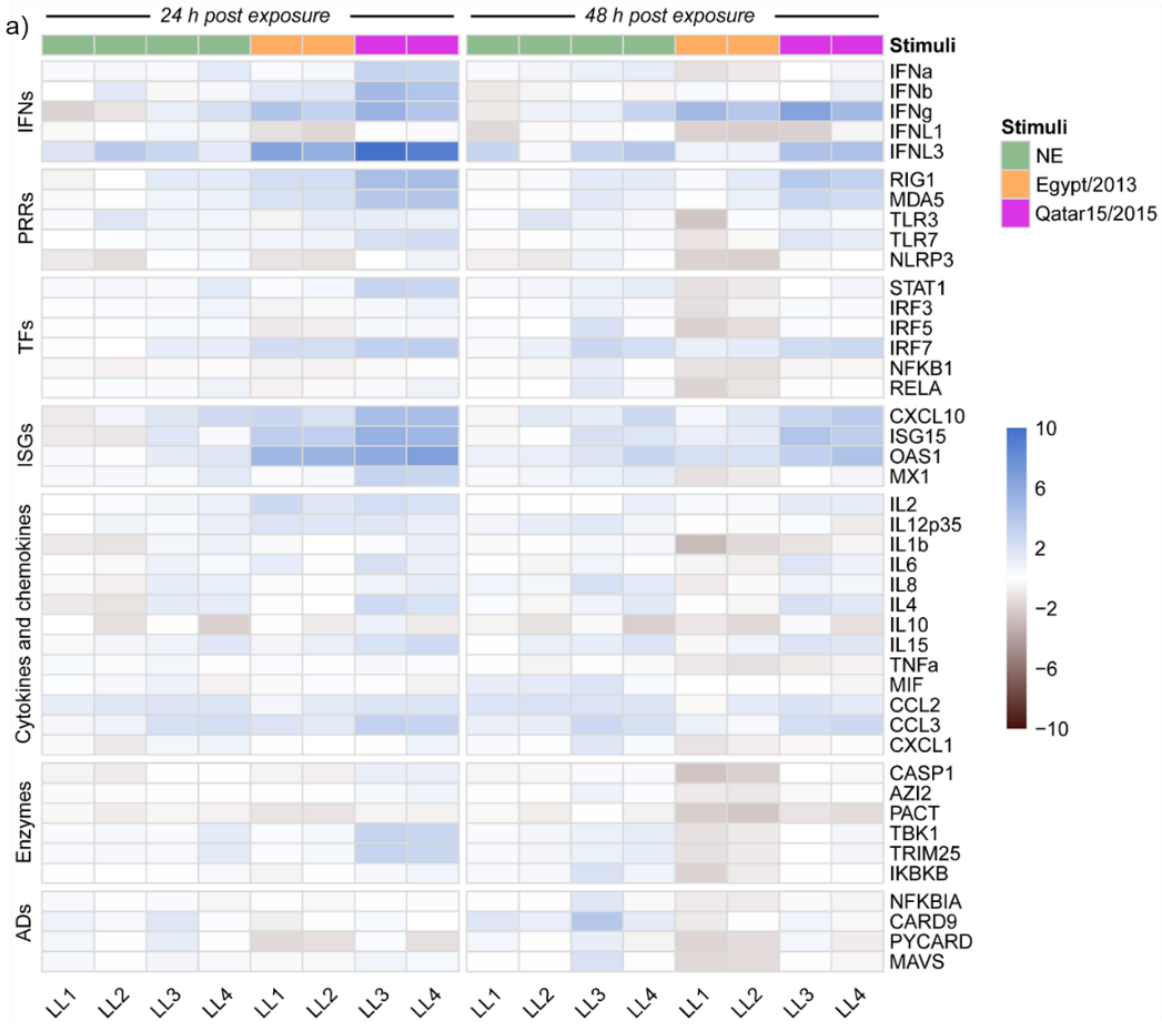

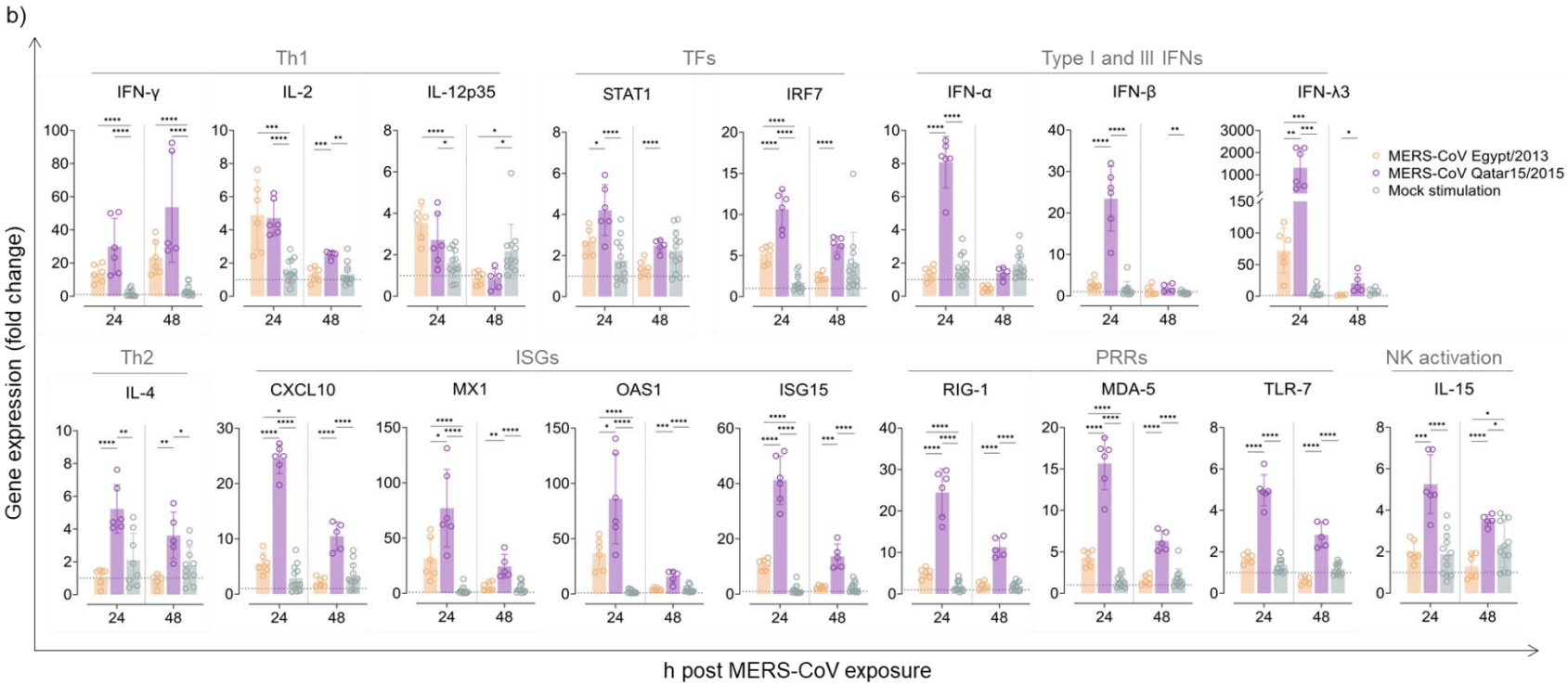
b)
Th1
TFs
Type I and III IFNs
IFN-γ
IL-2
IL-12p35
STAT1
IRF7
IFN-α
IFN-β
IFN-λ3
MERS-CoV Egypt/2013
MERS-CoV Qatar15/2015
Mock stimulation
Th2
ISGs
PRRs
NK activation
IL-4
CXCL10
MX1
OAS1
ISG15
RIG-1
MDA-5
TLR-7
IL-15
Gene expression (fold change)
h post MERS-CoV exposure

Figure 7.2. Expression of immune response genes by llama lymph node (LN) cells pulsed with MERS-CoV. A microfluidic RT-qPCR assay was used to quantify transcripts of immune-related genes at different h post MERS-CoV exposure (hpe). (a) After relative normalization, mean expression values (triplicates) of llama LN cells exposed for 24 and 48 h to MERS-CoV Qatar15/2015 (purple rectangles), Egypt/2013 (orange rectangles), or cultured in media only (NS, green rectangles) were calculated respective to non-cultured control cells. Mean log2 fold-change expression values of each studied gene are represented in a heat-map plot with colour variations; blue for up-regulated and black for down-regulated gene expression, respectively. Panel (b) display the relative expression values of some differentially regulated genes at 24 and 48 h after exposure to MERS-CoV Qatar15/2015 (purple), Egypt/2013 (orange) or cultured in media only (green). Boxes indicate mean expression values and error bars represent SD intervals. Individual relative expression measurements are shown as empty circles. Grey dashed lines display basal expression levels from freshly isolated control cells. *, *p*-value < 0.05; **, *p*-value < 0.001; ***, *p*-value < 0.0001; ****, *p*-value < 0.00001; ADs, adaptors; IFNs, interferons; ISGs, IFN stimulated genes; LL, llama; NK, natural killer T cells, PRRs, pattern-recognition receptors; TFs, transcription factors; Th1, T-helper 1; Th2, T-helper 2.

7.4 Discussion

In this study, we demonstrated that cervical LN cells from llamas do not support MERS-CoV replication *in vitro*. There is no data on the replication of MERS-CoV in LNs of other susceptible species. Nonetheless, our findings support the concept that camelid dendritic-like cells carry MERS-CoV to LNs [207,208,236] without active viral replication, and they might be the drivers of potent immune responses that prevent virus spread.

We investigated if llamas could mount cellular adaptive immune responses to counteract MERS-CoV infection. Indeed, llama LN cells re-exposed to the virus developed an early induction of *IL-12* in all MERS-CoV pulsed cells, suggesting that both Qatar15/2015 and Egypt/2013

strains were effectively mounting an immune response accompanied by an increase of *IFN-γ* over time. The concomitant induction of *IL-2* suggested activation of Th1 lymphocytes, similar to previous findings in PBMCs from convalescent human patients pulsed with MERS-CoV peptide pools [246,247]. Alternatively, or in addition, NK cells residing in camelid LN could be responsible for the up-regulation of *IFN-γ*, as previously described in cattle and human [418,419]. On the other hand, the absence of *IL-10* up-regulation would indicate that Th2 cells were not induced or recalled. Further detailed studies are needed to deeply characterize T- and B- cell responses in LNs.

Importantly, significant induction of type I, II and III IFNs was noticed in LN cells of animals primed and re-stimulated with at least the Qatar15/2015 isolate, with a consequent up-regulation of ISGs, PRRs and TFs involved in antiviral responses. Strikingly, pro-inflammatory cytokines (*TNF-α*, *IL-1β*, *IL-6* and *IL-8*), *CARD9* (an activator of NF-κB) and components of the inflammasome (*NLRP3*, *CASP1*, *PYCARD*) remained at basal transcription levels or were slightly up- or down-regulated. This would imply specific mechanisms of camelids for dampening inflammation as observed in bats [279,280]. In these virus-tolerant animals, NF-κB-dependent inflammatory genes are inhibited under the action of C-Rel [279]. Similar studies should be performed in camelid species to precisely determine mechanisms controlling inflammation and their similarity to those engaged in bats. Nonetheless, like bats, camelids can control inflammation mediating an impaired NLRP3 inflammasome. In the present study, *IFN-λ3* but not *IFN-λ1* was highly up-regulated and might contribute to counterbalancing the inflammatory effects of type I IFNs [420]. Moreover, control of inflammation is not specific to LN cells, since we previously described

dampened inflammatory responses in the nose, trachea, and lungs of MERS-CoV-challenged alpacas. Early and transient type I and III IFNs were also produced by the nasal epithelium of these animals [8,32]. A previous study unravelled the high production of type I and III IFNs by human pDCs in the absence of productive MERS-CoV replication [199]. Camelid pDCs sensing MERS-CoV might also contribute to the pronounced *IFN-λ3* response in LNs. Altogether, our results highlight that *IFN-λ3* might have a key role in bridging innate and adaptive immunity from the infected respiratory mucosa to secondary lymphoid organs, as previously described for other viral infection [421,422]. Thus, camelid species own key mechanisms to host MERS-CoV in the absence of clinical disease.

At 24 hpe, the Qatar15/2015 strain induced higher antiviral transcripts than the Egypt/2013 strain, while levels of cytokine mRNAs decayed thereafter except for *IFN-γ*. Possibly, pathogen-associated molecular patterns (PAMPs) of the Qatar15/2015 strain better activated type I and III IFN pathways. Alternatively, the peak of antiviral responses could be elicited earlier with the Egypt/2013 strain. However, our observations should be confirmed with samples from a larger number of animals, being also collected at early time points after viral exposure. Overall, llama cervical LN cells elicited early antiviral responses in the absence of inflammation to MERS-CoV re-exposure, which were higher for the clade B strain compared to its clade C counterpart. Although animals inoculated with a high dose of either MERS-CoV Egypt/2013 or Qatar15/2015 had similar levels of viral shedding, *Chapters 3* and *4* provide experimental data supporting an increased replication, shedding and transmission potential of MERS-CoV clade B viruses compared to clade C strains in llamas. Further studies are needed to understand if a

differential viral replication and tropism in respiratory tissues could explain the differential immune response intensities observed between MERS-CoV strains.

A potential limitation of our study is the lack of comparison with LN cells from healthy, non-convalescent animals, which may help to discern unique features of camelid memory T-cell responses *versus* those occurring in a primary infection. Further studies using this experimental control would complement our work. Finally, the use of peptide pools to stimulate camelid LN lymphocytes would reveal the most immunogenic MERS-CoV-specific T cell epitopes, and thus, improve animal vaccine design.

In conclusion, we found that MERS-CoV does not replicate in camelid LN cells. Also, convalescent llamas develop strong cellular antiviral responses that are rapidly activated *in vitro* following a secondary viral exposure, in the absence of inflammation.

Appendix 7

Appendix Table 7.1 is available online at:

https://drive.google.com/drive/folders/1Ltz1bGtYWrmTBvfYz2YBalGhXT1azwIC

Chapter 8

Protective efficacy of an RBD-based Middle East respiratory syndrome coronavirus (MERS-CoV) particle vaccine in llamas

---

Chapter published at:

Rodon, J., Mykytyn, A. Z., Cantero, G., Albulescu, I. C., Bosch, B. J., Brix, A., Audonnet, J. C., Bensaid, A., Vergara-Alert, J., Haagmans, B. L., & Segalés, J. (2022). Protective efficacy of an RBD-based Middle East respiratory syndrome coronavirus (MERS-CoV) particle vaccine in llamas. *One Health Outlook*, *4*(1), 12. https://doi.org/10.1186/s42522-022-00068-9

8.1 Introduction

MERS-CoV is associated with severe pneumonia and lethal disease in humans with high case-fatality rates in the Middle East [4,23]. The virus still poses a public health concern since ongoing zoonotic transmission events from dromedary camels, the main source of infection, and several major travel-associated outbreaks have been documented [26].

Dromedaries are the main reservoir, although other camelid species such as llamas and alpacas are also susceptible to MERS-CoV [8,16,65,115,116,234,235]. Camelids, as opposed to humans, undergo a mild to subclinical infection upon MERS-CoV infection, characterized by upper respiratory tract replication and rapid clearance of the virus within 1-2 weeks after infection [207,208]. Robust and timely innate immune responses occurring in camelids might play a crucial role in controlling MERS-CoV infection and disease development [8]. Importantly, animals showing nasal discharges and asymptomatic carriers shed abundant quantities of MERS-CoV [65,207,208], which may result in a potential spillover to humans.

To date, commercial vaccines and therapeutics against MERS-CoV are lacking, and the World Health Organization has advised animal vaccination as a strategy to control the spread of MERS-CoV to animals and humans [237]. Different vaccine prototypes have been tested in camelids to counteract MERS-CoV, all of them focusing on the full-length or specific regions of the S protein [203,207,209]. This protein mediates viral entry by binding to the host cell receptor dipeptidyl peptidase-4 [47] and subsequent fusion of the viral and cellular membrane. The spike protein is highly immunogenic and the main target of neutralizing antibodies and, therefore, the antigen of choice for vaccine development

against MERS-CoV and other betacoronaviruses [285]. Viral-vector vaccines expressing the full-length S protein induced partial immunity and, in some instances, when exposed to MERS-CoV, reduced rhinorrhea and viral shedding in dromedaries [203,207]. Importantly, an increase in nAb titers was observed after one vaccination of seropositive animals, resulting in minimum excretion of viral RNA after exposure to naturally infected camels [203]. This fact is of special relevance due to the high prevalence of seropositive camels found in the Middle East.

Further, to mimic the natural transmission occurring in the field, we previously developed a direct-contact llama transmission challenge model to demonstrate that can be a useful setting for vaccine efficacy studies. Here, we used the same direct-contact model to assess the efficacy of a virus-like particle vaccine to block MERS-CoV transmission in llamas. The vaccine was composed of self-assembling multimeric protein scaffold particles (MPSP) expressing the RBD of the MERS-CoV S protein [226]. The MPSP vaccine prototype allows the self-assembly of antigens into 60-mer particles and offers enhanced immune responses in comparison to other multivalent and monomeric recombinant vaccines [226,424,425]. Indeed, the proposed vaccine prototype induced strong protective immune responses that reduced MERS-CoV replication in the upper and lower respiratory tract of experimentally infected rabbits [226]. Since rabbits do not develop severe disease upon MERS-CoV inoculation as occurs in humans, nor a subclinical infection with high viral secretions that camelid reservoirs experience [232], this study provided a rationale for testing the MPSP-RBD vaccine prototype in camelids.

8.2 Material and methods

Animal welfare and ethics

Animal experiments with MERS-CoV were performed at the BSL-3 facilities of the Biocontainment Unit of IRTA-CReSA. The present study was approved by the CEEA-IRTA and by the Ethical Commission of Animal Experimentation of the Autonomous Government of Catalonia (file No. CEA-OH/10942/1).

Cell culture and virus

Vero E6 cells were cultured as described in *Chapter 3*. The MERS-CoV Qatar15/2015 stock was prepared as indicated in *Chapters 3*.

Vaccine design and expression

The vaccine immunogen was prepared by coupling purified RBD of MERS-CoV spike onto the surface of the mi3 60-mer MPSP using the SpyTag-SpyCatcher strategy [226,426]. Recombinant mi3 fused to the SpyCatcher was expressed in *E. coli* cells, as follows. A bacterial culture with an OD_{600} of ~0.5 was induced for expression with 0.1 mM IPTG (isopropyl β-D-1-thiogalactopyranoside) and incubated overnight at 18°C in a shaking incubator. Next the bacteria were pelleted by centrifugation at 8,000×g, incubated for 30 min in lysis buffer at 25°C, followed by sonication on ice. Unlysed bacteria, debris and the insoluble protein fraction were removed by centrifugation (100min/4°C/18,000×g). Purification was performed by an initial heat treatment step (30 min, 60°C), followed by another centrifugation step (see above) and size exclusion chromatography (Superdex^{TM} 75). Recombinant RBD of MERS-CoV spike with a C-terminal SpyTag was expressed and purified as previously described [226] and coupled to the

SpyCatcher containing mi3 MPSP at a molar ratio of 1:3 RBD:mi3, in DPBS without calcium and magnesium (Lonza). Concentrations of all purified proteins were determined with the NanoDrop ND-1000 spectrophotometer.

Study design

Seven healthy llamas were purchased from a private animal facility and housed at the IRTA farm of Alcarràs (Catalonia, Spain) during the immunization period. Animals were transferred to the BSL-3 animal facilities of the Biocontainment Unit of IRTA-CReSA for experimental procedures involving MERS-CoV.

Three llamas were intramuscularly immunized in the right side of the neck with 40 µg of a MERS-CoV RBD coupled with 120 µg mi3 and emulsified (1:1 volume) with Montanide™ ISA 206 VG (Seppic, France) adjuvant, administering a total volume of 2 mL per animal and dose. A second immunization was conducted 3 weeks later as described above but in the left side of the neck. Two other animals received an emulsion of PBS and Montanide™ ISA 206 VG (1:1 volume) at the vaccination days, while the two remaining animals were kept naïve. Five weeks after the first immunization, two naïve llamas were intranasally inoculated with a 10^7 $TCID_{50}$ of MERS-CoV Qatar15/2015 strain (GenBank Accesion MK280984) in 3 mL saline solution using a nebulization device (LMA® MADgic®, Teleflex Inc., USA), administrating 1.5 mL into each nostril. At 2 dpi, vaccinated (n=3) and naïve llamas (n=2) were brought into contact with inoculated llamas (**Figure 8.1**). The box in the BSL-3 facility was set up as in previous MERS-CoV transmission study in *Chapter 3* and as represented in **Figure 8.1**.

Animals were monitored daily for respiratory clinical signs, including sneezing, coughing, nasal discharge and/or dyspnea. Rectal temperatures were recorded with a fast display digital thermometer (AccuVet®, Infratec, Italy) until 15 dpi plus the day of necropsy. NS were obtained daily until 15 dpi, and then at 17 and 22 dpi (**Figure 8.1**). Whole blood samples of all animals were collected from the jugular vein using Vacutainer® tubes (Beckton Dickinson, USA) and serum samples were obtained before the first and the second immunizations, prior to challenge, and weekly after the MERS-CoV challenge (**Figure 8.1**). Animals were euthanized at 22 dpi with an overdose of pentobarbital and a complete necropsy was performed, with special emphasis on upper and lower respiratory tract lesions.

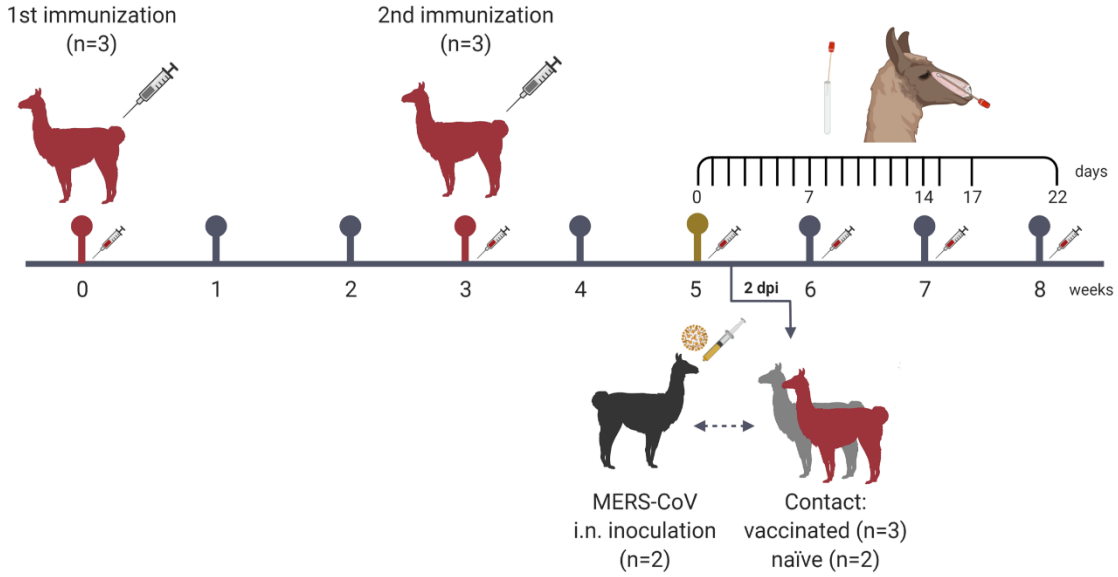
1st immunization
(n=3)
2nd immunization
(n=3)
days
0
7
14
17
22
0
1
2
3
4
5
2 dpi
6
7
8
weeks
MERS-CoV
i.n. inoculation
(n=2)
Contact:
vaccinated (n=3)
naïve (n=2)

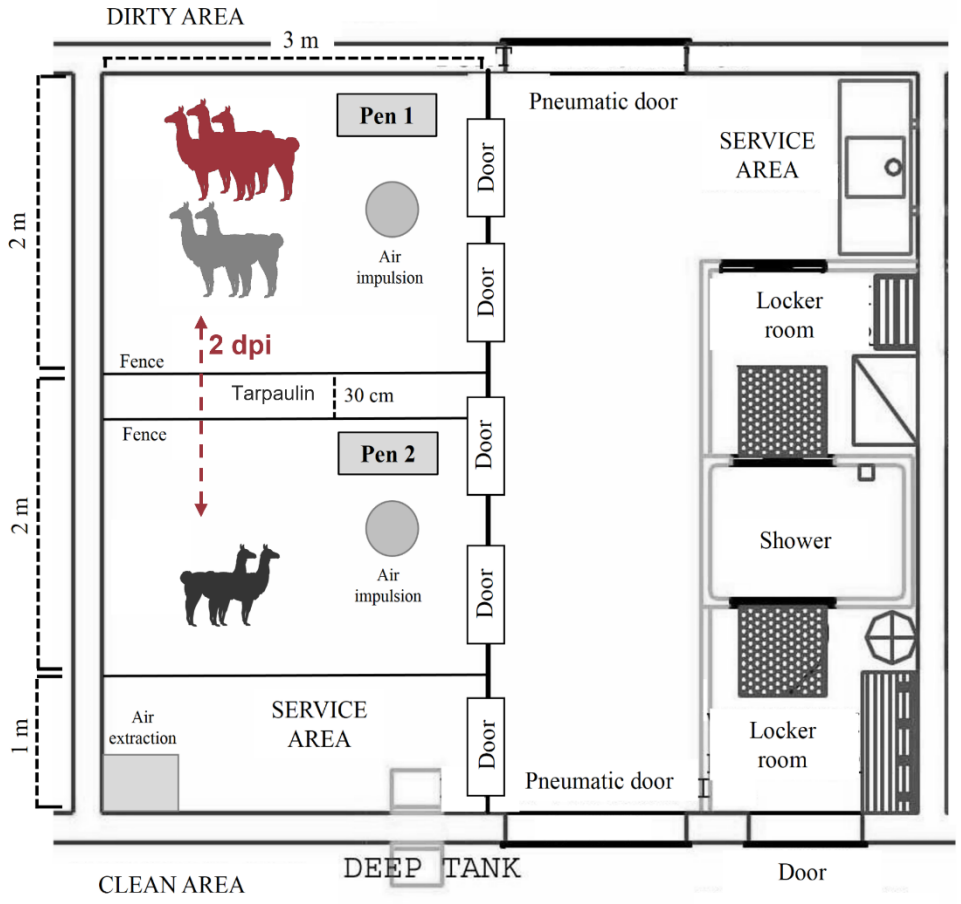
DIRTY AREA
3 m
Pen 1
Pneumatic door
SERVICE
AREA
Door
Door
Air
impulsion
Locker
room
2 m
2 dpi
Fence
Tarpaulin
30 cm
Fence
Pen 2
Door
Shower
Air
impulsion
2 m
Door
Air
extraction
SERVICE
AREA
Locker
room
1 m
Pneumatic door
DEEP TANK
Door
CLEAN AREA

Figure 8.1. Schematic representation of the experimental design. Two llamas (black) were intranasally inoculated with MERS-CoV (Qatar15/2015) and placed in contact with two naïve (grey) and three vaccinated (red) llamas. Experimental groups were kept in different compartments of an experimental box separated by a tarpaulin to prevent animal contact until two days after inoculation procedure, when the tarpaulin was removed, and experimentally infected llamas were brought in direct contact. Immunization dates are shown in red timeline points and with grey syringes. MERS-CoV-inoculation procedure is stressed as a gold time point. Blood collection days are represented with a red syringe symbol on the weeks scale. Sampling scheme of nasal swabs in all animals is shown using black lines in a daily scale. Dpi, days post-inoculation; i.n., intranasal.

MERS-CoV genomic and subgenomic RNA detection

Viral genomic and subgenomic RNA was extracted from nasal swab samples as previously described in *Chapter 4*. Samples with a Cq value ≤40 were considered positive for MERS-CoV genomic or subgenomic RNA.

Virus titration

Nasal swabs samples with lower Cq value ≤ 30 to MERS-CoV RNA, as determined by RT-qPCR, were evaluated for the presence of infectious virus by titration in Vero E6 cells, as previously reported in *Chapter 3*.

Plaque reduction neutralization assay

The levels of nAbs in serum samples collected at different time-points were determined as previously described in *Chapter 4*. with minor modifications. The PRNT titre was calculated using GraphPad Prism 9, calculating a 50% reduction in infected cell counts based on non-linear regression with bottom constraints of 0% and top constraints of 100%.

8.3 Results

Rectal temperatures of all animals remained basal (37-40°C) throughout the study (**Figure 8.2a**). None of the inoculated llamas showed clinical signs at any dpi. One contact-control animal showed moderate rhinorrhea at 5-9 dpi, and one vaccinated animal from 8 to 19 dpi (**Figure 8.2b** and **c**, respectively). MERS-CoV-inoculated llamas had detectable genomic and subgenomic viral RNA in nasal swabs for a period of 2 weeks (**Figure 8.3a** and **b**) and shed high titers of infectious virus during the first week after inoculation (**Figure 8.3c**). These animals seroconverted for MERS-CoV and nAbs were detected from 2 weeks after infection onwards (**Figure 8.3d**).

a)

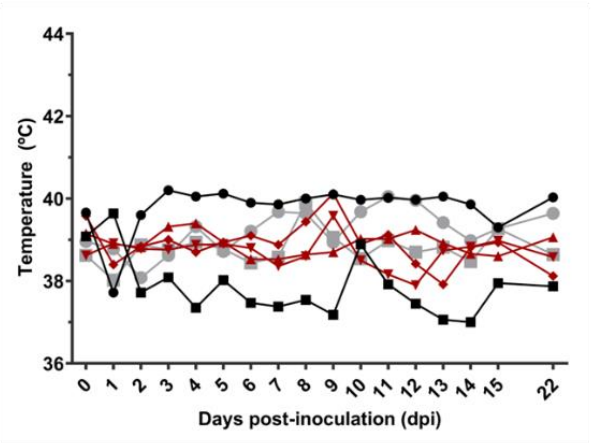

b)

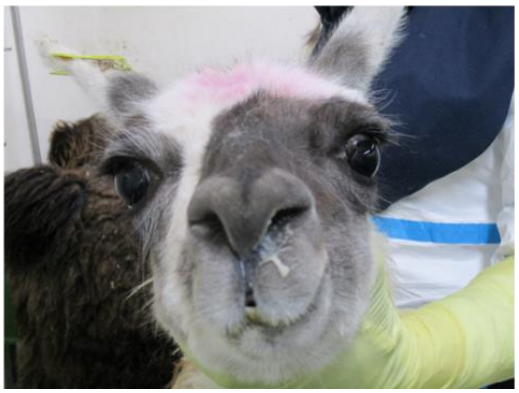

c)

Figure 8.2. Temperature and rhinorrhoea after MERS-CoV exposure to llamas. MERS-CoV experimentally inoculated llamas (black) were, two days later, put in contact with naïve (grey) and vaccinated (red). (a) Rectal temperature was measured daily after MERS-CoV. Each line/sign represents an individual animal. One naïve (b) and one vaccinated, contact animal (c) showed moderate mucus excretion at 5-9 and 8-19 days post-inoculation procedure, respectively.

As determined by RT-qPCR and virus titration in cell culture, MERS-CoV was transmitted to all adjuvant-administered and two out of three vaccinated, in-contact animals at 5-7 dpi (**Figure 8.3a**, **b** and **c**). With the exception of one vaccinated llama, all animals had similar profiles in the duration and levels of viral RNA and infectious virus shedding (**Figure 8.3a**, **b** and **c**). These results are comparable to previous ones obtained in inoculated and naïve contact animals (*Chapter 3*); therefore, individual differences observed in the current study may account for minor variations in viral shedding patterns of vaccinated and control-contact animals. The remaining vaccinated-contact llama was protected against MERS-CoV infection. Only minor traces of MERS-CoV genomic RNA were detected in nasal swabs of this animal along the experiment, evidencing its exposure to the virus (**Figure 8.3a**). Moreover, subgenomic RNA was not detected at any time point of the study in this vaccinated llama and the animal did not shed infectious virus (**Figure 8.3b** and **c)**. Furthermore, all inoculated and in-contact naïve llamas developed a comparable neutralizing humoral response to MERS-CoV (**Figure 8.3d**). MPSP-RBD vaccination induced high titres of virus nAbs in sera, which were boosted in 2 out of 3 animals three weeks after contact with MERS-CoV-inoculated llamas shedding high titres of infectious virus (**Figure 8.3d**). Thus, the MPSP-RBD vaccine candidate was able to partially prevent MERS-CoV transmission among

camelids, being effective in 1/3 of the animals vaccinated in this exploratory study.

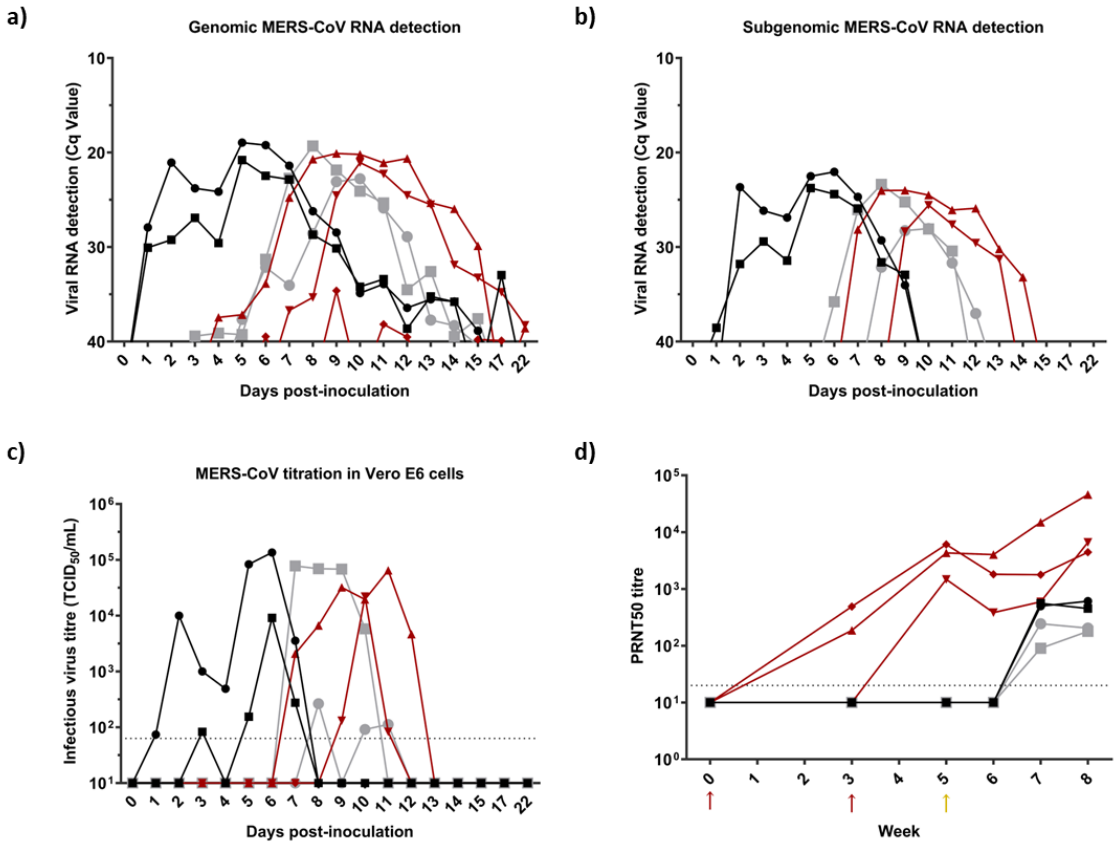

Figure 8.3. MERS-CoV RNA and infectious virus shedding and development of neutralizing antibodies in llamas. Experimentally infected llamas (black) were placed in contact with naïve (grey) and vaccinated (red) animals two days after MERS-CoV inoculation. Genomic (a) and subgenomic (b) viral RNA was quantified in nasal swab specimens collected at different times after MERS-CoV inoculation. Plot (c) show infectious MERS-CoV titres in nasal swabs collected on different days after MERS-CoV inoculation. Plot (d) displays serum neutralizing antibodies elicited against MERS-CoV in vaccinated, experimentally inoculated and in-contact naïve llamas. Each line represents an individual animal. Dashed lines depict the detection limits of the assays. Red and yellow arrows indicate the two MPSP-RBD immunizations and MERS-CoV inoculation days, respectively. Cq, quantification cycle; MERS-CoV, Middle East respiratory syndrome coronavirus; PRNT50, 50% plaque reduction neutralization titre; $TCID_{50}$, 50% tissue culture infective dose.

8.4 Discussion

Vaccination of livestock reservoir species is a recommended strategy to prevent spread of MERS-CoV among animals and potential spillover to humans [170]. Based on the enhanced immune response offered by MPSP-displayed immunogens and the *in vivo* protective capacity of the MPSP-RBD vaccine prototype against MERS-CoV [226], we evaluated its potential to inhibit MERS-CoV transmission among camelid reservoirs. While MERS-CoV was transmitted to naïve animals exposed to virus-inoculated llamas, immunization with the MPSP-RBD formulated with a commercial adjuvant elicited robust nAbs to MERS-CoV and prevented transmission in 1/3 vaccinated, in-contact animals. Since high MERS-CoV seroprevalence and evidence of reinfection have been found in camelids [121], further studies would be needed to investigate whether MPSP-RBD administration can boost sufficient protective immune responses to MERS-CoV and decrease the transmission rate in previously exposed animals. Our exploratory study supports further improvement of the RBD-based vaccine to reduce MERS-CoV transmission. The monomeric RBD displayed by MPSP may induce lower protective responses than a prototype shaping a trimeric conformation or the combination with other S subunits. Nonetheless, the capabilities of MPSP-RBD to prevent animal-to-animal transmission of MERS-CoV and, eventually, human spillover, seem limited.

Chapter 9

Blocking transmission of Middle East respiratory syndrome coronavirus (MERS-CoV) in llamas by vaccination with a recombinant spike protein

---

Chapter published as a part (II) of the article:

Rodon, J., Okba, N., Te, N., van Dieren, B., Bosch, B. J., Bensaid, A., Segalés, J., Haagmans, B. L., & Vergara-Alert, J. (2019). Blocking transmission of Middle East respiratory syndrome coronavirus (MERS-CoV) in llamas by vaccination with a recombinant spike protein. *Emerging Microbes & Infections*, *8*(1), 1593–1603. DOI: 10.1080/22221751.2019.1685912

9.1 Introduction

The current MERS-CoV vaccine candidates mainly use the entire or sub regions of the S protein or its coding gene. This virus surface structural glycoprotein binds to the host receptor, the DPP4 [47], through its S1 subunit and is therefore the target of choice to raise nAbs [285,290]. The S1 subunit protein is immunogenic and can induce both T-cell mediated and NAb responses mainly directed towards the RBD (or $S1^B$ domain) [285,286]. Recently, it was reported that although most nAbs target the $S1^B$ domain, antibodies targeting the sialic acid-binding $S1^A$ domain can also provide protection against lethal MERS-CoV challenge in a mouse model [288].

Several vaccine prototypes to control MERS-CoV have been tested using a wide variety of delivery systems, including DNA vaccines, protein-based vaccines, vector-based vaccines and live attenuated vaccines [290,427]. Vector-based-vaccines have been developed using the orthopox modified virus Ankara (MVA) [207], different host-origin adenovirus (AdV) [316,317,319,428], measles virus (MeV) [325], rabies virus (RABV) [328], and Venezuelan equine encephalitis replicons (VRP) [227,428], all expressing different lengths of the S protein. These vector-based candidates were tested in hDPP4 transgenic or transduced mice, except the orthopox-based recombinant vaccine, which expresses the full-length MERS-CoV spike protein and induced efficient protective immunity in dromedaries [207]. Due to reticence in applying live genetically modified organisms, protein recombinant subunit or DNA vaccines mainly based on the S1 protein or gene, respectively, are also under study. A DNA-based vaccine expressing the full-length S protein was shown to induce MERS-CoV specific nAbs and confer protection in rhesus macaques [334]. In addition, MERS-CoV protein-based vaccines using the full-length or fragments of the S protein

were produced in the form of virus-like particles, nanoparticles, peptides, or recombinant protein. Partial protection efficacy for some candidates has been demonstrated in NHP [332,347] and hDPP4 transgenic mice [229,287,342,346,429–431]. A more recent study demonstrated that an S protein subunit vaccine conferred protection to MERS-CoV (EMC/2012 strain) in an alpaca model, although in dromedary camels the vaccine was only able to reduce and delay viral shedding [209]. However, there is no evidence that any of the MERS-CoV vaccine candidates developed so far can block MERS-CoV transmission in camelids when tested in a direct-contact virus transmission setting, mimicking natural transmission in the field. Vaccinating the MERS-CoV animal reservoirs can potentially reduce transmission to humans and provide a simple and economical solution to avoid expansion of this threatening disease.

In the present study, we have successfully used a llama direct-contact transmission model (described in *Chapter 3*) to demonstrate the efficacy of a recombinant S1-protein vaccine, using a registered adjuvant, to block MERS-CoV transmission.

9.2 Materials and methods

Animal welfare and ethics

Experiments with MERS-CoV were performed at the BSL-3 facilities of the Biocontainment Unit of IRTA-CReSA. The present study was approved by the CEEA-IRTA and by the Ethical Commission of Animal Experimentation of the Autonomous Government of Catalonia (file No. FUE-2017-00561265).

Cell culture and MERS-CoV

Cell culture and preparation of viral stocks were performed as described in *Chapter 3*.

Vaccine

Full-length MERS-CoV S1 recombinant protein, including A and B domains, was produced in house using baculovirus and HEK 293T cells production systems as previously described [54,288]. In brief, to produce soluble MERS-CoV S1 using the baculovirus expression system, the gene fragment encoding the MERS-CoV S1 subunit (amino acid 19 – 748; EMC/2012 isolate; GenBank Accession YP_009047204.1) was codon-optimized for insect cell expression and cloned in-frame between honeybee melittin secretion signal peptide and a triple StrepTag purification tag in the pFastbac transfer vector. Generation of bacmid DNA and recombinant baculovirus was performed according to protocols from Bac-to-Bac system (Invitrogen), and expression of MERS-CoV S1 was performed by infection of recombinant baculovirus of Sf-9 cells. Recombinant proteins were harvested from cell culture supernatants 3 days post infection and purified using StrepTactin sepharose affinity chromatography (IBA).

Production of recombinant MERS-S1 in HEK 293T cells was described previously [54,288]. In brief, the MERS-S1 (amino acid 1-747; EMC/2012 isolate; GenBank Accession YP_009047204.1) encoding sequence was C-terminally fused to a gene fragment encoding the Fc region of human IgG and cloned into the pCAGGS mammalian expression vector, expressed by plasmid transfection in HEK-293T cells, and affinity purified from the culture supernatant using Protein-A affinity chromatography. The Fc part of S1-Fc fusion protein was proteolytically removed by thrombin following Protein-A affinity purification using the thrombin cleavage site

present at the S1-Fc junction.

Animals, vaccination and experimental design

Eight healthy llamas were purchased and housed at IRTA farm facilities at Alcarràs (Catalonia, Spain) during the immunization period and transferred for challenge at the BSL-3 animal facilities of the Biocontainment Unit of IRTA-CReSA, in Barcelona (Spain).

Five llamas were prime vaccinated each with 35 µg of a recombinant S1 protein produced in a baculovirus system, emulsified (1:1 volume) with Montanide™ ISA 206 VG (Seppic) adjuvant and intramuscularly administered (2 mL per animal and dose) in the right side of the neck. A boosting immunization was conducted 3 weeks later as above (left side of the neck) but with 50 µg of recombinant S1 protein produced in HEK 293T cells, emulsified (1:1 volume) with Montanide™ ISA 206 VG (Seppic) adjuvant. The correct structure of the S1 antigens was previously confirmed by reactivity of conformational antibodies, DPP4 solid phase and sialic acid binding assays [288]. Two weeks later, MERS-CoV challenge was performed. A group of llamas (n=3) were intranasally inoculated with a 10^7 $TCID_{50}$ dose of MERS-CoV Qatar15/2015 strain (GenBank Accesion MK280984) in 3 ml saline solution (1.5 ml in each nostril) using a nebulization device (LMA® MADgic®, Teleflex Inc.). At 2 days post-inoculation (dpi) vaccinated llamas (n=5) were put in contact with infected llamas (**Figure 9.1**, see also **Figure 3.1** from *Chapter 3*). Llamas from the previous study on transmission to naïve in-contact animals (Chapter 3) were used as control group; both studies were performed concomitantly.

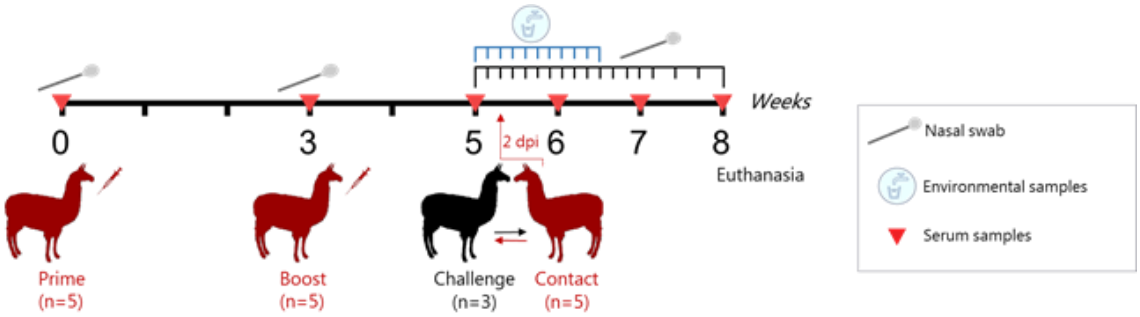

Fig. 9.1. Schematic diagram of the llama vaccination study. Vaccination, challenge and sampling scheme showing vaccinated llamas (red, n=5, LL12-16) and directly inoculated llamas (black, n=3; LL9-11) used as a transmission challenge model for MERS-CoV. Dpi, days post-inoculation.

Regarding to the nomenclature used in this study, animals 9-11 corresponded to intranasally inoculated llamas. Llamas 12-16 were immunized contact animals.

Animals were monitored daily for clinical signs (sneezing, coughing, nasal discharge, or dyspnea). Rectal temperatures were recorded with a fast display digital thermometer (AccuVet®) until day 15 post-inoculation (pi). NS were collected daily until day 15 pi and two extra collections were performed on 17 and 19 dpi. Serum samples were obtained before the first and the second immunizations, prior to challenge, and weekly after the MERS-CoV challenge. Animals were euthanized 3-weeks after challenge, with an overdose of pentobarbital. An extra sampling of NS was performed prior to necropsy procedures.

Viral RNA detection by RT-qPCR

MERS-CoV RNA extraction from NS and genomic RNA detection by RT-qPCR were performed as previously described in *Chapter 3*. Viral replication was assessed with an RT-qPCR for subgenomic RNA detection performed as indicated in *Chapter 4*.

Viral RNA Sequencing

Viral RNA was extracted from llama NS using the QIAamp viral RNA mini kit (Qiagen) according to the manufacturer's instructions. cDNA was produced from RNA using Superscript III first strand synthesis system (Invitrogen Corp) using random hexamers. The cDNA was then used as a template to PCR amplify the MERS-CoV spike S1 encoding region (nucleotides positions 21,304 to 25,660, GenBank Accession JX869059) using the PfuUltra II Fusion HS DNA polymerase (Aligent Technologies). The PCR was carried out as follows: 95°C for 5 min, 39 cycles of 20 sec at 95°C, 20 sec at 48°C, and 45 sec at 72°C, and a final extension at 72°C for 1 min. The amplicons were sequenced bidirectionally using the BigDye Terminator v3.1 cycle sequencing kit on an ABI PRISM 3130XL Genetic analyzer (Applied Biosystems).

Virus titration

Presence of infectious MERS-CoV titres in NS collected at different times pi were determined as previously described in *Chapter 3*.

MERS-CoV S1-ELISA

Specific S1-antibodies in serum samples from all collected time-points and from all animals were determined by a MERS-CoV S1-ELISA as previously described in *Chapter 3*.

MERS-CoV N-LIPS

Llama sera was tested for MERS-CoV N antibodies using a luciferase LIPS assay, as previously described in *Chapter 3*.

HI assay

Llama sera was assayed for the presence of functional antibodies against

the $S1^A$ domain of the S protein using a nanoparticle-based HI assay, as previously described in *Chapter 3*.

RBI inhibition assay

We tested llama sera from the vaccine efficacy study for antibodies able to block MERS-CoV binding to DPP4 as indicated in *Chapter 3*.

Plaque reduction neutralization assay

Serum samples and nasal swabs were tested for neutralizing antibodies against MERS-CoV (Qatar15/2015 and EMC/2012 isolates) using a PRNT assay, as previously described in *Chapter 3*.

9.3 Results

Clinical signs

Two directly-inoculated llamas (No. 9 and 10) showed moderate nasal mucus secretion from 9 to 13 dpi. No clinical signs were noticed in any of the five vaccinated llamas throughout the study. Body temperatures in inoculated and vaccinated in-contact llamas remained constant all along the experiment and never exceeded 39.5ºC.

MERS-CoV RNA and Infectious Virus

All MERS-CoV inoculated llamas shed viral RNA in the nasal cavity during a 2-week period (**Figure 9.2a**). The amount of viral RNA was still high (Cq values < 25) in all inoculated llamas at 6-7 dpi, but a decrease in RNA load was observed from 8 dpi onwards. Only one out of the five vaccinated llamas (No. 15) had viral RNA in the nasal cavity to levels comparable to non-vaccinated in-contact animals, while the other four animals had very low levels of viral RNA (**Figure 9.2a**). Additionally, the

viral RNA from this llama was sequenced at days 9-12 pi and used for comparative analysis of the S1 protein (see **Figure 9.3**). A substitution of serine for phenylalanine was found at the amino acid position 465 (S465F) in comparison with the inoculum isolate S1 protein (see **Figure 9.3a**). This mutation was also found in another vaccinated llama (No. 13) at 10 dpi. Interestingly, we identified the S465F mutation arising at 5-6 dpi in two directly inoculated llamas (No. 9, 10). Furthermore, the same mutation was found in animals from the transmission control group (described in *Chapter 3*), including an inoculated llama (No. 1) and a sentinel (No. 6) llama (see **Figure 9.3b**). To ensure that this mutant is not a neutralization escape mutant, the mutant virus was plaque-purified form the nasal swab of llama No. 9 at 6 dpi. The virus was sequenced (Llama-passaged-Qatar15; GenBank Accession MN507638) to ensure no other mutations were present in the spike protein and then used to carry out neutralization assays. The virus was neutralized by serum of all five vaccinated animals (**Figure 9.4a**).

RT-qPCR positive nasal swab samples were tested for the presence of infectious virus. All intranasally inoculated llamas excreted infectious MERS-CoV at some point until 8 dpi (**Figure 9.2b**). The duration of infectious virus shedding varied among individual animals ranging from 1 up to 6 consecutive days. One inoculated llama (animals No. 10) shed infectious virus continuously from days 1 to 6 pi (**Figure 9.2b**). The peaks of viral RNA coincided with the highest levels of infectious virus shed. Although llama No. 15 had MERS-CoV mRNA indicative of replication in the nasal cavity to levels comparable to non-vaccinated in-contact animals (**Figure 9.5**), as assessed by the specific RT-qPCR described by Coleman and collaborators[41], none of the vaccinated animals (including llama No. 15) shed infectious virus at any point in the study (**Figure 9.2b**).

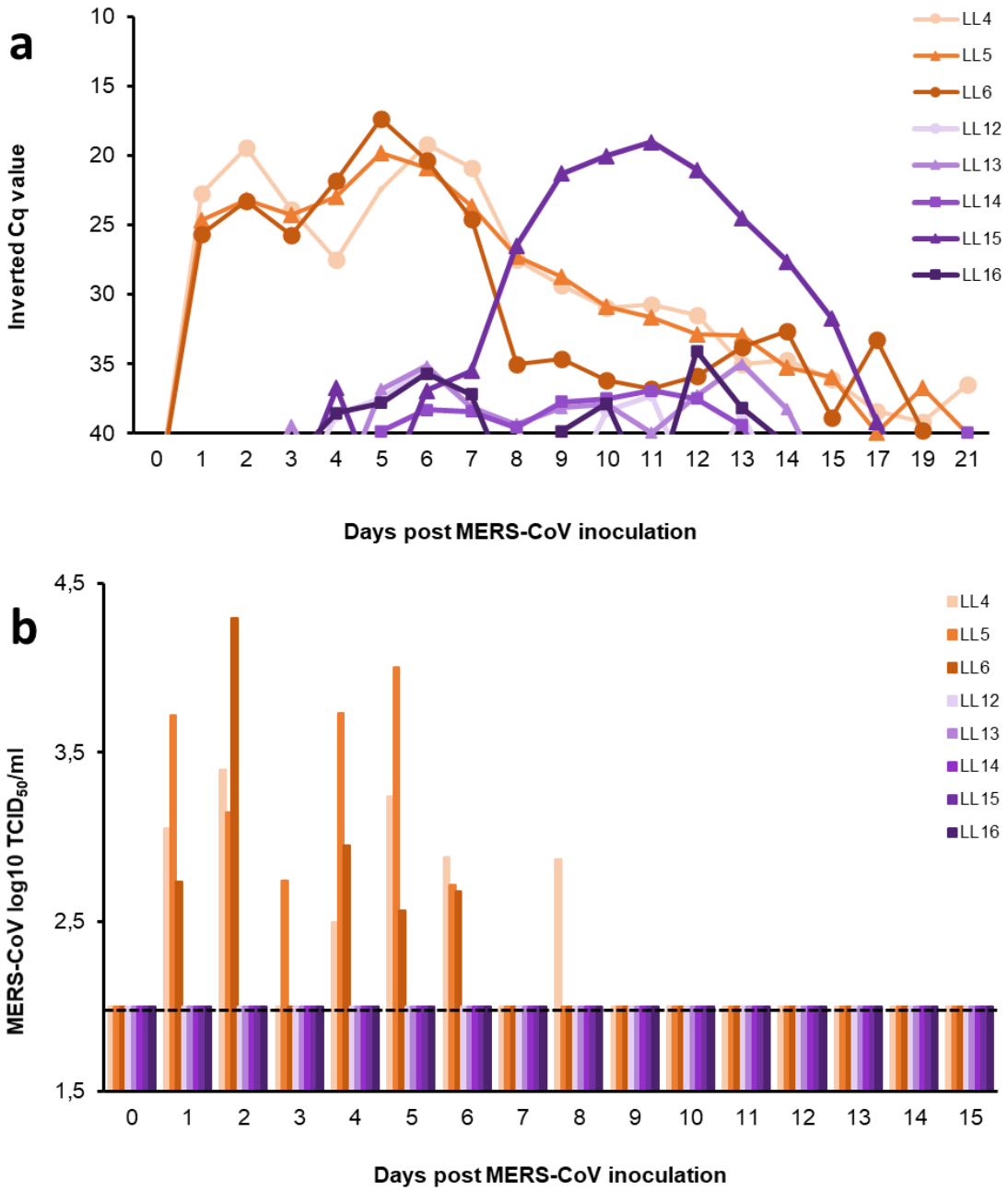

Fig. 9.2 Viral shedding in llamas after experimental inoculation or contact with MERS-CoV-infected llamas. Viral RNA detected in nasal swab samples collected from S1 vaccinated **(a)** llamas at different time points after contact with directly inoculated animals. Panels **b)** display infectious MERS-CoV in nasal swab samples collected from S1 vaccinated animals at different time points after inoculation. Each line/bar represents an individual animal. Orange lines/bars

indicate experimentally inoculated llamas, while purple lines/bars indicate vaccinated llamas. Dashed lines depict the detection limit of the assays. Cq, quantification cycle; MERS-CoV, Middle East respiratory syndrome coronavirus; $TCID_{50}$, 50% tissue culture infective dose.

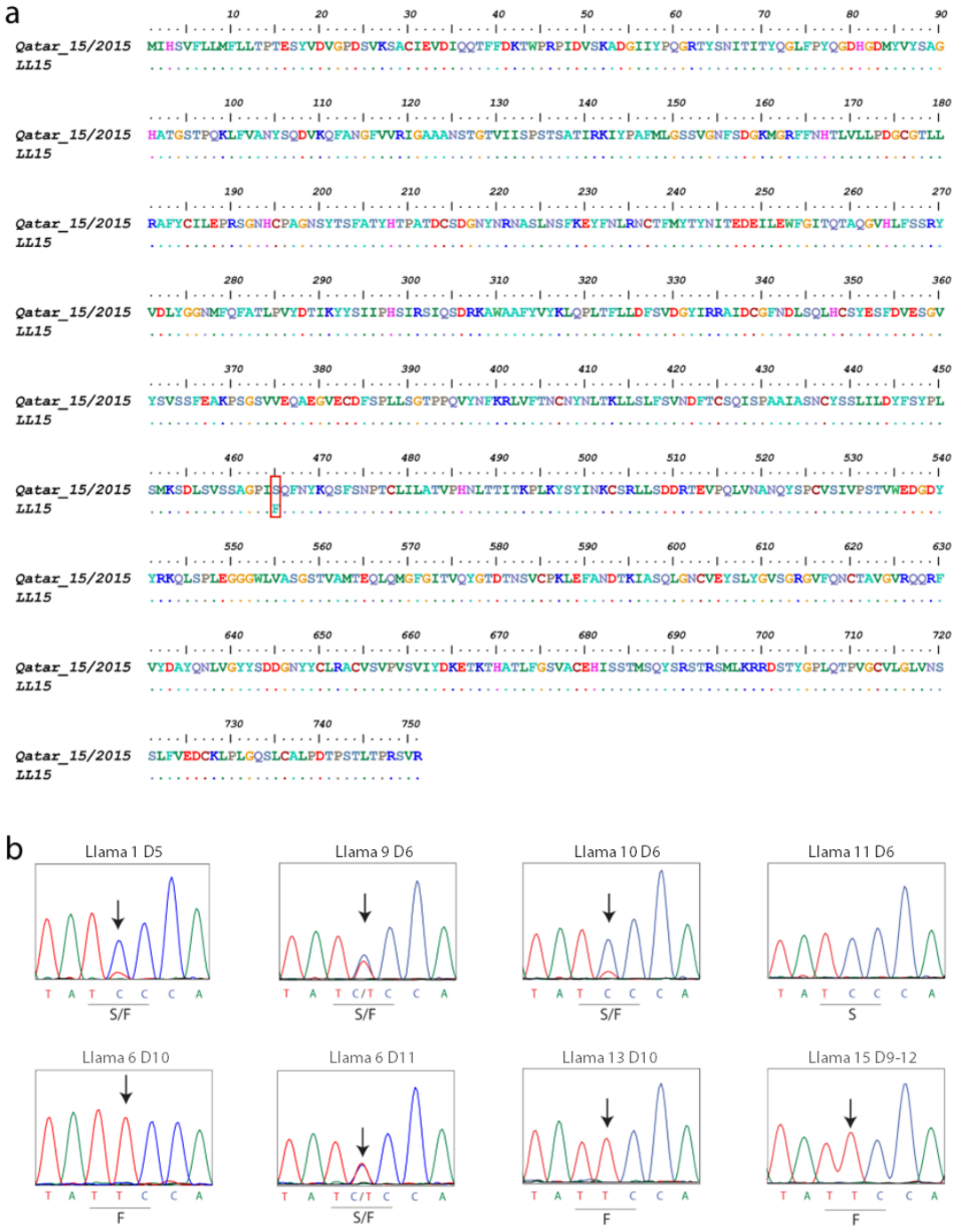

Figure 9.3. Sequence analysis of the spike S1 protein of MERS-CoV. **(a)** The amino acid sequence of the S1 domain of MERS-CoV spike protein obtained by sequencing of the viral RNA isolated from an S1-vaccinated llama (LL15) at day 11 post-inoculation was compared to the sequence of the S1 of the virus used to

directly inoculate the animals (Qatar_15/2015; GenBank Accession MK280984). **(b)** Sanger sequencing chromatograms of MERS-CoV spike S1 subunit from four directly inoculated llamas (No. 1 at day 5 pi and No. 9-11, day 6 pi), one in-contact naïve animal (No. 6 at days 10 and 11 pi) and two in-contact vaccinated llamas (No. 13 and 15, at 10 and 9-12 dpi, respectively). Arrows indicate emerging mutations.

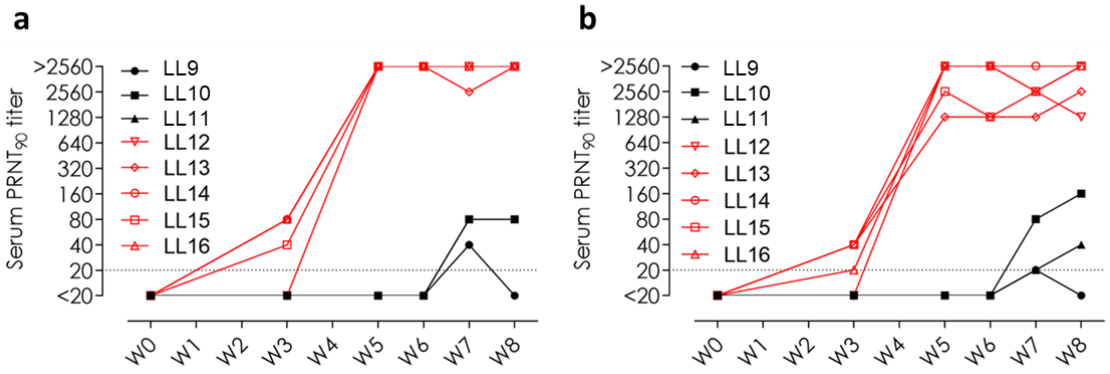

Figure 9.4. Virus neutralizing antibodies against MERS-CoV **(a)** Llama-passaged-Qatar15 isolate and **(b)** EMC/2012 strain elicited in sera of directly inoculated (LL9-11; black) and in-contact MERS-CoV S1 vaccinated (LL12-16; red) llamas. The horizontal dotted lines indicate the cutoff of the assay. LL, llama; PRNT, plaque reduction neutralization assay; W, week.

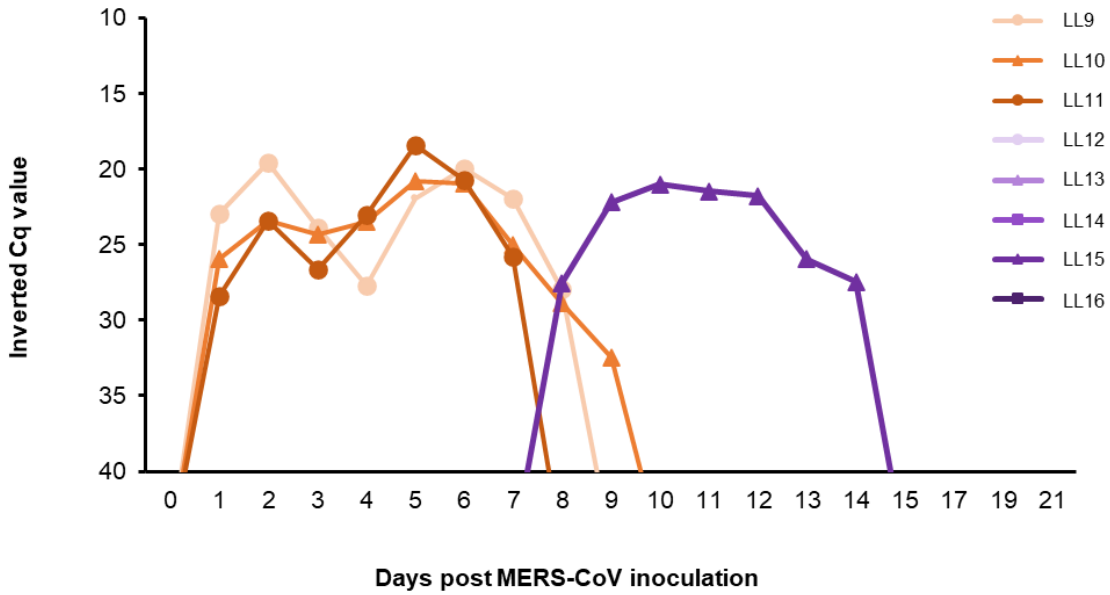

Figure 9.5. Viral M mRNA detected in nasal swab samples collected from S1 vaccinated llamas at different time points after contact with directly inoculated animals.

Humoral immune response

We evaluated the MERS-CoV specific antibody responses induced in llamas following infection and MERS-CoV S1 vaccination. All vaccinated animals (**Figure 9.6a-d**, red) developed high titres of serum S1-reactive antibodies (**Fig. 9.6a**) and virus neutralizing antibodies against both clade B Qatar15/2015 and a clade A EMC/2102 isolates as detected by PRNT (**Fig. 9.6b**, **Figure 9.4b**). In particular, the vaccination induced antibodies against the two functional domains of S1, the $S1^A$ binding N-terminal domain as detected by HI assay (**Fig. 9.6c**) and the RBD as detected by a competitive RBI ELISA (**Fig. 9.6d**). Additionally, only one directly inoculated but none of the vaccinated animals developed antibodies against the N protein (**Figure 9.7**). Aiming to assess mucosal immunity elicited upon vaccination, we evaluated the presence of antibodies in the nasal cavity. Remarkably, we detected low levels of both MERS-CoV S1-directed and neutralizing antibodies in the nasal swabs of three out of the five vaccinated animals (**Fig. 9.6e, f**).

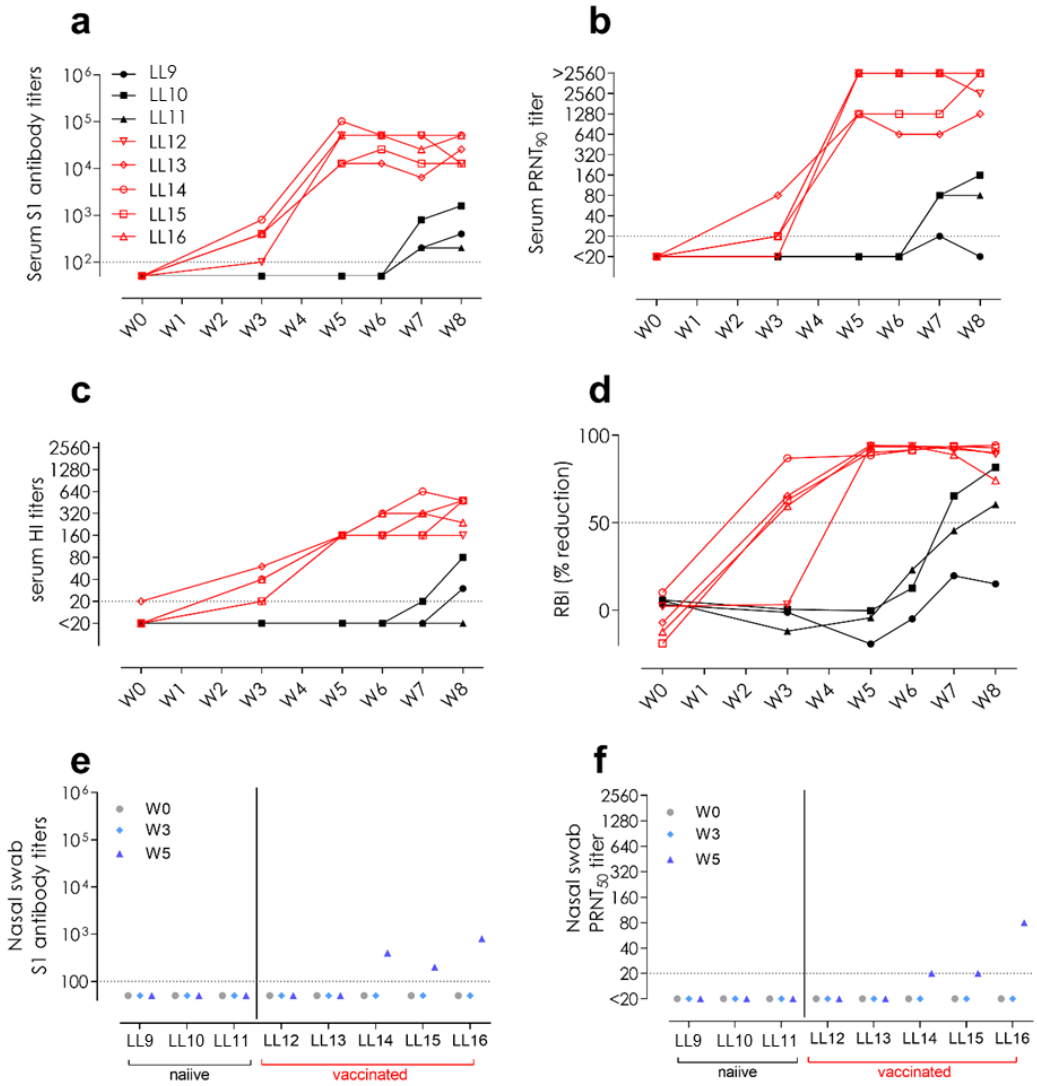

Figure 9.6. Antibody responses to MERS-CoV elicited in directly inoculated (LL9-11; black) and in-contact MERS-CoV S1 vaccinated (LL12-16; red) llamas in sera **(a-d)** and nasal swabs **(e,f)**. **(a,e)** MERS-CoV S1-reactive antibodies, **(b,f)** MERS-CoV neutralizing antibodies (Qatar15/2015 strain), **(c)** hemagglutination inhibition (HI; anti-$S1^{A}$ N terminal domain) antibodies, and **(d)** receptor binding inhibition (RBI; anti-S1 receptor binding domain) antibodies. The horizontal dotted lines indicate the cutoff of each assay. HI, hemagglutination inhibition; LL, llama; PRNT, plaque reduction neutralization assay; RBI, receptor binding inhibition; W, week.

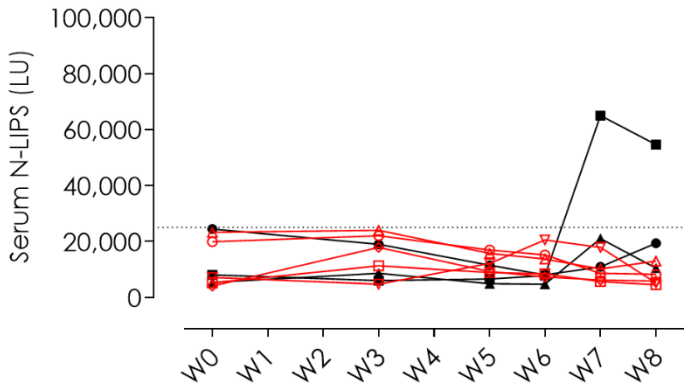

Figure. 9.7. Sera MERS-CoV nucleocapsid (N)-directed antibodies elicited in directly inoculated (LL4-6; black) and in-contact MERS-CoV S1 vaccinated (LL12-16; red) llamas. The horizontal dotted lines indicate the cutoff of the assay. LU, luminescence units; N-LIPS, nucleocapsid luciferase immunoprecipitation assay; W, week.

9.4 Discussion

Based on the *in vivo* protective capacity of monoclonal antibodies directed against different domains of the spike protein [288], a broader protective immune response can be achieved using multi-domain vaccines ($S1^A$ and $S1^B$ domains) compared to RBD-focused vaccines. Thus, the efficacy of an S1 recombinant protein emulsified with the adjuvant Montanide™ ISA 206 VG was evaluated as a potential vaccine candidate. We showed that immunized llamas were efficiently protected against MERS-CoV infection; no infectious virus was detected in the nose of any of the vaccinated animals and viral RNA shedding remained low (Cq ≥ 34), except for one llama (No. 15). Viral mRNA was also detected in the nasal cavity of this llama, which might be from intracellular viral mRNA from cells harvested in the nasal swabs; nonetheless, we could not detect any infectious virus. Neutralization of the virus by antibodies at mucosal level may have inhibited infectious viral particle production. The lack of

detectable infectious virus in the vaccinated llamas despite being infected, renders these animals unlikely to transmit the virus further to other animals and thus blocking the transmission chain. In addition, our studies revealed a mutation (S465F) in the spike protein encoded by this viral RNA, which may suggest a potential escape variant being produced. However, the emergence of the same mutation in another vaccinated llama, in one naïve in-contact animal and in other three directly inoculated llamas was revealed. In addition, the capacity of vaccinated animals to induce nAbs against this variant when isolated, indicate that it is unlikely an escape variant induced under antibody pressure. Mutation at this site (S465F) is not directly involved in receptor binding but has been previously reported to occur as a result of virus adaptation to its host receptor [432]. Overall, this indicates a probable adaptive mutation rather than a vaccine escape mutation.

Immunization with the S1 protein induced antibodies against the RBD as confirmed by the RBI and virus neutralization assays as well as antibodies to the $S1^{A}$ domain as confirmed by HI assay. These latter antibodies may be important in blocking virus attachment to sialic acid present in camelids, as it has been demonstrated in the dromedary camel upper respiratory tract [51]. Importantly, serum nAbs were generated in all vaccinated animals after the boosting immunization and were maintained during challenge. Therefore, a correlation of nAb levels in serum upon vaccination and protection occurred, as previously described in another vaccination study in camelids [209]. Notably, we detected mucosal nAb in the nasal cavity of 3 out of 5 vaccinated llamas, as also reported in dromedary camels immunized with an MVA-based candidate [207]. In addition, we demonstrate that vaccination of llamas with a spike protein from a clade A MERS-CoV (EMC/2012 isolate) provides protection

against a challenge with a clade B virus (Qatar15/2015 isolate). Since evidence of MERS-CoV reinfection has been reported in camels in the field [121], further studies to determine whether intramuscular administration of the subunit vaccine can boost mucosal immunity in the upper respiratory tract of animals that have been previously exposed to MERS-CoV are needed.

A critical component of a vaccine that influences the duration and the quality of immune responses is the adjuvant. Here we used the Montanide™ ISA 206 VG adjuvant, which was shown to induce long-term protective immunity in large animal species by stimulating both cell-mediated and humoral immune responses [433]. Further studies should be conducted in target species to determine the optimal antigen dose and the persistence of NAb following S1 recombinant vaccination. In fact, here, two doses of 35 and 50 µg were enough to induce protection, as opposed to a recent study which used 3 doses of 400 µg of the S1 antigen with a combination of adjuvants[37]. Unlike vector-based vaccines, protein-based vaccines do not require safety testing in high containment facilities and field studies could be directly conducted; thus, reducing the cost of the proposed vaccine. The registered adjuvant used in this study, Montanide™ ISA 206 VG, offers economical and practical use for field applications. Therefore, the S1 recombinant vaccine tested in this study appears as a good candidate to prevent animal-to-animal and, eventually, animal-to-human transmission.

Overall, immunization with the MERS-CoV S1 recombinant protein, in combination with a commercial adjuvant, efficiently limits infectious viral shedding from vaccinated llamas upon exposure to directly inoculated ones.

Chapter 10

General discussion

The ongoing zoonotic spread of MERS-CoV to the human population poses a serious public health risk, not only locally but worldwide, as demonstrated in a travel-associated outbreak in the Republic of Korea in 2015 [26]. Infected humans can develop fatal pulmonary disease due to the massive infiltration of inflammatory leukocytes into the lungs, which produces a dysregulated inflammatory cytokine storm [189,190,239]. Particularly, MERS-CoV-infected macrophages produce high and prolonged amounts of pro-inflammatory cytokines and chemokines that exacerbate lung pathology [200–202]. Nonetheless, humans are merely dead-end hosts suffering from disease and possibly playing a fairly neglectable role in MERS-CoV evolution [127]. MERS-CoV is known to be carried and evolve in a singular animal reservoir, the dromedary camel [16,127]. Dromedaries, as well as other camelid species [8,32,65,209,233–235], only experience a subclinical MERS-CoV infection, characterized by high viral loads in the URT and abundant infectious viral shedding [141].

At the beginning of the current Ph.D. thesis, there was a lack of reagents and little bibliographical information to study innate and adaptive immune responses of camelid species. Therefore, we developed and validated a panel of primers to monitor camelid immune responses at the transcriptomic level, which were used to understand how camelids respond to MERS-CoV. Local, robust, and timely antiviral innate immune responses (IFNs and ISGs) are thought to be key determinants for viral clearance in less than a week [8,32]. Like in bats [7,280], dampened pro-inflammatory responses during MERS-CoV infection prevent the development of severe lesions in the respiratory tract of camelids [8,32]. During the peak of infection, mononuclear leukocytes infiltrate into the lungs of alpacas concomitant with a transient induction of pro-

inflammatory cytokines (TNF-α, IL-1β and NLPR3)[8,32]. In addition, using llamas, we elucidated that alveolar macrophages do not support MERS-CoV replication *in vitro*. Opposed to the productive viral replication described in human MDMs [200–202], we determined that LAMs capture, internalize, and degrade MERS-CoV particles. Moreover, these cells did not produce efficient antiviral or pro-inflammatory responses upon viral sensing. Importantly, IRF5, a relevant marker of inflammatory M1 macrophage polarization [274,275], was not upregulated in LAMs sensing MERS-CoV *in vitro* or in lungs of infected animals [8,32]. Thus, alveolar macrophages could be important mediators of MERS-CoV clearance in respiratory tissues while poorly participating in the mild pro-inflammatory responses described in the LRT of camelids *in vivo*.

Additionally, previous studies using experimentally-inoculated camelids showed that dendritic-like cells carried MERS-CoV antigen to cervical LNs [207,208,236], from where infectious virus could be isolated [207,208]. Consistent with the absence of tissue damage in secondary lymphoid organs, we determined that MERS-CoV replication does not occur in camelid LNs, at least using an *in vitro* approach. We used cervical LN cells from previously inoculated llamas to mimic a secondary exposure to MERS-CoV (clade B and C strains) *in vitro*. In particular, LN cells pulsed with a MERS-CoV clade B strain induced remarkable antiviral responses involving various innate immune pathways, including type I and III IFNs, ISGs, PRRs and TFs. Nonetheless, independently of the MERS-CoV used, viral re-exposure did not elicit pro-inflammatory responses, such as expression of pro-inflammatory cytokines (*TNF-α*, *IL-1β*, *IL-6* and *IL-8*). Also, the NF-κB activator *CARD9* and different components of the NLRP3 inflammasome (*NLRP3*, *CASP1*, *PYCARD*) remained at baseline levels in all studied conditions. Thus, not only MERS-CoV-infected respiratory

tissues [8,32], but also secondary lymphoid organs, exhibit high and transient inductions of *IFN-λ3* and dimmed pro-inflammatory responses to MERS-CoV. Of note, relative expressions of *IFN-λ3* were higher for LN cells re-challenged with the MERS-CoV clade B strain. Such differences between strains need to be clarified but might be related to the display of different PAMPs or, alternatively, to genetic variations between animals. These hypotheses should be tested in a larger number of animals. Indeed, despite numerous efforts to understand pathological mechanisms in humans or animal models, the exact nature of MERS-CoV PAMPs remains elusive. A comparative study of PAMPs interactions with molecules from species resistant or susceptible to disease might shed light on the host pathways conducting to different pathological fates. Nonetheless, *IFN-λ3* might have a key role in bridging innate and adaptive immunity from the infected respiratory mucosa to secondary lymphoid organs, as described in other viral infections [421,422]. We hypothesize that the high relative expression of *IFN-λ3* upon viral sensing might counterbalance the inflammatory responses elicited by type I IFNs [420]. Moreover, since inflammation was controlled in these relevant anatomical compartments for MERS-CoV pathogenesis, camelid species own specific mechanisms for dampening inflammatory processes and consequently experience asymptomatic MERS-CoV infection. Similar mechanisms for inhibiting inflammation have been described in bats [279,280], which allow viral replication in the absence of clinical disease. Further research is needed to identify key immunological mechanisms of camelids that confer tolerance to MERS-CoV. Such mechanisms might also account for the absence of disease in camelids after being infected with a variety of viruses (i.e., RVFV, HEV or CCHFV) that are of serious human health concern [365,366,434,435]. Camelid

species might restrict the development of acute disease by controlling inflammatory processes upon viral infection.

Regarding adaptive immune responses, the development of T-cell responses were required to fully achieve viral clearance in hDPP4-transduced mice [227], but cell-mediated immunity to MERS-CoV had never been studied in camelids. We indirectly demonstrated that successful viral-antigen presentation occurs in camelid draining LNs, probably prompting the development of efficient T- and B-cell adaptive immune responses to MERS-CoV. Importantly, immunologically recalled llama LN cells mounted appeared to mount a Th1-skewed cellular immune response, as evidenced by the enhanced transcription of *IL-12*, *IL-2* and *IFN-γ* in LN cells exposed to both clade B and C viruses. Activation of Th1 responses was also described in PBMCs from recovered MERS patients [246,247]. As previously described in humans and cattle [418,419], functional NK cells residing in LNs could also contribute to *IFN-γ* up-regulation in camelids. More studies using camelid LN cells combining flow cytometry [436] and/or single-cell RNA sequencing would help in characterizing which immune cell subsets play a key role in the development of innate and adaptive immune responses in camelids. Furthermore, the high prevalence of MERS-CoV antibodies found in African and Arabian dromedaries [23,110] indicates that camelids develop efficient B lymphocyte responses. Camelids can elicit protective humoral immunity, including nAbs, after natural and experimental MERS-CoV infection [65,115,116,208,234,235]. All llamas used in the current Ph.D. thesis developed moderate levels of nAbs and binding-antibodies directed to the $S1^A$ and $S1^B$ domains of the S protein. Nonetheless, studies in dromedary camels from endemic countries reported a significant waning of humoral responses over time [120], as well as the rapid re-infection of seropositive animals (re-infection has been

described in less than a month since the previous infection) [23,120–122,130–133]. Thus, camelid species mount effective T- and B-cell responses with relatively short memory that contribute to viral clearance and host disease resistance while not interfering with MERS-CoV circulation within dromedary populations.

Intrinsic immunological characteristics of dromedary camels would allow MERS-CoV persistance, evolution and spread. Infected dromedaries shed abundant infectious virus with a high transmission potential to animals and humans [134,140,141,207,208]. High seroprevalence and active circulation of MERS-CoV have been determined in dromedary camels from the Arabian Peninsula and African countries [23]. However, despite that more than 80% of the camel population is found in Africa (https://www.fao.org/faostat) and that MERS-CoV infection is widespread in African dromedaries, zoonotic disease has only been reported in the Arabian Peninsula. There is serological and molecular evidence of MERS-CoV infection in camel handlers of Africa [358–360] but no zoonotic MERS has been reported across this continent so far. Despite a continuous trade of dromedaries into the Arabian Peninsula [33,135], no African clade C MERS-CoV strains have been detected in this region. One explanation for the dominance of clade B strains in the Middle East could be their increased fitness compared to the African clade C viruses. A recent study demonstrated increased replication competence of MERS-CoV clade B Arabian viruses compared to different clade C African strains in human lung *ex vivo* cultures and in a transgenic mouse model expressing the hDPP4 receptor [30]. However, the differential replication and transmission competence of Arabian and African viruses in camelid reservoir species remained unknown before the current Ph.D. thesis. Llamas were proposed as valuable surrogates for dromedary camels because they reproduce a very similar MERS-CoV infection and shedding

than dromedary camels [65]. Here we demonstrated efficient MERS-CoV (clade B and C) transmission from experimentally-inoculated llamas to naïve in-contact animals. Furthermore, we used the llama model to set up a valuable direct-contact transmission scenario that mimics field-like conditions and is useful for MERS-CoV transmission and vaccination studies.

To understand differential transmission patterns between MERS-CoV clades, we retrieved experimental data from previous MERS-CoV Qatar15/2015 (clade B; *Chapters 3, 8* and *9*) and Egypt/2013 (clade C; *Chapter 4*) transmission studies and performed comparative analyses of all naïve and non-protected llamas. Animals inoculated with a high dose of either MERS-CoV Egypt/2013 or Qatar15/2015 had similar levels of genomic and subgenomic viral RNA, as well as infectious viral shedding. Data analyses showed no significant differences in viral shedding of llamas inoculated with high doses of MERS-CoV regardless of the strain used. Instead, comparative analyses revealed a statistically higher and extended shedding of the MERS-CoV clade B strain in naïve-contact llamas than the clade C strain (**Figure 10.1**). Therefore, the Egypt/2013 strain seemed to have a lower transmission potential than the Qatar15/2015 strain in a camelid model. Additionally, IHC studies in animals inoculated with the Egypt/2013 strain would be required to monitor virus replication and tropism in respiratory tissues, revealing the differential fitness of both strains in camelids. Nonetheless, our results might explain why MERS-CoV clade C strains are unable to establish themselves in the Arabian Peninsula after being introduced via imported camels and competing with enzootic clade B viruses. However, further studies are needed to determine whether this potentially reduced transmissibility is a common feature of the diverse MERS-CoV lineages found in African dromedaries. Specific

amino acid substitutions in the S protein or in other genomic regions of African clade C viruses might be determinant of the low replication phenotype observed in in-contact camelids, as previously observed in human cells [30]. However, viral or host factors that play a key role in conferring replication and transmission competence remain to be explored in camelid reservoirs. Nonetheless, studies of the present Ph.D. thesis provide *in vivo* experimental data demonstrating reduced MERS-CoV fitness of one African clade C isolate to in-contact camelids compared with an Arabian Clade B isolate. In addition, if confirmed in the field, the reduced MERS-CoV Clade C shedding from infected camels might limit spillover to humans. Importantly, introduction of MERS-CoV clade B strains to Africa through infected camelids must be avoided as they might outcompete African MERS-CoV clade C strains and pose greater zoonotic and pandemic threat in Africa.

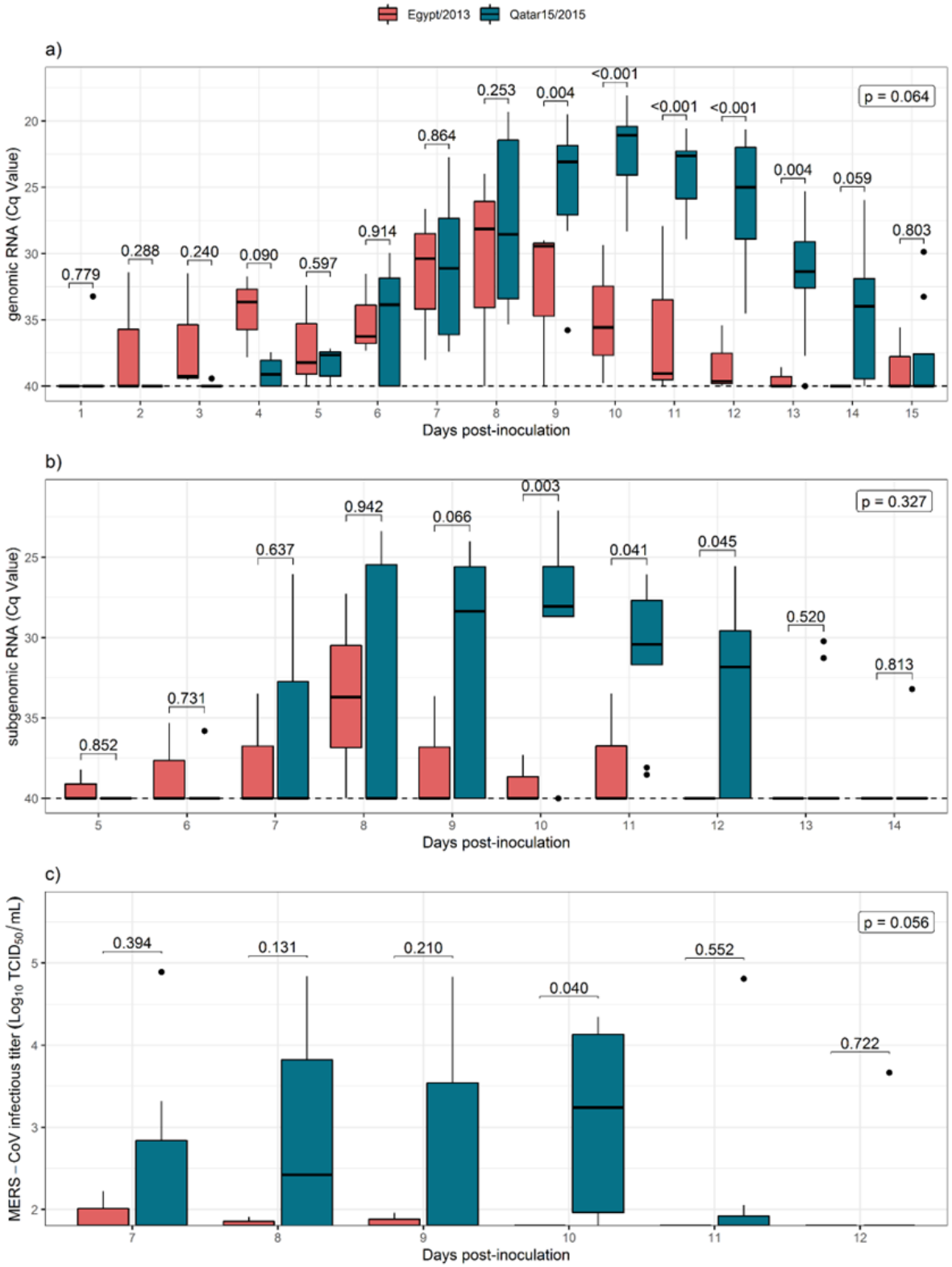
Egypt/2013
Qatar15/2015
a)
genomic RNA (Cq Value)
Days post-inoculation
p = 0.064
0.779
0.288
0.240
0.090
0.597
0.914
0.864
0.253
0.004
<0.001
<0.001
<0.001
0.004
0.059
0.803
b)
subgenomic RNA (Cq Value)
Days post-inoculation
p = 0.327
0.852
0.731
0.637
0.942
0.066
0.003
0.041
0.045
0.520
0.813
c)
MERS – CoV infectious titer (Log10 TCID50/mL)
Days post-inoculation
p = 0.056
0.394
0.131
0.210
0.040
0.552
0.722

Figure 10.1. Mixed model to statistically analyse the transmission competence of each MERS-CoV strain over time. A mixed model was adjusted using the shedding data of each individual as a fixed factor and the corresponding MERS-CoV strain and days post-inoculation as random factors, along with a contrast of the estimated marginal means. Only the days whose values differed from the limit of detection were used for the mixed models are represented. The boxplot shows daily virus shedding of sentinel llamas infected with MERS-CoV Egypt/2013 (red) or Qatar15/2015 strains (blue), after direct exposition to inoculated llamas. Panels a) and b) show genomic and subgenomic viral RNA quantification in nasal swabs collected throughout the study, expressed in Cq values. Panel c) displays infectious MERS-CoV titres in $TCID_{50}$/mL. The *p*-values obtained in the models are indicated above the boxes. The *p*-values shown at the top right corner of the plots determine statistical differences between areas under the curve of the experimental groups, as calculated in the Wilcoxon test.

Nowadays, MERS-CoV clade B strains are dominant among dromedaries from the Arabian Peninsula and cause continuous human outbreaks. These strains have an increased replicative fitness and pose a higher epidemic and pandemic threat [32,169].

Due to the current absence of vaccines or treatments to counteract MERS-CoV, Middle Eastern countries implemented measures to control MERS outbreaks [27,28]. Strengthening diagnosis and surveillance improved human outbreak control, preventing human-to-human transmission and deaths [168]. Nonetheless, further preparedness and efforts are required to prevent MERS-CoV spillover from animal reservoirs to humans. Enhanced surveillance in dromedary populations and restriction of camel movement in affected areas could rapidly help in preventing animal-to-human transmission [170]. Moreover, the WHO, the FAO and the WOAH recommend dromedary camel vaccination to prevent primary human cases [170], which may be a less costly and faster solution than licensing human vaccines [237]. In this regard, effective vaccine prototypes were developed for camel use, which elicited protective humoral immunity and reduced MERS-CoV shedding after infection [203,207,209]. Although they are useful

vaccine candidates to be evaluated in animal clinical trials, none of them impeded infectious viral shedding in dromedary camels, implying that MERS-CoV transmission among animals and to humans would still be possible during a limited window of time.

In the current Ph.D. thesis, we explored the possibility to completely block MERS-CoV transmission among camelids using two different vaccine candidates. Both vaccine efficacy studies used the llama direct-contact transmission model to simulate MERS-CoV infection as it occurs under natural conditions. The first vaccine candidate was based on self-assembling MPSP expressing the RBD domain of the MERS-CoV S protein [226], formulated with a registered adjuvant (Montanide™ ISA 206 VG). Immunization with MPSP-RBD induced humoral immunity and reduced MERS-CoV replication in experimentally-inoculated rabbits [226]. Antigens delivered with the MPSP platform were shown to enhance immune responses compared to other multivalent and/or conventional recombinant protein-based vaccines [424,425]. Indeed, MPSP-RBD immunization elicited high levels of MERS-CoV nAbs in all vaccinated llamas and partially blocked viral transmission (one out of three vaccinated animals) in our exploratory study. Thus, the potential of MPSP-RBD to prevent MERS-CoV transmission to animals or humans seems limited. We hypothesized that a monomeric RBD may confer reduced protection to MERS-CoV infection than a vaccine prototype displaying the natural trimeric conformation. Also, based on the protective capacity of monoclonal antibodies targeting different domains of the S protein [288], broader protective immune responses could be achieved using multi-domain ($S1^A$ and $S1^B$) vaccines compared to others based on the RBD only. Then, we evaluated the efficacy of a recombinant S1 protein emulsified with the Montanide™ ISA 206 VG adjuvant as a potential

vaccine candidate. Immunization with the S1-based vaccine induced high levels of humoral responses toward $S1^A$ and RBD, including nAbs to MERS-CoV. Antibodies targeting $S1^A$ could expand protective responses by impeding viral attachment to sialoglycans present in the upper respiratory tract of camelids [51]. Furthermore, nAb responses were generated both systemically and at the mucosal level. We demonstrated that S1-immunized animals were efficiently protected against MERS-CoV infection after being in contact with inoculated llamas shedding high titres of infectious virus. Although viral replication was found in the URT of one out of five vaccinated llamas, none of the immunized animals shed infectious at any point of the study. Neutralizing Abs elicited at the nasal cavity of the animal shedding viral RNA might have been immune complexed with MERS-CoV particles, preventing infection of Vero cells. Alternatively, generation of defective viral particles in this animal might explain shedding of viral RNA without presence of infectious virus. Thus, the recombinant S1 vaccine candidate completely prevented infectious MERS-CoV shedding and, consequently, interrupted viral transmission in this experimental setting.

Technical issues are key to license and market an efficient vaccine prototype, such as the recombinant S1 prototype. Immunization studies in dromedary camels would confirm that the target species responds to vaccination similar than llamas. Further studies should be performed to establish the optimal immunization dose, as well as to assess the duration and quality of immune responses. The absence of immunity might explain the higher incidence and viral loads found in juvenile animals compared to adults [23,98,106,112,128,129], thus, the vaccination of newborn camels or young calves is recommended to reduce MERS-CoV shedding in camel herds. Nonetheless, a previous study showed a narrow window of

opportunity for vaccinating seronegative dromedary camels [129]. Due to the high MERS-CoV seroprevalence in endemic countries [23], the vaccination of seropositive animals must also be considered. Additional field studies would be needed to ascertain whether vaccination can boost protective immunity and reduce MERS-CoV transmission from seropositive animals. Overall, our immunization studies support that vaccination can curtail virus transmission among dromedary reservoirs and, eventually, prevent zoonotic spillover to humans. Vaccine formulation with a new generation of approved adjuvants would probably improve our experimental vaccine by conferring long lasting immunity [437].

The next MERS-CoV zoonotic outbreak is only matter of time; the challenge remains in anticipating when and where it will occur, whilst being prepared. Exploring camelid reservoirs and exploiting their inherent biology would aid in finding solutions for MERS-CoV control. The research performed in the current Ph.D. thesis is highly devoted to the 'One Health' initiative. The global community bear a collective and shared responsibility for containing MERS-CoV, a major health security threat in the Middle East, Africa and beyond.

Chapter 11

Conclusions

1. A comprehensive set of primers for the simultaneous quantification of cytokines and immune-related genes involved in major innate and adaptive immune response signalling pathways, which can be used for all camelid species, has been successfully designed and validated with state-of-the-art methodologies. The novel assay appears as an accurate and easily reproducible tool that can be used to investigate camelid immune responses and is widely accessible to the veterinary and health research community.

2. Llama alveolar macrophages do not support MERS-CoV replication, although these cells effectively capture, internalize, and degrade viral particles. Contrary to human MDMs, these cells do not produce pro-inflammatory cytokine responses upon viral sensing. Thus, alveolar macrophages could be important effectors of MERS-CoV clearance in respiratory tissues of camelids during the early phase of infection.

3. Cervical LN cells from llama do not support MERS-CoV replication. Convalescent llamas develop strong antiviral cellular responses (i.e., Th1-like, type III IFNs, ISGs) that are rapidly induced *in vitro* upon immunological recall, in the absence of inflammation.

4. Llamas can be useful surrogates for dromedary camel in MERS-CoV transmission and vaccination studies. As such, currently circulating MERS-CoV strains (clade B and C) are efficiently transmitted among llamas in an experimental direct-contact set up.

5. A MERS-CoV clade B strain (Qatar15/2015) exhibits extended viral shedding compared to an African clade C strain (Egypt/2013) in llamas. Introduction of MERS-CoV clade B strains to Africa should be

avoided as they could outcompete endemic clade C strains, potentiating the risk of zoonotic disease in this continent.

6. The MPSP-RBD-based vaccine candidate showed limited capabilities to curtail MERS-CoV transmission among llamas, as infection was only prevented in 1/3 vaccinated, in-contact animals. However, the S1-recombinant based-candidate formulated with a commercial adjuvant efficiently prevented infectious viral shedding in llamas and, thus, blocked MERS-CoV transmission among animals. This finding represents a step forward in the application of animal vaccines to prevent zoonotic spillover.

References

1. Zhang, L. *et al.* Biological invasions facilitate zoonotic disease emergences. *Nat. Commun.* **13**, 1–11 (2022).

2. Jones, K. E. *et al.* Global trends in emerging infectious diseases. *Nature* **451**, 990–993 (2008).

3. Carlson, C. J. *et al.* Climate change increases cross-species viral transmission risk. *Nature* (2022) doi:10.1038/s41586-022-04788-w.

4. Millet, J. K., Jaimes, J. A. & Whittaker, G. R. Molecular diversity of coronavirus host cell entry receptors. *FEMS Microbiol. Rev.* **45**, 1–16 (2021).

5. Lu, G., Wang, Q. & Gao, G. F. Bat-to-human: Spike features determining 'host jump' of coronaviruses SARS-CoV, MERS-CoV, and beyond. *Trends Microbiol.* **23**, 468–478 (2015).

6. Cui, J., Li, F. & Shi, Z. L. Origin and evolution of pathogenic coronaviruses. *Nat. Rev. Microbiol.* **17**, 181–192 (2019).

7. Irving, A. T., Ahn, M., Goh, G., Anderson, D. E. & Wang, L. F. Lessons from the host defences of bats, a unique viral reservoir. *Nature* **589**, 363–370 (2021).

8. Te, N. *et al.* Type I and III IFNs produced by the nasal epithelia and dimmed inflammation are features of alpacas resolving MERS-CoV infection. *PLoS Pathog.* **17**, 1–28 (2021).

9. Zaki, A. M., van Boheemen, S., Bestebroer, T. M., Osterhaus, A. D. M. E. & Fouchier, R. A. M. Isolation of a Novel Coronavirus from a Man with Pneumonia in Saudi Arabia. *N. Engl. J. Med.* **367**, 1814–1820 (2012).

10. de Groot, R. J. *et al.* Commentary: Middle East Respiratory Syndrome Coronavirus (MERS-CoV): Announcement of the Coronavirus Study Group. *J. Virol.* **87**, 7790–7792 (2013).

11. Corman, V. M. *et al.* Rooting the Phylogenetic Tree of Middle East Respiratory Syndrome Coronavirus by Characterization of a Conspecific Virus from an African Bat. *J. Virol.* **88**, 11297–11303 (2014).

12. Ithete, N. L. *et al.* Close relative of human middle east respiratory syndrome coronavirus in bat, South Africa. *Emerg. Infect. Dis.* **19**, 1697–1699 (2013).

13. Memish, Z. A. *et al.* Middle East respiratory syndrome coronavirus in Bats, Saudi Arabia. *Emerg. Infect. Dis.* **19**, 1819–1823 (2013).

14. Wang, Q. *et al.* Bat origins of MERS-CoV supported by bat Coronavirus HKU4 usage of human receptor CD26. *Cell Host Microbe* **16**, 328–337 (2014).

15. Hu, B., Ge, X., Wang, L. F. & Shi, Z. Bat origin of human coronaviruses Coronaviruses. *Virol. J.* **12**, 1–10 (2015).

16. Sabir, J. S. M. *et al.* Co-circulation of three camel coronavirus species and recombination of MERS-CoVs in Saudi Arabia. *Science.* **351**, 81–84 (2016).

17. Corman, V. M. *et al.* Antibodies against MERS coronavirus in dromedary camels, Kenya, 1992-2013. *Emerg. Infect. Dis.* **20**, 1319–1322 (2014).

18. Meyer, B. *et al.* Antibodies against MERS coronavirus in dromedaries, United Arab Emirates, 2003 and 2013. *Emerg. Infect. Dis.* **20**, 552–559 (2014).

19. Azhar, E. I. *et al.* Evidence for Camel-to-Human Transmission of MERS Coronavirus. *N. Engl. J. Med.* **370**, 2499–2505 (2014).

20. Stalin Raj, V. *et al.* Isolation of MERS coronavirus from dromedary camel, Qatar, 2014. *Emerg. Infect. Dis.* **20**, 1339–1342 (2014).

21. Reusken, C. B. E. M. *et al.* Middle East respiratory syndrome coronavirus neutralising serum antibodies in dromedary camels: A comparative serological study. *Lancet Infect. Dis.* **13**, 859–866 (2013).

22. Müller, M. A. *et al.* MERS coronavirus neutralizing antibodies in camels, eastern Africa, 1983–1997. *Emerg. Infect. Dis.* **20**, 2093–2095 (2014).

23. Dighe, A., Jombart, T., van Kerkhove, M. D. & Ferguson, N. A systematic review of MERS-CoV seroprevalence and RNA prevalence in dromedary camels: Implications for animal vaccination. *Epidemics* **29**, 100350 (2019).

24. Perlman, S. & Zumla, A. MERS-CoV in Africa—an enigma with relevance to COVID-19. *Lancet Infect. Dis.* **21**, 303–305 (2021).

25. World Health Organization (WHO). MERS Situation Update - March 2022. http://www.emro.who.int/health-topics/mers-cov/mers-outbreaks.html (2022).

26. Kim, K. H., Tandi, T. E., Choi, J. W., Moon, J. M. & Kim, M. S. Middle East respiratory syndrome coronavirus (MERS-CoV) outbreak in South Korea, 2015: epidemiology, characteristics and public health implications. *J. Hosp. Infect.* **95**, 207–213 (2017).

27. Kumar, A. & Chaterjee, S. Outbreak of Middle East respiratory syndrome coronavirus, Saudi Arabian experience. *Curr. Med. Res. Pract.* **7**, 132–134 (2017).

28. Baharoon, S. & Memish, Z. A. MERS-CoV as an emerging respiratory illness: A review of prevention methods. *Travel Med. Infect. Dis.* **32**, 101520 (2019).

29. Lefkowitz, E. J. *et al.* Virus taxonomy: The database of the International Committee on Taxonomy of Viruses (ICTV). *Nucleic Acids Res.* **46**, D708–D717 (2018).

30. Zhou, Z. *et al.* Phenotypic and genetic characterization of MERS coronaviruses from Africa to understand their zoonotic potential. *Proc. Natl.*

Acad. Sci. **118**, e2103984118 (2021).

31. Farrag, M. A., Amer, H. M., Bhat, R. & Almajhdi, F. N. Sequence and phylogentic analysis of MERS-CoV in Saudi Arabia, 2012–2019. *Virol. J.* **18**, 1–10 (2021).

32. Te, N. *et al.* Enhanced replication fitness of MERS-CoV clade B over clade A strains in camelids explains the dominance of clade B strains in the Arabian Peninsula. *Emerg. Microbes Infect.* **11**, 260–274 (2022).

33. El-Kafrawy, S. A. *et al.* Enzootic patterns of Middle East respiratory syndrome coronavirus in imported African and local Arabian dromedary camels: a prospective genomic study. *Lancet Planet. Heal.* **3**, e521–e528 (2019).

34. Chu, D. K. W. *et al.* MERS coronaviruses from camels in Africa exhibit region-dependent genetic diversity. *Proc. Natl. Acad. Sci. U. S. A.* **115**, 3144–3149 (2018).

35. Boheemen, S. van *et al.* Genomic Characterization of Newly Discovered Coronavirus Associated with Acute Respiratory Distress Syndrome in Humans. *MBio* **3**, e00473-12 (2012).

36. V'kovski, P., Kratzel, A., Steiner, S., Stalder, H. & Thiel, V. Coronavirus biology and replication: implications for SARS-CoV-2. *Nat. Rev. Microbiol.* **19**, 155–170 (2021).

37. Wang, Y., Grunewald, M. & Perlman, S. Coronaviruses: An Updated Overview of Their Replication and Pathogenesis. in *Methods in Molecular Biology* (eds. Maier, H. J. & Bickerton, E.) 1–29 (Springer US, 2020). doi:10.1007/978-1-0716-0900-2_1.

38. Pasternak, A. O., Spaan, W. J. M. & Snijder, E. J. Nidovirus transcription: How to make sense...? *J. Gen. Virol.* **87**, 1403–1421 (2006).

39. Sawicki, S. G. & Sawicki, D. L. Coronaviruses use discontinuous extension for synthesis of subgenome-length negative strands. *Adv. Exp. Med. Biol.* **380**, 499–506 (1995).

40. Scobey, T. *et al.* Reverse genetics with a full-length infectious cDNA of the Middle East respiratory syndrome coronavirus. *Proc. Natl. Acad. Sci. U. S. A.* **110**, 16157–16162 (2013).

41. Almazán, F. *et al.* Engineering a replication-competent, propagation-defective middle east respiratory syndrome coronavirus as a vaccine candidate. *MBio* (2013) doi:10.1128/mBio.00650-13.

42. Li, Y. H., Hu, C. Y., Wu, N. P., Yao, H. P. & Li, L. J. Molecular Characteristics, Functions, and Related Pathogenicity of MERS-CoV Proteins. *Engineering* **5**, 940–947 (2019).

43. Rabouw, H. H. *et al.* Middle East Respiratory Coronavirus Accessory

Protein 4a Inhibits PKR-Mediated Antiviral Stress Responses. *PLoS Pathog.* **12**, 1–26 (2016).

44. Niemeyer, D. *et al.* Middle East Respiratory Syndrome Coronavirus Accessory Protein 4a Is a Type I Interferon Antagonist. *J. Virol.* **87**, 12489–12495 (2013).

45. Menachery, V. D. *et al.* MERS-CoV accessory ORFs play key role for infection and pathogenesis. *MBio* **8**, (2017).

46. Snijder, E. J. *et al.* A unifying structural and functional model of the coronavirus replication organelle: Tracking down RNA synthesis. *PLoS Biol.* **18**, 1–25 (2020).

47. Raj, V. S. *et al.* Dipeptidyl peptidase 4 is a functional receptor for the emerging human coronavirus-EMC. *Nature* **495**, 251–254 (2013).

48. Iwanaga, T. & Nio-Kobayashi, J. Cellular expression of CD26/dipeptidyl peptidase IV. *Biomed. Res.* **42**, 229–237 (2021).

49. Boonacker, E. & van Noorden, C. J. F. The multifunctional or moonlighting protein CD26/DPPIV. *Eur. J. Cell Biol.* **82**, 53–73 (2003).

50. Lambeir, A.-M., Durinx, C., Scharpé, S. & De Meester, I. Dipeptidyl-Peptidase IV from Bench to Bedside: An Update on Structural Properties, Functions, and Clinical Aspects of the Enzyme DPP IV. *Crit. Rev. Clin. Lab. Sci.* **40**, 209–294 (2003).

51. Li, W. *et al.* Identification of sialic acid-binding function for the Middle East respiratory syndrome coronavirus spike glycoprotein. *Proc. Natl. Acad. Sci.* **114**, E8508 LP-E8517 (2017).

52. Alejandra Tortorici, M. *et al.* Structural basis for human coronavirus attachment to sialic acid receptors. *Nat. Struct. Mol. Biol.* **26**, 481–489 (2019).

53. Park, Y. J. *et al.* Structures of MERS-CoV spike glycoprotein in complex with sialoside attachment receptors. *Nat. Struct. Mol. Biol.* **26**, 1151–1157 (2019).

54. Mou, H. *et al.* The Receptor Binding Domain of the New Middle East Respiratory Syndrome Coronavirus Maps to a 231-Residue Region in the Spike Protein That Efficiently Elicits Neutralizing Antibodies. *J. Virol.* **87**, 9379–9383 (2013).

55. Lu, G. *et al.* Molecular basis of binding between novel human coronavirus MERS-CoV and its receptor CD26. *Nature* **500**, 227–231 (2013).

56. Lu, L. *et al.* Structure-based discovery of Middle East respiratory syndrome coronavirus fusion inhibitor. *Nat. Commun.* **5**, (2014).

57. Gao, J. *et al.* Structure of the Fusion Core and Inhibition of Fusion by a Heptad Repeat Peptide Derived from the S Protein of Middle East

Respiratory Syndrome Coronavirus. *J. Virol.* **87**, 13134–13140 (2013).

58. Alsaadi, E. A. J., Neuman, B. W. & Jones, I. M. A Fusion Peptide in the Spike Protein of MERS Coronavirus. *Viruses* **11**, 1–9 (2019).

59. Yuan, Y. *et al.* Cryo-EM structures of MERS-CoV and SARS-CoV spike glycoproteins reveal the dynamic receptor binding domains. *Nat. Commun.* **8**, 1–9 (2017).

60. Gierer, S. *et al.* The Spike Protein of the Emerging Betacoronavirus EMC Uses a Novel Coronavirus Receptor for Entry, Can Be Activated by TMPRSS2, and Is Targeted by Neutralizing Antibodies. *J. Virol.* **87**, 5502–5511 (2013).

61. Shirato, K., Kawase, M. & Matsuyama, S. Middle East Respiratory Syndrome Coronavirus Infection Mediated by the Transmembrane Serine Protease TMPRSS2. *J. Virol.* **87**, 12552–12561 (2013).

62. Du, L. *et al.* MERS-CoV spike protein: a key target for antivirals. *Expert Opin. Ther. Targets* **21**, 131–143 (2017).

63. Chan, J. F. W. *et al.* Differential cell line susceptibility to the emerging novel human betacoronavirus 2c EMC/2012: Implications for disease pathogenesis and clinical manifestation. *J. Infect. Dis.* **207**, 1743–1752 (2013).

64. Müller, M. A. *et al.* Human coronavirus EMC does not require the SARS-coronavirus receptor and maintains broad replicative capability in mammalian cell lines. *MBio* **3**, 1–5 (2012).

65. Vergara-Alert, J. *et al.* Livestock Susceptibility to Infection with Middle East Respiratory Syndrome Coronavirus. *Emerg. Infect. Dis.* **23**, 232–240 (2017).

66. Widagdo, W. *et al.* Differential Expression of the Middle East Respiratory Syndrome Coronavirus Receptor in the Upper Respiratory Tracts of Humans and Dromedary Camels. *J. Virol.* **90**, 4838–4842 (2016).

67. De Wit, E. *et al.* Domestic pig unlikely reservoir for MERS-CoV. *Emerg. Infect. Dis.* **23**, 985–988 (2017).

68. Widagdo, W. *et al.* Tissue Distribution of the MERS-Coronavirus Receptor in Bats. *Sci. Rep.* **7**, 1–8 (2017).

69. De Wit, E. *et al.* Middle East respiratory syndrome coronavirus (MERS-CoV) causes transient lower respiratory tract infection in rhesus macaques. *Proc. Natl. Acad. Sci. U. S. A.* **110**, 16598–16603 (2013).

70. Haagmans, B. L. *et al.* Asymptomatic Middle East Respiratory Syndrome Coronavirus Infection in Rabbits. *J. Virol.* **89**, 6131–6135 (2015).

71. Raj, V. S. *et al.* Adenosine Deaminase Acts as a Natural Antagonist for Dipeptidyl Peptidase 4-Mediated Entry of the Middle East Respiratory

Syndrome Coronavirus. *J. Virol.* **88**, 1834–1838 (2014).

72. Li, F. Receptor Recognition Mechanisms of Coronaviruses: a Decade of Structural Studies. *J. Virol.* **89**, 1954–1964 (2015).

73. Barlan, A. *et al.* Receptor Variation and Susceptibility to Middle East Respiratory Syndrome Coronavirus Infection. *J. Virol.* **88**, 4953–4961 (2014).

74. de Wit, E. *et al.* The Middle East Respiratory Syndrome Coronavirus (MERS-CoV) Does Not Replicate in Syrian Hamsters. *PLoS One* **8**, 3–8 (2013).

75. Coleman, C. M., Matthews, K. L., Goicochea, L. & Frieman, M. B. Wild-type and innate immune-deficient mice are not susceptible to the Middle East respiratory syndrome coronavirus. *J. Gen. Virol.* **95**, 408–412 (2014).

76. Widagdo, W., Na Ayudhya, S. S., Hundie, G. B. & Haagmans, B. L. Host determinants of MERS-CoV transmission and pathogenesis. *Viruses* **11**, (2019).

77. Baggen, J., Vanstreels, E., Jansen, S. & Daelemans, D. Cellular host factors for SARS-CoV-2 infection. *Nat. Microbiol.* **6**, 1219–1232 (2021).

78. Wolff, G., Melia, C. E., Snijder, E. J. & Bárcena, M. Double-Membrane Vesicles as Platforms for Viral Replication. *Trends Microbiol.* **28**, 1022–1033 (2020).

79. Sachse, M. *et al.* Unraveling the antiviral activity of plitidepsin against SARS-CoV-2 by subcellular and morphological analysis. *Antiviral Res.* **200**, 105270 (2022).

80. Blanchard, E. & Roingeard, P. Virus-induced double-membrane vesicles. *Cell. Microbiol.* **17**, 45–50 (2015).

81. Wolff, G. *et al.* A molecular pore spans the double membrane of the coronavirus replication organelle. *Science.* **369**, 1395–1398 (2020).

82. de Breyne, S. *et al.* Translational control of coronaviruses. *Nucleic Acids Res.* **48**, 12502–12522 (2020).

83. Memish, Z. A., Perlman, S., van Kerkhove, M. D. & Zumla, A. Middle East respiratory syndrome. *Lancet* **395**, 1063–1077 (2020).

84. Omrani, A. S., Al-Tawfiq, J. A. & Memish, Z. A. Middle east respiratory syndrome coronavirus (MERS-CoV): Animal to human interaction. *Pathog. Glob. Health* **109**, 354–362 (2015).

85. Woo, P. C. Y., Lau, S. K. P., Li, K. S. M., Tsang, A. K. L. & Yuen, K. Y. Genetic relatedness of the novel human group C betacoronavirus to Tylonycteris bat coronavirus HKU4 and Pipistrellus bat coronavirus HKU5. *Emerg. Microbes Infect.* **1**, 0 (2012).

86. Annan, A. *et al.* Human betacoronavirus 2c EMC/2012-related viruses in bats, Ghana and Europe. *Emerg. Infect. Dis.* **19**, 456–459 (2013).

87. Anthony, S. J. *et al.* Coronaviruses in bats from Mexico. *J. Gen. Virol.* **94**, 1028–1038 (2013).

88. De Benedictis, P. *et al.* Alpha and lineage C betaCoV infections in Italian bats. *Virus Genes* **48**, 366–371 (2014).

89. Lelli, D. *et al.* Detection of coronaviruses in bats of various species in Italy. *Viruses* **5**, 2679–2689 (2013).

90. Giammanco, G. M. *et al.* Group C Betacoronavirus in Bat Guano Fertilizer, Thailand. *Emerg. Infect. Dis.* **19**, 1349–1351 (2013).

91. Guan, Y. *et al.* Isolation and characterization of viruses related to the SARS coronavirus from animals in Southern China. *Science.* **302**, 276–278 (2003).

92. Mahalingam, S. *et al.* Hendra virus: An emerging paramyxovirus in Australia. *Lancet Infect. Dis.* **12**, 799–807 (2012).

93. Reusken, C. B. *et al.* Middle east respiratory syndrome coronavirus (MERS-CoV) serology in major livestock species in an affected region in Jordan, june to September 2013. *Eurosurveillance* **18**, (2013).

94. Farag, E. *et al.* MERS-CoV in camels but not camel handlers, Sudan, 2015 and 2017. *Emerg. Infect. Dis.* **25**, 2333–2335 (2019).

95. Hemida, M. G. *et al.* Middle east respiratory syndrome (MERS) coronavirus seroprevalence in domestic livestock in Saudi Arabia, 2010 to 2013. *Eurosurveillance* **18**, 1–7 (2013).

96. Perera, R. A. *et al.* Seroepidemiology for MERS coronavirus using microneutralisation and pseudoparticle virus neutralisation assays reveal a high prevalence of antibody in dromedary camels in Egypt, june 2013. *Eurosurveillance* **18**, 1–7 (2013).

97. Tolah, A. M. *et al.* Cross-sectional prevalence study of MERSCoV in local and imported dromedary camels in Saudi Arabia, 2016-2018. *PLoS One* **15**, 2016–2018 (2020).

98. Kasem, S. *et al.* Cross-sectional study of MERS-CoV-specific RNA and antibodies in animals that have had contact with MERS patients in Saudi Arabia. *J. Infect. Public Health* **11**, 331–338 (2018).

99. Ali, M. *et al.* Cross-sectional surveillance of Middle East respiratory syndrome coronavirus (MERS-CoV) in dromedary camels and other mammals in Egypt, August 2015 to January 2016. *Eurosurveillance* **22**, (2017).

100. Chu, D. K. W. *et al.* MERS Coronaviruses in Dromedary Camels, Egypt. *Emerg. Infect. Dis.* **20**, 1049–1053 (2014).

101. Kandeil, A. *et al.* Middle east respiratory syndrome coronavirus (Mers-cov) in dromedary camels in africa and middle east. *Viruses* **11**, (2019).

102. Chu, D. K. *et al.* Middle east respiratory syndrome coronavirus (MERSCoV) in dromedary camels in nigeria, 2015. *Eurosurveillance* **20**, 1–7 (2015).

103. Nowotny, N. & Kolodziejek, J. Middle East Respiratory Syndrome coronavirus (MERS-CoV) in dromedary camels, Oman, 2013. *Eurosurveillance* **19**, 1–5 (2014).

104. Alexandersen, S., Kobinger, G. P., Soule, G. & Wernery, U. Middle east respiratory syndrome coronavirus antibody reactors among camels in Dubai, United Arab Emirates, in 2005. *Transbound. Emerg. Dis.* **61**, 105–108 (2014).

105. Haagmans, B. L. *et al.* Middle East respiratory syndrome coronavirus in dromedary camels: An outbreak investigation. *Lancet Infect. Dis.* **14**, 140–145 (2014).

106. Miguel, E. *et al.* Risk factors for MERS coronavirus infection in dromedary camels in Burkina Faso, Ethiopia, and Morocco, 2015. *Eurosurveillance* **22**, (2017).

107. Deem, S. L. *et al.* Serological evidence of MERS-CoV antibodies in dromedary camels (camelus dromedaries) in laikipia county, Kenya. *PLoS One* **10**, 11–15 (2015).

108. Hemida, M. G. *et al.* Seroepidemiology of middle east respiratory syndrome (MERS) coronavirus in Saudi Arabia (1993) and Australia (2014) and characterisation of assay specificity. *Eurosurveillance* **19**, 1–6 (2014).

109. Sayed, A. S. M., Malek, S. S. & Abushahba, M. F. N. Seroprevalence of Middle East Respiratory Syndrome Corona Virus in dromedaries and their traders in upper Egypt. *J. Infect. Dev. Ctries.* **14**, 191–198 (2020).

110. Reusken, C. B. E. M. E. M. *et al.* Geographic Distribution of MERS Coronavirus among Dromedary Camels, Africa. *Emerg. Infect. Dis.* **20**, 1370–1374 (2014).

111. Eckstein, S. *et al.* Prevalence of middle east respiratory syndrome coronavirus in dromedary camels, tunisia. *Emerg. Infect. Dis.* **27**, 1964–1968 (2021).

112. van Doremalen, N. *et al.* High prevalence of middle east respiratory coronavirus in young dromedary camels in Jordan. *Vector-Borne Zoonotic Dis.* **17**, 155–159 (2017).

113. Ommeh, S. *et al.* Genetic Evidence of Middle East Respiratory Syndrome Coronavirus (MERS-Cov) and Widespread Seroprevalence among Camels in Kenya. *Virol. Sin.* **33**, 484–492 (2018).

114. Falzarano, D. *et al.* Dromedary camels in northern Mali have high seropositivity to MERS-CoV. *One Heal.* **3**, 41–43 (2017).

115. Reusken, C. B. E. M. E. M. *et al.* MERS-CoV infection of alpaca in a region where MERS-CoV is endemic. *Emerg. Infect. Dis.* **22**, 1129–1131 (2016).

116. David, D. *et al.* Middle East respiratory syndrome coronavirus specific antibodies in naturally exposed Israeli llamas, alpacas and camels. *One Heal.* **5**, 65–68 (2018).

117. Chan, S. M. S. *et al.* Absence of MERS-Coronavirus in bactrian camels, Southern Mongolia, November 2014. *Emerg. Infect. Dis.* **21**, 1269–1271 (2015).

118. Miguel, E. *et al.* Absence of Middle East respiratory syndrome coronavirus in camelids, Kazakhstan, 2015. *Emerg. Infect. Dis.* **22**, 555–557 (2016).

119. So, R. T. Y. *et al.* Lack of serological evidence of Middle East respiratory syndrome coronavirus infection in virus exposed camel abattoir workers in Nigeria, 2016. *Eurosurveillance* **23**, (2018).

120. Ali, M. A. *et al.* Systematic, active surveillance for Middle East respiratory syndrome coronavirus in camels in Egypt. *Emerg. Microbes Infect.* **6**, e1-7 (2017).

121. Hemida, M. G. *et al.* Longitudinal study of Middle East Respiratory Syndrome coronavirus infection in dromedary camel herds in Saudi Arabia, 2014–2015. *Emerg. Microbes Infect.* **6**, 1–7 (2017).

122. Yusof, M. F. *et al.* Diversity of Middle East respiratory syndrome coronaviruses in 109 dromedary camels based on full-genome sequencing, Abu Dhabi, United Arab Emirates. *Emerg. Microbes Infect.* **6**, 1–10 (2017).

123. Kiambi, S. *et al.* Detection of distinct MERS-Coronavirus strains in dromedary camels from Kenya, 2017. *Emerg. Microbes Infect.* **7**, (2018).

124. Khalafalla, A. I. *et al.* MERS-CoV in upper respiratory tract and lungs of dromedary camels, Saudi Arabia, 2013–2014. *Emerg. Infect. Dis.* **21**, 1153–1158 (2015).

125. Kasem, S. *et al.* The prevalence of Middle East respiratory Syndrome coronavirus (MERS-CoV) infection in livestock and temporal relation to locations and seasons. *J. Infect. Public Health* **11**, 884–888 (2018).

126. Food And Agriculture Organization Of the United Nations (FAO). *MERS-CoV situation update*. https://www.fao.org/ag/againfo/programmes/en/empres/mers/situation_update.html (2021).

127. Dudas, G., Carvalho, L. M., Rambaut, A. & Bedford, T. MERS-CoV spillover at the camel-human interface. *Elife* **7**, 1–23 (2018).

128. Alagaili, A. N. *et al.* Middle east respiratory syndrome coronavirus infection

in dromedary camels in Saudi Arabia. *MBio* **5**, (2014).

129. Meyer, B. *et al.* Time course of MERS-CoV infection and immunity in dromedary camels. *Emerg. Infect. Dis.* **22**, 2171–2173 (2016).

130. Al Hammadi, Z. M. *et al.* Asymptomatic MERS-CoV infection in humans possibly linked to infected dromedaries imported from Oman to United Arab Emirates, May 2015. *Emerg. Infect. Dis.* **21**, 2197–2200 (2015).

131. Wernery, U. *et al.* Acute middle East respiratory syndrome coronavirus infection in livestock Dromedaries, Dubai, 2014. *Emerg. Infect. Dis.* (2015) doi:10.3201/eid2106.150038.

132. Muhairi, S. Al *et al.* Epidemiological investigation of Middle East respiratory syndrome coronavirus in dromedary camel farms linked with human infection in Abu Dhabi Emirate, United Arab Emirates. *Virus Genes* **52**, 848–854 (2016).

133. Hemida, M. G. *et al.* MERS coronavirus in dromedary camel herd, Saudi Arabia. *Emerg. Infect. Dis.* **20**, 1231–1234 (2014).

134. Hemida, M. G. *et al.* Dromedary Camels and the Transmission of Middle East Respiratory Syndrome Coronavirus (MERS-CoV). *Transbound. Emerg. Dis.* **64**, 344–353 (2017).

135. Younan, M., Bornstein, S. & Gluecks, I. V. MERS and the dromedary camel trade between Africa and the Middle East. *Trop. Anim. Health Prod.* **48**, 1277–1282 (2016).

136. Memish, Z. A. *et al.* Human Infection with MERS coronavirus after exposure to infected camels, Saudi Arabia, 2013. *Emerg. Infect. Dis.* **20**, 1012–1015 (2014).

137. Müller, M. A. *et al.* Presence of Middle East respiratory syndrome coronavirus antibodies in Saudi Arabia: A nationwide, cross-sectional, serological study. *Lancet Infect. Dis.* **15**, 559–564 (2015).

138. Reusken, C. B. E. M. *et al.* Occupational exposure to dromedaries and risk for MERS-CoV infection, Qatar, 2013–2014. *Emerg. Infect. Dis.* **21**, 1422–1425 (2015).

139. Al-Tawfiq, J. A. & Memish, Z. A. Middle East respiratory syndrome coronavirus: Transmission and phylogenetic evolution. *Trends Microbiol.* **22**, 573–579 (2014).

140. Sikkema, R. S. *et al.* Risk factors for primary middle east respiratory syndrome coronavirus infection in camel workers in Qatar during 2013-2014: A case-control study. *J. Infect. Dis.* **215**, 1702–1705 (2017).

141. Te, N. *et al.* Middle East respiratory syndrome coronavirus infection in camelids. *Vet. Pathol.* **5**, 1–6 (2022).

142. Arwady, M. A. *et al.* Middle east respiratory syndrome coronavirus

transmission in extended family, Saudi Arabia, 2014. *Emerg. Infect. Dis.* **22**, 1395–1402 (2016).

143. Memish, Z. A., Zumla, A. I., Al-Hakeem, R. F., Al-Rabeeah, A. A. & Stephens, G. M. Family Cluster of Middle East Respiratory Syndrome Coronavirus Infections. *N. Engl. J. Med.* **368**, 2487–2494 (2013).

144. Drosten, C. *et al.* Transmission of MERS-Coronavirus in Household Contacts. *N. Engl. J. Med.* **371**, 828–835 (2014).

145. Omrani, A. S. *et al.* A family cluster of middle east respiratory syndrome coronavirus infections related to a likely unrecognized asymptomatic or mild case. *Int. J. Infect. Dis.* **17**, e668–e672 (2013).

146. The Health Protection Agency (HPA) UK Novel Coronavirus Investigation team. Evidence of person-to-person transmission within a family cluster of novel coronavirus infections, United Kingdom, February 2013. *Eurosurveillance* **18**, 1–7 (2013).

147. Al-Abdallat, M. M. *et al.* Hospital-associated outbreak of middle east respiratory syndrome coronavirus: A serologic, epidemiologic, and clinical description. *Clin. Infect. Dis.* **59**, 1225–1233 (2014).

148. Assiri, A. *et al.* Hospital outbreak of Middle East respiratory syndrome coronavirus. *N. Engl. J. Med.* **369**, 407–16 (2013).

149. Memish, Z. A., Zumla, A. I. & Assiri, A. Middle East Respiratory Syndrome Coronavirus Infections in Health Care Workers. *N. Engl. J. Med.* **369**, 884–886 (2013).

150. Nam, H. S. *et al.* High fatality rates and associated factors in two hospital outbreaks of MERS in Daejeon, the Republic of Korea. *Int. J. Infect. Dis.* **58**, 37–42 (2017).

151. Oboho, I. K. *et al.* 2014 MERS-CoV Outbreak in Jeddah — A Link to Health Care Facilities. *N. Engl. J. Med.* **372**, 846–854 (2015).

152. Alenazi, T. H. *et al.* Identified Transmission Dynamics of Middle East Respiratory Syndrome Coronavirus Infection during an Outbreak: Implications of an Overcrowded Emergency Department. *Clin. Infect. Dis.* **65**, 675–679 (2017).

153. Al Hosani, F. I. *et al.* Response to emergence of middle east respiratory syndrome coronavirus, Abu Dhabi, United Arab Emirates, 2013-2014. *Emerg. Infect. Dis.* **22**, 1162–1168 (2016).

154. Alfaraj, S. H. *et al.* Middle East respiratory syndrome coronavirus transmission among health care workers: Implication for infection control. *Am. J. Infect. Control* **46**, 165–168 (2018).

155. Hunter, J. C. *et al.* Transmission of middle east respiratory syndrome coronavirus infections in healthcare settings, abu dhabi. *Emerg. Infect. Dis.*

22, 647–656 (2016).

156. Alanazi, K. H. *et al.* Scope and extent of healthcare-associated Middle East respiratory syndrome coronavirus transmission during two contemporaneous outbreaks in Riyadh, Saudi Arabia, 2017. *Infect. Control Hosp. Epidemiol.* **40**, 79–88 (2019).

157. Amer, H., Alqahtani, A. S., Alzoman, H., Aljerian, N. & Memish, Z. A. Unusual presentation of Middle East respiratory syndrome coronavirus leading to a large outbreak in Riyadh during 2017. *Am. J. Infect. Control* **46**, 1022–1025 (2018).

158. Kang, C. K. *et al.* Clinical and epidemiologic characteristics of spreaders of middle east respiratory syndrome coronavirus during the 2015 outbreak in Korea. *J. Korean Med. Sci.* **32**, 744–749 (2017).

159. Cho, S. Y. *et al.* MERS-CoV outbreak following a single patient exposure in an emergency room in South Korea: an epidemiological outbreak study. *Lancet* **388**, 994–1001 (2016).

160. Kim, S. W. *et al.* Risk factors for transmission of Middle East respiratory syndrome coronavirus infection during the 2015 outbreak in South Korea. *Clin. Infect. Dis.* **64**, 551–557 (2017).

161. Hui, D. S. *et al.* Middle East respiratory syndrome coronavirus: risk factors and determinants of primary, household, and nosocomial transmission. *Lancet Infect. Dis.* **18**, e217–e227 (2018).

162. Alraddadi, B. M. *et al.* Risk factors for middle east respiratory syndrome Coronavirus infection among healthcare personnel. *Emerg. Infect. Dis.* **22**, 1915–1920 (2016).

163. Grant, R., Malik, M. R., Elkholy, A. & van Kerkhove, M. D. A review of asymptomatic and subclinical middle east respiratory syndrome coronavirus infections. *Epidemiol. Rev.* **41**, 69–81 (2019).

164. van Doremalen, N., Bushmaker, T. & Munster, V. J. Stability of middle east respiratory syndrome coronavirus (MERS-CoV) under different environmental conditions. *Eurosurveillance* **18**, 20590 (2013).

165. Lee, J. Y. *et al.* The clinical and virological features of the first imported case causing MERS-CoV outbreak in South Korea, 2015. *BMC Infect. Dis.* **17**, 498 (2017).

166. Al-Gethamy, M. *et al.* A Case of Long-term Excretion and Subclinical Infection With Middle East Respiratory Syndrome Coronavirus in a Healthcare Worker. *Clin. Infect. Dis.* **60**, 973–974 (2015).

167. Choi, S., Jung, E., Choi, B. Y., Hur, Y. J. & Ki, M. High reproduction number of Middle East respiratory syndrome coronavirus in nosocomial outbreaks: mathematical modelling in Saudi Arabia and South Korea. *J. Hosp. Infect.* **99**, 162–168 (2018).

168. Donnelly, C. A., Malik, M. R., Elkholy, A., Cauchemez, S. & van Kerkhove, M. D. Worldwide reduction in MERS cases and deaths since 2016. *Emerg. Infect. Dis.* **25**, 1758–1760 (2019).

169. Schroeder, S. *et al.* Functional comparison of MERS-coronavirus lineages reveals increased replicative fitness of the recombinant lineage 5. *Nat. Commun.* **12**, (2021).

170. Aguanno, R. *et al.* MERS: Progress on the global response, remaining challenges and the way forward. *Antiviral Res.* **159**, 35–44 (2018).

171. Alyami, M. H., Alyami, H. S. & Warraich, A. Middle East Respiratory Syndrome (MERS) and novel coronavirus disease-2019 (COVID-19): From causes to preventions in Saudi Arabia. *Saudi Pharm. J.* **28**, 1481–1491 (2020).

172. Aleanizy, F. S., Mohmed, N., Alqahtani, F. Y. & El Hadi Mohamed, R. A. Outbreak of Middle East respiratory syndrome coronavirus in Saudi Arabia: A retrospective study. *BMC Infect. Dis.* **17**, 1–7 (2017).

173. Assiri, A. *et al.* Epidemiological, demographic, and clinical characteristics of 47 cases of Middle East respiratory syndrome coronavirus disease from Saudi Arabia: A descriptive study. *Lancet Infect. Dis.* **13**, 752–761 (2013).

174. Al-Tawfiq, J. A. *et al.* Middle east respiratory syndrome coronavirus: A case-control study of hospitalized patients. *Clin. Infect. Dis.* **59**, 160–165 (2014).

175. Memish, Z. A. *et al.* Middle East respiratory syndrome coronavirus disease in children. *Pediatr. Infect. Dis. J.* **33**, 904–906 (2014).

176. Guery, B. *et al.* Clinical features and viral diagnosis of two cases of infection with Middle East Respiratory Syndrome coronavirus: A report of nosocomial transmission. *Lancet* **381**, 2265–2272 (2013).

177. Arabi, Y. M. *et al.* Clinical Course and Outcomes of Critically Ill Patients With Middle East Respiratory Syndrome Coronavirus Infection. *Ann. Intern. Med.* **160**, 389–397 (2014).

178. Ajlan, A. M., Ahyad, R. A., Jamjoom, L. G., Alharthy, A. & Madani, T. A. Middle East respiratory syndrome coronavirus (MERS-CoV) infection: Chest CT findings. *Am. J. Roentgenol.* **203**, 782–787 (2014).

179. Alsahafi, A. J. & Cheng, A. C. The epidemiology of Middle East respiratory syndrome coronavirus in the Kingdom of Saudi Arabia, 2012-2015. *Int. J. Infect. Dis.* **45**, 1–4 (2016).

180. Elkholy, A. A. *et al.* MERS-CoV infection among healthcare workers and risk factors for death: Retrospective analysis of all laboratory-confirmed cases reported to WHO from 2012 to 2 June 2018. *J. Infect. Public Health* **13**, 418–422 (2020).

181. Badawi, A. & Ryoo, S. G. Prevalence of comorbidities in the Middle East respiratory syndrome coronavirus (MERS-CoV): a systematic review and meta-analysis. *Int. J. Infect. Dis.* **49**, 129–133 (2016).

182. Alqahtani, F. Y. *et al.* Prevalence of comorbidities in cases of Middle East respiratory syndrome coronavirus: A retrospective study. *Epidemiol. Infect.* **147**, (2019).

183. Yang, Y. M. *et al.* Impact of Comorbidity on Fatality Rate of Patients with Middle East Respiratory Syndrome. *Sci. Rep.* **7**, 1–9 (2017).

184. Seys, L. J. M. *et al.* DPP4, the Middle East Respiratory Syndrome Coronavirus Receptor, is Upregulated in Lungs of Smokers and Chronic Obstructive Pulmonary Disease Patients. *Clin. Infect. Dis.* **66**, 45–53 (2018).

185. Batawi, S. *et al.* Quality of life reported by survivors after hospitalization for Middle East respiratory syndrome (MERS). *Health Qual. Life Outcomes* **17**, 1–7 (2019).

186. Park, W. B. *et al.* Correlation between pneumonia severity and pulmonary complications in Middle East respiratory syndrome. *J. Korean Med. Sci.* **33**, 1–5 (2018).

187. Alsaad, K. O. *et al.* Histopathology of Middle East respiratory syndrome coronovirus (MERS-CoV) infection – clinicopathological and ultrastructural study. *Histopathology* **72**, 516–524 (2018).

188. Ng, D. L. *et al.* Clinicopathologic, immunohistochemical, and ultrastructural findings of a fatal case of middle east respiratory syndrome coronavirus infection in the United Arab Emirates, April 2014. *Am. J. Pathol.* **186**, 652–658 (2016).

189. Alosaimi, B. *et al.* MERS-CoV infection is associated with downregulation of genes encoding Th1 and Th2 cytokines/chemokines and elevated inflammatory innate immune response in the lower respiratory tract. *Cytokine* **126**, 154895 (2020).

190. Min, C. K. *et al.* Comparative and kinetic analysis of viral shedding and immunological responses in MERS patients representing a broad spectrum of disease severity. *Sci. Rep.* **6**, 1–12 (2016).

191. Widagdo, W. *et al.* Species-Specific Colocalization of Middle East Respiratory Syndrome Coronavirus Attachment and Entry Receptors. *J. Virol.* **93**, (2019).

192. Shinya, K. *et al.* Influenza virus receptors in the human airway. *Nature* **440**, 435–436 (2006).

193. Drosten, C. *et al.* Clinical features and virological analysis of a case of Middle East respiratory syndrome coronavirus infection. *Lancet Infect. Dis.* **13**, 745–751 (2013).

194. van Den Brand, J. M. A., Smits, S. L. & Haagmans, B. L. Pathogenesis of Middle East respiratory syndrome coronavirus. *J. Pathol.* **235**, 175–184 (2015).

195. Meyerholz, D. K., Lambertz, A. M. & McCray, P. B. Dipeptidyl Peptidase 4 Distribution in the Human Respiratory Tract Implications for the Middle East Respiratory Syndrome. *Am. J. Pathol.* **186**, 78–86 (2016).

196. Kindler, E. *et al.* Efficient replication of the novel human betacoronavirus EMC on primary human epithelium highlights its zoonotic potential. *MBio* **4**, (2013).

197. Zhou, J., Chu, H., Chan, J. F. W. & Yuen, K. Y. Middle East respiratory syndrome coronavirus infection: Virus-host cell interactions and implications on pathogenesis. *Virol. J.* **12**, 1–7 (2015).

198. Chu, H. *et al.* Middle East Respiratory Syndrome Coronavirus Efficiently Infects Human Primary T Lymphocytes and Activates the Extrinsic and Intrinsic Apoptosis Pathways. *J. Infect. Dis.* **213**, 904–914 (2016).

199. Scheuplein, V. a. *et al.* High Secretion of Interferons by Human Plasmacytoid Dendritic Cells upon Recognition of Middle East Respiratory Syndrome Coronavirus. *J. Virol.* **89**, JVI.03607-14 (2015).

200. Tynell, J. *et al.* Middle east respiratory syndrome coronavirus shows poor replication but significant induction of antiviral responses in human monocyte-derived macrophages and dendritic cells. *J. Gen. Virol.* **97**, 344–355 (2016).

201. Zhou, J. *et al.* Active replication of middle east respiratory syndrome coronavirus and aberrant induction of inflammatory cytokines and chemokines in human macrophages: Implications for pathogenesis. *J. Infect. Dis.* **209**, 1331–1342 (2014).

202. Cong, Y. *et al.* MERS-CoV pathogenesis and antiviral efficacy of licensed drugs in human monocyte-derived antigen-presenting cells. *PLoS One* **13**, 1–17 (2018).

203. Alharbi, N. K. *et al.* Humoral Immunogenicity and Efficacy of a Single Dose of ChAdOx1 MERS Vaccine Candidate in Dromedary Camels. *Sci. Rep.* **9**, 16292 (2019).

204. Alnaeem, A. *et al.* Some pathological observations on the naturally infected dromedary camels (Camelus dromedarius) with the Middle East respiratory syndrome coronavirus (MERS-CoV) in Saudi Arabia 2018–2019. *Vet. Q.* **40**, 190–197 (2020).

205. Alnaeem, A. *et al.* Scanning electron microscopic findings on respiratory organs of some naturally infected dromedary camels with the lineage-b of the middle east respiratory syndrome coronavirus (Mers-cov) in Saudi Arabia—2018. *Pathogens* **10**, 1–12 (2021).

206. Alnaeem, A. *et al.* The dipeptidyl peptidase-4 expression in some MERS-CoV naturally infected dromedary camels in Saudi Arabia 2018–2019. *VirusDisease* **31**, 200–203 (2020).

207. Haagmans, B. L. *et al.* An orthopoxvirus-based vaccine reduces virus excretion after MERS-CoV infection in dromedary camels. *Science.* **351**, 77–81 (2016).

208. Adney, D. R. *et al.* Replication and shedding of MERS-CoV in upper respiratory tract of inoculated dromedary camels. *Emerg. Infect. Dis.* **20**, 1999–2005 (2014).

209. Adney, R. D. *et al.* Efficacy of an Adjuvanted Middle East Respiratory Syndrome Coronavirus Spike Protein Vaccine in Dromedary Camels and Alpacas. *Viruses* vol. 11 (2019).

210. Haverkamp, A. K. *et al.* Experimental infection of dromedaries with Middle East respiratory syndrome-Coronavirus is accompanied by massive ciliary loss and depletion of the cell surface receptor dipeptidyl peptidase. *Sci. Rep.* **8**, 1–15 (2018).

211. Munster, V. J. *et al.* Replication and shedding of MERS-CoV in Jamaican fruit bats (Artibeus jamaicensis). *Sci. Rep.* **6**, 1–10 (2016).

212. Peck, K. M. *et al.* Glycosylation of Mouse DPP4 Plays a Role in Inhibiting Middle East Respiratory Syndrome Coronavirus Infection. *J. Virol.* **89**, 4696–4699 (2015).

213. de Wit, E. *et al.* Middle East respiratory syndrome coronavirus (MERS-CoV) causes transient lower respiratory tract infection in rhesus macaques. *Proc Natl Acad Sci U S A* **110**, 16598–16603 (2013).

214. Falzarano, D. *et al.* Treatment with interferon-α2b and ribavirin improves outcome in MERS-CoV-infected rhesus macaques. *Nat. Med.* **19**, 1313–1317 (2013).

215. Yao, Y. *et al.* An animal model of MERS produced by infection of rhesus macaques with MERS coronavirus. *J. Infect. Dis.* **209**, 236–242 (2014).

216. Rockx, B. *et al.* Comparative pathogenesis of COVID-19, MERS, and SARS in a nonhuman primate model. *Science.* **368**, 1012–1015 (2020).

217. Baseler, L. J. *et al.* An acute immune response to Middle East respiratory syndrome coronavirus replication contributes to viral pathogenicity. *Am. J. Pathol.* **186**, 630–638 (2016).

218. Yu, P. *et al.* Comparative pathology of rhesus macaque and common marmoset animal models with Middle East respiratory syndrome coronavirus. *PLoS One* **12**, (2017).

219. Falzarano, D. *et al.* Infection with MERS-CoV Causes Lethal Pneumonia in the Common Marmoset. *PLoS Pathog.* **10**, (2014).

220. Nelson, M. *et al.* Comparison of Experimental Middle East Respiratory Syndrome Coronavirus Infection Acquired by Three Individual Routes of Infection in the Common Marmoset. *J. Virol.* **96**, (2022).

221. Johnson, R. F. *et al.* Intratracheal exposure of common marmosets to MERS-CoV Jordan-n3/2012 or MERS-CoV EMC/2012 isolates does not result in lethal disease. *Virology* **485**, 422–430 (2015).

222. Chan, J. F. W. *et al.* Treatment with lopinavir/ritonavir or interferon-β1b improves outcome of MERSCoV infection in a nonhuman primate model of common marmoset. *J. Infect. Dis.* **212**, 1904–1913 (2015).

223. de Wit, E. *et al.* Prophylactic efficacy of a human monoclonal antibody against MERS-CoV in the common marmoset. *Antiviral Res.* **163**, 70–74 (2019).

224. Widagdo, W. *et al.* Lack of Middle East respiratory syndrome coronavirus transmission in rabbits. *Viruses* **11**, 1–13 (2019).

225. Houser, K. V. *et al.* Enhanced inflammation in New Zealand white rabbits when MERS-CoV reinfection occurs in the absence of neutralizing antibody. *PLoS Pathog.* **13**, 1–25 (2017).

226. Okba, N. M. A. *et al.* Particulate multivalent presentation of the receptor binding domain induces protective immune responses against MERS-CoV. *Emerg. Microbes Infect.* **9**, 1080–1091 (2020).

227. Zhao, J. *et al.* Rapid generation of a mouse model for Middle East respiratory syndrome. *Proc. Natl. Acad. Sci.* **111**, 4970–5 (2014).

228. Agrawal, A. S. *et al.* Generation of Transgenic Mouse Model of Middle East Respiratory Syndrome-Coronavirus Infection and Disease. *J. Virol.* **89**, JVI.03427-14 (2015).

229. Tao, X. *et al.* Characterization and Demonstration of the Value of a Lethal Mouse Model of Middle East Respiratory Syndrome Coronavirus Infection and Disease. *J. Virol.* **90**, 57–67 (2016).

230. Li, K. *et al.* Middle east respiratory syndrome coronavirus causes multiple organ damage and lethal disease in mice transgenic for human dipeptidyl peptidase 4. *J. Infect. Dis.* **212**, 712–722 (2015).

231. Pascal, K. E. *et al.* Pre- and postexposure efficacy of fully human antibodies against Spike protein in a novel humanized mouse model of MERS-CoV infection. *Proc. Natl. Acad. Sci. U. S. A.* **112**, 8738–8743 (2015).

232. Vergara-Alert, J., Vidal, E., Bensaid, A. & Segalés, J. Searching for animal models and potential target species for emerging pathogens: Experience gained from Middle East respiratory syndrome (MERS) coronavirus. *One Heal.* **3**, 34–40 (2017).

233. Adney, D. R. *et al.* Bactrian camels shed large quantities of Middle East

respiratory syndrome coronavirus (MERS-CoV) after experimental infection*. *Emerg. Microbes Infect.* **8**, 717–723 (2019).

234. Adney, D. R., Bielefeldt-Ohmann, H., Hartwig, A. E. & Bowen, R. A. Infection, replication, and transmission of Middle East respiratory syndrome coronavirus in alpacas. *Emerg. Infect. Dis.* **22**, 1031–1037 (2016).

235. Crameri, G. *et al.* Experimental infection and response to rechallenge of alpacas with Middle East respiratory syndrome coronavirus. *Emerg. Infect. Dis.* **22**, 1071–1074 (2016).

236. Te, N. *et al.* Co-localization of Middle East respiratory syndrome coronavirus (MERS-CoV) and dipeptidyl peptidase-4 in the respiratory tract and lymphoid tissues of pigs and llamas. *Transbound. Emerg. Dis.* **66**, 831–841 (2019).

237. World Health Organization (WHO). *WHO Target Product Profiles for MERS-CoV Vaccines.* http://www.who.int/blueprint/what/research-development/MERS_CoV_TPP_15052017.pdf (2017).

238. Faure, E. *et al.* Distinct immune response in two MERS-CoV-infected patients: Can we go from bench to bedside? *PLoS One* **9**, (2014).

239. Kim, E. J. S. *et al.* Clinical progression and cytokine profiles of Middle East respiratory syndrome coronavirus infection. *J. Korean Med. Sci.* **31**, 1717–1725 (2016).

240. Hamed, M. E. *et al.* Elevated Expression Levels of Lung Complement Anaphylatoxin, Neutrophil Chemoattractant Chemokine IL-8, and RANTES in MERS-CoV-Infected Patients: Predictive Biomarkers for Disease Severity and Mortality. *J. Clin. Immunol.* **41**, 1607–1620 (2021).

241. Zielecki, F. *et al.* Human Cell Tropism and Innate Immune System Interactions of Human Respiratory Coronavirus EMC Compared to Those of Severe Acute Respiratory Syndrome Coronavirus. *J. Virol.* **87**, 5300–5304 (2013).

242. Chan, R. W. Y. *et al.* Tropism and replication of Middle East respiratory syndrome coronavirus from dromedary camels in the human respiratory tract: an in-vitro and ex-vivo study. *Lancet Respir. Med.* **2**, 813–822 (2014).

243. Hocke, A. C. *et al.* Emerging human middle east respiratory syndrome coronavirus causes widespread infection and alveolar damage in human lungs. *Am. J. Respir. Crit. Care Med.* **188**, 882–886 (2013).

244. Lau, S. K. P. *et al.* Delayed induction of proinflammatory cytokines and suppression of innate antiviral response by the novel Middle East respiratory syndrome coronavirus: Implications for pathogenesis and treatment. *J. Gen. Virol.* **94**, 2679–2690 (2013).

245. Chu, H. *et al.* Productive replication of Middle East respiratory syndrome coronavirus in monocyte-derived dendritic cells modulates innate immune

response. *Virology* **454**–**455**, 197–205 (2014).

246. Zhao, J. *et al.* Recovery from the Middle East respiratory syndrome is associated with antibody and T-cell responses. *Sci. Immunol.* **2**, 1–11 (2017).

247. Shin, H. S. *et al.* Immune Responses to Middle East Respiratory Syndrome Coronavirus during the Acute and Convalescent Phases of Human Infection. *Clin. Infect. Dis.* **68**, 984–992 (2019).

248. Shin, H.-S. *et al.* Longitudinal Analysis of Memory T-Cell Responses in Survivors of Middle East Respiratory Syndrome. *Clin. Infect. Dis.* 1–8 (2021) doi:10.1093/cid/ciab1019.

249. Cheon, S. *et al.* Longevity of seropositivity and neutralizing antibodies in recovered MERS patients: a 5-year follow-up study. *Clin. Microbiol. Infect.* **28**, 292–296 (2022).

250. Channappanavar, R., Selvaraj, M., More, S. & Perlman, S. Alveolar macrophages protect mice from MERS-CoV-induced pneumonia and severe disease. *Vet. Pathol.* (2022) doi:10.1177/03009858221095270.

251. Junhee Seok *et al.* Genomic responses in mouse models poorly mimic human inflammatory diseases. *Proc. Natl. Acad. Sci. U. S. A.* **110**, 3507–3512 (2013).

252. Takao, K. & Miyakawa, T. Genomic responses in mouse models greatly mimic human inflammatory diseases. *Proc. Natl. Acad. Sci. U. S. A.* **112**, 1167–1172 (2015).

253. Kotsias, F., Cebrian, I. & Alloatti, A. Chapter Two - Antigen processing and presentation. in *Immunobiology of Dendritic Cells Part A* (eds. Lhuillier, C. & Galluzzi, L. B. T.-I. R. of C. and M. B.) vol. 348 69–121 (Academic Press, 2019).

254. Kelly, A. & Trowsdale, J. Genetics of antigen processing and presentation. *Immunogenetics* **71**, 161–170 (2019).

255. Janeway Jr, C. A., Travers, P., Walport, M. & Shlomchik, M. J. The major histocompatibility complex and its functions. in *Immunobiology: The Immune System in Health and Disease. 5th edition* (Garland Science, 2001).

256. Hamers-Casterman, C. *et al.* Naturally occurring antibodies devoid of light chains. *Nature* **363**, 446–448 (1993).

257. Greenberg, A. S. *et al.* A new antigen receptor gene family that undergoes rearrangement and extensive somatic diversification in sharks. *Nature* **374**, 168–173 (1995).

258. Nuttall, S. D. *et al.* Isolation of the new antigen receptor from wobbegong sharks, and use as a scaffold for the display of protein loop libraries. *Mol. Immunol.* **38**, 313–326 (2001).

259. De Genst, E., Saerens, D., Muyldermans, S. & Conrath, K. Antibody repertoire development in camelids. *Dev. Comp. Immunol.* **30**, 187–198 (2006).

260. Harmsen, M. M. & De Haard, H. J. Properties, production, and applications of camelid single-domain antibody fragments. *Appl. Microbiol. Biotechnol.* **77**, 13–22 (2007).

261. Muyldermans, S. Nanobodies: Natural single-domain antibodies. *Annu. Rev. Biochem.* **82**, 775–797 (2013).

262. Hussen, J. & Schuberth, H. J. Recent Advances in Camel Immunology. *Front. Immunol.* **11**, 1–17 (2021).

263. Plasil, M. *et al.* The major histocompatibility complex of Old World camelids: Class I and class I-related genes. *HLA* **93**, 203–215 (2019).

264. Plasil, M. *et al.* The major histocompatibility complex in Old World camelids and low polymorphism of its class II genes. *BMC Genomics* **17**, 1–17 (2016).

265. Ciccarese, S. *et al.* The camel adaptive immune receptors repertoire as a singular example of structural and functional genomics. *Front. Genet.* **10**, 1–14 (2019).

266. Le Page, L., Baldwin, C. L. & Telfer, J. C. γδ T cells in artiodactyls: Focus on swine. *Dev. Comp. Immunol.* **128**, 104334 (2022).

267. Ciccarese, S. *et al.* Characteristics of the somatic hypermutation in the Camelus dromedarius T cell receptor gamma (TRG) and delta (TRD) variable domains. *Dev. Comp. Immunol.* **46**, 300–313 (2014).

268. Chen, H. *et al.* Characterization of arrangement and expression of the T cell receptor γ locus in the sandbar shark. *Proc. Natl. Acad. Sci. U. S. A.* **106**, 8591–8596 (2009).

269. Chen, H., Bernstein, H., Ranganathan, P. & Schluter, S. F. Somatic hypermutation of TCR γ V genes in the sandbar shark. *Dev. Comp. Immunol.* **37**, 176–183 (2012).

270. Antonacci, R. *et al.* Expression and genomic analyses of Camelus dromedarius T cell receptor delta (TRD) genes reveal a variable domain repertoire enlargement due to CDR3 diversification and somatic mutation. *Mol. Immunol.* **48**, 1384–1396 (2011).

271. Vaccarelli, G. *et al.* Generation of diversity by somatic mutation in the Camelus dromedarius T-cell receptor gamma variable domains. *Eur. J. Immunol.* **42**, 3416–3428 (2012).

272. Futas, J. *et al.* Natural killer cell receptor genes in camels: Another mammalian model. *Front. Genet.* **10**, 1–15 (2019).

273. Lado, S. *et al.* Innate and adaptive immune genes associated with mers-cov

infection in dromedaries. *Cells* **10**, 1–20 (2021).

274. Krausgruber, T. *et al.* IRF5 promotes inflammatory macrophage polarization and TH1-TH17 responses. *Nat. Immunol.* **12**, 231–238 (2011).

275. Weiss, M., Blazek, K., Byrne, A. J., Perocheau, D. P. & Udalova, I. A. IRF5 is a specific marker of inflammatory macrophages in vivo. *Mediators Inflamm.* **2013**, (2013).

276. Banerjee, A., Falzarano, D., Rapin, N., Lew, J. & Misra, V. Interferon regulatory factor 3-mediated signaling limits middle-east respiratory syndrome (MERS) coronavirus propagation in cells from an insectivorous bat. *Viruses* **11**, (2019).

277. Mandl, J. N., Schneider, C., Schneider, D. S. & Baker, M. L. Going to bat(s) for studies of disease tolerance. *Front. Immunol.* **9**, 1–13 (2018).

278. Zhou, P. *et al.* Contraction of the type i IFN locus and unusual constitutive expression of IFN-α in bats. *Proc. Natl. Acad. Sci. U. S. A.* **113**, 2696–2701 (2016).

279. Banerjee, A., Rapin, N., Bollinger, T. & Misra, V. Lack of inflammatory gene expression in bats: A unique role for a transcription repressor. *Sci. Rep.* **7**, 1–15 (2017).

280. Ahn, M. *et al.* Dampened NLRP3-mediated inflammation in bats and implications for a special viral reservoir host. *Nat. Microbiol.* **4**, 789–799 (2019).

281. Banerjee, A. *et al.* Novel Insights Into Immune Systems of Bats. *Front. Immunol.* **11**, 1–15 (2020).

282. Agnihothram, S. *et al.* Evaluation of serologic and antigenic relationships between middle eastern respiratory syndrome coronavirus and other coronaviruses to develop vaccine platforms for the rapid response to emerging coronaviruses. *J. Infect. Dis.* **209**, 995–1006 (2014).

283. Ma, C. *et al.* Searching for an ideal vaccine candidate among different MERS coronavirus receptor-binding fragments – the importance of immunofocusing in subunit vaccine design. *Vaccine* **32**, 6170–6176 (2014).

284. Wang, L. *et al.* Evaluation of candidate vaccine approaches for MERS-CoV. *Nat. Commun.* **6**, (2015).

285. Okba, N. M., Raj, V. S. & Haagmans, B. L. Middle East respiratory syndrome coronavirus vaccines: current status and novel approaches. *Curr. Opin. Virol.* **23**, 49–58 (2017).

286. Stalin Raj, V. *et al.* Chimeric camel/human heavy-chain antibodies protect against MERS-CoV infection. *Sci. Adv.* **4**, eaas9667–eaas9667 (2018).

287. Tai, W. *et al.* A recombinant receptor-binding domain of MERS-CoV in trimeric form protects human dipeptidyl peptidase 4 (hDPP4) transgenic

mice from MERS-CoV infection. *Virology* **499**, 375–382 (2016).

288. Widjaja, I. *et al.* Towards a solution to MERS: protective human monoclonal antibodies targeting different domains and functions of the MERS-coronavirus spike glycoprotein. *Emerg. Microbes Infect.* **8**, 516–530 (2019).

289. Tai, W., Zhang, X., Yang, Y., Zhu, J. & Du, L. Advances in mRNA and other vaccines against MERS-CoV. *Transl. Res.* **242**, 20–37 (2022).

290. Cho, H., Excler, J.-L., Kim, J. H. & Yoon, I.-K. Development of Middle East Respiratory Syndrome Coronavirus vaccines – advances and challenges. *Hum. Vaccin. Immunother.* (2018) doi:10.1080/21645515.2017.1389362.

291. Zhang, N., Jiang, S. & Du, L. Current advancements and potential strategies in the development of MERS-CoV vaccines. *Expert Rev. Vaccines* **13**, 761–74 (2014).

292. Modjarrad, K. *et al.* Safety and immunogenicity of an anti-Middle East respiratory syndrome coronavirus DNA vaccine: a phase 1, open-label, single-arm, dose-escalation trial. *Lancet Infect. Dis.* **19**, 1013–1022 (2019).

293. Folegatti, P. M. *et al.* Safety and immunogenicity of a candidate Middle East respiratory syndrome coronavirus viral-vectored vaccine: a dose-escalation, open-label, non-randomised, uncontrolled, phase 1 trial. *Lancet Infect. Dis.* **20**, 816–826 (2020).

294. Koch, T. *et al.* Safety and immunogenicity of a modified vaccinia virus Ankara vector vaccine candidate for Middle East respiratory syndrome: an open-label, phase 1 trial. *Lancet Infect. Dis.* **20**, 827–838 (2020).

295. Zhou, B. *et al.* Reversion of Cold-Adapted Live Attenuated Influenza Vaccine into a Pathogenic Virus. *J. Virol.* **90**, 8454–8463 (2016).

296. Jimenez-Guardeño, J. M. *et al.* Identification of the Mechanisms Causing Reversion to Virulence in an Attenuated SARS-CoV for the Design of a Genetically Stable Vaccine. *PLoS Pathog.* **11**, 1–36 (2015).

297. Weyer, C. T. *et al.* African horse sickness caused by genome reassortment and reversion to virulence of live, attenuated vaccine viruses, South Africa, 2004–2014. *Emerg. Infect. Dis.* **22**, 2087–2096 (2016).

298. Nielsen, H. S. *et al.* Reversion of a live porcine reproductive and respiratory syndrome virus vaccine investigated by parallel mutations. *J. Gen. Virol.* **82**, 1263–1272 (2001).

299. Gutiérrez-Álvarez, J. *et al.* Middle East respiratory syndrome coronavirus vaccine based on a propagation-defective RNA replicon elicited sterilizing immunity in mice. *Proc. Natl. Acad. Sci. U. S. A.* **118**, (2021).

300. Haut, L. H., Ratcliffe, S., Pinto, A. R. & Ertl, H. Effect of preexisting

immunity to adenovirus on transgene product-specific genital T cell responses on vaccination of mice with a homologous vector. *J. Infect. Dis.* **203**, 1073–1081 (2011).

301. McCoy, K. *et al.* Effect of Preexisting Immunity to Adenovirus Human Serotype 5 Antigens on the Immune Responses of Nonhuman Primates to Vaccine Regimens Based on Human- or Chimpanzee-Derived Adenovirus Vectors. *J. Virol.* **81**, 6594–6604 (2007).

302. Pandey, A. *et al.* Impact of preexisting adenovirus vector immunity on immunogenicity and protection conferred with an adenovirus-based H5N1 influenza vaccine. *PLoS One* **7**, 1–9 (2012).

303. Nayak, S. & Herzog, R. W. Progress and prospects: immune responses to viral vectors. *Gene Ther.* **17**, 295–304 (2010).

304. Suschak, J. J., Williams, J. A. & Schmaljohn, C. S. Advancements in DNA vaccine vectors, non-mechanical delivery methods, and molecular adjuvants to increase immunogenicity. *Hum. Vaccines Immunother.* **13**, 2837–2848 (2017).

305. Hobernik, D. & Bros, M. DNA vaccines—How far from clinical use? *Int. J. Mol. Sci.* **19**, 1–28 (2018).

306. Ma, C. *et al.* Intranasal vaccination with recombinant receptor-binding domain of MERS-CoV spike protein induces much stronger local mucosal immune responses than subcutaneous immunization: Implication for designing novel mucosal MERS vaccines. *Vaccine* **32**, 2100–2108 (2014).

307. Liang, Z. *et al.* Adjuvants for Coronavirus Vaccines. *Front. Immunol.* **11**, (2020).

308. Gartlan, C. *et al.* Vaccine-Associated Enhanced Disease and Pathogenic Human Coronaviruses. *Front. Immunol.* **13**, 1–18 (2022).

309. Deng, Y. *et al.* Enhanced protection in mice induced by immunization with inactivated whole viruses compare to spike protein of middle east respiratory syndrome coronavirus. *Emerg. Microbes Infect.* **7**, (2018).

310. Kun, L. *et al.* Single-Dose, Intranasal Immunization with Recombinant Parainfluenza Virus 5 Expressing Middle East Respiratory Syndrome Coronavirus (MERS-CoV) Spike Protein Protects Mice from Fatal MERS-CoV Infection. *MBio* **11**, e00554-20 (2022).

311. Agrawal, A. S. *et al.* Immunization with inactivated Middle East Respiratory Syndrome coronavirus vaccine leads to lung immunopathology on challenge with live virus. *Hum. Vaccines Immunother.* **12**, 2351–2356 (2016).

312. Menachery, V. D. *et al.* Middle East Respiratory Syndrome Coronavirus Nonstructural Protein 16 Is Necessary for Interferon Resistance and Viral Pathogenesis. *mSphere* **2**, (2017).

313. Zhao, J. *et al.* Airway Memory CD4+ T Cells Mediate Protective Immunity against Emerging Respiratory Coronaviruses. *Immunity* **44**, 1379–1391 (2016).

314. Song, F. *et al.* Middle East Respiratory Syndrome Coronavirus Spike Protein Delivered by Modified Vaccinia Virus Ankara Efficiently Induces Virus-Neutralizing Antibodies. *J. Virol.* **87**, 11950–11954 (2013).

315. Volz, A. *et al.* Protective Efficacy of Recombinant Modified Vaccinia Virus Ankara Delivering Middle East Respiratory Syndrome Coronavirus Spike Glycoprotein. *J. Virol.* **89**, 8651–8656 (2015).

316. Kim, E. *et al.* Immunogenicity of an adenoviral-based Middle East Respiratory Syndrome coronavirus vaccine in BALB/c mice. *Vaccine* **32**, 5975–5982 (2014).

317. Guo, X. *et al.* Systemic and mucosal immunity in mice elicited by a single immunization with human adenovirus type 5 or 41 vector-based vaccines carrying the spike protein of Middle East respiratory syndrome coronavirus. *Immunology* (2015) doi:10.1111/imm.12462.

318. Jung, S. Y. *et al.* Heterologous prime–boost vaccination with adenoviral vector and protein nanoparticles induces both Th1 and Th2 responses against Middle East respiratory syndrome coronavirus. *Vaccine* **36**, 3468–3476 (2018).

319. Hashem, A. M. *et al.* A Highly Immunogenic, Protective, and Safe Adenovirus-Based Vaccine Expressing Middle East Respiratory Syndrome Coronavirus S1-CD40L Fusion Protein in a Transgenic Human Dipeptidyl Peptidase 4 Mouse Model. *J. Infect. Dis.* **220**, 1558–1567 (2019).

320. Kim, M. H., Kim, H. J. & Chang, J. Superior immune responses induced by intranasal immunization with recombinant adenovirus-based vaccine expressing fulllength Spike protein of Middle East respiratory syndrome coronavirus. *PLoS One* **14**, 1–20 (2019).

321. Dolzhikova, I. V. *et al.* Preclinical Studies of Immunogenity, Protectivity, and Safety of the Combined Vector Vaccine for Prevention of the Middle East Respiratory Syndrome. *Acta Naturae* **12**, 114–123 (2020).

322. Munster, V. J. *et al.* Protective efficacy of a novel simian adenovirus vaccine against lethal MERS-CoV challenge in a transgenic human DPP4 mouse model. *npj Vaccines* **2**, 1–3 (2017).

323. Alharbi, N. K. *et al.* ChAdOx1 and MVA based vaccine candidates against MERS-CoV elicit neutralising antibodies and cellular immune responses in mice. *Vaccine* **35**, 3780–3788 (2017).

324. van Doremalen, N. *et al.* A single dose of ChAdOx1 MERS provides protective immunity in rhesus macaques. *Sci. Adv.* **6**, (2020).

325. Malczyk, A. H. *et al.* A Highly Immunogenic and Protective Middle East

Respiratory Syndrome Coronavirus Vaccine Based on a Recombinant Measles Virus Vaccine Platform. *J. Virol.* (2015) doi:10.1128/JVI.01815-15.

326. Liu, R. qiang *et al.* Newcastle disease virus-based MERS-CoV candidate vaccine elicits high-level and lasting neutralizing antibodies in Bactrian camels. *J. Integr. Agric.* **16**, 2264–2273 (2017).

327. Liu, R. *et al.* A recombinant VSV-vectored MERS-CoV vaccine induces neutralizing antibody and T cell responses in rhesus monkeys after single dose immunization. *Antiviral Res.* **150**, 30–38 (2018).

328. Wirblich, C. *et al.* One-Health: a Safe, Efficient, Dual-Use Vaccine for Humans and Animals against Middle East Respiratory Syndrome Coronavirus and Rabies Virus. *J. Virol.* **91**, 1–15 (2017).

329. Li, E. *et al.* Characterization of the Immune Response of MERS-CoV Vaccine Candidates Derived from Two Different Vectors in Mice. *Viruses* **12**, (2020).

330. Kato, H. *et al.* Development of a recombinant replication-deficient rabies virus-based bivalent-vaccine against MERS-CoV and rabies virus and its humoral immunogenicity in mice. *PLoS One* **14**, 1–17 (2019).

331. Lan, J. *et al.* Significant Spike-Specific IgG and Neutralizing Antibodies in Mice Induced by a Novel Chimeric Virus-Like Particle Vaccine Candidate for Middle East Respiratory Syndrome Coronavirus. *Virol. Sin.* **33**, 453–455 (2018).

332. Wang, C. *et al.* MERS-CoV virus-like particles produced in insect cells induce specific humoural and cellular imminity in rhesus macaques. *Oncotarget* **8**, 12686–12694 (2017).

333. Wang, C. *et al.* Novel chimeric virus-like particles vaccine displaying MERS-CoV receptor-binding domain induce specific humoral and cellular immune response in mice. *Antiviral Res.* **140**, 55–61 (2017).

334. Karuppiah, M. *et al.* A synthetic consensus anti–spike protein DNA vaccine induces protective immunity against Middle East respiratory syndrome coronavirus in nonhuman primates. *Sci. Transl. Med.* **7**, 301ra132-301ra132 (2015).

335. Patel, A. *et al.* Intradermal delivery of a synthetic DNA vaccine protects macaques from Middle East respiratory syndrome coronavirus. *JCI Insight* **6**, (2021).

336. Chi, H. *et al.* DNA vaccine encoding Middle East respiratory syndrome coronavirus S1 protein induces protective immune responses in mice. *Vaccine* **35**, 2069–2075 (2017).

337. Al-Amri, S. S. *et al.* Immunogenicity of Candidate MERS-CoV DNA Vaccines Based on the Spike Protein. *Sci. Rep.* **7**, 1–8 (2017).

338. Jung-ah, C. *et al.* Cross-Protection against MERS-CoV by Prime-Boost Vaccination Using Viral Spike DNA and Protein. *J. Virol.* **94**, e01176-20 (2022).

339. Cho, H. *et al.* Human endogenous retrovirus-enveloped baculoviral DNA vaccines against MERS-CoV and SARS-CoV2. *npj Vaccines* **6**, 1–9 (2021).

340. Veit, S., Jany, S., Fux, R., Sutter, G. & Volz, A. CD8+ T cells responding to the middle east respiratory syndrome coronavirus nucleocapsid protein delivered by vaccinia virus MVA in mice. *Viruses* **10**, (2018).

341. Pallesen, J. *et al.* Immunogenicity and structures of a rationally designed prefusion MERS-CoV spike antigen. *Proc. Natl. Acad. Sci. U. S. A.* **114**, E7348–E7357 (2017).

342. Jiaming, L. *et al.* The recombinant N-terminal domain of spike proteins is a potential vaccine against Middle East respiratory syndrome coronavirus (MERS-CoV) infection. *Vaccine* **35**, 10–18 (2017).

343. Jung, B. K., An, Y. H., Park, J. E., Chang, K. S. & Jang, H. Development of a recombinant vaccine containing a spike S1-Fc fusion protein induced protection against MERS-CoV in human DPP4 knockin transgenic mice. *J. Virol. Methods* **299**, 114347 (2022).

344. Du, L. *et al.* A truncated receptor-binding domain of MERS-CoV spike protein potently inhibits MERS-CoV infection and induces strong neutralizing antibody responses: Implication for developing therapeutics and vaccines. *PLoS One* **8**, 2–10 (2013).

345. Nyon, M. P. *et al.* Engineering a stable CHO cell line for the expression of a MERS-coronavirus vaccine antigen. *Vaccine* **36**, 1853–1862 (2018).

346. Lan, J. *et al.* Tailoring Subunit Vaccine Immunity with Adjuvant Combinations and Delivery Routes Using the Middle East Respiratory Coronavirus (MERS-CoV) Receptor-Binding Domain as an Antigen. *PLoS One* **9**, e112602 (2014).

347. Lan, J. *et al.* Recombinant Receptor Binding Domain Protein Induces Partial Protective Immunity in Rhesus Macaques Against Middle East Respiratory Syndrome Coronavirus Challenge(). *EBioMedicine* **2**, 1438–1446 (2015).

348. Kim, J., Yang, Y. L., Jeong, Y. & Jang, Y. S. Conjugation of human β-defensin 2 to spike protein receptor-binding domain induces antigen-specific protective immunity against middle east respiratory syndrome coronavirus infection in human dipeptidyl peptidase 4 transgenic mice. *Vaccines* **8**, 1–15 (2020).

349. Lin, L. C. W. *et al.* Viromimetic STING Agonist-Loaded Hollow Polymeric Nanoparticles for Safe and Effective Vaccination against Middle East Respiratory Syndrome Coronavirus. *Adv. Funct. Mater.* **29**, (2019).

350. Coleman, C. M. *et al.* Purified coronavirus spike protein nanoparticles

induce coronavirus neutralizing antibodies in mice. *Vaccine* **32**, 3169–3174 (2014).

351. Coleman, C. M. *et al.* MERS-CoV spike nanoparticles protect mice from MERS-CoV infection. *Vaccine* **35**, 1586–1589 (2017).

352. Mohd, H. A., Al-Tawfiq, J. A. & Memish, Z. A. Middle East Respiratory Syndrome Coronavirus (MERS-CoV) origin and animal reservoir. *Virol. J.* **13**, 87 (2016).

353. Vergara-Alert, J. *et al.* Middle East respiratory syndrome coronavirus experimental transmission using a pig model. *Transbound. Emerg. Dis.* **64**, 1342–1345 (2017).

354. Corman, V. M. *et al.* Detection of a novel human coronavirus by real-time reverse-transcription polymerase chain reaction. *Eurosurveillance* **17**, (2012).

355. Okba, N. M. A. *et al.* Sensitive and specific detection of low-level antibody responses in mild Middle East respiratory syndrome coronavirus infections. *Emerg. Infect. Dis.* **25**, 1868–1877 (2019).

356. Burbelo, P. D., Goldman, R. & Mattson, T. L. A simplified immunoprecipitation method for quantitatively measuring antibody responses in clinical sera samples by using mammalian-produced Renilla luciferase-antigen fusion proteins. *BMC Biotechnol.* (2005) doi:10.1186/1472-6750-5-22.

357. Burbelo, P. D., Ching, K. H., Klimavicz, C. M. & Iadarola, M. J. Antibody Profiling by Luciferase Immunoprecipitation Systems (LIPS). *J. Vis. Exp.* (2009) doi:10.3791/1549.

358. Munyua, P. *et al.* Low-Level Middle East Respiratory Syndrome Coronavirus among Camel Handlers, Kenya, 2019. *Emerg. Infect. Dis. J.* **27**, 1201 (2021).

359. Liljander, A. *et al.* MERS-CoV Antibodies in Humans, Africa, 2013–2014. *Emerg. Infect. Dis. J.* **22**, 1086 (2016).

360. Kiyong'a, A. N. *et al.* Middle East Respiratory Syndrome Coronavirus (MERS-CoV) Seropositive Camel Handlers in Kenya. *Viruses* vol. 12 396 (2020).

361. Mok, C. K. P. *et al.* T-cell responses to MERS coronavirus infection in people with occupational exposure to dromedary camels in Nigeria: an observational cohort study. *Lancet Infect. Dis.* **21**, 385–395 (2021).

362. Coleman, C. M. & Frieman, M. B. Growth and Quantification of MERS-CoV Infection. *Curr. Protoc. Microbiol.* **37**, 15E.2.1-15E.2.9 (2015).

363. Food and Agriculture Organization of the United Nations Statistics Division. FAOSTAT Statistical Database. www.fao.org/faostat (2021).

364. Halsby, K. *et al.* Zoonotic diseases in South American camelids in England and Wales. *Epidemiol. Infect.* **145**, 1037–1043 (2017).

365. Khalafalla, A. I. Emerging Infectious Diseases in Camelids BT - Emerging and Re-emerging Infectious Diseases of Livestock. in (ed. Bayry, J.) 425–441 (Springer International Publishing, 2017). doi:10.1007/978-3-319-47426-7_20.

366. Zhu, S., Zimmerman, D. & Deem, S. L. A Review of Zoonotic Pathogens of Dromedary Camels. *Ecohealth* **16**, 356–377 (2019).

367. Dinarello, C. A. Historical insights into cytokines. *Eur. J. Immunol.* **37**, S34–S45 (2007).

368. Svanborg, C., Godaly, G. & Hedlund, M. Cytokine responses during mucosal infections: role in disease pathogenesis and host defence. *Curr. Opin. Microbiol.* **2**, 99–103 (1999).

369. Smeed, J. A., Watkins, C. A., Rhind, S. M. & Hopkins, J. Differential cytokine gene expression profiles in the three pathological forms of sheep paratuberculosis. *BMC Vet. Res.* **3**, 18 (2007).

370. van Reeth, K. & Nauwynck, H. Proinflammatory cytokines and viral respiratory disease in pigs. *Vet. Res.* **31**, 187–213 (2000).

371. Premraj, A., Aleyas, A. G., Nautiyal, B. & Rasool, T. J. Camelid type I interferons: Identification and functional characterization of interferon alpha from the dromedary camel (Camelus dromedarius). *Mol. Immunol.* **119**, 132–143 (2020).

372. Nagarajan, G. *et al.* Cloning and sequence analysis of IL-2, IL-4 and IFN-γ from Indian Dromedary camels (Camelus dromedarius). *Res. Vet. Sci.* **92**, 420–426 (2012).

373. Odbileg, R. *et al.* Complete cDNA sequences and phylogenetic analyses of the Th1 and Th2 cytokines of the bactrian camel (Camelus bactrianus). *J. Vet. Med. Sci.* **68**, 941–946 (2006).

374. Odbileg, R. *et al.* Cloning and sequence analysis of llama cytokines related to cell-mediated immunity. *Vet. Immunol. Immunopathol.* **102**, 93–102 (2004).

375. Odbileg, R., Lee, S. Il, Ohashi, K. & Onuma, M. Cloning and sequence analysis of llama (lama glama): Th2 (IL-4, IL-10 and IL-13) cytokines. *Vet. Immunol. Immunopathol.* **104**, 145–153 (2005).

376. Odbileg, R., Konnai, S., Ohashi, K. & Onuma, M. Molecular cloning and phylogenetic analysis of inflammatory cytokines of Camelidae (llama and camel). *J. Vet. Med. Sci.* **67**, 921–5 (2005).

377. Odbileg, R., Konnai, S., Usui, T., Ohashi, K. & Onuma, M. Quantification of llama inflammatory cytokine mRNAs by real-time RT-PCR. *J. Vet. Med.*

Sci. **67**, 195–8 (2004).

378. Odbileg, R. *et al.* Cytokine responses in camels (Camelus bactrianus) vaccinated with Brucella abortus strain 19 vaccine. *J. Vet. Med. Sci.* **70**, 197–201 (2008).

379. Wu, H. *et al.* Camelid genomes reveal evolution and adaptation to desert environments. *Nat. Commun.* **5**, (2014).

380. Bustin, S. A. *et al.* The MIQE guidelines: Minimum information for publication of quantitative real-time PCR experiments. *Clin. Chem.* **55**, 611–622 (2009).

381. Ballester, M., Cordón, R. & Folch, J. M. DAG expression: High-throughput gene expression analysis of real-time PCR data using standard curves for relative quantification. *PLoS One* **8**, 8–12 (2013).

382. Wernery, U., Kinne, J. & Schuster, R. K. *Camelid infectious disorders*. (OIE (World Organisation for Animal Health), 2014).

383. Taylor, S., Wakem, M., Dijkman, G., Alsarraj, M. & Nguyen, M. A practical approach to RT-qPCR-Publishing data that conform to the MIQE guidelines. *Methods* **50**, S1 (2010).

384. Cicinnati, V. R. *et al.* Validation of putative reference genes for gene expression studies in human hepatocellular carcinoma using real-time quantitative RT-PCR. *BMC Cancer* **8**, 350 (2008).

385. Mehta, R. *et al.* Validation of endogenous reference genes for qRT-PCR analysis of human visceral adipose samples. *BMC Mol. Biol.* **11**, 39 (2010).

386. Souza, A. F. D., Brum, I. S., Neto, B. S., Berger, M. & Branchini, G. Reference gene for primary culture of prostate cancer cells. *Mol. Biol. Rep.* **40**, 2955–2962 (2013).

387. Albershardt, T. C., Iritani, B. M. & Ruddell, A. Evaluation of reference genes for quantitative PCR analysis of mouse lymphocytes. *J. Immunol. Methods* **384**, 196–199 (2012).

388. Bas, A., Forsberg, G., Hammarström, S. & Hammarström, M.-L. Utility of the housekeeping genes 18S rRNA, beta-actin and glyceraldehyde-3-phosphate-dehydrogenase for normalization in real-time quantitative reverse transcriptase-polymerase chain reaction analysis of gene expression in human T lymphocytes. *Scand. J. Immunol.* **59**, 566–573 (2004).

389. Dheda, K. *et al.* Validation of housekeeping genes for normalizing RNA expression in real-time PCR. *Biotechniques* **37**, 112–119 (2004).

390. Resa, C. *et al.* Development of an efficient qRT-PCR assay for quality control and cellular quantification of respiratory samples. *J. Clin. Virol.* **60**, 270–275 (2014).

391. Sullivan, K. E. *et al.* Measurement of cytokine secretion, intracellular

protein expression, and mRNA in resting and stimulated peripheral blood mononuclear cells. *Clin. Diagn. Lab. Immunol.* **7**, 920–924 (2000).

392. Baran, J., Kowalczyk, D., Ozog, M. & Zembala, M. Three-color flow cytometry detection of intracellular cytokines in peripheral blood mononuclear cells: Comparative analysis of phorbol myristate acetate-ionomycin and phytohemagglutinin stimulation. *Clin. Diagn. Lab. Immunol.* **8**, 303–313 (2001).

393. Nakatsumi, H., Matsumoto, M. & Nakayama, K. I. Noncanonical Pathway for Regulation of CCL2 Expression by an mTORC1-FOXK1 Axis Promotes Recruitment of Tumor-Associated Macrophages. *Cell Rep.* **21**, 2471–2486 (2017).

394. Norian, R., Delirezh, N. & Azadmehr, A. Evaluation of proliferation and cytokines production by mitogen-stimulated bovine peripheral blood mononuclear cells. *Vet. Res. Forum* **6**, 265–271 (2015).

395. Rostaing, L. *et al.* Kinetics of intracytoplasmic Th1 and Th2 cytokine production assessed by flow cytometry following in vitro activation of peripheral blood mononuclear cells. *Cytometry* **35**, 318–328 (1999).

396. Liu, T., Zhang, L., Joo, D. & Sun, S. C. NF-κB signaling in inflammation. *Signal Transduct. Target. Ther.* **2**, (2017).

397. Sen, N., Sung, P., Panda, A. & Arvin, A. M. Distinctive Roles for Type I and Type II Interferons and Interferon Regulatory Factors in the Host Cell Defense against Varicella-Zoster Virus. *J. Virol.* **92**, (2018).

398. Wang, W., Xu, L., Su, J., Peppelenbosch, M. P. & Pan, Q. Transcriptional Regulation of Antiviral Interferon-Stimulated Genes. *Trends Microbiol.* **25**, 573–584 (2017).

399. Rabin, R. L. CC, C, and CX3C Chemokines. in *Encyclopedia of Hormones* (eds. Henry, H. L. & Norman, A. W. B. T.-E. of H.) 255–263 (Academic Press, 2003). doi:https://doi.org/10.1016/B0-12-341103-3/00044-9.

400. Gao, Y. *et al.* Transcriptome analysis of porcine PBMCs after in vitro stimulation by LPS or PMA/ionomycin using an expression array targeting the pig immune response. *BMC Genomics* **11**, 1–25 (2010).

401. Lin, Z. *et al.* Functional differences and similarities in activated peripheral blood mononuclear cells by lipopolysaccharide or phytohemagglutinin stimulation between human and cynomolgus monkeys. *Ann. Transl. Med.* **9**, 257–257 (2021).

402. Ciliberti, M. G. *et al.* Peripheral blood mononuclear cell proliferation and cytokine production in sheep as affected by cortisol level and duration of stress. *J. Dairy Sci.* **100**, 750–756 (2017).

403. Wagner, B. & Freer, H. Development of a bead-based multiplex assay for simultaneous quantification of cytokines in horses. *Vet. Immunol.*

Immunopathol. **127**, 242–248 (2009).

404. Zhou, Z. *et al.* Type III Interferon (IFN) Induces a Type I IFN-Like Response in a Restricted Subset of Cells through Signaling Pathways Involving both the Jak-STAT Pathway and the Mitogen-Activated Protein Kinases. *J. Virol.* **81**, 7749–7758 (2007).

405. Stanifer, M. L., Pervolaraki, K. & Boulant, S. Differential regulation of type I and type III interferon signaling. *Int. J. Mol. Sci.* **20**, 1–22 (2019).

406. Huang, C. C. *et al.* A pathway analysis of poly(I:C)-induced global gene expression change in human peripheral blood mononuclear cells. *Physiol. Genomics* **26**, 125–133 (2006).

407. Murata, K. *et al.* Ex vivo induction of IFN-λ3 by a TLR7 agonist determines response to Peg-IFN/Ribavirin therapy in chronic hepatitis C patients. *J. Gastroenterol.* **49**, 126–137 (2014).

408. Booth, J. S., Buza, J. J., Potter, A., Babiuk, L. A. & Mutwiri, G. K. Co-stimulation with TLR7/8 and TLR9 agonists induce down-regulation of innate immune responses in sheep blood mononuclear and B cells. *Dev. Comp. Immunol.* **34**, 572–578 (2010).

409. Docampo, M. J., Cabrera, J. & Bassols, A. Hyaluronan mediates the adhesion of porcine peripheral blood mononuclear cells to poly (I:C)-treated intestinal cells and modulates their cytokine production. *Vet. Immunol. Immunopathol.* **184**, 8–17 (2017).

410. Wang, J. *et al.* Transcriptomic analysis identifies candidate genes and gene sets controlling the response of porcine peripheral blood mononuclear cells to poly I:C stimulation. *G3 Genes, Genomes, Genet.* **6**, 1267–1275 (2016).

411. Mahallawi, W. H., Khabour, O. F., Zhang, Q., Makhdoum, H. M. & Suliman, B. A. MERS-CoV infection in humans is associated with a pro-inflammatory Th1 and Th17 cytokine profile. *Cytokine* **104**, 8–13 (2018).

412. Mubarak, A. *et al.* In vivo and in vitro evaluation of cytokine expression profiles during middle east respiratory syndrome coronavirus (Mers-cov) infection. *J. Inflamm. Res.* **14**, 2121–2131 (2021).

413. Zhao, X. *et al.* Activation of C-Type Lectin Receptor and (RIG)-I-Like Receptors Contributes to Proinflammatory Response in Middle East Respiratory Syndrome Coronavirus-Infected Macrophages. *J. Infect. Dis.* **221**, 647–659 (2020).

414. Rodon, J. *et al.* Blocking transmission of Middle East respiratory syndrome coronavirus (MERS-CoV) in llamas by vaccination with a recombinant spike protein. *Emerg. Microbes Infect.* **8**, 1593–1603 (2019).

415. Livak, K. J. & Schmittgen, T. D. Analysis of relative gene expression data using real-time quantitative PCR and the 2-ΔΔCT method. *Methods* **25**, 402–408 (2001).

416. Tenorio, R. *et al.* Reovirus σNS and μNS proteins remodel the endoplasmic reticulum to build replication neo-organelles. *MBio* **9**, (2018).

417. Perez-Zsolt, D. *et al.* SARS-CoV-2 interaction with Siglec-1 mediates trans-infection by dendritic cells. *Cell. Mol. Immunol.* **18**, 2676–2678 (2021).

418. Dogra, P. *et al.* Tissue Determinants of Human NK Cell Development, Function, and Residence. *Cell* **180**, 749-763.e13 (2020).

419. Boysen, P., Gunnes, G., Pende, D., Valheim, M. & Storset, A. K. Natural killer cells in lymph nodes of healthy calves express CD16 and show both cytotoxic and cytokine-producing properties. *Dev. Comp. Immunol.* **32**, 773–783 (2008).

420. Dowling, J. W. & Forero, A. Beyond Good and Evil: Molecular Mechanisms of Type I and III IFN Functions. *J. Immunol.* **208**, 247–256 (2022).

421. Ye, L., Schnepf, D. & Staeheli, P. Interferon-λ orchestrates innate and adaptive mucosal immune responses. *Nat. Rev. Immunol.* **19**, 614–625 (2019).

422. Hemann, E. A. *et al.* Interferon-λ modulates dendritic cells to facilitate T cell immunity during infection with influenza A virus. *Nat. Immunol.* **20**, 1035–1045 (2019).

423. World Health Organisation (WHO). *MERS situation update - August 2021*. https://applications.emro.who.int/docs/WHOEMCSR451E-eng.pdf?ua=1 (2021).

424. Aebischer, A. *et al.* Development of a Modular Vaccine Platform for Multimeric Antigen Display Using an Orthobunyavirus Model. *Vaccines* vol. 9 (2021).

425. Wichgers Schreur, P. J. *et al.* Vaccine Efficacy of Self-Assembled Multimeric Protein Scaffold Particles Displaying the Glycoprotein Gn Head Domain of Rift Valley Fever Virus. *Vaccines* vol. 9 (2021).

426. Bruun, T. U. J., Andersson, A.-M. C., Draper, S. J. & Howarth, M. Engineering a Rugged Nanoscaffold To Enhance Plug-and-Display Vaccination. *ACS Nano* **12**, 8855–8866 (2018).

427. Xu, J. *et al.* Antibodies and vaccines against Middle East respiratory syndrome coronavirus. *Emerg. Microbes Infect.* **8**, 841–856 (2019).

428. Cockrell, A. S. *et al.* A mouse model for MERS coronavirus-induced acute respiratory distress syndrome. *Nat. Microbiol.* **2**, 16226 (2016).

429. Zhang, N. *et al.* Identification of an ideal adjuvant for receptor-binding domain-based subunit vaccines against Middle East respiratory syndrome coronavirus. *Cell. Mol. Immunol.* **13**, 180 (2015).

430. Tang, J. *et al.* Optimization of antigen dose for a receptor-binding domain-

based subunit vaccine against MERS coronavirus. *Hum. Vaccin. Immunother.* **11**, 1244–1250 (2015).

431. Tai, W. *et al.* Recombinant Receptor-Binding Domains of Multiple Middle East Respiratory Syndrome Coronaviruses (MERS-CoVs) Induce Cross-Neutralizing Antibodies against Divergent Human and Camel MERS-CoVs and Antibody Escape Mutants. *J. Virol.* **91**, e01651-16 (2017).

432. Letko, M. *et al.* Adaptive Evolution of MERS-CoV to Species Variation in DPP4. *Cell Rep.* **24**, 1730–1737 (2018).

433. Ibrahim, E. E.-S. *et al.* Comparative study on the immunopotentiator effect of ISA 201, ISA 61, ISA 50, ISA 206 used in trivalent foot and mouth disease vaccine. *Vet. World* **8**, 1189–1198 (2015).

434. Camp, J. V. *et al.* Crimean-Congo hemorrhagic fever virus endemicity in United Arab Emirates, 2019. *Emerg. Infect. Dis.* **26**, 1019–1021 (2020).

435. Khalafalla, A. I. *et al.* Identification of a novel lineage of Crimean-Congo haemorrhagic fever virus in dromedary camels, United Arab Emirates. *J. Gen. Virol.* **102**, 1–4 (2021).

436. Davis, W. C. *et al.* Flow cytometric analysis of an immunodeficiency disorder affecting juvenile llamas. *Vet. Immunol. Immunopathol.* **74**, 103–120 (2000).

437. Savoji, M. A., Sereshgi, M. M. A., Ghahari, S. M. M., Asgarhalvaei, F. & Mahdavi, M. Formulation of HBsAg in Montanide ISA 51VG adjuvant: Immunogenicity study and monitoring long-lived humoral immune responses. *Int. Immunopharmacol.* **96**, 107599 (2021).

About the author

Jordi Rodon Aldrufeu was born on the 19th September 1994 in Vilassar de Mar, Barcelona, where he grew up. For a long time, science has been one of his passions. He obtained a Bachelor's degree in Biology at the University of Girona (2012-2016). He coursed the last year of his B. Sc. at the Ghent University (Belgium), achieving a special mention on fundamental biotechnology and sanitary biology. Afterwards, he completed a Master's degree in Molecular Biotechnology at the University of Barcelona (2016-2017) that introduced him to the world of infectious diseases. He was delighted by the possibility of integrating this branch of science in his research. Therefore, he enrolled a Ph.D. fellowship at IRTA-CReSA, which provided him with the unique opportunity to work with zoonotic diseases and large animal models (camelid species) in BSL-3 conditions.

His Ph.D. research was focused on MERS-CoV; however, during the last 2 years he was intensively working with SARS-CoV-2. He is studying MERS-CoV pathogenesis and immune responses upon infection and vaccination in camelids, and why camelid reservoir species do not experience severe disease as opposed to humans. Nonetheless, since the beginning of the current COVID-19 pandemic, our research group has been focused on developing and testing therapeutic treatments and vaccine prototypes to fight MERS-CoV and SARS-CoV-2 infections, in both the natural host and animal models. Thus, his research is highly devoted to the 'One Health' initiative.

Ph.D. Portfolio

EDUCATION

July 2018 – *currently*
Autonomous University of Barcelona (UAB) – Barcelona, Spain
Ph.D. student in Animal Medicine and Health

2016 – 2017
University of Barcelona (UB) – Barcelona, Spain
M.Sc. in Molecular Biotechnology

2016
Institut de Formació Contínua IL3 - Universitat de Barcelona (UB) – Barcelona, Spain
Course in Education of Research User of Laboratory Animals (FELASA categories B+C+D)

2015 – 2016
Ghent University (UGent) – Ghent, Belgium
Exchange student at Ghent University

2012 – 2016
University of Girona (UdG) – Girona, Spain
B.Sc. in Biology with a distinguished mention in Fundamental and Sanitary Biology

OTHER EDUCATION

Nov., 2020
Course: Scientific writing and other documents
Autonomous University of Barcelona (UAB) – Barcelona, Spain

May., 2020
Course: Research Papers
Autonomous University of Barcelona (UAB) – Barcelona, Spain

Oct., 2019
Guest Researcher at Ghent University (UGent) – Ghent, Belgium
Guest Researcher at Hans Nauwynck's Lab – Laboratory of Virology, Faculty of Veterinary Medicine, Ghent, Belgium

Jul. 7-13, 2019
15th HKU-Pasteur Virology Course: Coronaviruses
Hong Kong University (HKU)-Pasteur Research Pole – LKS Faculty of Medicicne, Hong Kong, China

May - Jun.,
Course: Research Papers
Autonomous University of Barcelona (UAB) – Barcelona, Spain

Dec. 14, 2017
Course: Sending Biologic Material
IRTA-CReSA – Barcelona, Spain

Dec. 12, 2017
Course: Personal Protection Equipment (PPE)
IRTA-CReSA – Barcelona, Spain

Nov. 30, 2017
Course: Use and Management of Critical Equipment
IRTA-CReSA – Barcelona, Spain

Jun. 6-7, 2017
Course in Modern Designs and Analyses of Experimental Data (16h)
IRTA – Barcelona, Spain

Jan. 20, 2017
Course: General Rules at BSL-2 and BSL-3 Laboratories
IRTA-CReSA – Barcelona, Spain

TEACHING, SEMINARS and CONGRESSES

May 2022

14th Annual Meeting of EPIZONE, Barcelona (Spain) – *Oral Communication*
MERS-CoV internalized by llama alveolar macrophages do not result in replication and induction of inflammatory cytokines. **Rodon, J**, Sachse, M, Te, N, Bensaid, A, Segalés, J, Risco, C, Vergara-Alert, J.

May 2022

14th Annual Meeting of EPIZONE, Barcelona (Spain) – *Poster Communication*
MERS-coronavirus clade C Egypt/2013 isolate exhibits poor transmission potential in camelid reservoir hosts. **Rodon, J**, Mykytyn, A, Te, N, Okba, N, Lamers, M, Pailler-Garcia, L, Cantero, G, Albulescu, I, Bosch, B, Bensaid, A, Vergara-Alert, J, Haagmans, B, Segalés, J.

Apr. 2022

Viruses 2022 - At the Leading Edge of Virology Research, Virtual edition – *Poster Communication*
Unraveling the antiviral activity of plitidepsin by subcellular and morphological analysis. Sachse, M, Tenorio, R, Fenrández, I, Muñoz-Basagoiti, J, Pérez-Zsolt, D, **Rodon, J**, Losada, A, Avilés, P, Cuevas, C, Paredes, R, Segalés, J, Clotet, B, Vergara-Alert, J, Izquierdo-Useros, N, Risco, C.

Feb. 2022

29th Conference on Retroviruses and Opportunistic Infections (CROI), Virtual edition – *Poster Communication*
Unraveling the antiviral activity of plitidepsin by ultrastuctural analysis. Sachse, M, Tenorio, R, Fenrández, I, Muñoz-Basagoiti, J, Pérez-Zsolt, D, **Rodon, J**, Losada, A, Avilés, P, Cuevas, C, Paredes, R, Segalés, J, Clotet, B, Vergara-Alert, J, Izquierdo-Useros, N, Risco, C.

Nov. 2021

3rd Research Symposium on Coronavirus by the Societat Catalana de Virologia, Virtual edition – *Oral Communication*
Monitoring natural SARS-CoV-2 infection in lions (*Panthera leo*) at Barcelona Zoo: viral dynamics and host responses. **Rodon, J**, Fernández-Bellón, H, Fernández-Bastit, L, Almagro, V, Padilla-Solé, P, Lorca-Oró, C, Valle, R, Roca, N, Graziolini, S, Trogu, T, Bensaid, A, Carrillo, J, Izquierdo-Useros, N, Blanco, J, Parera, M, Noguera-Julián, M, Clotet, B, Moreno, A, Segalés, J, Vergara-Alert, J.

Sep. 2021

Seminar at Virologie et Immunologie Moléculaires (VIM), Institut national de recherche pour l'agriculture (INRAe), Paris (France) – *Oral Communication*
Unravelling the role of early immune responses in camelid hosts controlling MERS-CoV infection. **Rodon, J**.

Jun. 2021

5th Conference of Predoctoral Researchers, University of Girona (Spain) – *Oral Communication*
Round table: Consequences of COVID-19 in the PhD.

Jan. 2021

M.Sc. Infectious Disease One Health, Autonomous University of Barcelona (Spain) – *Oral Communication*
SARS and MERS Coronaviruses: the role of Animals in virus transmission. **Rodon, J**, Vergara-Alert, J.

Dec. 2020

IRTA PhD Student Annual Seminar 2020, Barcelona (Spain) – *Oral Communication*
Development of cellular models for testing antiviral and anti-inflammatory compounds counteracting COVID-19. **Rodon, J**, Perez-Zsolt, D, Muñoz-Basagoiti, J, Valencia, A, Guallar, V, Carrillo, J, Blanco, J, Segalés, J, Clotet, B, Vergara-Alert, J, Izquierdo-Useros, N.

Dec. 2020

IRTA PhD Student Annual Seminar 2020, Barcelona (Spain) – *Oral Communication*

Development of cellular models for testing antiviral and anti-inflammatory compounds counteracting COVID-19. **Rodon, J**, Perez-Zsolt, D, Muñoz-Basagoiti, J, Valencia, A, Guallar, V, Carrillo, J, Blanco, J, Segalés, J, Clotet, B, Vergara-Alert, J, Izquierdo-Useros, N.

Nov. 2020

6th World One Health Congress (WOHC2020), Virtual edition – *Oral Communication*

Respiratory explants from alpaca as a tool for studying the Middle East respiratory syndrome coronavirus (MERS-CoV) infection in camelids. **Rodon, J**, Te, N, Pérez, M, Pujols, J, Segalés, J, Bensaid, A, Vergara-Alert, J.

Oct. 2020

2nd Research Symposium on Coronavirus by the Societat Catalana de Virologia, Virtual edition – *Oral Communication*

Search of SARS-CoV-2 inhibitors and their combinations within approved drugs to tackle COVID-19 pandemic. **Rodon, J**, Muñoz-Basagoiti, J, Perez-Zsolt, D, Noguera, M, Paredes, R, Mateu, L, Quiñones, C, Erkizia, I, Blanco, I, Valencia, A, Guallar, V, Carrillo, J, Blanco, J, Segalés, J, Clotet, B, Vergara-Alert, J, Izquierdo-Useros, N.

May 2020

Research Symposium on Coronavirus by the Societat Catalana de Virologia, Virtual edition – *Oral Communication*

Search for SARS-CoV-2 inhibitors in currently approved drugs to tackle COVID-19 pandemia. **Rodon, J**, Noguera, M, Erkizia, I, Valencia, A, Guallar, V, Carrillo, J, Blanco, J, Segalés, J, Clotet, B, Vergara-Alert, J, Izquierdo-Useros, N.

Jan. 2020

M.Sc. Infectious Disease One Health, Autonomous University of Barcelona (Spain) – *Oral Communication*

SARS and MERS Coronaviruses: the role of Animals in virus transmission. **Rodon, J**, Vergara-Alert, J.

Nov. 2019

IRTA PhD Student Annual Seminar 2019, Barcelona (Spain) – *Chair of one session and speaker, oral Communication*

Blocking transmission of Middle East respiratory syndrome coronavirus (MERS-CoV) in llamas by vaccination with a recombinant spike protein. **Rodon, J**, Okba M.A., N, Te, N, van Dieren, B, Bosch, B-J, Bensaid, A, Segalés, J, Haagmans, B, Vergara-Alert, J.

Aug. 2019

13th Annual Meeting of EPIZONE, Berlin (Germany) – *Oral Communication*

An experimental vaccine based on a recombinant MERS-CoV S1-protein induces broad protective immune responses in llama. **Rodon, J**, Okba M.A., N, Te, N, van Dieren, B, Bosch, B-J, Bensaid, A, Segalés, J, Haagmans, B, Vergara-Alert, J.

Aug. 2019

13th Annual Meeting of EPIZONE, Berlin (Germany) – *Poster Communication*

Middle East respiratory syndrome coronavirus (MERS-CoV) early immune responses in an alpaca infection model., Te, N, **Rodon, J,** Vergara-Alert, J, Pérez, M, Segalés, J, Bensaid, A,.

Jun. 2019

SEV-GVN, XV Congress of the Spanish Society of Virology (Sociedad Española de Virología, SEV) and 11th International Global Virus Network (GVN) Meeting, Barcelona (Spain) – *Oral Communication*

Middle East respiratory syndrome coronavirus (MERS-CoV) replicates in alpaca respiratory tissue explants. **Rodon, J**, Te, N, Pérez, M, Pujols, J, Haagmans, B, Segalés, J, Bensaid, A, Vergara-Alert, J.

Jun. 2019

SEV-GVN, XV Congress of the Spanish Society of Virology (Sociedad Española de Virología, SEV) and 11th International Global Virus Network (GVN) Meeting, Barcelona (Spain) – *Oral Communication*

Expression of cytokines and pro-inflammatory response induced in the nasal epithelium of MERS-CoV infected alpacas (Vicugna pacos). Te, N, **Rodon, J**, Pérez, M, Haagmans, B, Vergara-Alert, J, Segalés, J, Bensaid, A.

Nov. 2018

X International Global Virus Network (GVN) Meeting, Annecy (France) – *Poster Communication*

Cytokine expression in the respiratory tract of MERS-CoV infected alpacas (Vicugna pacos). Te N, **Rodon J**, Pérez M, Haagmans BL, Vergara-Alert J, Segalés, J, Bensaid A.

Oct. 2018

XVII JORNADA DE VIROLOGIA de la Societat Catalana de Virologia, Barcelona (Spain), – *Poster Communication*

Middle East Respiratory Syndrome coronavirus (MERS-CoV) vaccination efficacy in a direct-contact transmission model in llamas. **Rodon, J**, Te, N, Saporiti, V, Okba M.A., N, Pujols, J, Abad, X, Haagmans, B, Bosch, B-J, van Dieren, B, Vergara-Alert, J, Bensaid, A, Segalés, J.

Aug. 2018

ESVV-EPIZONE, 11th International Congress for Veterinary Virology and 12th Annual Meeting of EPIZONE, Vienna (Austria) – *Oral Communication*

Middle East Respiratory Syndrome coronavirus (MERS-CoV) vaccination efficacy in a direct-contact transmission model in llamas. **Rodon, J**, Te, N, Saporiti, V, Okba M.A., N, Pujols, J, Abad, X, Haagmans, B, Bosch, B-J, van Dieren, B, Vergara-Alert, J, Bensaid, A, Segalés, J.

Aug. 2018

ESVV-EPIZONE, 11th International Congress for Veterinary Virology and 12th Annual Meeting of EPIZONE, Vienna (Austria) – *Oral Communication*

Middle East respiratory syndrome coronavirus (MERS-CoV) early infection in alpacas. Te, N, **Rodon, J**, Vergara-Alert, J, Pérez, M, Segalés, J, Bensaid, A.

AWARDS, HONORS and SCHOLARSHIPS

2020 **Fellowship Grant by the One Health Platform, WOHC2020 - 6th World One Health Congress –** June 2020, Edinburgh (Postponed and finally converted to virtual edition)

2020 **Early Career Scientist Meeting Grant by the Federation of European Microbiological Societies (FEMS), NIDO2020 - XVth International Nidovirus Symposium** – May 2020, The Netherlands (Postponed and finally converted to virtual edition)

2019 **Travel grant award, 13th Annual Meeting EPIZONE, EPIZONE European Research Group**

2018 **Best communication award, XVII Virology Congress, Catalan Society of Biology** – October 2018, Barcelona

List of scientific publications – As a 1st author

1. **Rodon, J.**, Mykytyn, A. Z., Cantero, G., Albulescu, I. C., Bosch, B. J., Brix, A., Audonnet, J. C., Bensaid, A., Vergara-Alert, J., Haagmans, B. L., & Segalés, J. (2022). Protective efficacy of an RBD-based Middle East respiratory syndrome coronavirus (MERS-CoV) particle vaccine in llamas. *One health outlook*, *4*(1), 12.

2. Te, N., **Rodon, J.**, Pérez, M., Segalés, J., Vergara-Alert, J., & Bensaid, A. (2021). Enhanced replication fitness of MERS-CoV clade B over clade A strains in camelids explains the dominance of clade B strains in the Arabian Peninsula. *Emerging microbes & infections*, *11*(1), 260-274.

3. Perez-Zsolt, D., Muñoz-Basagoiti, J., **Rodon, J.**, Elosua-Bayes, M., Raïch-Regué, D., Risco, C., ... & Izquierdo-Useros, N. (2021). SARS-CoV-2 interaction with Siglec-1 mediates trans-infection by dendritic cells. *Cellular & molecular immunology*, *18*(12), 2676-2678.

4. Fernández-Bellon, H., **Rodon, J.**, Fernández-Bastit, L., Almagro, V., Padilla-Solé, P., Lorca-Oró, C., ... & Vergara-Alert, J. (2021). Monitoring natural SARS-CoV-2 infection in lions (*Panthera leo*) at the Barcelona Zoo: Viral dynamics and host responses. *Viruses*, *13*(9), 1683.

5. Te, N., **Rodon, J.**, Ballester, M., Pérez, M., Pailler-García, L., Segalés, J., ... & Bensaid, A. (2021). Type I and III IFNs produced by the nasal epithelia and dimmed inflammation are features of alpacas resolving MERS-CoV infection. *PLoS pathogens*, *17*(5), e1009229.

6. Brustolin, M., **Rodon, J.**, Rodríguez de la Concepción, M. L., Ávila-Nieto, C., Cantero, G., Pérez, M., ... & Segalés, J. (2021). Protection against reinfection with D614-or G614-SARS-CoV-2 isolates in golden Syrian hamster. *Emerging Microbes & Infections*, *10*(1), 797-809.

7. **Rodon, J.**, Muñoz-Basagoiti, J., Perez-Zsolt, D., Noguera-Julian, M., Paredes, R., Mateu, L., ... & Izquierdo-Useros, N. (2021). Identification of plitidepsin as potent inhibitor of SARS-CoV-2-induced cytopathic effect after a drug repurposing screen. *Frontiers in pharmacology*, *12*, 278.

8. **Rodon, J.**, Okba, N. M., Te, N., van Dieren, B., Bosch, B. J., Bensaid, A., ... & Vergara-Alert, J. (2019). Blocking transmission of Middle East respiratory syndrome coronavirus (MERS-CoV) in llamas by vaccination with a recombinant spike protein. *Emerging microbes & infections*, *8*(1), 1593-1603.

As a co-author

9. Varona, J. F., Landete, P., Lopez-Martin, J. A., Estrada, V., Paredes, R., Guisado-Vasco, P., ... & Garcia-Sastre, A. (2022). Preclinical and randomized phase I studies of plitidepsin in adults hospitalized with COVID-19. *Life Science Alliance*, *5*(4).

10. Sachse, M., Tenorio, R., de Castro, I. F., Muñoz-Basagoiti, J., Perez-Zsolt, D., Raïch-Regué, D., ... & Risco, C. (2022). Unraveling the antiviral activity of plitidepsin against SARS-CoV-2 by subcellular and morphological analysis. *Antiviral Research*, *200*, 105270.

11. Pradenas, E., Trinité, B., Urrea, V., Marfil, S., Tarrés-Freixas, F., Ortiz, R., ... & Blanco, J. (2022). Clinical course impacts early kinetics, magnitude, and amplitude of SARS-CoV-2 neutralizing antibodies beyond 1 year after infection. *Cell Reports Medicine*, *3*(2).

12. Te, N., Ciurkiewicz, M., van den Brand, J. M., **Rodon, J.**, Haverkamp, A. K., Vergara-Alert, J., ... & Segalés, J. (2022). Middle East respiratory syndrome coronavirus infection in camelids. *Veterinary pathology*, 03009858211069120.

13. Vidal, E., López-Figueroa, C., **Rodon, J.**, Pérez, M., Brustolin, M., Cantero, G., ... & Segalés, J. (2021). Chronological brain lesions after SARS-CoV-2 infection in hACE2-transgenic mice. *Veterinary pathology*, 03009858211066841.

14. Fernández-Bastit, L., **Rodon, J.**, Pradenas, E., Marfil, S., Trinité, B., Parera, M., ... & Segalés, J. (2021). First Detection of SARS-CoV-2 Delta (B. 1.617. 2) Variant of Concern in a Dog with Clinical Signs in Spain. *Viruses*, *13*(12), 2526.

15. Sikkema, R. S., Tobias, T., Oreshkova, N., de Bruin, E., Okba, N., Chandler, F., ... & Stegeman, A. (2022). Experimental and field investigations of exposure, replication and transmission of SARS-CoV-2 in pigs in the Netherlands. *Emerging microbes & infections*, *11*(1), 91-94.

16. Barreiro, A., Prenafeta, A., Bech-Sabat, G., Roca, M., March, R., Gonzalez, L., ... & Torroella, E. (2021). Preclinical efficacy, safety, and immunogenicity of PHH-1V, a second-generation COVID-19 vaccine candidate based on a novel recombinant RBD fusion heterodimer of SARS-CoV-2. *bioRxiv*.

17. Lorca-Oró, C., Vila, J., Pleguezuelos, P., Vergara-Alert, J., **Rodon, J.**, Majó, N., ... & Abad, X. (2022). Rapid SARS-CoV-2 Inactivation in a Simulated Hospital Room Using a Mobile and Autonomous Robot Emitting Ultraviolet-C Light. *The Journal of infectious diseases, 225*(4), 587-592.

18. Massanella, M., Martin-Urda, A., Mateu, L., Marín, T., Aldas, I., Riveira-Muñoz, E., ... & Paredes, R. (2021, July). Critical Presentation of a SARS-CoV-2 Reinfection: a case report. In *Open Forum Infectious Diseases*.

19. Trinité, B., Pradenas, E., Marfil, S., Rovirosa, C., Urrea, V., Tarrés-Freixas, F., ... & Blanco, J. (2021). Previous SARS-CoV-2 infection increases B. 1.1. 7 cross-neutralization by vaccinated individuals. *Viruses*, *13*(6), 1135.

20. Roca, O., Pacheco, A., **Rodon, J.**, Antón, A., Vergara-Alert, J., Armadans, L., ... & Rodríguez-Garrido, V. (2021). Nasal high-flow oxygen therapy in COVID-19 patients does not cause environmental surface contamination. *Journal of Hospital Infection*, *116*, 103-105.

21. Pradenas, E., Trinité, B., Urrea, V., Marfil, S., Ávila-Nieto, C., de la Concepción, M. L. R., ... & Blanco, J. (2021). Stable neutralizing antibody levels 6 months after mild and severe COVID-19 episodes. *Med*, *2*(3), 313-320.

22. Trinité, B., Tarrés-Freixas, F., **Rodon, J.**, Pradenas, E., Urrea, V., Marfil, S., ... & Blanco, J. (2021). SARS-CoV-2 infection elicits a rapid neutralizing antibody response that correlates with disease severity. *Scientific reports*, *11*(1), 1-10.

23. Alemany, A., Baró, B., Ouchi, D., Rodó, P., Ubals, M., Corbacho-Monné, M., ... & Mitjà, O. (2021). Analytical and clinical performance of the panbio COVID-19 antigen-detecting rapid diagnostic test. *Journal of Infection*, *82*(5), 186-230.

24. Vergara-Alert, J., **Rodon, J.**, Carrillo, J., Te, N., Izquierdo-Useros, N., Rodríguez de la Concepción, M. L., ... & Segalés, J. (2021). Pigs are not susceptible to SARS-CoV-2 infection but are a model for viral immunogenicity studies. *Transboundary and emerging diseases*, *68*(4), 1721-1725.

25. Segalés, J., Puig, M., **Rodon, J.**, Avila-Nieto, C., Carrillo, J., Cantero, G., ... & Vergara-Alert, J. (2020). Detection of SARS-CoV-2 in a cat owned by a COVID-19− affected patient in Spain. *Proceedings of the National Academy of Sciences*, *117*(40), 24790-24793.

26. Díez, J. M., Romero, C., Vergara-Alert, J., Belló-Perez, M., **Rodon, J.**, Honrubia, J. M., ... & Gajardo, R. (2020). Cross-neutralization activity against SARS-CoV-2 is present in currently available intravenous immunoglobulins. *Immunotherapy*, *12*(17), 1247-1255.

Acknowledgements

Passant aquesta pàgina acaba una etapa que m'ha fet créixer molt, professional i personalment. Durant aquest camí he tingut l'oportunitat de conèixer i compartir grans moments amb gent fantàstica. Us estaré sempre molt agraït de tot cor! No voldria pas començar una nova etapa sense dedicar unes paraules a algunes d'aquestes persones.

Trulli, Dani, Anna i Kuki, us vull agrair la relació que tenim i m'hagueu donat suport fins aquí. El veure'ns intermitent, degut situacions vàries, no camufla res del que heu fet per mi durant tants anys. El suport del dia a dia me'l dona sempre *la meva clicka*, una família d'amics que es van trobar per casualitat jugant a futbol i que la vida ha portat molt més enllà. Vull agrair-vos molt tot el que feu per mi diàriament, i tot el que fem per mantenir aquest grup humà de gent tan diferent, tan unit i tan viu. Sense que suposi cap mena d'esforç, sou el pilar amb qui un es pot recolzar en qualsevol moment i davant qualsevol situació. En especial m'agradaria mencionar el suport incondicional d'en Pau, Carrasco, Axel, Guille, Jau, Aleix, Balles, Gella, Lui i Vera.

Mar i Aitor, la vida ens va tancar un temps en una gàbia de ciment i vau fer que passés ràpid i tot! No és fàcil conviure amb persones molt diferents i penso que ho hem fet més que bé, moltes gràcies per tants moments conviscuts. La pandèmia també m'ha portat a conèixer gent amb qui he passat moltes hores últimament i espero que això no canviï. Elena, Mimi i els *nenes*, sou el *highlight* de la meva pandèmia.

El camí fins a culminar aquesta tesi és llarg. Agraeixo profundament que tot això comences amb els amics biòlegs gironins 'de para siempre', quina família més maca que vam crear durant el grau. És genial retrobar-nos sovint i que els anys no passin. No només a ells però també vull agrair molt a la María tot el que va fer per mi durant aquella època. Sense el teu suport no hagués aconseguit graduar-me i qui sap si seguir estudiant. Gràcies per trobar-me en una època estranya de la meva vida i ajudar-me a estar centrat on tocava. Fio i, especialment, Laura, gràcies per transmetre la ciència que porteu dins. Tot i que no sempre he encarat de la millor manera les decisions que prenc a la vida, gràcies per intentar entendre-les i seguir avançant.

Només tinc paraules d'agraïment cap a la família del CReSA. Em vau acollir amb 22 anyets i em deixeu volar a dia d'avui, amb una preparació sòlida per afrontar nous reptes professionals. Heu fet que hagi gaudit de cada moment d'aquesta tesi, i n'hem passat molts i de tots colors. Moltes gràcies als equips d'estabulari i gestió de laboratoris, sense vosaltres hagués sigut impossible dur a terme els experiments que s'han fet al llarg d'aquesta tesi. Agrair profundament el treball realitzat pels col·laboradors d'EMC i UU als Països Baixos, en especial al Prof. Bart Haagmans i el seu equip. També a l'equipàs d'IrsiCaixa, que ha fet molt fàcil i fructíferes les nostres col·laboracions, i a tots els altres col·laboradors que no cito explícitament i que sense la vostra aportació no hagués sigut possible arribar fins al punt on sóc. Agrair a la família de doctorands tot el suport professional i personal que m'heu donat. Vaig estar un temps preocupat perquè ningú donava continuïtat a la família d'Old Scool PhDs però puc marxar molt tranquil veient les últimes incorporacions. Tots i cadascun de vosaltres sou genials, i us desitjo molt d'èxit professional i sobretot personal. Aquí la menció especial va cap als 'papitos muertovivos'. Doctorsitos Alejo i Laia, gràcies per tot el suport que m'heu donat des del moment que vaig trepitjar el CReSA. Sou dues persones molt especials i sóc molt afortunat de formar part de la vostra vida. Tot i que la vida ens separi, almenys un temps, tots teniu casa en algun indret del món on acabi fent arrels.

Tot el que he viscut durant aquesta tesi mai hagués estat possible sense el suport del grup corona. Moltes gràcies Carlos, Carla, Cris, Lei, Lore, Marco i Núria pel vostre suport diari al laboratori i en alguns casos fora del laboratori. Sou un gran equip professional i humà. Lei Jr. T'has espero que cuidis al/la pròxim Jr. Igual de bé o millor del que jo he fet amb tu, segur que t'ho agrairà moltíssim. It should not have been easy dealing with me on a daily basis in the lab, but you did an amazingly well. Thank you for all of our fruitful works; they were far too brief. I hope our paths cross again someday, my lab brother!

I a qui més he d'agrair poder aconseguir aquest títol de doctor és als meus directors, gràcies pel vostre suport incondicional, econòmic i moral. Sou tres persones molt especials, tres caràcters molt forts i diferents que sorprenentment troben un equilibri òptim. Ha sigut un plaer ser aprenent vostre, i no ho vull deixar de ser mai. Si pogués tornar a

començar el doctorat ho faria amb els ulls tancats sota la vostra direcció. Gràcies per fer-me fet créixer molt com a professional i persona. Quim, moltes gràcies per compartir els teus coneixements i les teves ensenyances en el món de les malalties infeccioses. Per l'intent d'ensenyar-me temes de patologia on sóc i seguiré sent un negat... sort que sempre et podré venir a molestar. I sobretot gràcies per ensenyar-me a veure-ho tot des d'un punt de vista sistèmic. La teva energia i dedicació són espectaculars i les admiro profundament, fins i tot dins de la pista de pàdel. Albert, siempre estaré en deuda contigo por todo lo que me has aportado científicamente. Quién lo diría que pasaríamos de las broncas a tus PhDs novatos a las discusiones científicas de gran interés (al menos para mí). Es una pena que te jubiles pronto, todo doctorando merece a alguien que le pueda ayudar a analizar cada simple detalle profesional como lo has hecho conmigo. Muchas gracias por abrirme las puertas al mundo de la inmunología y la biología celular, y por confiar siempre en mí. Sé que lo has hecho más de lo que muchas veces reflejas, y lo valoro muchísimo. Espero poder visitarte en Tailandia o dónde sea tu jubilación y poder seguir con muchas discusiones científicas y no científicas, de estas para no arreglar el mundo. Júlia, no sé com agrair tot el que has fet per mi. Has estat sense dubte el meu principal pilar durant tot aquest temps, dins i fora del laboratori. Vas agafar un estudiant ingenu però motivat, i el vas fer créixer en tots els àmbits. Gràcies per fer-me de germana gran i guiar-me dins i fora el laboratori. Per ensenyar-me com funciona gairebé tot a nivell professional i tècnic, i alhora donar-me responsabilitats i apretar-me per aflorar el millor de mi. Gràcies per dirigir-me també com a persona, i posar-me en sintonia quan em podia descentrar. Sé del cert que la relació que surt d'aquest doctorat no acaba aquí, m'emporto una amistat de per vida, de les que no es troben.

Finalment, vull agrair a la meva família tot el que ha fet i fa per mi a diari. La menció especial va per la meva cosina Maria per acollir-me en hores intempestives tornant del laboratori o quan ha fet falta acabar unes bones copes, bona música i arreglant el món. He tingut la sort de compartir aquest doctorat amb els quatre avis, mai m'hagués imaginat que tots veurien com avui em faig doctor. Moltes gràcies Josep, Montse, Joan i Teresa per posar-me sempre un plat a taula i mimar-me tan com heu pogut. A la Duna, que recentment ens ha deixat, i ha sigut durant

gairebé 18 anys la germaneta que mai havia tingut. He fet moltes hores de ‘colzes’ per arribar fins aquí i ella és sense dubte és la que en va fer més amb mi. La meva més sincera gratitud per la Tina, qui ha sigut en tot moment un suport durant el darrer any. Tens un cor transparent i gegant, entre moltes altres qualitats, que tothom al teu voltant admira. Que res faci que s'embruti, deixa'l brillar i que surti tot el potencial que té. Espero que seguim vivint moltes més experiències junts, gràcies per tant en tan poc temps!

A qui vull dedicar sobretot aquesta tesi és a la meva mare i al meu pare. Mama, ets els fonaments de tot això. Gràcies per forjar-me tossut i treballador, i sobretot per no interferir en res del que he volgut fer a la vida, fins i tot quan no he pres bones decisions i m'has deixat ‘fotre'm l'hòstia’. Tot i la poca comunicació que ens caracteritza, res hagués d'això hagués sigut possible sense el teu suport. Papa, vas marxar massa aviat i t'has perdut alguns moments i persones especials que m'envolten. Qui ho hagués dit fa uns anys que tindríem un doctor a la família, eh?! Des d'allà on siguis, gràcies per acompanyar-me, guiar-me i adreçar-me pel bon camí.

Passant pàgines

Observes la portada ponderant
si et ve de gust seguir endavant.
El revers sembla prou bo,
i la crítica el qualifica d'intens i interessant.

El principi és temptador
amb trames de tots colors.
Cada frase ve de nou, sembla que el guió promet,
i hi estàs enganxada per complet.

I segueixes avançant,
res és simple com abans.
Hi ha camins que s'entrecreuen
i contratemps inesperats.
El batec se t'accelera amb cada gir argumental,
i la por a topar-te amb la última pàgina al final,
et recorda de tant en tant
què segueixes fent allà.

Poc a poc vas fent la història teva,
descobrint-ne dins la trama
com hi encaixa cada peça.
Fins arribat al punt que
t'atreviries a afirmar,
que predir-ne em pròxim moviment
no et seria complicat.

Però segueixes avançant,
res és simple com abans.
Hi ha camins que s'entrecreuen
i contratemps inesperats.
El batec se t'accelera amb cada gir argumental,
i la por a topar-te amb la última pàgina al final,
et recorda de tant en tant
què segueixes fent allà.

I seguiràs devorant-me fins que un dia
ja no tremolis al llegir-me,
o jo ja no m'exalti en observar-te embadalida.
Amb cada línia que escrivim, amb cada nova aportació,
a vegades per més que s'intenti, la resposta sempre és no.

I amb sort ho veurem a temps,
i ens desfarem d'uns sentiments,
d'estima i de 'carinyo'
que ens lliguen al que coneixem.
I sabrem dir-nos adéu.

Despedint-nos però contents, tot esbossant,
a corre-cuita, unes frases que deixaran
l'obra a mitges.
Qui sap si mai tindrem ganes de rellegir-nos.

Adaptació de *Bruç i Adriana Pla*

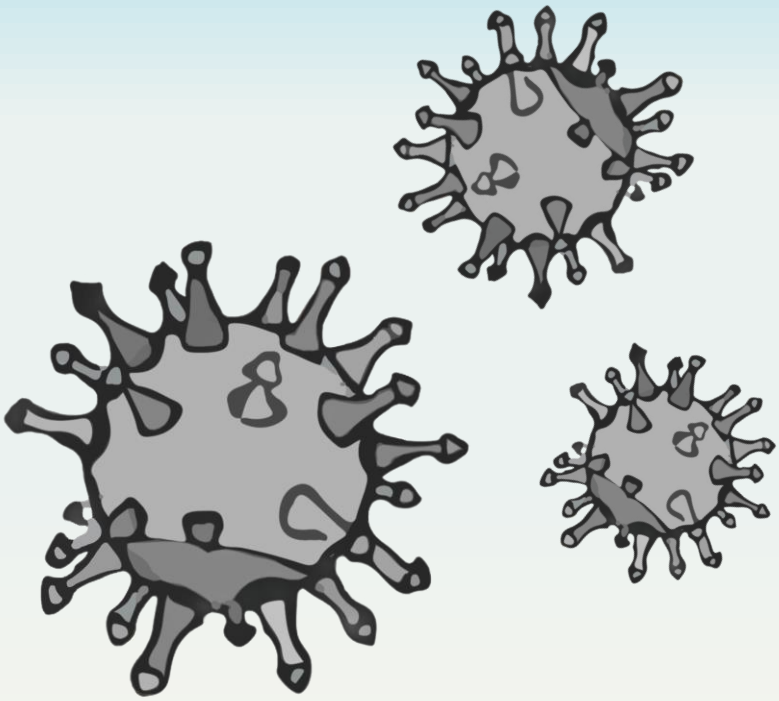

UAB
Universitat Autònoma
de Barcelona

IRTA
CReSA